Lab Medicine

Science

Evaluation of the Impact of Changing Quality Control Rules and Frequency on the Risk Management Index: Results from the Clinical Routine of a Medical Laboratory

Daniela Karnutsch,[1] Francesca Occhipinti,[1] Daniel Tumiatti,[1] Thomas Mueller, MD[1,]*

ABSTRACT

Objective: The consideration of the principles of risk management in the analytical process is a current trend. The aim of this study was to evaluate whether the risk management index (RMI) for various laboratory parameters can be influenced by interventions that change the internal quality control (IQC) strategy.

Methods: We selected 10 laboratory parameters associated with cardiovascular disease for the study (myoglobin, N-terminal fragment of the pro B-type natriuretic polypeptide, cardiac troponin T, creatinine kinase, lactate dehydrogenase, glucose, triglycerides, total cholesterol, and low-density lipoprotein and high-density lipoprotein cholesterol). The study-specific interventions included changing the IQC rules and changing the IQC schedule. This was a one-armed intervention study in which changes in the RMI, a measure of patient harm risk, was recorded over time.

Results: Before the intervention, the mean RMI was 1.022 (95% confidence interval [CI], 0.269–1.776). After the intervention, the mean RMI was 0.934 (95% CI, 0.088–1.956). The RMI values before and after the intervention were not significantly different ($P =.89$).

Conclusion: The study-specific interventions did not lead to an improvement of the RMI in the clinical routines of a medical laboratory. There is a great need to further explore this subject area with interventional studies to clarify how the risk of unintended patient harm can be measurably improved.

Keywords: analytical quality, patient harm, quality control, rejection rules, risk management, intervention study

In a medical laboratory, analyses are performed to support medical decisions.[1] The results of laboratory analyses are an aid to diagnosis, prognosis estimation, and therapy control.[1-3] It is important that the laboratory values obtained are analytically correct.[1] To ensure the quality of analysis, medical laboratories participate in external quality assurance programs and use daily internal quality control (IQC).[4-6] The use of appropriate IQC strategies has been accepted in medical laboratories for decades[4-6] and has been included in international recommendations and guidelines.[7,8] The term *IQC strategy* is defined as (i) the number of IQC materials to measure, (ii) the number of IQC results and the IQC rule to use at each IQC event, and (iii) the frequency of IQC events.[7]

A current trend with regard to the IQC strategy in a medical laboratory is the consideration of the principles of risk management in the analytical process.[8-10] In the literature, the term *risk management index* (RMI) has been introduced in this context.[11,12] The RMI is the predicted probability of harm (predicted P_H) divided by the acceptable probability of harm (acceptable P_H).[11,12] According to the literature, one should aim for an RMI ≤ 1.[11,12] An RMI ≤ 1 would mean that the capability and reliability of the respective measurement system combined with the

Abbreviations

RMI, risk management index; IQC, internal quality control; CI, confidence interval; P_H, probability of harm; NT-proBNP, N-terminal fragment of the pro B-type natriuretic polypeptide; cTnT, cardiac troponin T; CK, creatine kinase; LDH, lactate dehydrogenase; LDLC, low-density lipoprotein cholesterol; HDLC, high-density lipoprotein cholesterol; CV, coefficient of variation; SD, standard deviation; TEa, allowable total error; ND, estimated number of patients who are run (on average) each day; MTBF, mean time between failures; $P_{h|u}$, probability of harm given an unreliable result.

[1]Department of Clinical Pathology, Hospital of Bolzano, Bolzano, Italy

*To whom correspondence should be addressed.
thomas.mueller@sabes.it

IQC strategy of the medical laboratory maintains the risk of unintended patient harm at an acceptable level.[11,12] An RMI >1 would indicate that the medical laboratory has not reduced the risk of accidental patient harm to an acceptable level.[11]

There is, however, no scientific evidence in the form of published studies showing that changing the IQC strategy will have an impact on the RMI in the clinical routine of a medical laboratory. Thus, the aim of this study was to evaluate, under routine clinical conditions, whether the RMI for various laboratory parameters can be influenced by interventions that change the IQC strategy.

Materials and Methods

Study Design

This prospectively conducted study was performed at the Department of Clinical Pathology, Hospital of Bolzano, Italy. Before starting the study, the local ethics committee approved the study protocol. In the study, we collected the RMI over time for several laboratory parameters. The study hypothesis was "By tightening the IQC strategy, the RMI will decrease." The null hypothesis was "By tightening the IQC strategy, the RMI will not decrease." The study-specific interventions were staggered, and they included a change in the applicable IQC rules and a change in the IQC schedule. The study period spanned April 30, 2019, to September 2, 2019 (ie, 18 weeks). This was thus a single-arm intervention study in which changes of RMI were recorded over time. The study design is detailed in **Figure 1**. To calculate the RMI at different points in time, we used the commercially available software solution Mission Control 2 (Bio-Rad Laboratories, Plano, TX), which we also used routinely in the Department of Clinical Pathology, Hospital of Bolzano, Italy, before initiating the study.

Laboratory Parameters

To test the study hypotheses, we selected 10 laboratory parameters that were (i) associated with cardiovascular diseases; (ii) determined in daily routine diagnostics on 1 of the 2 clinical chemical analyzers in the laboratory, a Cobas 8000 (Roche Diagnostics, Rotkreuz, Switzerland) with Roche

reagents; (iii) checked with "third-party" IQCs by Bio-Rad Laboratories; and (iv) subject to the same IQC rules.

The following laboratory parameters were investigated in this study: myoglobin, the N-terminal fragment of the pro B-type natriuretic polypeptide (NT-proBNP), cardiac troponin T (cTnT), creatine kinase (CK), lactate dehydrogenase (LDH), glucose, triglycerides, total cholesterol, low-density lipoprotein cholesterol (LDLC), and high-density lipoprotein cholesterol (HDLC).

We determined myoglobin, NT-proBNP, and cTnT by electrochemiluminescence immunoassays on a Cobas e801 system (Elecsys Myoglobin, Elecsys proBNP II, and Elecsys Troponin T highly sensitive) in lithium heparin plasma. According to the package inserts, the total coefficient of variation (CV) is <3.1% for myoglobin and <12.6% for NT-proBNP. According to the package insert, the total CV of cTnT at the 99th percentile of a healthy reference population of 14 ng/L is <10%.

We determined CK, LDH, and glucose with UV tests on a Cobas c702 (CK, LDHI2, and Gluc3) in lithium heparin plasma. According to the package insert, the total CV is <1.4% for CK, <2.7% for LDH, and <1.8% for glucose.

We determined triglycerides, total cholesterol, LDLC, and HDLC with enzymatic color tests on a Cobas c702 (trigl, Chol2, LDLC3, and HDLC4) in lithium heparin plasma. According to the package insert, the total CV is <2.0% for triglycerides, <1.6% for total cholesterol, <2.3% for LDLC, and <1.8% for HDLC.

During the entire study period, we used only 1 batch of reagents for myoglobin, NT-proBNP, CK, LDH, glucose, triglycerides, total cholesterol, LDLC, and HDLC. For cTnT, we used 2 different batches of reagents during the study period; one lot (number 345850) was used until May 4, 2019, and another lot (number 370695) was used thereafter.

IQC Material

We purchased third-party IQCs from Bio-Rad Laboratories. For the parameters CK, LDH, glucose, triglycerides, total cholesterol, LDLC, and HDLC, we used "Multiqual 1,2,3" (batch number: 45800; date of expiry: October 31, 2020). For myoglobin and NT-proBNP, we used "Cardiac Markers LT" (batch number: 31440; date of expiry: April 30, 2020). For cTnT, we used "Cardiac Troponins" (batch number: 56330; date of expiry: March 31, 2020). Thus, for all 10
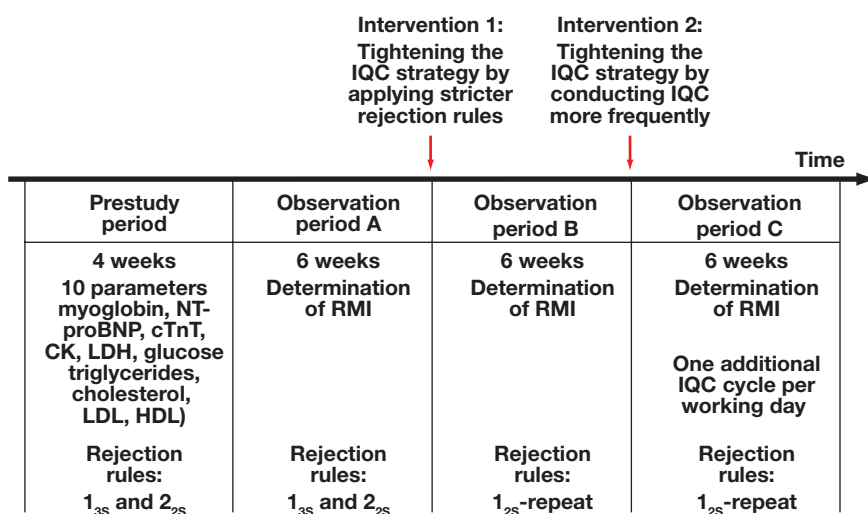
Figure 1

Study design—interventions and observation periods.

laboratory parameters we used the same IQC material during the entire study period without any change to the batches.

Study-Specific Interventions

Figure 1 highlights the different study periods and the 2 study-specific interventions.

Prestudy Period

Since April 2, 2019 we used the Westgard Rules[4] 1_{3s} and 2_{2s} as rejection rules for all 10 laboratory parameters. Beginning April 2, the IQC rules were related to the laboratory mean (which was a mobile mean) and the corresponding standard deviation (SD) of the laboratory. For the parameters myoglobin, NT-proBNP, and cTnT, we measured IQCs with 2 different concentration levels at 7:00 a.m. every operating day. For the parameters CK, LDH, glucose, triglycerides, total cholesterol, LDLC, and HDLC, we measured IQCs with 2 different concentration levels at 7:00 a.m. and 12:30 p.m. every operating day.

Observation Period A

From April 30 to June 10, 2019, inclusive (ie, during a study period of 6 weeks), we evaluated the IQC of all 10 laboratory parameters using Westgard Rules[4] 1_{3s} and 2_{2s} as rejection rules (**Figure 1**) and the same IQC timetable as in the prestudy period. In observation period A, the IQC rules were

still related to the laboratory mean (which was a mobile mean) and the corresponding SD of the laboratory. If a control had violated the 1_{3s} or 2_{2s}, then the analytical process had to be interrupted and the cause of the rule violation had to be determined and corrected.

Intervention 1 (Change in the Rejection Rules)

In the afternoon of June 10, 2019 (after the analyzer had been shut down), the rejection rules for all 10 laboratory parameters were changed. As of this date, the 1_{2s}-repeat was activated as a rejection rule[13] and the 1_{3s} and 2_{2s} were disactivated (**Figure 1**). For the parameters myoglobin, NT-proBNP, and cTnT, we measured IQCs with 2 different concentration levels at 7:00 a.m. every operating day. Likewise, the rule remained that for the parameters CK, LDH, glucose, triglycerides, total cholesterol, LDLC, and HDLC, we measured IQCs with 2 different concentration levels at 7:00 a.m. and 12:30 p.m. every operating day.

Observation Period B

From June 11 to July 22, 2019, inclusive (ie, for a study period of 6 weeks), the IQC of all 10 laboratory parameters were evaluated using the 1_{2s}-repeat as a rejection rule (**Figure 1**) and the same IQC timetable as in the prestudy period and in observation period A. Even in observation period B, the IQC rules were based on the laboratory mean (which was a mobile mean) and the corresponding SD of the laboratory. If a control violated

the 1_{2s}-repeat, then the analytical process had to be interrupted and the cause of the rule violation had to be determined and corrected.

Intervention 2 (Change in the Frequency of IQC)

In the afternoon of July 22, 2019 (after the analyzer had been shut down), the IQC system was changed in such a way that from the following day onward, not only 1 IQC but 2 IQCs with 2 different concentration levels were measured for the parameters myoglobin, NT-proBNP, and cTnT every day of operation at 7:00 a.m. and 12:30 p.m. Likewise, the rule for the parameters CK, LDH, glucose, triglycerides, total cholesterol, LDLC, and HDLC was changed to the extent that on each operating day, not only 2 but 3 IQCs with 2 different concentration levels each were measured at 7:00 a.m., 9:30 a.m., and 12:30 p.m. In contrast, the rejection rule for all 10 laboratory parameters remained unchanged in comparison with observation period B (**Figure 1**). The 1_{2s}-repeat was still valid as the rejection rule.

Observation Period C

From July 23 to September 2, 2019, inclusive (ie, for a study period of 6 weeks), the IQC of all 10 laboratory parameters was evaluated using the 1_{2s}-repeat as the rejection rule (**Figure 1**) and the IQC schedule described in the paragraph above. As in observational periods A and B, the IQC rules were based on the laboratory mean (which was a mobile mean) and the corresponding SD of the laboratory. If a control violated the 1_{2s}-repeat, then the analytical process had to be interrupted and the cause of the rule violation had to be determined and corrected.

Bias and CV

The bias and CV of the 10 laboratory parameters were determined using the software solution Unity Real Time (Bio-Rad Laboratories, Plano, TX). In Unity Real Time, the bias for all 10 laboratory parameters at 2 concentration levels in the 3 observation periods was calculated with the following formula:

$$Bias = \frac{(Lab\ mean - Group\ mean) \cdot 100}{Group\ mean}$$

In this formula, "Lab mean" was the mean of our own IQC controls and "Group mean" was the mean of the homogeneous group of all other laboratories with the same

analytical method in Unity Real Time (ie, a consensus group that encompasses all laboratories using the exact same methodology, instrument, and reagents). To calculate the bias for the observation periods A, B, and C in Unity Real Time, we formulated the setting in such a way that the time used to calculate the bias in the Group mean was 6 months, and in the Lab mean it was exactly the time of the respective observation period (**Figure 1**).

In Unity Real Time, the CV for all 10 laboratory parameters at 2 concentration levels in the 3 observation periods was calculated with the following formula:

$$CV\% = \left(\frac{SD}{Lab\ mean}\right) \cdot 100\%$$

In this formula, "Lab mean" was the mean of our own IQC controls and "SD" was the corresponding SD of our own IQC controls. To calculate the CV for the observation periods A, B, and C in Unity Real Time, we formulated the setting in such a way that Lab mean and the corresponding SD referred exactly to the time of the respective observation period (**Figure 1**).

The RMI

As explained in the introduction, the RMI is the predicted P_H divided by the acceptable P_H:[11,12]

$$RMI = \frac{predicted\ P_H}{acceptable\ P_H}$$

The formula for calculating the predicted P_H is published elsewhere.[11,12] The acceptable P_H is derived from a 5-part scale for both the probability of the occurrence of unintended patient harm and the severity of that patient harm from CLSI EP23-A.[9,11] We determined the RMI values of all 10 laboratory parameters by using Mission Control 2. In the input screen of Mission Control 2, we had to fill in the following 7 fields for each laboratory parameter: We changed "QC Per Day" and "QC-Rules" in time course according to the study design (**Figure 1**). We did not change the inputs "Number of Patients," "*T*Ea," "Mean Time Between Failures in Days," "Severity of Harm," and "Probability of Harm Given an Unreliable Result" for the duration of the study (**Table 1**).

Detailed information on the RMI in general and how we calculated the RMI can be found in the Supplementary Material for this article.

Table 1. Input Variables for Mission Control 2 Necessary to Calculate RMI

	ND	TEa	MTBF	Severity of Harm	Acceptable P_H	$P_{h|u}$
Myoglobin	14	10%	90 days	Serious	0.0001	5%
NT-proBNP	22	20%	90 days	Critical	0.00001	5%
cTnT	40	18%	90 days	Critical	0.00001	5%
CK	27	5%	30 days	Serious	0.0001	5%
LDH	107	5%	30 days	Serious	0.0001	5%
Glucose	107	4%	30 days	Critical	0.00001	5%
Triglycerides	143	6%	6 days	Serious	0.0001	5%
Total cholesterol	139	6%	7 days	Serious	0.0001	5%
LDLC	52	6%	120 days	Serious	0.0001	5%
HDLC	105	6%	30 days	Serious	0.0001	5%

RMI, risk management index; ND, estimated number of patients who are run (on average) each day on the study analyzer; TEa, allowable total error; MTBF, mean time between failures; acceptable P_H, acceptable probability of harm; $P_{h|u}$, probability of harm given an unreliable result; NT-proBNP, N-terminal fragment of the pro B-type natriuretic polypeptide; cTnT, cardiac troponin T; CK, creatine kinase; LDH, lactate dehydrogenase; LDLC, low-density lipoprotein cholesterol; HDLC, high-density lipoprotein cholesterol.
Listed specifications for input variables remained unchanged for the duration of the study (input variables "QC Per Day" and "QC-Rules" not listed because both were changed during the study).

Table 2. Bias, CV, and RMI in the 3 Observation Periods

Parameter	IQC Level and Mean[a]	Period A			Period B			Period C		
		Bias	CV (%)	RMI	Bias	CV (%)	RMI	Bias	CV (%)	RMI
Myoglobin	1 → 47 ng/mL	+0.07	2.45	0.849	+3.69	2.02	0.070	+4.44	1.76	0.110
	2 → 84 ng/mL	−3.43	2.62		+0.68	1.80		+1.82	1.93	
NT-proBNP	1 → 121 pg/mL	+7.87	3.52	1.110	+10.94	3.62	7.980	+3.63	3.29	0.010
	2 → 284 pg/mL	+3.02	4.16		+5.18	3.61		+4.02	3.29	
cTnT	1 → 15 pg/mL	+3.31	5.26	0.817	+3.53	4.81	0.832	+4.27	5.51	2.680
	2 → 96 pg/mL	+4.49	2.23		+4.66	2.93		+2.66	3.38	
CK	1 → 77 U/L	+1.40	1.46	0.344	+1.65	1.24	0.109	+2.38	1.31	0.990
	2 → 614 U/L	+0.70	0.82		+0.64	0.69		+0.87	0.83	
LDH	1 → 127 U/L	−0.25	1.68	0.599	+0.00	1.27	0.014	+0.28	1.09	0.001
	2 → 420 U/L	−0.44	1.29		−0.50	1.00		−0.47	0.90	
Glucose	1 → 60 mg/dL	−0.31	0.94	0.342	−0.55	1.08	0.954	−0.94	0.98	1.260
	2 → 352 mg/dL	+0.02	0.91		−0.36	0.94		−0.44	0.97	
Triglycerides	1 → 98 mg/dL	−1.31	1.23	0.060	−1.24	1.17	0.003	-1.35	1.34	0.067
	2 → 207 mg/dL	−0.56	1.17		−0.53	0.87		−0.65	1.27	
Total cholesterol	1 → 111 mg/dL	−2.37	1.57	1.270	−2.42	1.20	0.075	-2.53	1.07	0.034
	2 → 268 mg/dL	−1.28	1.27		−1.16	0.93		-1.52	0.91	
LDLC	1 → 76 mg/dL	−4.11	0.83	3.820	−3.50	0.92	0.997	-2.99	0.75	0.026
	2 → 184 mg/dL	−3.72	0.96		−3.36	0.93		-2.68	0.90	
HDLC	1 → 21 mg/dL	−2.67	1.49	1.010	−1.75	2.11	7.860	-1.19	1.81	4.160
	2 → 51 mg/dL	−0.50	1.56		−1.12	2.18		-0.66	2.28	

[a]Group mean (i.e., mean of the homogeneous group in "Unity Real Time").
CV, coefficient of variation; RMI, risk management index; NT-proBNP, N-terminal fragment of the pro B-type natriuretic polypeptide; cTnT, cardiac troponin T; CK, creatine kinase; LDH, lactate dehydrogenase; LDLC, low-density lipoprotein cholesterol; HDLC, high-density lipoprotein cholesterol.

Statistics

For testing the study hypothesis, we chose an alpha error level of 0.025 (instead of the usual alpha error level of 0.05) because of the 1-sided testing of the hypothesis. For the statistical analysis, we used the Student t-test for dependent samples. We compared the RMI of the 10 laboratory parameters in observation period A with those in observation period C. The data set consisted of 10 pairs of RMI values that were compared. We used IBM SPSS Statistics Version 24 (IBM Germany, Ehningen, Germany) and MedCalc version 17.2 (MedCalc Software, Ostend, Belgium) for data entry and statistics.

Results

Table 2 lists the study results for all 10 study parameters in terms of bias, CV, and RMI. In observation period A, the

mean RMI was 1.022 (95% CI, 0.269–1.776). In observation period C, the mean RMI was 0.934 (95% CI, 0.088–1.956). The RMI values of observation period A and observation period C were not significantly different (paired *t*-test; *P* =.89). **Figure 2** shows the graphical presentation of the RMI for all 10 laboratory parameters in the 3 observation periods of the study.

Table 3 lists (i) in how many instances an IQC identified violations of the rejection rules applicable during the respective observation period (A, B, or C) and (ii) in how many cases the IQC could be brought back into the acceptable range by the respective technician who operated the device. During observation period A, there were 28 situations in which an IQC violated a rejection rule; in all 28 cases, the IQC could be brought back into the acceptable range by the technician who operated the device. During observation period B, there were 35 situations in which an IQC violated a rejection rule—in 33 cases the IQC could be brought back into the acceptable range by the technician, but in 2 cases it was not possible. During observation period C, there were 30 situations in which an IQC violated a rejection rule—in 26 cases the IQC could be brought back into the acceptable range by the technician, but in 4 cases it was not possible.

Discussion

The study hypothesis was that by tightening the IQC strategy—ie, by applying stricter rejection rules and by conducting IQC more frequently—the analytical quality would improve, represented by a smaller RMI. This hypothesis could not be confirmed with the available results. In principle, therefore, this is a study with negative results.

Although we did not find a global reduction in RMI across the 10 laboratory parameters, it is interesting to note (**Table 2**) that the change in RMI varied dramatically by assay, with some parameters showing a large reduction in RMI and others showing a large increase in RMI. In comparing the RMI values in observation period A and observation period C, we found that the RMI of 5 parameters decreased (myoglobin, NT-proBNP, LDH, total cholesterol, and LDLC) and that the RMI of 5 parameters increased (cTnT, CK, glucose, triglycerides, and HDLC). If we treated the RMI as a qualitative variable with a cutoff value of 1
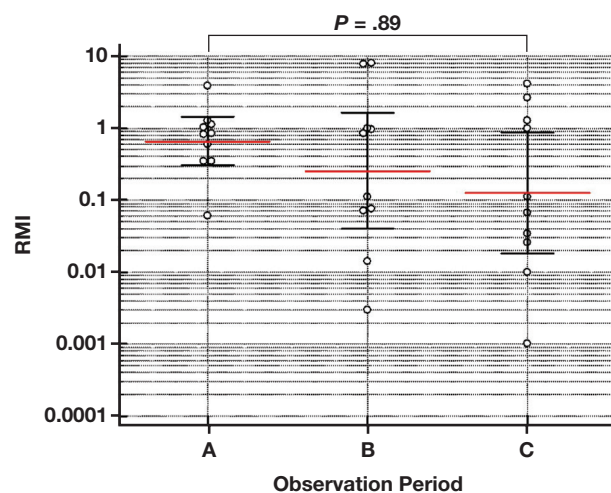
Figure 2

Graphical presentation of RMI for all 10 laboratory parameters in the 3 observation periods. All values plotted as open circles. Red horizontal lines indicate the mean RMI of each observation period and corresponding black whisker bars represent the 95% CI of the mean. RMI, risk management index; CI, confidence interval.

(ie, RMI ≤1, meaning that the capability and reliability of the respective measurement system combined with the IQC strategy of the laboratory maintains the risk of unintended patient harm at an acceptable level, and RMI >1, meaning that the laboratory has not reduced the risk of accidental patient harm to an acceptable level), then we found that 4 parameters remained in the same category after the study intervention (myoglobin, CK, LDH, and triglycerides), 3 parameters moved into the better category (NT-proBNP, total cholesterol, and LDLC), and 3 parameters shifted into the worse category (cTnT, glucose, and HDLC).

Because this is a study with negative results, a fundamental question arises as to whether a change in the IQC strategy in the clinical routine of a medical laboratory leads to a change in the RMI at all or whether perhaps the design of the present study was not optimal for addressing this question.

In our study we tried to establish a study plan that was as simple and comprehensible as possible for our research question. To test our study hypothesis, we tried to change only the IQC rules and the IQC schedule but otherwise keep all other variables necessary for the calculation of the RMI constant throughout the study. This effort was to ensure that

Table 3. Frequency of IQC-Identified Violations of Rejection Rule

Parameter	Period A		Period B		Period C	
	Number of cases in which IQC had violated a rejection rule	Number of cases in which IQC could be brought back into the acceptable range	Number of cases in which IQC had violated a rejection rule	Number of cases in which IQC could be brought back into the acceptable range	Number of cases in which IQC had violated a rejection rule	Number of cases in which IQC could be brought back into the acceptable range
Myoglobin	0		12	10	0	
NT-proBNP	3	3	0		0	
cTnT	0		0		3	3
CK	3	3	0		4	1
LDH	11	11	2	2	0	
Glucose	4	4	0		8	8
Triglycerides	2	2	10	10	5	5
Total cholesterol	2	2	4	4	2	2
LDLC	3	3	2	2	1	1
HDLC	0		5	5	7	6

IQC, internal quality control; NT-proBNP, N-terminal fragment of the pro B-type natriuretic polypeptide; cTnT, cardiac troponin T; CK, creatine kinase; LDH, lactate dehydrogenase; LDLC, low-density lipoprotein cholesterol; HDLC, high-density lipoprotein cholesterol.

only the impact of changing IQC rules and frequency on the RMI was evaluated.

It is of course possible that the theoretical assumptions of the IQC strategy described in the relevant scientific literature would be correct under very specific ideal conditions but would be so weakened in clinical routine, with all its deviations from ideal conditions, that the intended effect would be very small or even nonexistent. Possible reasons for the nonfunctioning of a tightened IQC strategy in clinical routine could theoretically include a batch change in reagents, a batch change in IQC (did not occur during this study), defective measuring instruments (did not occur during this study), or faulty work by the instrument operators.

However, an answer to the question of whether the tightening of an IQC strategy in clinical routine generally has no significant effect on the RMI cannot be determined with the available results. In this sense, the answer must be restricted to concluding that the 2 study-specific interventions (the replacement of rejection rules 1_{3s} and 2_{2s} by the rejection rule 1_{2s}-repeat and the change in the frequency of IQC—ie, the introduction of an additional daily IQC cycle) have produced a negative study result. Other interventions might have resulted in the study hypothesis being accepted.

In this study, the RMI was treated as a metric value (according to the formula on which it was based). Perhaps this approach should be reconsidered. To date, the literature has provided only sparse descriptions of how to use or interpret the RMI.[11,12] One could argue that the RMI should be treated as a qualitative value rather than a quantitative value. Further, it may make sense not to subject parameters with an RMI ≤1 to any change in the IQC strategy because the risk is acceptable anyway. It is thus possible that only those parameters with an RMI >1 should be subjected to a tightened IQC strategy (in this study, these would have been NT-proBNP, total cholesterol, LDLC, and HDLC). Furthermore, only 1 RMI was calculated for each analyte (Table 2), but the severity of harm and the probability of unintentionally harming patients could be different based on concentration level. Because Mission Control 2 does not allow this calculation, this restriction might be a limitation of our study.

Another possible limitation of our study is that we defined the TEa before starting the study by consensus. In laboratory medicine, TEa is a commonly used key figure that defines the quality requirements of a laboratory parameter with regard to the medical use of this parameter. There are no generally accepted limit values for TEa, but it is the task of laboratory management staff to determine the maximum analytical error that may occur for each laboratory

parameter without influencing medical decisions.[4-7,9] However, the criteria we used to define the TEa do not comply with some recent international consensus recommendations. For our study, the absolute value of TEa was not of primary importance because we used it as a "computing parameter" that was not changed during the entire study period. In addition, throughout the entire study period we did not use the TEa values as rejection rules.

Conclusion

The current study did not prove that applying stricter rejection rules and conducting IQC more frequently improves the RMI in the clinical routine of a medical laboratory. This is therefore a study with negative results. However, the results of this study are important because they provide indications for future studies on the topic. There is a great need to further explore the subject area with interventional studies to clarify how the RMI in the clinical routine of a medical laboratory can be measurably improved. **LM**

Acknowledgments

Supplementary Data

Supplemental figures and tables can be found in the online version of this article at www.labmedicine.com.

References

1. Hallworth MJ, Epner PL, Ebert C, et al.; IFCC Task Force on the Impact of Laboratory Medicine on Clinical Management and Outcomes. Current evidence and future perspectives on the effective practice of patient-centered laboratory medicine. *Clin Chem.* 2015;61(4):589–599.

2. Libby P, King K. Biomarkers: a challenging conundrum in cardiovascular disease. *Arterioscler Thromb Vasc Biol.* 2015;35(12):2491–2495.

3. Plebani M, Laposata M, Lippi G. A manifesto for the future of laboratory medicine professionals. *Clin Chim Acta.* 2019;489:49–52.

4. Badrick T. Quality leadership and quality control. *Clin Biochem Rev.* 2003;24(3):81–93.

5. Westgard JO. Managing quality vs. measuring uncertainty in the medical laboratory. *Clin Chem Lab Med.* 2010;48(1):31–40.

6. Burnett D, Ceriotti F, Cooper G, Parvin C, Plebani M, Westgard J. Collective opinion paper on findings of the 2009 convocation of experts on quality control. *Clin Chem Lab Med.* 2010;48(1):41–52.

7. CLSI C24-Ed4. *Statistical Quality Control for Quantitative Measurement Procedures: Principles and Definitions.* 4th ed. Wayne, PA: Clinical and Laboratory Standards Institute; 2016.

8. Parvin CA. Planning statistical quality control to minimize oatient risk: it's about time. *Clin Chem.* 2018;64(2):249–250.

9. CLSI EP23-A. *Laboratory Quality Control Based on Risk Management*. Wayne, PA: Clinical and Laboratory Standards Institute; 2011.

10. Parvin CA. What's new in laboratory statistical quality control guidance? The 4th edition of CLSI C24, statistical quality control for quantitative measurement procedures: principles and definitions. *J Appl Lab Med* 2017;1(5):581–584.

11. Yundt-Pacheco JC, Parvin CA. Computing a risk management index: correlating a quality control strategy to patient risk. *Clin Chem* 2017;63:s227–s228.

12. Parvin CA, Baumann NA. Assessing quality control strategies for HbA1c measurements from a patient risk perspective. *J Diabetes Sci Technol.* 2018;12(4):786–791.

13. Parvin CA, Kuchipudi L, Yundt-Pacheco JC. Should I repeat my 1:2s QC rejection? *Clin Chem.* 2012;58(5):925–929.

Comparison of Serum Free and Bioavailable 25-Hydroxyvitamin D Levels in Alzheimer's Disease and Healthy Control Patients

Esra Ertilav, MD,[1,] Nur Ebru Barcin, MD,[2] Sebahat Ozdem, MD[3]*

ABSTRACT

Objective: Many studies have investigated lower 25-hydroxyvitamin D (25[OH]D) levels in patients with Alzheimer's disease (AD) compared with those in control patients. In the present study, we aimed to evaluate serum free and bioavailable 25(OH)D levels in patients with AD and in healthy control patients.

Methods: The AD group consisted of 85 patients aged >60 years who were diagnosed with possible AD according to National Institute on Aging-Alzheimer's Association criteria and 85 healthy control patients. Serum levels of total 1,25-dihydroxyvitamin D, total 25(OH)D, vitamin D binding protein (VDBP), parathormone, calcium, phosphorus and albumin, free 25(OH)D, bioavailable 25(OH)D, and the bioavailable 25(OH)D/total 25(OH)D ratio were compared in both groups.

Results: Total 25(OH)D, free 25(OH)D, bioavailable 25(OH)D, and the bioavailable 25(OH)D/total 25(OH)D ratio were significantly lower (P <.001, P <.001, P <.001, P <.05, respectively) in the AD group, whereas the VDBP level was significantly higher (P <.05) in the AD than in the control group.

Conclusion: Free and bioavailable 25(OH)D detected at lower levels in patients with AD limit the target central effects of 25(OH)D; this result suggests that reduced levels of the active free form of vitamin D may be a risk factor for AD and dementia.

Keywords: Alzheimer's disease, free 25-hydroxyvitamin D, bioavailable 25-hydroxyvitamin D, cognitive impairment, dementia, vitamin D binding protein

Alzheimer's disease (AD) is a neurodegenerative disease that is the most common cause of dementia.[1] Accounting for 60% to 80% of all dementias,[2] AD is a chronic degenerative and inflammatory brain disorder that leads to inflammation, oxidative injury, neuronal dysfunction, and loss that is linked to the accumulation of fragments amyloid beta fragments (Aβ) and tau protein derivatives.[3]

Vitamin D is a steroid hormone that plays a role in calcium homeostasis, bone mineralization, and immune system

Abbreviations

25(OH)D, 25-hydroxyvitamin D; AD, Alzheimer's disease; VDBP, vitamin D binding protein; Aβ, amyloid beta fragments; 1,25(OH)2D, 1,25-dihydroxyvitamin D; MMSE, Mini Mental State Examination; PTH, parathormone; CV, coefficient of variation; ELISA, enzyme-linked immunosorbent assay; SD, standard deviation.

[1]Department of Neurology, Adnan Menderes University Faculty of Medicine, Aydın, Turkey, [2]Department of Neurology, and [3]Department of Biochemistry, Akdeniz University Faculty of Medicine, Antalya, Turkey

*To whom correspondence should be addressed.
eertilav@gmail.com

differentiation. It is synthesized in the skin by the effect of sunlight from 7-dehydrocholesterol, which is the precursor of cholesterol. Taken from the skin by synthesis or diet, vitamin D binds to the vitamin D binding protein (VDBP) and is transported to the liver, where its 25-hydroxylation occurs with cytochrome P450 enzymes (CYP27A1, CYP2J2, CYP3A4). The main circulating metabolite of vitamin D is 25(OH)D.[4]

In the kidneys, 25(OH)D is rehydroxylated with the other cytochrome P450 enzyme, CYP27B1, and the synthesis of the biologically active form 1,25 dihydroxyvitamin D (1,25[OH]2D) occurs.[5] Renal synthesis of this biologically active form is regulated by whether 25(OH)D is bound to VDBP. The uptake of 25(OH)D-bounded VDBP into renal proximal tubule cells is mediated by the endocytic receptor megalin. In the absence of megalin, the free form of 25(OH)D and 1,25(OH)2D enters the target cell by diffusion. Although vitamin D bounded to VDBP is taken up by megalin in the proximal tubule, the physiological importance of the free form in intestinal absorption is even more

prominent. In this case, the level of free vitamin D may be very important for the efficiency of biologically active vitamin D for calcium and phosphate homeostasis and for other important functions such as anti-inflammatory and immunomodulatory effects.

The optimal level of 25(OH)D is unknown; this level is influenced by factors such as binding proteins, vitamin D receptor genetic polymorphisms, and metabolic enzymes. Therefore, 25(OH)D serum levels are insufficient to measure vitamin D activity, but it is important to evaluate them together with free-form and binding proteins.[6-8]

Although the primary function of vitamin D is known to be the maintenance of calcium and phosphate homeostasis, other functions of vitamin D include anti-inflammatory and immunomodulatory effects, control of cell growth, differentiation and apoptosis, and defense against tumorigenesis.[9] Oxidative stress, inflammation, and neuronal calcium signaling defects are known to play an important role in the pathogenesis of AD. Vitamin D shows an anti-inflammatory effect via apolipoprotein A1 and the proinflammatory cytokine tumor necrosis factor-alpha.[10] It protects the brain from oxidative stress by reducing the formation of reactive oxygen species with its antioxidant effect through nitric oxide synthase and glutamyl transpeptidase.[11]

The interaction of vitamin D with Aβ, which is at the center of AD pathology, has made vitamin D an attractive molecule in the pathophysiology of AD.[12] Vitamin D and its metabolites show neuroprotective effects by inhibiting the abnormal accumulation of amyloid fibrils that are responsible for the pathogenesis of AD via amyloid phagocytosis and clearance and by regulating the activation of the phosphatase-2A enzyme that dephosphorylates the tau protein.[13,14] Vitamin D receptors are expressed in several regions of the brain that play a key role in cognition—primarily in the hippocampus, but also in the prefrontal cortex, cingulate gyrus, caudate-putamen, thalamus, substantia nigra, hypothalamus, lateral geniculate ganglion, and cerebellum.[15]

In the present study, our objective was to draw attention particularly to the levels of the effective form of 25(OH)D in AD by measuring serum levels of free and bioavailable 25(OH)D in patients with AD and healthy volunteers.

Materials and Methods

Study Design and Participants

The study was performed in the Neurology Outpatient Clinic of Akdeniz University, Faculty of Medicine in Antalya, Turkey. After informed consent, all participants were routinely examined at the Neurology Outpatient Clinic and evaluated in terms of inclusion and exclusion criteria. Eighty-five patients who were diagnosed with AD according to the National Institute on Aging-Alzheimer's Association criteria (AD group) who were evaluated using the Mini Mental State Examination (MMSE) and 85 control patients with normal cognitive function (control group) were included in the study. Patients with severe depression, other medical or neurological conditions (eg, seizures, stroke, head trauma) that would cause cognitive impairment were excluded from the study, as were those with renal and/or hepatic impairment and those with malignancies.

Demographic data, examination findings, medications (including anticholinesterases and preparations containing calcium and vitamin D), and concomitant diseases of the participants were recorded. Neurocognitive tests were performed in a quiet room so as not to distract the patients. The MMSE was used to evaluate cognitive areas such as place-time orientation, recording memory, attention and calculation, anterograde and retrograde memory, verbal fluency, language and visuospatial abilities, clock-drawing, perceptual abilities, recall, and recognition.

Patients with AD were divided into stages according to their MMSE scores: MMSE scores between 20 and 24 were considered as early-stage dementia, scores between 10 and 19 were considered as intermediate-stage dementia, and scores between 0 and 9 were considered as advanced-stage dementia.

Blood Specimens and Serum Investigations

Venous blood specimens of the participants were collected into Becton-Dickinson serum separator tubes (Becton-Dickinson, Franklin Lakes, NJ). Serum was separated by centrifuging the specimens at 4°C at 4000 rpm for 4 minutes and storing them at –80°C until analysis. Serum levels of total 25(OH)D, total 1,25(OH)2D, VDBP, parathormone (PTH),

calcium, phosphorus, and albumin were measured in all patients.

Serum total 25(OH)D levels were measured by chemilumin-escence immunoassay with the Siemens Centaur XP device (Siemens Healthcare Diagnostics, Forchheim, Germany). Intra- and inter-assay coefficients of variations (CV) of the 25(OH) vitamin D3 ELISA kit were 3.9% (control value: 46.1 ng/mL) and 6.1% (control value: 46.1 ng/mL), respec-tively. The minimal detectable serum 25(OH) vitamin D3 level was 4.2 ng/mL.

Serum PTH levels were measured by chemilumines-cence immunoassay with the Siemens Centaur XP device (Siemens Healthcare Diagnostics, Forchheim, Germany). The minimal detectable limit of the PTH kit was 2.5 pg/mL. Intra- and inter-assay CVs of the PTH kit were both 4.3% with the same control value of 107.6 pg/mL.

Serum calcium levels were measured by the spectro-photometric method using the Siemens Advia Chemistry XP device (Siemens Healthcare Diagnostics, Forchheim, Germany) based on the measurement of the colored com-pound formed by calcium ions with an arsenazo III reagent. The minimal detectable serum calcium level was 0.9 mg/dL. Intra- and inter-assay CVs of the calcium kit were 0.6% (control value: 8.9 mg/dL) and 0.9% (control value: 8.9 mg/dL), respectively.

Serum phosphorus levels were measured using the spectro-photometric method, based on the principle that phosphorus ions form phosphomolybdate complex with molybdate in a sulfuric acid medium, using the Siemens Advia Chemistry XP autoanalyzer (Siemens Healthcare Diagnostics, Forchheim, Germany). Intra- and inter-assay CVs of the phosphorus kit were 0.6% (control value: 2.31 mg/dL) and 0.4% (control value: 2.31 mg/dL), respectively. The minimal detectable serum phosphorus level was 0.3 mg/dL.

Serum albumin was measured by the bromocresol green dye-binding method using the Siemens Advia 2400 autoanalyzer (Siemens Healthcare Diagnostics, Forchheim, Germany). The minimal detectable serum albumin level was 1.0 g/dL. Intra- and inter-assay CVs of the albumin kit were 1.8% (control value: 2.3 g/dL) and 0.6% (control value: 3.6 g/dL), respectively.

Serum 1,25(OH)2D levels were measured using the enzyme-linked immunosorbent assay (ELISA) method with a kit specific for recombinant human 1,25(OH)2D (Elabscience Biotechnology Co, Ltd, Hubei Province, China). Intra- and inter-assay CVs of the kit (catalog number E-EL-0016; lot number AK0017APR17020) were <10% for both. The min-imal detectable serum 1.25(OH)2D level was 4.7 pg/mL. The kit was stored at 2°C to 8°C until use.

Serum vitamin D binding protein levels were measured using ELISA with a recombinant human vitamin D binding protein–specific kit (Elabscience Biotechnology Co, Ltd, Hubei Province, China). The intra- and inter-assay CVs of the kit (catalog number E-EL-H1604; lot number AK0017APR17021) were <10% for both. The minimal detectable limit of the vitamin D binding protein level was 2.35 ng/mL. The kit was stored at 2°C to 8°C until use.

Free and bioavailable 25(OH)D levels in serum were calcu-lated using the formula by Bikle et al[16]:

$$\text{Free 25(OH)D} = \frac{\text{Total 25(OH)D}}{1 + (6 \times 10^5 \times [\text{albumin}]) + (7 \times 10^8 \times [\text{DBP}])}$$

$$\text{Bioavailable 25(OH)D} = (6 \times 10^5 \times [\text{albumin}] + 1) \times \text{free 25(OH)D}$$

$$[\text{Albumin}]: \text{Serum albumin in g/L} \div 66,430 \text{ g/mol}$$
$$[\text{DBP}]: \text{Serum DBP in g/L} \div 58,000 \text{ g/mol}$$

Statistical Analysis

Descriptive statistics were presented as frequency, per-centage, mean, standard deviation (SD), median, and min-imum and maximum values. Results of measured parameters were given as mean ± SD. Fisher's exact or Pearson χ^2 tests were used to analyze categorical data. Normality assump-tion was evaluated using the Kolmogorov-Smirnov test. The difference between the groups was analyzed using the independent-samples *t*-test for normally distributed vari-ables and the Mann-Whitney *U* test for variables that were not normally distributed. The Kruskal-Wallis test was used to analyze the difference in free, bioavailable, and total 25(OH)D levels of patients with AD in different stages of the disease. All analyses were performed with SPSS Version 23.0. We considered *P* <.05 statistically significant.

Table 1. Demographic Characteristics of Groups

		Groups			
		Control Patients		Patients	
		n	%	n	%
Sex	Female	40	47.1	50	58.8
	Male	45	52.9	35	41.2
Age, y	Mean	70.16		75.54	
	Minimum–maximum	(61–84)		(60–99)	
Disease stage	Early stage			44	51.8
	Intermediate stage			26	30.6
	Advanced stage			15	17.6
Drugs used	Ginkgo biloba			3	3.6
	Donepezil			26	31.0
	Donepezil + memantine			29	34.5
	Rivastigmine			9	10.7
	Rivastigmine + memantine			17	20.2
Vitamin D replacement (6000 IU/d)	No	61	71.8	65	76.5
	Yes	24	28.2	20	23.5

Results

The mean ages of the AD and control groups were 75.46 ± 8.66 and 70.16 ± 6.06 years, respectively. Among patients, 31% were using donepezil, 10.7% were using rivastigmine, 20.2% were using rivastigmine plus memantine, 34.5% were using donepezil plus memantine, and 3.6% were using ginkgo biloba. Both patients in the AD group (23.5%) and patients in the control group (28.2%) were receiving vitamin D replacement at 6000 IU/day (P =.484). Demographic characteristics of both groups are shown in **Table 1**.

Serum levels of measured biochemical parameters are shown in **Table 2**. Serum 25(OH)D levels were significantly higher (23.9 ± 12.7 ng/mL) in the control group compared with the AD group (16.8 ± 12.0 ng/mL; P <.001). However, in the control group there was no significant difference in 25(OH)D levels between women (19.8 ± 13.8 ng/mL) and men (21.0 ± 11.7 ng/mL; P =.208). In the AD group, 25(OH)D levels were 16.5 ± 13.5 ng/mL in women and 17.3 ± 9.7 ng/mL in men (P =.251); 70.6% of patients in the AD group and 41.2% of patients in the control group had 25(OH)D deficiency (vitamin D deficiency was defined as a serum concentration <20 ng/mL based on the cut off of the kit).

When 25(OH)D levels of patients with AD in different stages of disease were analyzed, we found that 25(OH)D levels were 18.6 ± 13.4 ng/mL in the early-stage AD group,

14.9 ± 10 ng/mL in the intermediate-stage AD group, and 15.0 ± 10.6 ng/mL in the advanced-stage AD group. There were no significant correlations between disease stages and 25(OH)D levels (P =.278).

The VDBP levels were significantly higher (P =.035) in the AD group (192.6 ± 151.1 µg/mL) compared with the control group (146.5 ± 129.6 µg/mL). However, 1,25(OH)2D levels were similar (P = .689) in both the AD and the control groups (72.6 ± 37.1 pg/mL vs 71.1 ± 39.7 pg/mL, respectively).

There were significant differences in the levels of free 25(OH)D and bioavailable 25(OH)D and the bioavailable 25(OH)D/total 25(OH)D ratios between the groups; free 25(OH)D (9.4 ± 9.3 pg/mL) and bioavailable 25(OH)D (3.6 ± 3.7 ng/mL) levels in the AD group were significantly low (P <.001 for both) as compared with those in the control group (17.8 ± 14.8 pg/mL and 6.9 ± 5.9 ng/mL, respectively). Bioavailable 25(OH)D/total 25(OH)D ratios were also significantly low (P =.041) in patients with AD compared with control patients (0.2 ± 0.2 vs 0.3 ± 0.2 in AD and control groups, respectively).

Whereas 25(OH)D levels in study participants receiving vitamin D replacement were 21.5 ± 9.4 ng/mL, they were 20.0 ± 13.8 ng/mL in those not receiving vitamin D replacement. However, there was no significant difference (P =.155) between the AD and control groups.

Table 2. Results of Biochemical Parameters in Patient and Control Groups (N = 85 in each group)

		Mean	SD	Median	Minimum	Maximum	P Value
Calcium (mg/dL)	Control	9.2	0.7	9.3	6.4	10.9	.738
	Patient	9.2	0.6	9.3	6.8	10.5	
Phosphorus (mg/dL)	Control	3.5	0.7	3.4	0.5	5.2	.645
	Patient	3.5	0.6	3.6	1.9	4.7	
Albumin (g/dL)	Control	4.2	0.5	4.3	2.6	5	.520
	Patient	4.2	0.4	4.3	3.0	5.0	
1,25(OH)2D (pg/mL)	Control	71.1	39.7	60.5	20.9	217.7	.689
	Patient	72.6	37.1	62.7	23.6	186.1	
VDBP (µg/mL)	Control	146.5	129.6	103.5	2.3	512.3	.035
	Patient	192.6	151.1	145.6	9.7	521.7	
25(OH)D (ng/mL)	Control	23.9	12.7	23.5	5.6	70.4	<.001
	Patient	16.8	12.0	13.0	4.4	78.1	
PTH (pg/mL)	Control	59.3	37.6	49.0	8.6	201.9	.803
	Patient	63.8	52.9	51.7	8.7	411.4	
Free 25(OH)D (pg/mL)	Control	17.8	14.8	13.8	1.2	82.1	<.001
	Patient	9.4	9.3	7.0	1.1	58.8	
Bioavailable 25(OH)D (ng/mL)	Control	6.9	5.9	5.7	0.4	36.0	<.001
	Patient	3.6	3.7	2.6	0.4	24.1	
Bioavailable 25(OH)D/total 25(OH)D ratio	Control	0.3	0.2	0.2	0.06	0.9	.041
	Patient	0.2	0.2	0.2	0.05	0.7	

SD, standard deviation; 1,25(OH)D, 1,25 dihydroxyvitamin D; VDBP, vitamin D binding protein; 25(OH)D, 25-hydroxyvitamin D; PTH, parathormone.

Serum calcium, phosphorus, albumin, and PTH levels did not differ significantly between the groups ($P > .05$) (**Table 2**).

Discussion

In the present study, we found that serum total 25(OH)D, free 25(OH)D, and bioavailable 25(OH)D levels and the bioavailable 25(OH)D/total 25(OH)D ratio were significantly lower in patients with AD than in control patients. However, VDBP levels were significantly higher in the AD group than in the control group. Although 25(OH)D levels were significantly lower in patients with AD as compared with control patients, we did not find a significant relationship in 1,25(OH)2D, the active form of vitamin D, between the AD and the control groups. In contrast to previous studies, in the present study we used several biochemical parameters including 25(OH)D and the active form 1,25(OH)2D, the free and bioavailable forms of vitamin D, and the binding protein, which limits the effectiveness of free hormone levels.

Previous studies have shown a correlation between AD and low vitamin D levels. Vitamin D has been shown to play a role in the etiopathogenesis of AD through different mechanisms: by regulating calcium-sensitive receptor expression, increasing clearance of amyloid beta peptides, decreasing and regulating matrix metalloproteinases, increasing heme oxygenase 1, regulating oxidative stress and neurotransmission, and modulating immune and inflammatory processes, ultimately improving cognitive functions.[17-20]

It is estimated that approximately 50% of the adult population has vitamin D deficiency in the world globally. Previous studies have shown that serum total vitamin D levels were lower than normal in approximately 70%–90% of patients with AD.[21,22] In the present study, we also found 25(OH)D deficiency in 70.6% in our group of patients with AD and in 41.2% of our control patients.

We found no significant difference in levels of 1,25(OH)2D, the active form of vitamin D, between patients with AD and control patients. Many tissues express 1α-hydroxylase and can locally convert circulating 25(OH)D into its active form. Therefore, it is possible that total or free 1.25(OH)2D levels in circulation are not good indicators of vitamin D efficacy.[23] This consideration is also supported by the findings of our study. In previous studies, 25(OH)D was found to be the best indicator of the depot form of vitamin D in the liver.[24]

In the present study, VDBP levels were found to be increased in the AD group compared with the control group. Because VDBP binds vitamin D, the increase in its levels reduces the effective free fraction of vitamin D. In this case, hormone activity decreases as the free form decreases even if there is sufficient vitamin D in serum. Formulas for calculating bioavailable 25(OH)D have been developed in previous studies. However, these methods define the bioavailable hormone as both the free and the albumin-bound fraction; that is, the fraction not bound to circulating binding proteins such as VDBP.[25] We calculated serum levels of free 25(OH)D and bioavailable 25(OH)D and the bioavailable 25(OH)D/total 25(OH)D ratio based on this information and found that they all were significantly lower in patients with AD. These findings suggest that even if serum total vitamin D concentrations are sufficient, vitamin D may not be effective if the levels of its free form are low.

Some studies have shown that cerebrospinal fluid VDBP levels are increased in patients with AD.[16,26] Others have also shown that VDBP injected into mice limits the biological activity of 1,25(OH)2D.[27,28] Therefore, the increased levels of VDBP in the patients with AD in our study are in agreement with previous studies and support the view that such increased levels of VDBP may limit the effects of the free and effective forms of vitamin D. Although it has been reported that the normal serum levels of VDBP are slightly higher in women than in men,[29] we could not show a significant difference in VDBP levels depending on sex in the present study. Because all of the female patients with AD and female control patients included in our study were in the postmenopausal period, this finding may be attributed to the effects of estrogen on VDBP levels.

Although many studies conducted to show a correlation between cognitive impairment and vitamin D deficiency have shown lower levels of 25(OH)D in patients with AD compared with those in age-matched healthy control patients, free 25(OH)D that corresponds to the effective forms of vitamin D and bioavailable 25(OH)D and the bioavailable 25(OH)D/total 25(OH)D ratio have not been studied before. In the present study, by studying 1,25(OH)2D, VDBP, bioavailable 25(OH)D, and the bioavailable 25(OH)D/total 25(OH)D ratio in addition to 25(OH)D we have provided evidence in support of the view that the effective form of vitamin D is lower in patients with AD compared with that in control patients.

We found no significant relationship between vitamin D levels and sex. There are contradicting results in the literature; although the majority of studies investigating the relationship between vitamin D levels and cognitive functions have reported sex differences,[30–32] some studies have argued that sex differences were not important.[33,34] Although the reasons for these conflicting results are not clear, factors such as lifestyle and sociocultural factors of the participants and the locations where different studies were performed may have some role in the observed findings.

Neurotrophic, neuroprotective, and neuromodulating effects of vitamin D are well known. In considering the effect of vitamin D deficiency in the etiopathogenesis of AD, one can argue that vitamin D deficiency may be a risk factor in the development of AD and dementia because it may be more common in the geriatric population because of poor dietary intake, malabsorption, and difficulty in oral intake. Therefore, it can be proposed that follow-up of serum vitamin D levels and vitamin D replacement in patients with vitamin D deficiency may improve cognitive function and protect against dementia.

Conclusion

We showed that serum 25(OH)D, free25(OH)D, and bioavailable 25(OH)D levels were lower in patients with AD. We also found increased VDBP levels in these patients compared to control patients. Increased VDBP may reduce the bioavailability of vitamin D by reducing the levels of the free and effective forms of vitamin D. Taken together, our findings suggest that vitamin D efficacy may be limited in patients with AD because of reduction in serum vitamin D including the serum free and bioavailable hormone levels, which are the effective forms of vitamin D. Findings of the present study also suggest that serum 1,25(OH)2D levels are not a good indicator of vitamin D activity, whereas the levels of free and bioavailable 25(OH)D may be more accurate measures of active and effective vitamin D. Long-term follow-up studies measuring baseline vitamin D levels (total, free, bioavailable 25[OH]D) in healthy control patients without dementia together with those assessing cognitive status in patients receiving replacement therapy for vitamin D deficiency may shed light on our findings. **LM**

Acknowledgments

References

1. Ballard C, Gauthier S, Corbett A, Brayne C, Aarsland D, Jones E. Alzheimer's disease. *Lancet.* 2011;377(9770):1019–1031.

2. Alzheimer's Association. 2014 Alzheimer's disease: facts and figures. *Alzheimer's Dement.* 2014;10(2):47–92.

3. Querfurth HW, LaFerla FM. Alzheimer's disease. *N Engl J Med.* 2010;362(4):329–344.

4. Deeb KK, Trump DL, Johnson CS. Vitamin D signalling pathways in cancer: potential for anticancer therapeutics. *Nat Rev Cancer.* 2007;7(9):684–700.

5. Eyles DW, Smith S, Kinobe R, Hewison M, McGrath JJ. Distribution of the vitamin D receptor and 1 alpha-hydroxylase in human brain. *J Chem Neuroanat.* 2005;29(1):21–30.

6. Nykjaer A, Dragun D, Walther D, et al. An endocytic pathway essential for renal uptake and activation of the steroid 25-(OH) vitamin D3. *Cell.* 1999;96(4):507–515.

7. Chun RF, Peercy BE, Orwoll ES, Nielson CM, Adams JS, Hewison M. Vitamin D and DBP: the free hormone hypothesis revisited. *J Steroid Biochem Mol Biol.* 2014;144(Pt A):132–137.

8. Landela V, Annweiler C, Millet P, Morello M, Féron F. Vitamin D, cognition and Alzheimer's disease: the therapeutic benefit is in the D-tails. *J Alzheimers Dis.* 2016;53(2):419–444.

9. Vuolo L, Di Somma C, Faggiano A, Colao A. Vitamin D and cancer. *Front Endocrinol (Lausanne).* 2012;3:58.

10. John WG, Noonan K, Mannan N, Boucher BJ. Hypovitaminosis D is associated with reductions in serum apolipoprotein A-I but not with fasting lipids in British Bangladeshis. *Am J Clin Nutr.* 2005;82(3):517–522.

11. Alvarez JA, Chowdhury R, Jones DP, et al. Vitamin D status is independently associated with plasma glutathione and cysteine thiol/disulphide redox status in adults. *Clin Endocrinol (Oxf).* 2014;81(3):458–466.

12. Gezen-Ak D, Yılmazer S, Dursun E. Why vitamin D in Alzheimer's disease? The hypothesis. *J Alzheimers Dis.* 2014;40(2):257–269.

13. Mizwicki MT, Liu G, Fiala M, et al. 1α, 25-dihydroxyvitamin D3 and resolvin D1 retune the balance between amyloid-β phagocytosis and inflammation in Alzheimer's disease patients. *Alzheimer's Dis.* 2013;34(1):155–170.

14. Briones TL, Darwish H. Decrease in age-related tau hyperphosphorylation and cognitive improvement following vitamin D supplementation are associated with modulation of brain energy metabolism and redox state. *Neuroscience.* 2014;262(2014):143–155.

15. Beydoun MA, Ding EL, Beydoun HA, Tanaka T, Ferrucci L, Zonderman AB. Vitamin D receptor and megalin gene polymorphisms and their associations with longitudinal cognitive change in US adults. *Am J Clin Nutr.* 2012;95(1):163–178.

16. Bikle DD, Gee E, Halloran B, Kowalski MA, Ryzen E, Haddad JG. Assessment of the free fraction of 25-hydroxyvitamin D in serum and its regulation by albumin and the vitamin D-binding protein. *J Clin Endocrinol Metab.* 1986;63(4):954–959.

17. Annweiler C, Allali G, Allain P, et al. Vitamin D and cognitive performance in adults: a systematic review. *Eur J Neurol.* 2009;16(10):1083–1089.

18. Etgen T, Sander D, Bickel H, Sander K, Förstl H. Vitamin D deficiency, cognitive impairment and dementia: a systematic review and meta-analysis. *Dement Geriatr Cogn Disord.* 2012;33(5):297–305.

19. Littlejohns TJ, Henley WE, Lang IA, et al. Vitamin D and the risk of dementia and Alzheimer disease. *Neurology.* 2014;83(10):920–928.

20. Afzal S, Bojesen SE, Nordestgaard BG. Reduced 25-hydroxyvitamin D and risk of Alzheimer's disease and vascular dementia. *Alzheimers Dement.* 2014;10(3):296–302.

21. Knekt P, Sääksjärvi K, Järvinen R, et al. Serum 25-hydroxyvitamin D concentration and risk of dementia. *Epidemiology.* 2014;25(6):799–804.

22. Annweiler C, Beauchet O. Vitamin D-mentia: randomized clinical trials should be the next step. *Neuroepidemiology.* 2011;37(3–4):249–258.

23. Bischoff-Ferrari HA. "Vitamin D–why does it matter?"–defining vitamin D deficiency and its prevalence. *Scand J Clin Lab Invest Suppl.* 2012;72(sup243):3–6.

24. van Driel M, Koedam M, Buurman CJ, et al. Evidence for auto/paracrine actions of vitamin D in bone: 1 alpha-hydroxylase expression and activity in human bone cells. *FASEB J.* 2006;20(13):2417–2419.

25. Holick MF. Vitamin D deficiency. *N Engl J Med.* 2007;357(3):266–281.

26. Abdi F, Quinn JF, Jankovic J, et al. Detection of biomarkers with a multiplex quantitative proteomic platform in cerebrospinal fluid of patients with neurodegenerative disorders. *J Alzheimers Dis.* 2006;9(3):293–348.

27. Zhang J, Sokal I, Peskind ER, et al. CSF multianalyte profile distinguishes Alzheimer and Parkinson diseases. *Am J Clin Pathol.* 2008;129(4):526–529.

28. Safadi FF, Thornton P, Magiera H, et al. Osteopathy and resistance to vitamin D toxicity in mice null for vitamin D binding protein. *J Clin Invest.* 1999;103(2):239–251.

29. Chun RF, Lauridsen AL, Suon L, et al. Vitamin D-binding protein directs monocyte responses to 25-hydroxy- and 1.25-dihydroxyvitamin D. *J Clin Endocrinol Metab.* 2010;95(7):3368–3376.

30. Bouillon R, van Baelen H, de Moor P. The measurement of the vitamin D-binding protein in human serum. *J Clin Endocrinol Metab.* 1977;45(2):225–231.

31. Lee DM, Tajar A, Ulubaev A, et al.; EMAS study group. Association between 25-hydroxyvitamin D levels and cognitive performance in middle-aged and older European men. *J Neurol Neurosurg Psychiatry.* 2009;80(7):722–729.

32. Slinin Y, Paudel ML, Taylor BC, et al.; Osteoporotic Fractures in Men (MrOS) Study Research Group. 25-Hydroxyvitamin D levels and cognitive performance and decline in elderly men. *Neurology.* 2010;74(1):33–41.

33. Annweiler C, Schott AM, Allali G, et al. Association of vitamin D deficiency with cognitive impairment in older women: cross-sectional study. *Neurology.* 2010;74(1):27–32.

34. Chei C, Raman P, Yin Z, et al. Vitamin D levels and cognition in the elderly population in China. *Am Geriatr Soc.* 2014;62(11):2125–2129.

Association of Mild Hyperbilirubinemia with Decreased ECG-Based Ventricular Repolarization Parameters in Young Men

Cihan Sengul, MD,[1*] Ahmet Sen, MD,[2] Suleyman Barutcu, MD,[1] Cayan Cakir, MD,[1] Remzi Sarikaya, MD[1]

ABSTRACT

Objective: Hyperbilirubinemia is associated with protection against various oxidative stress-mediated diseases. We aimed to investigate the association between bilirubin and novel electrocardiography (ECG)-based ventricular repolarization parameters.

Methods: We enrolled 201 healthy men with mild hyperbilirubinemia (group 1) and 219 healthy men with normal bilirubin levels (group 2). The Tpeak-Tend (Tp-e) interval (defined as the interval from the peak of the T wave to the end of the T wave), corrected (c) Tp-e interval, QT interval, cQT interval, and Tp-e interval/QT interval ratio were measured from leads V_5 and V_6 with 20 mm/mV amplitude and 50 mm/second rate.

Results: The Tp-e interval, cTp-e interval, and Tp-e interval/QT interval ratio were significantly lower in group 1 compared with group 2. The cTp-e interval showed a significant negative correlation with total bilirubin, conjugated bilirubin, and unconjugated bilirubin. The cTp-e interval (odds ratio [OR], 0.900; $P =.002$) and Tp-e interval/QT interval ratio (OR, 0.922; $P =.04$) were significantly associated with mild hyperbilirubinemia.

Conclusion: We showed the association of mild hyperbilirubinemia with decreased novel ECG-based ventricular repolarization parameters.

Keywords: bilirubin, Tp-e interval, Tp-e interval/QT interval ratio, QT interval, ventricular arrhythmia, ECG

Bilirubin, the final product of hemoglobin catabolism, was considered a threatening sign of an underlying liver and gallbladder diseases for years. However, recent data suggest that it is also a potent endogenous antioxidant because of a system of conjugated double bonds within its molecule.[1,2] There is growing evidence that bilirubin concentrations are associated with protection against various oxidative stress-mediated diseases, including cardiovascular diseases, diabetes, certain cancers, and autoimmune diseases.[3,4] In addition to the aforementioned diseases, accumulating evidence suggests a link between oxidative processes and cardiac arrhythmias.[5,6] In contrast to emerging data about the relationship of bilirubin with atrial fibrillation (AF) and with predictors of AF,[7-9] clinical trials studying the association of bilirubin with ventricular arrhythmia are limited.

In the past 2 decades, some ventricular repolarization markers have been found to be useful to predict arrhythmias, including the QT interval, QT dispersion, and T-wave alternans.[10,11] Recent studies have suggested that new indexes such as the Tpeak-Tend (Tp-e) interval (defined as the interval from the peak of the T wave to the end of the T wave), corrected (c) Tp-e interval, and Tp-e interval/QT interval (Tp-e/QT) ratio may be associated with ventricular arrhythmias in various clinical scenarios.[12-16]

No trial has evaluated the Tp-e interval, cTp-e interval, and Tp-e/QT ratio in patients with mild hyperbilirubinemia. The aim of this study was to investigate the association between serum bilirubin levels and ventricular repolarization using the Tp-e interval and Tp-e/QT ratio.

Abbreviations:

ECG, electrocardiography; c, corrected; Tp-e, Tpeak-Tend; OR, odds ratio; AF, atrial fibrillation; BP, blood pressure; BMI, body mass index; HR, heart rate; ROS, reactive oxygen species; HF, heart failure; SBP, systolic blood pressure; DBP, diastolic blood pressure; bil, bilirubin.

[1]Department of Cardiology, University of Health Sciences, Van Education and Research Hospital, Van, Turkey, [2]Department of Biochemistry, University of Health Sciences, Van Education and Research Hospital, Van, Turkey

*To whom correspondence should be addressed.
drcsengul@yahoo.com

Materials and Methods

Study Population and Study Protocol

The study population consisted of outpatients who were referred to our Army Check-Up Center for general youth health screening from January 2019 to July 2019. A total of 890 male patients whose age range was between 20 and 44 underwent electrocardiography (ECG), blood pressure (BP) measurement, basic transthoracic echocardiography, hepatic ultrasonography, and routine biochemical tests.

Of these patients, 201 patients with mild hyperbilirubinemia (total bilirubin level > 1.2 mg/dL and indirect bilirubin level > 1 mg/dL), normal hepatic enzymes, reticulocyte level < 2% measured by reticulocyte smear, lack of hemolytic disease, and normal hepatic ultrasonography were considered as group 1. There were 219 age-matched otherwise healthy patients with normal bilirubin levels included as the control group (group 2).

A total bilirubin level > 5.3 mg/dL, a history of coronary artery or valvular heart disease, systolic heart failure (HF), diabetes mellitus, liver disease, gallbladder disease, chronic renal disease, alcohol or drug abuse, hypo- or hyperthyroidism, previous use of antihypertensive drugs or statins, hypoalbuminemia, hematologic disease such as myelodysplastic syndrome, leukemia, lymphoma, and vitamin B_{12} deficiency were the exclusion criteria.

The study was approved by the Institutional Ethic Committee. All patients were informed and gave written consent. Patient age, height, and weight were recorded. Patients were questioned for smoking history. Smokers were defined as those who smoked ≥1 cigarettes per day or those who had quit smoking within < 2 years previously. The BP of all patients was measured with a sphygmomanometer following at least 15 minutes of resting. Body mass index (BMI) was calculated by dividing body weight in kilograms by the square of the height in meters (kg/m^2). Blood for biochemical analysis was taken after fasting for 12 hours. Routine biochemical investigations and cholesterol parameters of the patients were calculated using the Abbott ARCHITECT c16000 (Abbott Laboratories, USA) autoanalyzer. The hematologic tests were performed using the Abbott Cell Dyn Ruby analyzer (Abbott Diagnostics, USA). Thyrotropin test was performed using the chemiluminescent microparticle immunoassay method of the Abbott Architect I 2000 immunology analyzer (Abbott Diagnostics, USA). Serum bilirubin levels were measured 1 week later in patients with mild hyperbilirubinemia to confirm the diagnosis.

ECG

Twelve-lead resting ECGs were performed, with 20 mm/mV amplitude and 50 mm/second rate with standard lead derivations, on an ECG machine (Hewlett Packard, Pagewriter, USA). Patients were not allowed to talk during the ECG. The ECG measurements of Tp-e and QT intervals and heart rate (HR) were performed manually using a magnifying Glass (TorQ 150 mm Digital Caliper LCD) by 2 cardiologists blinded to the clinical data. Patients with U-waves on their ECGs were excluded from the study. The Tp-e interval was defined as the interval from the peak of the T wave to the end of the T wave using precordial lead V_5.[17,18] Measurements of the Tp-e interval were performed from precordial lead V_5 and corrected for HR using the Bazett formula: $cTp\text{-}e = Tp\text{-}e\sqrt{(R\text{-}R\ interval)}$. The QT interval was measured from the beginning of the QRS complex to the end of the T wave in precordial lead V_6, which best reflects the transmural axis of the left ventricle[19] and was corrected for HR using the Bazett formula: $cQT = QT\sqrt{(R\text{-}R\ interval)}$. The Tp-e/QT ratio and cTp-e/cQT ratio were calculated from these measurements. Interobserver and intraobserver coefficients of variation were each < 5%, respectively.

Statistical Analysis

Continuous variables were presented as mean ± standard deviation or median, and categorical variables were expressed as number and percentage. The Shapiro-Wilk test was used to identify the normally distributed variables. The continuous variables were compared across the groups using the Student's t-test or the Mann-Whitney U test. The categorical variables were compared using the χ^2 test. Spearman correlation analysis was performed to find the correlations between the cTp-e interval and bilirubin levels. To determine the independent predictors of mild hyperbilirubinemia, binary logistic regression analysis with the Enter method was performed. Variables that were found to be statistically significant in the univariate analysis were entered in the regression model. The results of the regression analysis were presented as odds ratio (OR) and 95% confidence interval. All data were analyzed with SPSS v16.0 for Windows (SPSS Inc, Chicago, IL). A P value <.05 was considered statistically significant.

Table 1. Baseline Demographic and Clinical Characteristics of Study Groups

	Group 1[c]	Group 2[d]	*P* Value
	n = 201	n = 219	
Age, y[a]	26.96 ± 3.87	27.51 ± 4.27	.35
SBP, mm Hg[b]	120 (96–140)	120 (101–140)	.53
DBP, mm Hg[b]	75 (50–89)	74 (53–93)	.99
BMI[a]	24.17 ± 2.50	24.47 ± 2.45	.52
Smoking, n (%)	35 (52.2)	37 (50.7)	.85
Fasting glucose[a]	87.81 ± 8.49	89.27 ± 8.73	.32
Total cholesterol[a]	164.34 ± 31.56	160.94 ± 39.78	.57
Thyrotropin[b]	1.66 (0.45–4.00)	1.44 (0.3–4.95)	.41
Creatinine[a]	0.86 ± 0.14	0.82 ± 0.14	.95
Total bil[b]	1.72 (1.37–3.82)	0.52 (0.23–1.00)	<.001
Conjugated bil[b]	0.31 (0.14–0.73)	0.21 (0.04–0.43)	<.001
Unconjugated bil[b]	1.41 (1.2–3.54)	0.34 (0.07–0.58)	<.001
Aspartate aminotransferase[b]	15.0 (6–35)	14.0 (8–24)	.42
Alanine aminotransferase[b]	18.0 (6–43)	19.0 (9–40)	.92
Sedimentation[b]	3 (1–19)	4 (4–11)	.25
Hematocrit[a]	52.27 ± 2.9	51.88 ± 2.9	.43

SBP, systolic blood pressure; DBP, diastolic blood pressure; BMI, body mass index; bil = bilirubin.
[a]Mean ± standard deviation.
[b]Median (min-max).
[c]Group 1 = patients with mild hyperbilirubinemia.
[d]Group 2 = patients with normal bilirubin levels.

Results

A total of 201 patients with mild hyperbilirubinemia as group 1 and 219 patients with normal bilirubin levels as group 2 were included in our study. Baseline demographic and clinical characteristics are shown in **Table 1**. Baseline characteristics of the study groups were similar regarding age, systolic BP, diastolic BP, BMI, smoking history, glucose, cholesterol panel, thyrotropin, creatinine, alanine aminotransferase, aspartate aminotransferase, sedimentation, and hematocrit. Total, conjugated, and unconjugated bilirubin levels were significantly higher in group 1 than in group 2 (*P* <.001). Patient ECG findings are shown in **Table 2**. The QRS interval and QT interval were similar between groups. The HR and cQT interval were lower in group 1 compared with group 2, but those findings did not achieve statistical significance. The Tp-e interval, cTp-e interval, and Tp-e/QT ratio were significantly lower in group 1 compared with group 2 (*P* <.001). Furthermore, in the Spearman correlation analysis, the cTp-e interval showed a significant negative correlation with total bilirubin (*r* = 0.555; *P* <.001), conjugated bilirubin (*r* = 0.529; *P* <.001), and unconjugated bilirubin (*r* = 0.521; *P* <.001). Multivariate logistic regression analysis showed that the cTp-e interval (OR, 0.900;

P =.002) and Tp-e/QT ratio (OR, 0.922; *P* =.04) were significantly and independently associated with mild hyperbilirubinemia (**Table 3**).

Discussion

In this study, we compared the repolarization parameters (Tp-e interval, QT interval, Tp-e/QT ratio, cTp-e interval, and cQT interval) among otherwise healthy men with a normal bilirubin level and otherwise healthy men with mild hyperbilirubinemia. Our study is the first report to show the relationship between cTp-e interval, Tp-e/QT ratio, and mild hyperbilirubinemia. First, we found a significantly lower Tp-e interval, cTp-e interval, and Tp-e/QT ratio in group 1 (patients with mild hyperbilirubinemia) compared with group 2 (patients with normal bilirubin levels). Second, the cTp-e interval showed a significant negative correlation with bilirubin levels. Third, the cTp-e interval and the Tp-e/QT ratio showed a significant and independent association with mild hyperbilirubinemia.

Previous research had suggested that bilirubin was a nonfunctional waste product of hemoglobin metabolism

Table 2. ECG Findings of Study Groups

	Group 1	Group 2	P Value
HR, bpm[a]	71.42 ± 12.51	74.12 ± 11.55	.18
QRS interval (ms)[b]	100 (80–120)	100 (80–130)	.87
QT interval (ms)[b]	360 (290–420)	360 (320–420)	.86
cQT (ms)[a]	391.64 ± 26.49	402.52 ± 27.04	.018
Tp-e (ms)[b]	80 (60–110)	100 (75–150)	<.001
cTp-e (ms)[a]	90.79 ± 13.80	112.18 ± 15.34	<.001
Tp-e/QT ratio[a]	0.23 ± 0.03	0.28 ± 0.03	<.001

ECG, electrocardiography; HR, heart rate; Tp-e, T-wave interval from peak to end; c, corrected.
[a]*Mean ± standard deviation.*
[b]*Median (min-max).*

Table 3. Multiple Linear Regression Model Identifying Independent Factors Associated with Mild Hyperbilirubinemia

Variable	B Value (95% confidence interval)	P Value
cQT	1.016 (0.995–1.037)	.136
Tp-e	0.984 (0.924–1.049)	.627
cTp-e	0.900 (0.843–0.961)	.002
Tp-e/QT	0.922 (0.816–0.975)	.04

c, corrected; Tp-e, T-wave interval from peak to end.

and that hyperbilirubinemia was even neurotoxic. However, Stocker et al suggested that bilirubin was also a potent endogenous antioxidant because of a system of conjugated double bonds within its molecule in their landmark study.[1] Other researchers also showed that bilirubin was more effective in protecting low-density lipoprotein against oxidation by reactive oxygen species (ROS) than several known antioxidants.[2,20] An inverse relationship between serum bilirubin and the risk of myocardial infarction, coronary artery disease, and peripheral vascular disease risk was found in several previous studies including the Framingham Offspring Study.[21-25] Although not as robust as the data regarding the aforementioned diseases, emerging data also link bilirubin to cardiac arrhythmias. Serum bilirubin levels were shown to be lower among patients with AF in a recent study by Demir et al.[8] Cüre et al[9] showed that increased bilirubin levels were associated with a decrease in HR, QT interval, and P-wave dispersion, a novel predictor of AF, in patients with mild hyperbilirubinemia. Ours is the first study linking bilirubin to the Tp-e interval and the Tp-e/QT ratio.

Ventricular arrhythmias, a common cause of sudden cardiac death, may present in apparently healthy individuals. It may be possible to predict the development of ventricular cardiac arrhythmias by analyzing several ventricular repolarization indicators in ECG. Of these, the QT interval, the cQT interval, and QT interval dispersion have been extensively studied in previous trials.[10,11] Recent studies have suggested the Tp-e interval as a novel index of the transmural dispersion of repolarization. A prolonged Tp-e interval has been shown to be associated with ventricular arrhythmias in various clinical scenarios.[12-16]

The relationship of mild hyperbilirubinemia to a decreased cTp-e interval and Tp-e/QT ratio, as shown in the present study, may result from the antioxidant properties of bilirubin. It is well known that arrhythmic conditions are associated with systemic and cardiac oxidative stress caused by ROS.[5] Excess amounts of ROS can result in focal activity by modifying many of the ionic currents in cardiomyocytes, cardiomyocyte coupling, and important elements of the extracellular matrix.[26,27] In addition, ROS may promote cardiac fibrosis and impair gap junction function, resulting in reduced myocyte coupling and facilitation of re-entry. The resulting heterogeneous action potential duration has been shown to be a possible mechanism for re-entry in oxidative stress.[28] Any situation associated with decreased oxidative stress may relate to less re-entry and subsequent ventricular arrhythmias. Interestingly, functional re-entry has been shown to be the underlying mechanism for arrhythmogenesis associated with a prolonged Tp-e interval.[29,30] We found a powerful association between mild hyperbilirubinemia and a decreased Tp-e interval. Our results suggest that hyperbilirubinemia, a potent antioxidant, may decrease re-entry–associated ventricular arrhythmias by lowering the cTp-e interval and modulating ventricular repolarization characteristics.

Moreover, recent trials using antioxidants as a potential antiarrhythmic drug may support the results of the present study and the potential benefits of bilirubin.[31,32] An experimental study showed that pretreatment with bilirubin significantly prevented bufadienolide (a novel anticancer drug)-induced premature ventricular complexes, ventricular tachycardia, ventricular fibrillation, and death.[33] Bakrania et al[34] showed that hyperbilirubinemia was associated with a negative inotropic effect on the heart of a male Gunn rat and decreased the levels of ventricular malondialdehyde and protein carbonyl content, indicating lower levels of cellular oxidative stress. In light of these findings, it is possible that the association of mild hyperbilirubinemia with a decreased cTp-e interval as shown in the present study may reflect the favorable impact of bilirubin on ventricular repolarization as a potent antioxidant.

Interestingly, bilirubin may be related to worse outcomes in some circumstances. Okada et al[35] showed that patients with acute decompensated HF with elevated bilirubin had a significantly higher rate of the composite endpoint of all-cause mortality or readmission compared with those with normal bilirubin. The same inverse relationship was also shown in patients with chronic HF and with acute myocardial infarction.[36,37] There is an apparent paradox that bilirubin may become antioxidant in certain situations, particularly when it is present in blood at moderately increased concentrations, which may reflect adverse outcomes in some pathological states. All patients in the present study were otherwise healthy, and their hepatic enzymes were in normal limits. The results of the present study may highlight the aforementioned paradox that hepatic functions should be normal to obtain antioxidant properties of bilirubin. In addition, the previous studies proved that hyperbilirubinemia because of underlying abnormal liver function did not only result in protection against vascular diseases but also eliminated the protective effects of bilirubin on all-cause mortality.[38,39]

The most important limitation of our study is the small number of patients enrolled. Although we used 2 blood specimens for measurement in the patients with mild hyperbilirubinemia, plasma bilirubin concentrations are known to exhibit substantial variability. We also could not assess the association between ventricular arrhythmias and the cTp-e interval and Tp-e/QT ratio because the study patients were not followed up prospectively for episodes of ventricular arrhythmias. Finally, this study sample is not representative of the general population. The enrollment of only men younger than age 45 years without comorbidity may limit the scope and generalizability of the present study. Large-scale prospective studies involving both men and women with multiple risk factors and comorbidities are needed to reveal the relationship between hyperbilirubinemia and ventricular repolarization parameters more clearly. Although specific bilirubin-based therapeutic approaches seem to have big therapeutic potential, further research targeting good clinical outcomes is required to uncover this promising field completely.

Conclusion

The present study showed the association of mild hyperbilirubinemia with a decreased cTp-e interval and Tp-e/QT ratio. Hyperbilirubinemia may decrease the incidence of ventricular arrhythmias by its antioxidant properties. The protective role of hyperbilirubinemia in the risk of ventricular arrhythmias needs clarification in further studies. **LM**

References

1. Stocker R, Yamamoto Y, McDonagh AF, Glazer AN, Ames BN. Bilirubin is an antioxidant of possible physiological importance. *Science.* 1987;235(4792):1043–1046.

2. Wu TW, Fung KP, Yang CC. Unconjugated bilirubin inhibits the oxidation of human low density lipoprotein better than Trolox. *Life Sci.* 1994;54(25):P477–P481.

3. Vítek L, Novotný L, Sperl M, et al. The inverse association of elevated serum bilirubin levels with subclinical carotid atherosclerosis. *Cerebrovasc Dis.* 2006;21(5-6):408–414.

4. Vítek L. Bilirubin and atherosclerotic diseases. *Physiol Res.* 2017;66(Supplement 1):S11–S20.

5. Jeong EM, Liu M, Sturdy M, et al. Metabolic stress, reactive oxygen species, and arrhythmia. *J Mol Cell Cardiol.* 2012;52(2):454–463.

6. Korantzopoulos P, Kolettis TM, Galaris D, Goudevenos JA. The role of oxidative stress in the pathogenesis and perpetuation of atrial fibrillation. *Int J Cardiol.* 2007;115(2):135–143.

7. Chen SC, Chung FP, Chao TF, et al. A link between bilirubin levels and atrial fibrillation recurrence after catheter ablation. *J Chin Med Assoc.* 2019;82(3):175–178.

8. Demir M, Demir C, Uyan U, Melek M. The relationship between serum bilirubin concentration and atrial fibrillation. *Cardiol Res.* 2013;4(6):186–191.

9. Cüre E, Yüce S, Ciçek Y, Cüre MC. The effect of Gilbert's syndrome on the dispersions of QT interval and P-wave: an observational study. *Anadolu Kardiyol Derg.* 2013;13(6):559–565.

10. Elming H, Holm E, Jun L, et al. The prognostic value of the QT interval and QT interval dispersion in all-cause and cardiac mortality and morbidity in a population of Danish citizens. *Eur Heart J.* 1998;19(9):1391–1400.

11. Tse G, Yan BP. Traditional and novel electrocardiographic conduction and repolarization markers of sudden cardiac death. *Europace.* 2017;19(5):712–721.

12. Kors JA, Ritsema van Eck HJ, van Herpen G. The meaning of the Tp-Te interval and its diagnostic value. *J Electrocardiol.* 2008;41(6):575–580.

13. Turgay Yıldırım Ö, Kaya Ş, Baloğlu Kaya F. Evaluation of the Tp-e interval and Tp-e/QTc ratio in patients with benign paroxysmal positional vertigo in the emergency department compared with the normal population. *J Electrocardiol.* 2020;58(1):51–55.

14. Akboğa MK, Gülcihan Balcı K, Yılmaz S, et al. Tp-e interval and Tp-e/QTc ratio as novel surrogate markers for prediction of ventricular arrhythmic events in hypertrophic cardiomyopathy. *Anatol J Cardiol.* 2017;18(1):48–53.

15. Castro Hevia J, Antzelevitch C, Tornés Bárzaga F, et al. Tpeak-Tend and Tpeak-Tend dispersion as risk factors for ventricular tachycardia/ventricular fibrillation in patients with the Brugada syndrome. *J Am Coll Cardiol.* 2006;47(9):1828–1834.

16. Smetana P, Schmidt A, Zabel M, et al. Assessment of repolarization heterogeneity for prediction of mortality in cardiovascular disease: peak to the end of the T wave interval and nondipolar repolarization components. *J Electrocardiol.* 2011;44(3):301–308.

17. Akcay M. The effect of moderate altitude on Tp-e interval, Tp-e/QT, QT, cQT and P-wave dispersion. *J Electrocardiol.* 2018;51(6):929–933.

18. Haarmark C, Graff C, Andersen MP, et al. Reference values of electrocardiogram repolarization variables in a healthy population. *J Electrocardiol.* 2010;43(1):31–39.

19. Gupta P, Patel C, Patel H, et al. T(p-e)/QT ratio as an index of arrhythmogenesis. *J Electrocardiol.* 2008;41(6):567–574.

20. Wu TW, Fung KP, Wu J, et al. Antioxidation of human low density lipoprotein by unconjugated and conjugated bilirubins. *Biochem Pharmacol.* 1996;51(6):859–862.

21. Franchini M, Targher G, Lippi G. Serum bilirubin levels and cardiovascular disease risk: a Janus Bifrons? *Adv Clin Chem.* 2010;50(1):47–63.

22. Lan Y, Liu H, Liu J, Zhao H, Wang H. Is serum total bilirubin a predictor of prognosis in arteriosclerotic cardiovascular disease? A meta-analysis. *Medicine (Baltimore).* 2019;98(42):e17544.

23. Ozeki M, Morita H, Miyamura M, et al. High serum bilirubin is associated with lower prevalence of peripheral arterial disease among cardiac patients. *Clin Chim Acta.* 2018;476(1):60–66.

24. Schwertner HA, Jackson WG, Tolan G. Association of low serum concentration of bilirubin with increased risk of coronary artery disease. *Clin Chem.* 1994;40(1):18–23.

25. Djoussé L, Levy D, Cupples LA, Evans JC, D'Agostino RB, Ellison RC. Total serum bilirubin and risk of cardiovascular disease in the Framingham Offspring Study. *Am J Cardiol.* 2001;87(10):1196–200.

26. Barth AS, Tomaselli GF. Cardiac metabolism and arrhythmias. *Circ Arrhythm Electrophysiol.* 2009;2(3):327–335.

27. Sovari AA. Cellular and molecular mechanisms of arrhythmia by oxidative stress. *Cardiol Res Pract.* 2016;2016:9656078. doi: 10.1155/2016/9656078.

28. Sovari AA, Vahdani N, Morita N, et al. Oxidative stress promotes ventricular fibrillation at early stages of hypertension: role of Ca2+/CaM kinase-II. *Heart Rhythm.* 2010;7(5):PO3–PO92.

29. Wang D, Patel C, Cui C, Yan GX. Preclinical assessment of drug-induced proarrhythmias: role of the arterially perfused rabbit left ventricular wedge preparation. *Pharmacol Ther.* 2008;119(2):141–151.

30. Yan GX, Wu Y, Liu T, et al. Phase 2 early afterdepolarization as a trigger of polymorphic ventricular tachycardia in acquired long-QT syndrome: direct evidence from intracellular recordings in the intact left ventricular wall. *Circulation.* 2001;103(23):2851–2856.

31. Adlam VJ, Harrison JC, Porteous CM, et al. Targeting an antioxidant to mitochondria decreases cardiac ischemia-reperfusion injury. *FASEB J.* 2005;19(9):1088–1095.

32. Graham D, Huynh NN, Hamilton CA, et al. Mitochondria-targeted antioxidant MitoQ10 improves endothelial function and attenuates cardiac hypertrophy. *Hypertension.* 2009;54(2):322–328.

33. Ma H, Zhang J, Jiang J, et al. Bilirubin attenuates bufadienolide-induced ventricular arrhythmias and cardiac dysfunction in guinea-pigs by reducing elevated intracellular Na(+) levels. *Cardiovasc Toxicol.* 2012;12(1):83–89.

34. Bakrania B, Du Toit EF, Ashton KJ, Wagner KH, Headrick JP, Bulmer AC. Chronically elevated bilirubin protects from cardiac reperfusion injury in the male Gunn rat. *Acta Physiol (Oxf).* 2017;220(4):461–470.

35. Okada A, Sugano Y, Nagai T, et al.; NaDEF Investigators. Usefulness of the direct and/or total bilirubin to predict adverse outcomes in patients with acute decompensated heart failure. *Am J Cardiol.* 2017;119(12):2035–2041.

36. Hosoda J, Ishikawa T, Matsumoto K, et al. Significance of change in serum bilirubin in predicting left ventricular reverse remodeling and outcomes in heart failure patients with cardiac resynchronization therapy. *J Cardiol.* 2017;70(5):416–419.

37. Shen H, Zeng C, Wu X, Liu S, Chen X. Prognostic value of total bilirubin in patients with acute myocardial infarction: a meta-analysis. *Medicine (Baltimore).* 2019;98(3):e13920.

38. Novotný L, Vítek L. Inverse relationship between serum bilirubin and atherosclerosis in men: a meta-analysis of published studies. *Exp Biol Med (Maywood).* 2003;228(5):568–571.

39. Fulks M, Stout RL, Dolan VF. Mortality associated with bilirubin levels in insurance applicants. *J Insur Med.* 2009;41(1):49–53.

Rapid Molecular Detection for Differentiation of Homozygous HbE and ß^0-Thalassemia/HbE in Samples Related With HbE >80% and Variable HbF Levels

Wanicha Tepakhan, PhD[1] Wittaya Jomoui, PhD[2*]

ABSTRACT

Objective: To validate a novel rapid molecular testing method for differentiation of homozygous hemoglobin (Hb)E and HbE/β^0-thalassemia genotypes using multiplex melt curve combined with high-resolution melt (HRM) analysis in a single test tube.

Methods: All 10 genotypes contained (β^N/β^N; n = 95), ($\beta^N/\beta^{3.5-kb}$; n = 71), (β^N/β^{45-kb}; n = 28), (β^N/β^E; n = 10), ($\beta^E/\beta^{3.5-kb}$; n = 6), (β^E/β^{45-kb}; n = 4), ($\beta^E/\beta^{41/42}$; n = 28), (β^E/β^{17}; n = 9), ($\beta^E/\beta^{IVSI\#1}$; n = 6), and (β^E/β^E; n = 76) were recruited for validation. A proposed strategy for rapid differentiation of β^0-thalassemia/HbE disease and homozygous Hb E in specimens with HbE greater than 80% and variable HbF levels was demonstrated.

Results: In the validation method, all genotypes showed 100% concordance, compared with the conventional reverse dot blot (RDB) and gap–polymerase chain reaction (PCR) methods.

Conclusions: Our newly developed method could be useful in routine laboratory settings. The method is rapid, simple, and cost effective; does not require a post-PCR step; and can be applied in routine settings.

Keywords: HbE/β0-thalassemia, homozygous HbE, HRM analysis, melt-curve analysis, 3.5-kb deletion, 45-kb deletion

Hemoglobin (Hb)E is a common hemoglobinopathic manifestation in Southeast Asian populations, especially in Thailand, where the prevalence has been reported to be as high as 50% in some areas.[1,2] This condition is caused by a single base substitution of GAG for AAG at codon 26 (HBB:c.79G>A) of the β-globin gene, resulting in changing glutamic acid to lysine substitution. Clinical manifestation of heterozygous HbE is usually asymptomatic; however,

homozygous HbE can present with mild anemia and hypochromic microcytic erythrocytes.[1]

The combination of HbE and β-thalassemia (HbE/β-thalassemia) results in a wide variety of clinical disorders, depending on the type of β-thalassemia mutation.[3] Screening for HbE is performed with the dichlorophenolindophenol (DCIP) precipitation test, and confirmation testing is carried out using high-performance liquid chromatography (HPLC) or capillary electrophoresis (CE). Normally, the levels of HbE/A2 and HbF in patients with homozygous HbE (Hb type: EE) range from 80% to 100% and less than 5%, respectively; those levels in HbE/β^0-thalassemia (Hb type: EF) range from 40% through 70% and 30% through 60%, respectively.[4,5] However, some cases of homozygous HbE or HbE/β^0-thalassemia (Hb type: EE/EF) have shown variable HbE and HbF levels, causing a frequent problem at routine Hb analysis among Southeast Asian populations.[6,7] Thus, further molecular analysis needs to be performed for differential diagnosis of these conditions.

The genotyping of HbE is usually performed using the amplification-refractory mutation system (ARMS) or reverse

Abbreviations:

Hb, hemoglobin; DCIP, dichlorophenolindophenol; HPLC, high-performance liquid chromatography; CE, capillary electrophoresis; ARMS, amplification-refractory mutation system; RDB, reverse dot blot; PCR, polymerase chain reaction; HRM, high-resolution melting; HREC, Human Research Ethics Committee; Tm, melting temperature; LOD, limits of detection; MCV, mean corpuscular volume

[1]Department of Pathology, Faculty of Medicine, Prince of Songkla University, Songkhla, Thailand, [2]Department of Pathology, Maha Chakri Sirindhorn Medical Center, Faculty of Medicine, Srinakharinwirot University, Nakhon Nayok, Thailand

*To whom correspondence should be addressed.
wittayaj@g.swu.ac.th

dot blot (RDB) analysis to detect point mutations. However, HbE with large deletional β^0-thalassemia can show similar results to homozygous HbE in those methods. Thus, the complete HbE genotyping should be performed using those techniques and gap–polymerase chain reaction (gap-PCR), respectively.[8–12]

These multiple techniques required to accurately determine the HbE genotype require considerable time, labor, and cost. In this study, we developed a new molecular analysis technique that can differentiate between homozygous HbE and HbE/β^0-thalassemia, which are prevalent among Southeast Asian populations, using multiplex melt curve and high-resolution melting (HRM) analysis in a single test tube.

Materials and Methods

Specimens

Ethical approval of the study protocol was obtained from the Human Research Ethics Committee (HREC), Faculty of Medicine, Prince of Songkla University (REC 62-073-5-2), Songkla, Thailand. Archival DNA specimens were obtained from the Thalassemia Service Unit, Department of Pathology, Faculty of Medicine, Prince of Songkla University. Identification of β-thalassemia is routinely performed in our laboratory using RDB analysis to detect point mutations and gap-PCR to detect large deletions, as described elsewhere.[10–12]

A total of 333 DNA specimens from healthy individuals and patients with β-thalassemia were used in this study. HbE/β^0-thalassemia genotypes were selected based on their high prevalence in this region (ie, $\beta^E/\beta^{41/42}$, β^E/β^{17}, $\beta^E/\beta^{IVSI\#1}$, $\beta^E/\beta^{3.5\text{-kb}}$, and $\beta^E/\beta^{45\text{-kb}}$). Further, we selected

specimens that were heterozygous for large deletion β^0-thalassemia, heterozygous HbE, and wildtype for validation of our novel testing method. Among these 333 specimens, 95 had a healthy beta globin gene (β^N/β^N), 71 specimens had heterozygous $\beta^{3.5\text{-kb}}$-thalassemia ($\beta^N/\beta^{3.5\text{-kb}}$), 28 had heterozygous $\beta^{45\text{-kb}}$-thalassemia ($\beta^N/\beta^{45\text{-kb}}$), 10 had heterozygous HbE (β^N/β^E), 6 had HbE/$\beta^{3.5\text{-kb}}$-thalassemia ($\beta^E/\beta^{3.5\text{-kb}}$), 4 had HbE/$\beta^{45\text{-kb}}$-thalassemia ($\beta^E/\beta^{45kb}$), 28 had HbE/$\beta^{41/42}$-thalassemia ($\beta^E/\beta^{41/42}$), 9 had HbE/$\beta^{17}$-thalassemia ($\beta^E/\beta^{17}$), 6 had HbE/$\beta^{IVSI\#1}$-thalassemia ($\beta^E/\beta^{IVSI\#1}$), and 76 had homozygous HbE (β^E/β^E). All specimens were anonymized before being used for validation with our newly developed method, to avoid interpretation bias.

Development and Validation of Multiplex Melt Curves and HRM Analysis

A novel method based on melt curve and HRM analysis was developed. We designed a process to differentiate β^0-thalassemia (3.5-kb deletion), β^0-thalassemia (45-kb deletion) and the β-globin gene (codon 26 fragment) using melt-curve analysis based on PCR product amplicons (melting temperature [Tm]). HbE was continually genotyped by HRM analysis based on selected PCR product amplicons of the β-globin gene (codon 26 fragment). The 3 primer pairs and PCR product details are shown in **Table 1**. Detection of β^0-thalassemia large deletions and HbE (HBB:c.79G>A) genotyping was performed using real-time PCR machine which is Quantstudio5 product of Thermo Fisher, systems. The single tube of multiplex melt-curve and HRM reaction mixture (20 µL) contained 2 µL of 20 ng per µL genomic DNA, 10 µL of 2X Sensifast HRM kit (Bioline), 0.4 µL of 10 µM primer pairs of β^0-thalassemia (45- and 3.5-kb deletion) (F1, R1, F2, R2), 0.2 µL of 10 µM primers pairs of codon 26 fragments (F3 and R3), and distilled water for the remainder. Thermal cycling was performed on mean real-time PCR namely Quanstudio5 (a model of Thermo fisher product), starting with the holding stage (95°C for

Table 1. List of the Primer Pairs and PCR Product Details

| No.	Primer		PCR Product		Method	Specific Fragment
	Forward (5′ > 3′)	Reverse (5′ > 3′)	bp	Tm (°C)		
1	(F1) AGACCTTATGATCTTGATAGGGA	(R1) ATCCTTTATTTCTTTCTCTTGCC	58	72.0	Melt-curve analysis	45-kb deletion
2	(F2) TCCCCAGTTAACCTCCTATT	(R2) CGGCTGCAACATGAATATTAG	140	77.0	Melt-curve analysis	3.5-kb deletion
3	(F3) ACGTGGATGAAGTTGGTG	(R3) GCCCAGTTTCTATTGGTCTC	85	80.5	Melt-curve and HRM analysis	Condon 26 fragment

PCR, polymerase chain reaction; Tm, melting temperature; HRM, high-resolution melt.

3 minutes) for activation of enzyme Taq polymerase by heating before PCR steps, followed by 40 cycles of PCR (95°C for 5 seconds, 64°C for 15 seconds). The final step was the melt-curve stage, which was started at 95°C for 10 seconds, followed by a melting cycle from 50°C to 95°C with temperature incrementation (rate, 0.025°C/seconds). HbE genotyping was selected at the specific melt curve of the β-globin gene (codon 26 fragment); then, we continued with HRM analysis performed on High Resolution Melt Software, version 3.1 (Thermo Fisher Scientific Inc.).

We determined the limits of detection (LOD) for our method using a DNA 10-fold serial dilution of 10 ng per reaction to 0.001 ng per reaction across duplicate dilutions. We calculated 4 genotypes with LOD, namely, $(\beta^N/\beta^{3.5\text{-kb}})$, $(\beta^N/\beta^{45\text{-kb}})$, $(\beta^E/\beta^{41/42})$, and (β^E/β^E). The values between Ct and log[DNA concentration] scatterplots were created by MINITAB statistical software, version 14.12.0. A total of 333 leftover DNA specimens collected at our routine setting were examined in masked trials with the developed method, and the results of genotyping were compared with conventional routine RDB and gap-PCR assay results.

Results

Our method, based on multiplex melt-curve analysis, differentiates 3 specific amplicons, namely, β^0-thalassemia (45-kb deletion), β^0-thalassemia (3.5-kb deletion), and the β-globin gene (codon 26 fragment). The amplified products were aligned according to Tm: 69.0°C to 74.0°C specific for β^0-thalassemia (45-kb deletion), 74.0°C to 78.0°C specific for β^0-thalassemia (3.5-kb deletion), and 78.0°C to 82.0°C specific for the β-globin gene (codon 26 fragment; **Figure 1**). The specific melt curve of the β-globin gene (codon 26 fragment) was further investigated for differentiation of HbE genotyping based on HRM analysis. HRM analysis related to HbE (HBB:c.79G>A) genotyping demonstrated 4 different patterns—GG, GA, AA, and GA—with $\beta^{IVSI\#1}$-thalassemia (**Figure 2**). HbE/β^0-thalassemia (point mutation) and heterozygous HbE displayed a GA pattern, and homozygous HbE and HbE/β^0-thalassemia (large deletion) showed an AA pattern. The normal β-globin gene codon 26 showed a GG pattern. Further, primer pairs
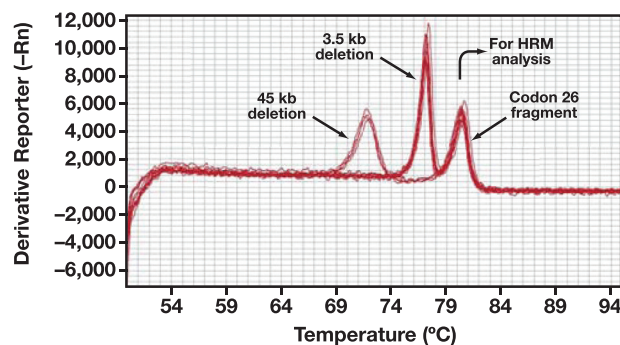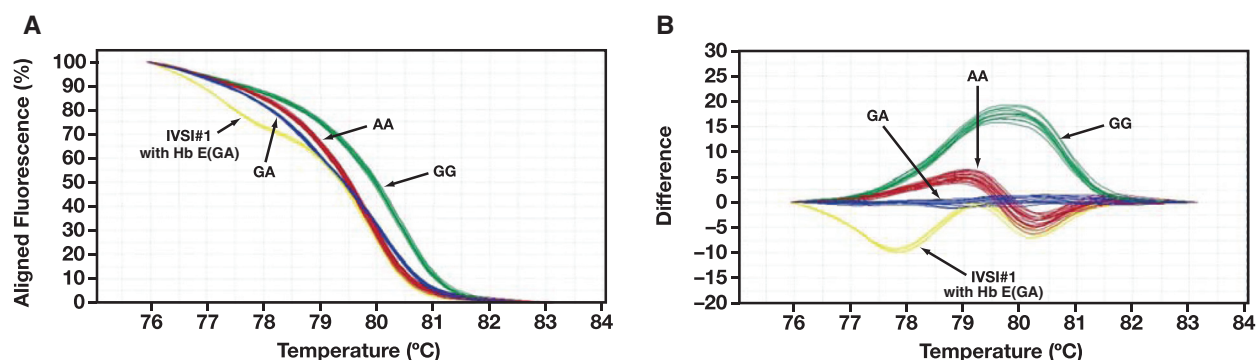

Figure 1

Melt-curve analysis with amplified products was aligned according to temperature melting, including 69.0°C–74.0°C specific for β^0-thalassemia (45-kb deletion), 74.0°C–78.0°C specific for β^0-thalassemia (3.5-kb deletion), and 78.0°C–82.0°C specific for the β-globin gene (codon 26 fragment). The specific melt curve of the β-globin gene (codon 26 fragment) was further investigated for hemoglobin E (HBB:c.79G>A) genotyping based on high-resolution melt (HRM) analysis.

of the β-globin gene (codon 26 fragment) could also be amplified to cover the common β^0-thalassemia mutation ($\beta^{IVSI\#1}$-thalassemia) in Southeast Asia. Thus, HbE/$\beta^{IVSI\#1}$-thalassemia would show the specific HRM pattern, as mentioned herein.

To assess the sensitivity of the method we developed, we determined LOD values, as shown in **Figure 3**. 10-fold serial DNA dilutions were started, with 10 ng per reaction for each of the 4 genotypes ($\beta^N/\beta^{3.5\text{-kb}}$, $\beta^N/\beta^{45\text{-kb}}$, $\beta^E/\beta^{41/42}$, and β^E/β^E). The LOD of the developed assay was 0.01 ng per reaction in all genotypes. To assess the correlation coefficient, a standard curve was also included for these serial dilutions. The results showed that R^2 values of 0.995, 0.997, 0.998, and 0.996 were related to $\beta^N/\beta^{3.5\text{-kb}}$, $\beta^N/\beta^{45\text{-kb}}$, $\beta^E/\beta^{41/42}$, and β^E/β^E, respectively (**Figure 3**).

The developed method was validated with 333 deidentified specimens. As the results show in **Table 2**, all 10 genotypes recruited in the study showed 100% concordant results, compared with the conventional RDB and gap-PCR methods, as described. Melt-curve analysis results revealed that 71 heterozygous $\beta^{3.5\text{-kb}}$-thalassemia ($\beta^N/\beta^{3.5\text{-kb}}$) and 6 HbE/$\beta^{3.5\text{-kb}}$-thalassemia ($\beta^E/\beta^{3.5\text{-kb}}$) specimens had the same specific melt curve as β^0-thalassemia (3.5-kb deletion). Also, 28 heterozygous $\beta^{45\text{-kb}}$-thalassemia ($\beta^N/\beta^{45\text{-kb}}$) and 4 HbE/$\beta^{45\text{-kb}}$-thalassemia

Figure 2

Hemoglobin E (HBB:c.79G>A) genotyping using high-resolution melt (HRM) analysis on the β-globin gene (codon 26 fragment). The differentiation of genotypes (GG, GA, AA, and GA with $\beta^{IVSI\#1}$-thalassemia) is shown in aligned melt curves (**A**) and difference-aligned melt curves (**B**).

($\beta^E/\beta^{45\text{-}kb}$) specimens had the same specific melt curve of β^0-thalassemia (45-kb deletion).

All 333 deidentified specimens represented the melt curve of the β-globin gene (codon 26 fragment) and were further investigated using HRM analysis. HRM specific to the G/G pattern was related to 95 specimens of β^N/β^N, 71 of $\beta^N/\beta^{3.5\text{-}kb}$, and 28 of $\beta^N/\beta^{45\text{-}kb}$. For the G/A pattern, HRM specificty was observed in 10 specimens of β^N/β^E, 28 of $\beta^E/\beta^{41/42}$, and 9 of β^E/β^{17}. In contrast, the A/A pattern was found in 76 specimens of β^E/β^E, 6 of $\beta^E/\beta^{3.5\text{-}kb}$, and 4 of $\beta^E/\beta^{45\text{-}kb}$. Finally, 6 specimens of HbE/$\beta^{IVSI\#1}$-thalassemia were represented to be specific to the G/A genotype pattern with the $\beta^{IVSI\#1}$-thalassemia pattern (**Figure 2**).

A proposed strategy using rapid melting curve combined HRM analysis for differentiation of β^0-thalassemia/HbE and homozygous HbE was demonstrated in **Figure 4**. According to the diagram, based on Hb analysis with EE or EE/EF, HbE of greater than 80% was usually diagnosed as homozygous HbE in molecular detection; however, β^0-thalassemia/HbE was rarely reported in these groups.[7,14,15] Thus, this strategy is suitable for rapid completely genotyping of homozygous Hb E in a single test tube.

Next we compared the cost-effectiveness of the conventional vs developed method. In our setting, the costs per specimen of RDB and gap-PCR methods are currently US$24.80, and US$16.00, respectively. The overall cost per specimen of molecular testing using the conventional method would be US$40.80, whereas the developed method would be US$4.30. Then, we compared the time consumed per test between the 2 methods. The conventional method takes more than 6 hours per run to perform. whereas our novel method takes less than 2 hours per run. This finding seems to be of such magnitude to merit the implementation of our method in the field, to realize a significant reduction in terms of time and cost.

Discussion

A high frequency of HbE, heterogeneity of β-thalassemia, and genotype interaction of β-globin gene defect in HbE and β-thalassemia have been observed in Southeast Asian populations.[13] The clinical manifestation of HbE is dependent on genotype (ie, heterozygous HbE usually presents with normal Hb levels and mean corpuscular volume [MCV], whereas homozygous HbE is usually associated with a low Hb level or mild anemia and presents with hypochromic microcytic RBC). Coinheritance of HbE with β^0-thalassemia is called HbE/β^0-thalassemia disease, which has a wide clinical manifestation ranging from mild anemia to severe thalassemia disease.[1,3]

Routine Hb analysis is used for initial differentiation of HbE genotypes based on HbA, HbE, and HbF. For homozygous HbE, the EE type (Hb F less than 5%) and compound heterozygous HbE/β^0-thalassemia disease, EF type (Hb F more than 20%) is usually used as diagnostic criterion in routine settings. However, HbF levels ranging from 5% to 20% have also been found in these genotypes.[4,5,7] Recently, the results of 2 studies[14,15] have suggested a simplified method using a score index for
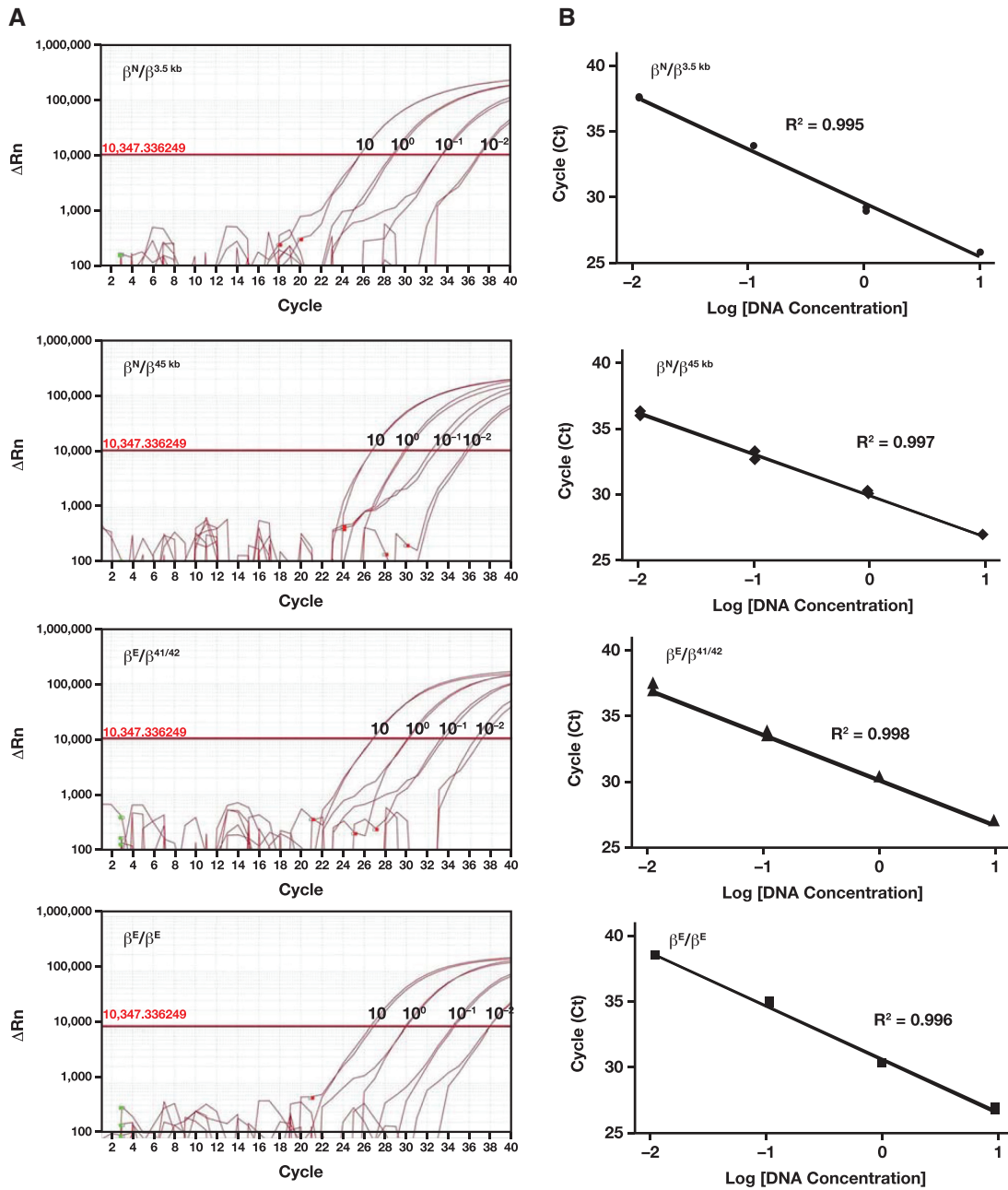
Figure 3

Limit of detection (LOD) values for our novel assay method. To determine the LOD, DNA 10-fold serial dilutions were started with 10 ng/reaction to 0.01 ng/reaction across duplicate dilutions for each of the 4 tested genotypes ($\beta^N/\beta^{3.5-kb}$, β^N/β^{45-kb}, $\beta^E/\beta^{41/42}$, and β^E/β^E) (**A**), To assess the correlation coefficients, the results showed that R^2 values of 0.995, 0.997, 0.998, and 0.996 were related to $\beta^N/\beta^{3.5-kb}$, β^N/β^{45-kb}, $\beta^E/\beta^{41/42}$, and β^E/β^E, respectively (**B**).

differentiation of homozygous HbE and HbE/β^0-thalassemia. However, some cases of E/β^0-thalassemia that was coinherited with α-thalassemia (ie, HbH disease)

showed limited results using these scores, resulting from lower levels of HbA2. Further, another limitation of these scores is that they can only be used to calculate cases in

Table 2. The Validation of Multiplex Melt Curves and HRM Analysis, Compared with the Conventional Method

No.	β-globin Genotype	No.	Development Method in a Single Test Tube			Conventional Method			Interpretation
			Multiplex Melt Curve and HRM Analysis			Multiplex Gap-PCR for β0-thalassemia		RDB Codon 26	
			Melt Curve Analysis for β0-thalassemia		HRM Analysis Codon 26				
			45-kb Deletion	3.5-kb Deletion		45-kb Deletion	3.5-kb Deletion		
1	β^N/β^N	95	−	−	G/G	−	−	G/G	Normal codon 26
2	$\beta^N/\beta^{3.5\text{-kb}}$	71	−	+	G/G	−	+	G/G	Heterozygous β^0-thalassemia (3.5-kb del)
3	$\beta^N/\beta^{45\text{-kb}}$	28	+	−	G/G	+	−	G/G	Heterozygous β^0-thalassemia (45-kb del)
4	β^N/β^E	10	−	−	G/A	−	−	G/A	Heterozygous HbE
5	$\beta^E/\beta^{3.5\text{-kb}}$	6	−	+	A/A	−	+	A/A	Compound heterozygous β^0-thalassemia (3.5-kb deletion)/HbE
6	$\beta^E/\beta^{45\text{-kb}}$	4	+	−	A/A	+	−	A/A	Compound heterozygous β^0-thalassemia (45-kb deletion)/HbE
7	$\beta^E/\beta^{41/42}$	28	−	−	G/A	−	−	G/A	Compound heterozygous β^0-thalassemia/HbE
8	β^E/β^{17}	9	−	−	G/A	−	−	G/A	Compound heterozygous β^0-thalassemia/HbE
9	$\beta^E/\beta^{IVSI\#1}$	6	−	−	E-IVSI#	−	−	G/A	Compound heterozygous β^0-thalassemia/HbE
10	β^E/β^E	76	−	−	A/A	−	−	A/A	Homozygous HbE

HRM, high-resolution melt; PCR, polymerase chain reaction; RDB, reverse dot blot; −, negative; +, positive; Hb, hemoglobin.
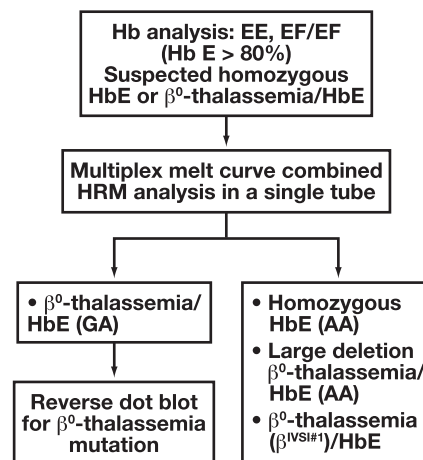

Figure 4

A proposed strategy using rapid melting curve–combined high-resolution melt (HRM) analysis for differentiation of β^0-thalassemia/hemoglobin (Hb)E and homozygous HbE.

which Hb analysis is performed by a method capable of reporting HbA2 (ie, CE but not HPLC).[15] Thus, differentiation of both genotypes needs to be solved by accurate diagnosis using DNA analysis.

DNA analysis for differentiation of homozygous HbE and HbE/β^0-thalassemia is also performed based on ARMS or RDB analysis.[8-10] However, a limitation of HbE/β^0-thalassemia (large deletion [ie, 3.5-kb, 45-kb deletion]) was observed when it was interpreted as homozygous HbE when only the ARMS or RDB analysis is used alone. Hence, β^0-thalassemia with common large deletion should be also applied in DNA analysis.

Two conventional tests, RDB and gap-PCR tests for large deletion are normally performed in our routine setting; however, both methods are time-consuming, labor-intensive, expensive, and require a further post-PCR step. Our newly developed method, validated in the study described herein, can detect HbE genotyping and large deletion in a single test tube, for differentiation of homozygous HbE and HbE/β^0-thalassemia. This novel method requires less time and labor and incurs lower cost, with no need for a post-PCR step, compared with the conventional RDB and gap-PCR methods. Further, gap-PCR in the conventional method should be replaced by our novel method for investigations of heterozygous large deletional β^0-thalassemia, as observed in a case with high HbA2 levels.[9]

LOD analysis was performed in our newly developed method on 4 genotypes: $\beta^N/\beta^{3.5\text{-kb}}$, $\beta^N/\beta^{45\text{-kb}}$, $\beta^E/\beta^{41/42}$,

and β^E/β^E (**Figure 3**). DNA concentration more than 0.01 ng per reaction is represented with accurate results in our newly developed method. However, DNA concentrations are measured before performing molecular analysis in our practical routine. DNA specimens are usually used when the concentration is more than 5 ng per µL. Further, the standard curve plotted between Ct and log[DNA concentration] of 10-fold serial dilutions showed that all 4 genotypes had high correlations with R^2 values of 0.995 to 0.998.

As shown in **Table 2**, the newly developed method showed 100% concordant results in all anonymized specimens, compared with the conventional RDB and gap-PCR methods. For validation, all genotypes were selected based on common β^0-thalassemia mutations in this region. Although a rare β^0-thalassemia at codon 26 mutation (GAG>TAG) has been reported in Thailand, this mutation has the lowest incidence in this region, with only 1 documented case.[16] Thus, a rare mutation (codon26; GAG>TAG) with HbE could have been expected to present in HRM analysis with a different pattern from the developed method. However, no specimen material was available from the archived specimen for validation of this theory.

For reduction of bias in the validation method, we performed the study using different researchers to assign the codes and laboratory practice (one researcher designs the code for de-identify and another one does the experiment). In our differentiation of homozygous HbE and HbE/β^0-thalassemia, specimens with G/A pattern, as determined by HRM analysis, could be identified as having HbE/β^0-thalassemia and should be further investigated for β^0-thalassemia mutations. In contrast, the A/A pattern could definitely be identified as homozygous HbE. Further, the HbE/$\beta^{IVSI\#1}$-thalassemia variant that is common in this region also showed a specific HRM pattern; thus, there was no need to further confirm the identification by performing RDB or ARMS. Sequencing-based confirmation is mandatory to claim the validation of the methodology and to avoid annotation errors in globin genes, as previously described.[17] Nevertheless, in this study, such confirmation was not available in all specimens. However, the other β^0-thalassemia mutations were also confirmed via RDB in our routine setting.

In conclusion, our newly developed method, which uses multiplex melt curve and HRM analysis, is rapid, simple, and cost-effective; does not require a post-PCR step; and can be performed using a single test tube, all of which present advantages compared with conventional methods. Further,

this novel method was validated in several genotypes in the study results. Thus, this method could be applied in routine settings where heterogeneity of HbE disorder and β-thalassemia are common. **LM**

Acknowledgements

Funding

References

1. Fucharoen S, Winichagoon P. Hemoglobinopathies in Southeast Asia. *Hemoglobin.* 1987;11(1):65–88.

2. Tritipsombut J, Sanchaisuriya K, Phollarp P, et al. Micromapping of thalassemia and hemoglobinopathies in different regions of northeast Thailand and Vientiane, Laos People's Democratic Republic. *Hemoglobin.* 2012;36(1):47–56.

3. Nuntakarn L, Fucharoen S, Fucharoen G, Sanchaisuriya K, Jetsrisuparb A, Wiangnon S. Molecular, hematological and clinical aspects of thalassemia major and thalassemia intermedia associated with Hb E-beta-thalassemia in Northeast Thailand. *Blood Cells Mol Dis.* 2009;42(1):32–35.

4. Fucharoen G, Trithipsombat J, Sirithawee S, et al. Molecular and hematological profiles of hemoglobin EE disease with different forms of alpha-thalassemia. *Ann Hematol.* 2006;85(7):450–454.

5. Sae-ung N, Srivorakun H, Fucharoen G, Yamsri S, Sanchaisuriya K, Fucharoen S. Phenotypic expression of hemoglobins A_2, E and F in various hemoglobin E related disorders. *Blood Cells Mol Dis.* 2012;48(1):11–16.

6. Pornprasert S, Moriyama A, Kongthai K, et al. Detection of beta-thalassemia/hemoglobin E disease in samples which initially were diagnosed as homozygous hemoglobin E. *Clin Lab.* 2013;59(5-6):693–697.

7. Wong P, Srichaiya A, Suannum P, et al. Frequency of hemoglobin E/β-thalassemia compound heterozygotes with low hemoglobin F phenotype among cases with a diagnosis of hemoglobin E homozygote, determined by high-performance liquid chromatography, in prenatal control program for β-thalassemia. *Ann Hematol.* 2017;96(10):1763–1765.

8. Fucharoen S, Fucharoen G, Ratanasiri T, Jetsrisuparb A, Fukumaki Y. A simple non-radioactive assay for hemoglobin E gene in prenatal diagnosis. *Clin Chim Acta.* 1994;229(1-2):197–203.

9. Yamsri S, Sanchaisuriya K, Fucharoen G, Sae-Ung N, Fucharoen S. Genotype and phenotype characterizations in a large cohort of β-thalassemia heterozygote with different forms of α-thalassemia in northeast Thailand. *Blood Cells Mol Dis.* 2011;47(2):120–124.

10. Sutcharitchan P, Saiki R, Fucharoen S, Winichagoon P, Erlich H, Embury SH. Reverse dot-blot detection of Thai beta-thalassaemia mutations. *Br J Haematol.* 1995;90(4):809–816.

11. Waye JS, Eng B, Hunt JA, Chui DH. Filipino beta-thalassemia due to a large deletion: identification of the deletion endpoints and polymerase chain reaction (PCR)-based diagnosis. *Hum Genet.* 1994;94(5):530–532.

12. Old J, Traeger-Synodinos J, Galanello R, et al. *Prevention of Thalassemias and Other Haemoglobin Disorders.* 1st ed. Vol. 2. Nicosia, Cyprus: Team Up Creations; 2005.

13. Fukumaki Y, Fucharoen S, Fucharoen G, et al. Molecular heterogeneity of beta-thalassemia in Thailand. *Southeast Asian J Trop Med Public Health.* 1992;23 Suppl 2:14–21.

14. Pornprasert S, Tookjai M, Punyamung M, Kongthai K. A formula to identify potential cases of β-thalassemia/HbE disease among patients with absent HbA, HbE >75% and HbF between 5 and 15. *Lab Med.* 2019;50(2):158–162.

15. Singha K, Fucharoen G, Sanchaisuriya K, Fucharoen S. EE score: an index for simple differentiation of homozygous hemoglobin E and hemoglobin E-β0-thalassemia. *Clin Chem Lab Med.* 2018;56(9):1507–1513.

16. Fucharoen G, Fucharoen S, Jetsrisuparb A, Fukumaki Y. Molecular basis of HbE-β-thalassemia and the origin of HbE in northeast Thailand: identification of one novel mutation using amplified DNA from buffy coat specimens. *Biochem Biophys Res Commun.* 1990;170(2):698–704.

17. Borgio JF. Impact of annotation error in α-globin genes on molecular diagnosis. *PLoS One.* 2017;12(10):e0185270.

Evaluation of HCV RNA by PCR and Signal-to-Cutoff Ratios of HCV Antibody Assays for Diagnosis of HCV Infection

Myeong Hee Kim, MD, So Young Kang, MD, Woo In Lee, MD, Min Young Lee, MD*

ABSTRACT

Objective: In this study, we assessed whether a hepatitis C virus (HCV) RNA test could replace recombinant immunoblot assay (RIBA) and reduce unnecessary supplemental tests as the signal-to-cutoff (S/Co) ratio from anti-HCV antibody (Ab) tests.

Methods: Anti-HCV Ab tests were performed to screen for HCV infections, and RIBA and real-time polymerase chain reaction were performed for HCV RNA to confirm HCV infection. Receiver operating characteristic curves were evaluated to determine the optimal S/Co ratios for predicting HCV infection.

Results: The cutoff value for the S/Co ratio was 3.63 for predicting RIBA results and 10.6 for predicting HCV RNA results. Our data suggested that an S/Co ratio ≥10.6 indicated a high risk of active HCV infection. An S/Co ratio of 3.63 to 10.6 needed further evaluation and repeat HCV RNA testing. No further testing was required for S/Co ratios <3.63 or ≥10.6.

Conclusion: We determined that the S/Co ratio of the anti-HCV Ab test provides useful information to confirm HCV infections, including the need for further laboratory testing or clinical follow-up.

Keywords: HCV infection, RIBA, Anti-HCV Ab, S/Co ratio, HCV RNA, RT-PCR

Hepatitis C virus (HCV) is a major cause of chronic liver disease globally and associated morbidity and mortality.[1] Laboratory testing is important in diagnosis and follow-up of patients with HCV infections. The methods for diagnosing HCV infection are detecting circulating antibodies (Abs) against HCV and detecting HCV RNA.[2] The traditional approach to HCV testing is initial screening for anti-HCV Ab followed by supplementary testing using a recombinant immunoblot assay (RIBA), because of the chance of false positives from anti-HCV Ab tests. Physicians use HCV RNA tests to monitor responses to treatment and sometimes to confirm anti-HCV Ab positivity. However, the strategy for diagnosing HCV infection changed after discontinuation of the RIBA reagent in the United States. In 2013, the Centers for Disease Control and Prevention (CDC)

updated its guidelines for testing for HCV infections, recommending that a reactive result for an anti-HCV Ab test should be followed by an HCV RNA test.[3] Meanwhile, the CDC stated that more studies are needed for a strategy to confirm a diagnosis of HCV infection.[3] Therefore, patients with negative HCV RNA tests are required to have confirmation by further evaluation. Several studies have suggested that RIBA can be substituted with the signal-to-cutoff (S/Co) ratio of the anti-HCV Ab concentration.[4] In this study, we analyzed whether HCV infection could be diagnosed correctly with an anti-HCV Ab test and an HCV RNA test without RIBA and evaluated the diagnostic performance with and without RIBA and the usefulness of the S/Co ratio.

Abbreviations:

HCV, hepatitis C virus; RIBA, recombinant immunoblot assay; S/Co, signal-to-cutoff; Ab, antibody; CDC, Centers for Disease Control and Prevention; ROC, receiver operating characteristic; PCR, polymerase chain reaction; CI, confidence interval.

Department of Laboratory Medicine, Kyung Hee University School of Medicine and Kyung Hee University Hospital at Gangdong, Seoul, Korea

*To whom correspondence should be addressed.
sykangmd@daum.net

Materials and Methods

Anti-HCV Ab Tests

The Centaur anti-HCV assay is an indirect 2-wash sandwich immunoassay that uses 2 recombinant antigens, c200 (derived from NS3 and NS4) and NS5, and 1 synthetic HCV

core peptide (c22). Specimens with a calculated index value of <0.8 were considered nonreactive. Those with an index value of 0.8 to 1.0 were considered equivocal, and those with a calculated index value >1.0 were considered reactive. We reviewed the S/Co ratio of all positive anti-HCV tests. For supplemental tests, specimens were stored at –70°C until testing.

The RIBA

Specimens that tested positive by the Centaur anti-HCV Ab assay were analyzed using the HCV BLOT 3.0 RIBA (MP Biomedicals, Illkirch, France). This assay uses nitrocellulose strips containing recombinant HCV proteins for the core, NS3-1, NS3-2, NS4, and NS5 antigens. The intensity of the reactive bands was compared to the intensity of the control bands of anti-IgG and IgG. The test results were interpreted according to the manufacturer's criteria: the absence of bands of 1+ or greater reactivity was considered negative, 1+ or greater reactivity to ≥2 HCV antigens or 2+ or greater reactivity to the core band only was considered positive, and any single band of 1+ or greater reactivity that did not meet the criteria for positivity was considered indeterminate.

HCV RNA Tests

Serum specimens were tested for HCV RNA using the COBAS AmpliPrep/COBAS TaqMan HCV Quantitative tests (Roche Diagnostics International Ltd, Rotkreuz, Switzerland) on a COBAS AmpliPrep/COBAS TaqMan Analyzer. This test detects genotypes 1 through 6 of HCV viral RNA with a detection range of 15 IU/mL to 1×10^8 IU/mL.

Data Analysis

The Ab S/Co ratio was evaluated and compared with the RIBA and HCV RNA status. Receiver operating characteristic (ROC) curves were constructed by plotting sensitivity vs 1-specificity; the ROC curves and the area under the ROC curves with a 95% confidence interval were determined using IBM SPSS20 (IBM Corp, Armonk, NY).

Results

We analyzed a total of 165 serum specimens that were positive for anti-HCV Ab for this study. The demographic

characteristics of donors are shown in **Table 1**. Of the 165 positive anti-HCV Ab specimens, 119 (72.1%) showed normal levels of alanine aminotransferase at 40 IU/L and 46 (27.9%) had levels ≥40 IU/L. One hundred twenty-five specimens (75.8%) were RIBA-positive, 7 (4.2%) were RIBA-indeterminate, and 33 (20.0%) were RIBA-negative. In addition, results indicated that 72 specimens (43.6%) were positive for HCV RNA according to polymerase chain reaction (PCR) and that 93 (56.4%) were negative.

The status of HCV infection was defined according to the results of the RIBA and HCV RNA tests among the anti-HCV Ab-positive specimens (**Table 2**). Of patients who provided anti-HCV Ab-positive specimens, 72 (43.6%) had current infections and 33 (20.0%) had false positives. If both RIBA and HCV RNA were negative, then false positive anti-HCV Ab tests were considered: 53 patients (32.1%) with RIBA-positives and HCV RNA-negatives were considered to be from "accidental finding of RIBA positivity" after chart reviews. Among these 53 patients, 18 received treatment for HCV infection and 35 had no history of infection. Seven cases were indeterminate for RIBA and were considered to need repeated tests.

The cutoff values for the S/Co ratio were determined by ROC curve analysis based on RIBA and HCV RNA results. The cutoff value for the S/Co ratio for predicting RIBA results was 3.63 (sensitivity 95.2%, specificity 67.5%), and

Table 1. Clinical and Laboratory Characteristics of Patients Who Were Anti-HCV Ab-Positive (n = 165)

Characteristics	Number
Male:female	90:75
Age, y (mean ± SD)	9–89 (56.2 ± 17.7)
Alanine aminotransferase (IU/L), median (range)	24 (2–1910)
<40	119 (72.1%)
≥40	46 (27.9%)
HCV Ab test (%)	
1.0 ≤ S/Co ratio < 3.6	33 (20.0)
3.6 ≤ S/Co ratio < 10.6	30 (18.2)
S/Co ratio ≥10.6	102 (61.8)
RIBA (%)	
Negative	33 (20.0)
Positive	125 (75.8)
Indeterminate	7 (4.2)
HCV RNA (%)	
Not detected	93 (56.4)
Detected	72 (43.6)

Ab, antibody; HCV, hepatitis C virus; RIBA, recombinant immunoblot assay; S/Co, signal-to-cutoff; SD, standard deviation.

the cutoff value for the S/Co ratio for predicting HCV RNA results was 10.6 (sensitivity 97.2%, specificity 65.6%). The results for RIBA and HCV RNA according to S/Co ratio are shown in **Table 3**.

Discussion

Accurate diagnosis of HCV infection is not simple. Anti-HCV Ab acts as a screening test for HCV infection, but this serology test is not definitive, only suggestive. The current standard for diagnosis of HCV infection is a combination of immunoassays for anti-HCV Ab and molecular assays for HCV RNA.[3] A reactive HCV Ab result indicates a current HCV infection or a past HCV infection that has resolved or is a false positive. Up to 25% of patients with HCV Ab-positive tests have undetectable HCV RNA because they have cleared the infection spontaneously.[5] A negative result does not exclude acute infection.[6] For anti-HCV Ab-positive and HCV RNA-negative tests, RIBA-positive results mean spontaneous healing from an HCV infection. However, because HCV RNA tests may be temporarily negative even during progression from acute hepatitis C infection to chronic hepatitis, even for RIBA-positive or HCV

RNA-negative tests, HCV RNA testing should be repeated after 4 months to 6 months to confirm natural healing.[7] Note that this strategy risks missing patients with HCV infection because the RIBA is not available at this time in most countries. Therefore, investigators are considering and applying various methods to replace RIBA.[4,6]

We analyzed whether HCV infection could be diagnosed correctly with an anti-HCV Ab test and an HCV RNA test without using RIBA. In patients with anti-HCV Ab-positive but negative HCV RNA tests, determining the infection status is difficult. These patients accounted for 93/165 (56.3%) of the specimens in our study (**Table 2**). Of the 93 specimens, 33 were negative on the RIBA test and were considered false positives for anti-HCV Ab. A review of medical records suggested that among the 53 patients with positive RIBA, 18 patients had a resolved infection and the remaining 35 were positive for anti-HCV Ab without symptoms or liver function test findings. It was likely that there were HCV occult infections, so further testing and follow-up were necessary. The remaining 7 patients with HCV RNA negativity had tests read as indeterminate per the RIBA, so additional testing was needed.

After RIBA discontinuation in the United States, HCV RNA PCR has become the supplementary test for diagnosis of HCV infections. However, ruling out low levels of viremia or HCV occult infections for HCV RNA-negative tests is difficult. Previous studies have reported that depending on the S/Co ratio of anti-HCV Ab tests, HCV infection could be diagnosed without additional RIBA.[4,8] In these studies, RIBA was not necessary to confirm a negative anti-HCV test for S/Co ratios <3.0 or to confirm a positive test for ratios ≥20. In our study, we used ROC curve analysis to determine the optimal S/Co ratio of anti-HCV to predict HCV infection. We determined that an S/Co ratio of 3.63 was the optimal cutoff for RIBA-positive HCV infections (**Figure 1** and **Table 3**). When the S/Co ratio was >10.6, all HCV RNA tests were positive and we confirmed HCV infections.

### Table 2. HCV Infection Status of Patients Who Were Anti-HCV Ab-Positive

	RIBA	HCV RNA	Number
False-positive HCV Ab screening	N	N	33 (20.0%)
Probably resolved state	P	N	53 (32.1%)
Treated HCV infection			18
Accidental finding of RIBA positivity			35
Current HCV infection	P	P	72 (43.6%)
Indeterminate	I	N	7 (4.2%)

Ab, antibody; HCV, hepatitis C virus; I, indeterminate; N, negative; P, positive; RIBA, recombinant immunoblot assay.

Table 3. Results of RIBA and HCV RNA PCR According to HCV Ab S/Co Ratio

RIBA	S/Co <3.63		3.63 ≤ S/Co < 10.6		S/Co ≥10.6	
	HCV RNA-positive	HCV RNA-negative	HCV RNA-positive	HCV RNA-negative	HCV RNA-positive	HCV RNA-negative
Positive	1	5	1	17	70	31
Indeterminate	0	3	0	4	0	0
Negative	0	22	0	10	0	1

Ab, antibody; HCV, hepatitis C virus; PCR, polymerase chain reaction; RIBA, recombinant immunoblot assay; S/Co, signal-to-cutoff.
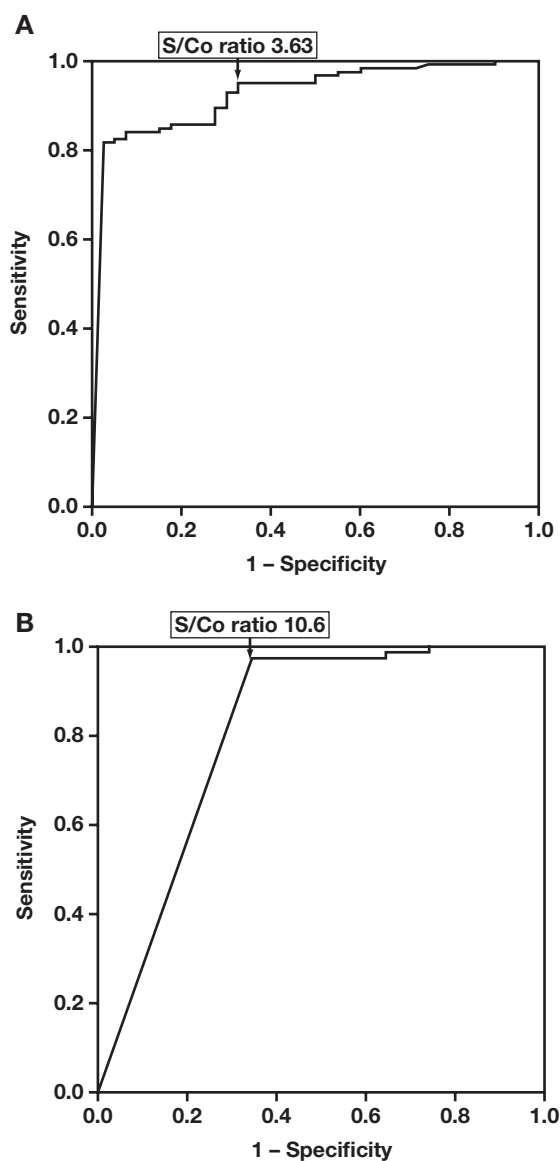
Figure 1

S/Co ratio of anti-HCV Ab tests. Image A, RIBA ROC curve. Image B, HCV RNA test ROC curve. The cutoffs of the S/Co ratios were 3.63 and 10.6. The areas under the curve were 0.927 (95% confidence interval [CI], 0.883–0.971) and 0.813 (95% CI, 0.747–0.880). Ab, antibody; HCV, hepatitis C virus; RIBA, recombinant immunoblot assay; ROC, receiver operating characteristic; S/Co, signal-to-cutoff.

For patients with negative HCV PCR results, the reported S/Co ratios for anti-HCV Ab tests may provide valuable information.[4,8] An S/Co ratio <3.63 in anti-HCV Ab-positive/HCV RNA-negative patients usually indicates a false-positive

reaction, as suggested by studies showing that very low Ab titers reliably indicate false positivity.[9,10] In contrast, a negative HCV RNA result with an S/Co ratio >10.6 means clearance of a past HCV infection. In our study, 97.2% (70/72) of patients with HCV RNA-positive tests had S/Co ratios >10.6 and 1 HCV RNA-positive patient had an S/Co ratio <3.63. Therefore, our data suggested that a S/Co ratio ≥10.6 carries a high risk of active HCV infection and that no further testing is required if the S/Co ratio is <3.63 or ≥10.6.

Patients with HCV RNA-negative specimens and anti-HCV Ab S/Co ratios ≥10.6 should repeat testing in 6 months to rule out active HCV infection because previous studies have reported that HCV RNA may not be detectable in some patients during the acute phase and that intermittent HCV positivity has been observed in patients with chronic HCV infection.[8,11,12] In addition, patients with anti-HCV Ab S/Co ratios between 3.63 and 10.6 need further evaluation and repeated HCV RNA tests. However, because the S/Co ratio for HCV confirmation varies with reagents, the appropriate cutoff must be determined in each laboratory. In addition, when conducting tests for HCV infection, physicians should consider the limitations of each test method. Each laboratory should adopt criteria and report results appropriately.

The limitations of this study include the fact that the number of specimens was relatively small to set the cutoff. Because the anti-HCV Ab test, RIBA, and HCV RNA were difficult to perform simultaneously, it was not easy to collect the specimens. In addition, because the anti-HCV Ab test was performed using only the Centaur anti-HCV Ab assay, it is difficult to apply the same cutoff value in a laboratory using other equipment. Therefore, more appropriate cutoff values can be obtained if more specimens are evaluated using various equipment.

Conclusion

We proposed the S/Co ratio for anti-HCV Ab tests as a method to help confirm HCV infection along with HCV RNA tests after discontinuation of the RIBA. To confirm HCV infection, specimens with an S/Co ratio between 3.63 and 10.6 should be followed up with HCV RNA tests when using the Centaur anti-HCV assay. However, if specimens have

an S/Co ratio <3.63 or ≥10.6, then physicians can confirm negative or positive results, respectively, without supplemental tests. We determined that an S/Co ratio for an anti-HCV Ab test can provide useful information to confirm HCV infection, including the need for further laboratory testing or clinical follow-up. **LM**

References

1. Global hepatitis report, 2017. World Health Organization website. http://www.who.int/hepatitis/publications/global-hepatitis-report2017/en/. Published April 2017. Accessed August 12, 2020.

2. Patel K, Muir AJ, McHutchison JG. Diagnosis and treatment of chronic hepatitis C infection. *BMJ.* 2006;332(7548):1013–1017.

3. Centers for Disease Control and Prevention (CDC). Testing for HCV infection: an update of guidance for clinicians and laboratorians. *MMWR Morb Mortal Wkly Rep.* 2013;62(18):362–365.

4. Lai KK, Jin M, Yuan S, Larson MF, Dominitz JA, Bankson DD. Improved reflexive testing algorithm for hepatitis C infection using signal-to-cutoff ratios of a hepatitis C virus antibody assay. *Clin Chem.* 2011;57(7):1050–1056.

5. Vine LJ, Sieberhagen C, Cramp ME. Diagnosis and management of hepatitis C. *Br J Hosp Med (Lond).* 2015;76(11):625–630.

6. Hassanin TM, Abdelraheem EM, Abdelhameed S, et al. Detection of hepatitis C virus core antigen as an alternative method for diagnosis of hepatitis C virus infection in blood donors negative for hepatitis C virus antibody. *Eur J Gastroenterol Hepatol.* 2019. [Epub ahead of print] doi: 10.1097/MEG.0000000000001647.

7. Ghany MG, Strader DB, Thomas DL, Seeff LB; American Association for the Study of Liver Diseases. Diagnosis, management, and treatment of hepatitis C: an update. *Hepatology.* 2009;49(4):1335–1374.

8. Gong S, Schmotzer CL, Zhou L. Evaluation of quantitative real-time PCR as a hepatitis C virus supplementary test after RIBA discontinuation. *J Clin Lab Anal.* 2016;30(5):418–423.

9. Contreras AM, Tornero-Romo CM, Toribio JG, et al. Very low hepatitis C antibody levels predict false-positive results and avoid supplemental testing. *Transfusion.* 2008;48(12):2540–2548.

10. Oethinger M, Mayo DR, Falcone J, Barua PK, Griffith BP. Efficiency of the ortho VITROS assay for detection of hepatitis C virus-specific antibodies increased by elimination of supplemental testing of samples with very low sample-to-cutoff ratios. *J Clin Microbiol.* 2005;43(5):2477–2480.

11. Hyland C, Seed CR, Kiely P, Parker S, Cowley N, Bolton W. Follow-up of six blood donors highlights the complementary role and limitations of hepatitis C virus antibody and nucleic acid amplification tests. *Vox Sang.* 2003;85(1):1–8.

12. Lemaire JM, Courouce AM, Defer C, et al. HCV RNA in blood donors with isolated reactivities by third-generation RIBA. *Transfusion.* 2000;40(7):867–870.

Evaluation of Transforming Growth Factor-β1 and Interleukin-35 Serum Levels in Patients with Placenta Accreta

Tayyebe Khamoushi, MD[1#], Moslem Ahmadi, PhD,[2#] Mohammad Ali-Hassanzadeh, PhD,[2,3]
Maryam Zare, MSc,[2] Fateme Hesampour, MSc,[2] Behrouz Gharesi-Fard, PhD,[2,4] Sedigheh Amooee, MD[1*]

ABSTRACT

Objective: Placenta accreta is a pregnancy-related disorder with extreme trophoblast invasion and the adherence of the placenta to the uterine wall. This study aimed to investigate the serum level of transforming growth factor-beta 1 (TGF-β1) and interleukin (IL)-35 in patients with placenta accreta.

Methods: Thirty-one women with placenta accreta and 57 healthy pregnant women were enrolled. The serum levels of TGF-β1 and IL-35 were measured using the enzyme-linked immunosorbent assay method.

Results: The serum levels of both TGF-β and IL-35 were significantly higher in the placenta accreta group compared with the group of healthy

women (1082.48 pg/mL vs 497.33 pg/mL and 4541.14 pg/mL vs 1306.04 pg/mL; $P <.001$, respectively). Moreover, the level of TGF-β1 positively correlated with the IL-35 level but other factors such as age, gestations, live births, and abortions did not correlate with IL-35 and TGF-β1 levels.

Conclusion: The serum levels of IL-35 and TGF-β1 may contribute to the pathogenesis of placenta accreta and could be considered as potential targets in clinical and diagnostic approaches.

Keywords: pregnancy, placenta accreta, interleukin-35, transforming growth factor-beta 1

Placenta accreta is a life-threatening condition occurring during pregnancy and characterized by extremely invasive placentation, adherence of the placenta to the uterine wall. and hemorrhage.[1,2] The frequency of this disease is dramatically increasing. Recent reports estimate that placenta accreta affects more than 0.3% of all pregnancies.[3] Several factors including previous Caesarean section, trauma, curettage, and in vitro fertilization pregnancy have been

proposed as main risk factors for the occurrence of placenta accreta.[4,5] Although the pathophysiology and etiology of placenta accreta are not fully understood and need more investigation, several mechanisms have been suggested to be involved in these processes. Extreme angiogenesis, uncontrolled proliferation signaling, increased invasion capacity of trophoblast cells, suppressed apoptosis, and changes in immune cell proportions at the feto-maternal interface are thought to be responsible for the occurrence of placenta accreta.[1]

The immune system and its components, such as immune cells and cytokines, play critical roles in the pregnancy process from conception to delivery.[6] In a successful pregnancy, a local and controlled inflammation is needed for conception and placentation in the first trimester.[7] During pregnancy and especially in the second trimester, a shift toward Th2 and regulatory T cells (Tregs) is critical to protect the fetus from rejection and to support fetus growth. In the third trimester, especially during the final days, a Th1 response is

Abbreviations:

TGF- β1, transforming growth factor-beta 1; IL-35, interleukin-35; Tregs, regulatory T cells.

[1]Department of Obstetrics and Gynecology and [2]Department of Immunology, School of Medicine, Shiraz University of Medical Sciences, Shiraz, Iran, [3]Department of Immunology, School of Medicine, Jiroft University of Medical Sciences, Jiroft, Iran, [4]Infertility Research Center, School of Medicine, Shiraz University of Medical Sciences, Shiraz, Iran

*To whom correspondence should be addressed.
sedighehamooee@gmail.com

#Tayyebe Khamoushi and Moslem Ahmadi contributed equally to the article and are considered as co-first authors.

required for successful delivery and a normal conclusion of pregnancy.[7] It is well documented that dysregulations in immune cells and their products, including cytokines, could lead to pregnancy-related pathological conditions such as intrauterine growth restriction, preterm birth, and pre-eclampsia.[8-10] In the case of placenta accreta, although few investigations have been conducted to spotlight the relationship between placenta accreta and the immune system, an increased level of Treg cells and a decreased level of T cells, decidual natural killer cells, and CD209 cells have been shown to be associated with placenta accreta.[11]

As noted earlier, cytokines play critical roles in a successful pregnancy. Transforming growth factor-beta 1 (TGF-β1) is one of the important cytokines produced mainly by Tregs.[12] This cytokine contributes to anti-inflammatory responses and induction of tolerance during pregnancy. Dysregulated levels of TGF-β1 have been shown in pregnancy-related complications.[13,14] In addition to its immunological roles, TGF-β1 seems to be critical in regulating the balance between proliferation and apoptosis in a large number of cells[15] and plays a role in angiogenesis, trophoblast proliferation, and invasion.[16] In the case of placenta accreta, 1 study investigated the expression of TGF-β1 in the maternal tissues of patients with placenta accreta and reported higher levels of TGF-β1 in myocytes of patients with placenta accreta compared with healthy tissues.[17]

Interleukin-35 (IL-35) is a member of the IL-12 cytokine family with anti-inflammatory properties.[18] The expression of IL-35 was first reported in Tregs but recent findings introduced the trophoblast cells as a constitutive producer of IL-35.[19] Research has indicated that IL-35 seems to be a critical player in the maintenance of normal pregnancy, and dysregulation of this cytokine is reported in association with several pregnancy-related complications.[20] In pre-eclampsia, a condition with impaired placentation and inhibited trophoblast invasion, a reduced level of IL-35 expression has been documented.[21] However, no study has investigated the role of IL-35 in women with placenta accreta so far. Therefore, to advance an understanding of the pathophysiology of placenta accreta and considering the importance of IL-35 and TGF-β1 in normal and complicated pregnancy, the current study was set as the first study to determine the serum levels of IL-35 and TGF-β1 in women with placenta accreta.

Materials and Methods

Study Population

In the current unblinded case-control study, 31 patients with placenta accreta and 51 healthy pregnant control patients were recruited from the gynecology department of Shiraz University of Medical Sciences. Patients and control patients were matched for age. Magnetic resonance imaging and sonography reports were used for diagnosis and confirmation of placenta accreta. Diagnosis of placenta accreta was confirmed by an expert gynecologist based on radiology specialist reports. Furthermore, after the cesarean section, placenta paraffin-embedded specimens were checked by a pathologist, and patients with the absence of pathological features of placenta accreta were excluded. Patients and control patients with other complications such as pre-eclampsia, intrauterine growth restriction, gestational diabetes mellitus, inflammatory or connective tissue disorders, thromboembolic disease, ischemic heart disease, cerebrovascular disease, and drug or substance abuse were also excluded from the study. All patients were also checked for anemia, and none were diagnosed with anemia. Clinical and demographic data such as age, number of gestations, live births, stillbirths, abortions, and previous Caesarean sections were recorded for all participants. Patients and control patients were Caesarean section candidates. All patients participated voluntarily, and the whole process was conducted under the supervision of the ethical committee of Shiraz University of Medical Sciences (ethical code: IR.SUMS.MED.REC.1397.342). Moreover, informed consent was obtained from all of the participants.

Specimen Collection and Cytokine Assay

We collected 5 ml peripheral blood from each patient at the 34th week of gestation. Blood specimens were centrifuged, and sera were separated and preserved at –70°C for further experiments.

The TGF-β1 and IL-35 were measured in the sera using commercially available enzyme-linked immunosorbent assay kits (Bioassay Technology Laboratory, China). Cytokine assays were performed in duplicate according to the manufacturers' protocols. The sensitivity of kits for measuring TGF-β1 and IL-35 was 5.11 pg/L and 0.047 pg/ml, respectively.

Statistical Analysis

Sample size calculation and data analysis were done using SPSS version 16 (SPSS Inc, Chicago, IL), and graphs were designed by GraphPad Prism version 5 (GraphPad Software Inc, San Diego, CA). We assumed 80% power for this study to calculate the sample size. To check the differences between the 2 participant groups, we used the independent-sample t-test and Pearson correlation test to evaluate the potential correlation between independent values. We considered $P < .05$ as significant.

Results

Patients and control patients were first checked for any potential differences in age, number of gestations, live births, abortions, and previous Caesarean sections. Results showed no differences regarding the studied parameters between patients and control patients. Detail data are presented in **Table 1**.

The evaluation of the TGF-β1 serum level indicated a significantly higher mean level of TGF-β1 in the placenta accreta group when compared with healthy women (1082.48 pg/mL vs 497.33 pg/mL; $P < .001$). Similarly, the mean level of IL-35 was significantly increased in patients with placenta accreta in comparison with healthy pregnant women (4541.14 pg/mL vs 1306.04 pg/mL; $P < .001$). Data are summarized in **Figure 1**.

An analysis of correlations between the studied cytokines showed a positive and significant correlation between TGF-β1 and IL-35 levels ($r = 0.537$; $P < .001$). Other factors such as age, number of gestations, live births, abortions, and previous Caesarean sections showed no significant correlations neither either IL-35 or TGF-β1.

Discussion

Generally, the findings of the current study indicated an increase in both IL-35 and TGF-β1 in women diagnosed with placenta accrete, whereas other factors such as age, number of gestations, live births, abortions, and previous Caesarean sections showed no differences between patients and healthy women.

In the case of TGF-β1, just 1 previous study investigated the expression of this cytokine in maternal tissue at the feto-maternal interface.[17] In accordance with our findings, the study showed the expression of TGF-β1 in myocytes isolated from patients with placenta accreta. Another study investigated the frequency of immune cells in placental tissue specimens from patients with placenta accreta.[11] Interestingly, that study showed a high frequency of Tregs in the investigated specimens. Considering that Tregs are the main source of TGF-β1 cytokines, this finding could also be considered in line with our results.[22]

Because the uncontrolled and extreme invasion of trophoblast and angiogenesis are 2 main features of placenta accreta pathology, factors contributing to trophoblast invasion and angiogenesis may be involved in placenta accreta etiology. Regarding TGF-β1, there are several pieces of evidence indicating the role of TGF-β1 in both trophoblast invasion and angiogenesis.[23,24] One previous study documented that the TGF-β1/SMAD signaling pathway is one of the main regulators of trophoblast proliferation and invasion and that TGF-β1 promotes the expression of downstream factors contributing to the proliferation and invasion of HTR-8/SVneo, a human trophoblast cell line.[16] In another study investigating the effects of TGF-β1 on JEG-3, another human trophoblast cell line, researchers showed that TGF-β1 not only induces downstream signaling pathways involved in the proliferation and invasion of trophoblast cells but also promotes the expression of matrix metalloproteinases, which are critical for invasion processes.[25]

Table 1. Comparative Analysis of Demographic and Clinical Data between Patients and Control Patients

	Patients (n = 31)	Control Patients (n = 57)	P Value
Age, y	34.25 ± 5.76[a]	32.03 ± 4.41	.067
Gestation	3.77 ± 1.54	3.45 ± 1.03	.30
Live birth	1.7 ± 0.73	1.68 ± 0.68	.87
Abortion	0.83 ± 0.89	0.71 ± 0.88	.55
Previous Caesarean section	1.74 ± 0.85	1.57 ± 0.68	.36

[a]Data are presented as mean ± SD.
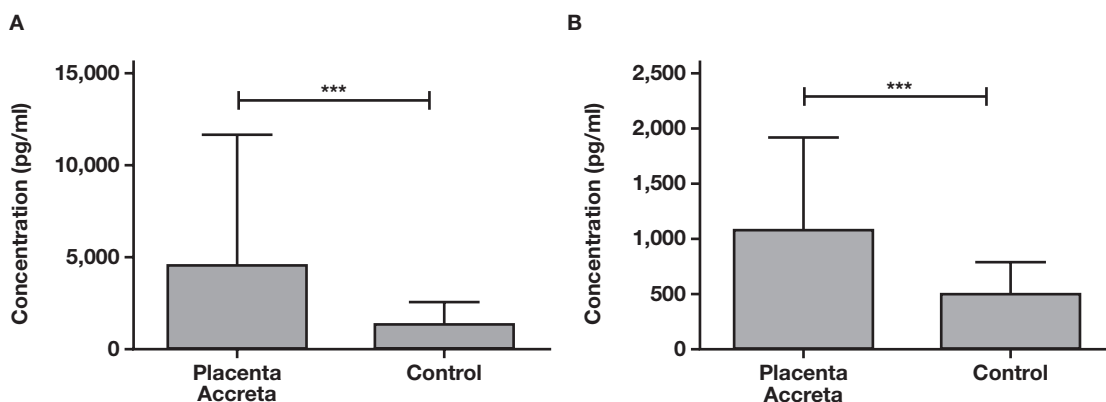
Figure 1

Comparison of IL-35 (**A**) and TGF-β1 (**B**) serum levels between placenta accreta and healthy women. Both IL-35 and TGF-β1 were significantly elevated in women complicated with placenta accreta.*** indicates *P* values less than .001.

In the absence of sufficient evidence about the serum level of cytokines in patients with placenta accreta, it may be useful to compare the findings of the current study to other pregnancy-related complications such as preeclampsia. Whereas in placenta accreta extreme and invasive placentation is the main feature, pre-eclampsia is associated with defective trophoblast invasion and incomplete placentation.[1,26] In terms of TGF-β1, previous studies have indicated a reduced level of TGF-β1 in the sera of patients with pre-eclampsia and have suggested that this reduced serum level of TGF-β1 is a bio-marker in these patients.[21] This finding could count as an in-direct documentation of the association of the TGF-β1 serum level in the placentation process with placenta accreta.

The higher level of IL-35 in patients with placenta accreta was another main finding of the current study. This is the first report on IL-35 in patients with placenta accreta. Research has shown that IL-35 was first noted as a cyto-kine produced by Tregs. Later investigations showed that trophoblast cells are the main source of IL-35 during pregnancy. These studies showed a higher level of IL-35 in normal pregnancies and suggested IL-35 as a key regulator of fetal-maternal immune tolerance.[19,20]

Although the effects of IL-35 on the placentation process, trophoblast invasion, and angiogenesis during pregnancy need further investigation, evidence from other diseases such as cancer may help elucidate the roles of IL-35 in in-vasion and angiogenesis. One study showed that a higher serum level of IL-35 contributes to the aggressive form of hepatocellular cancer and a higher invasion capacity of

cancer cells.[27] Furthermore, another study showed that IL-35 induces proliferation and invasion in cancer cells and is involved in the angiogenesis process in the tumor mi-lieu.[28] Similar to TGF-β1, IL-35 is also documented as being downregulated in patients with pre-eclampsia.[21,29] This factor may indirectly explain the role of IL-35 in the placentation process and consequently in placenta accrete, but more investigations are needed to understand the role of IL-35 in trophoblast proliferation and invasion and extreme placenta-tion in patients with placenta accreta.

Conclusion

Together, the current study proposed TGF-β1 and IL-35 as 2 cytokines involved in the pathogenesis of placenta accreta and introduced them as potential targets for further diagnostic and therapeutic studies and approaches. However, there are still several questions to be answered in further studies. Assessing the expression level of these cytokines in the placental tissue of patients with placenta accreta and investigating the direct effects of these cytokines in human primary trophoblast cells will provide a better perception of their roles in the induction of placenta accreta. We also recommend investigating other in-flammatory or anti-inflammatory cytokines that may contribute to the placentation process. Investigating other cytokines will help provide a more comprehensive understanding of the role of the cytokine network on placenta accreta. **LM**

Acknowledgments

References

1. Bartels HC, Postle JD, Downey P, Brennan DJ. Placenta accreta spectrum: a review of pathology, molecular biology, and biomarkers. *Dis Markers.* 2018;2018:1507674.

2. Jauniaux E, Chantraine F, Silver RM, Langhoff-Roos J; FIGO Placenta Accreta Diagnosis and Management Expert Consensus Panel. FIGO consensus guidelines on placenta accreta spectrum disorders: epidemiology. *Int J Gynaecol Obstet.* 2018;140(3):265–273.

3. Higgins MF, Monteith C, Foley M, O'Herlihy C. Real increasing incidence of hysterectomy for placenta accreta following previous caesarean section. *Eur J Obstet Gynecol Reprod Biol.* 2013;171(1):54–56.

4. Garmi G, Salim R. Epidemiology, etiology, diagnosis, and management of placenta accreta. *Obstet Gynecol Int.* 2012;2012(8):873929.

5. Esh-Broder E, Ariel I, Abas-Bashir N, Bdolah Y, Celnikier DH. Placenta accreta is associated with IVF pregnancies: a retrospective chart review. *BJOG.* 2011;118(9):1084–1089.

6. PrabhuDas M, Bonney E, Caron K, et al. Immune mechanisms at the maternal-fetal interface: perspectives and challenges. *Nat Immunol.* 2015;16(4):328–334.

7. Mor G, Cardenas I, Abrahams V, Guller S. Inflammation and pregnancy: the role of the immune system at the implantation site. *Ann N Y Acad Sci.* 2011;1221:80–87.

8. Gomez-Lopez N, StLouis D, Lehr MA, Sanchez-Rodriguez EN, Arenas-Hernandez M. Immune cells in term and preterm labor. *Cell Mol Immunol.* 2014;11(6):571–581.

9. Laresgoiti-Servitje E. A leading role for the immune system in the pathophysiology of preeclampsia. *Journal of Leukocyte Biology.* 2013;94(2):247–257.

10. Raghupathy R. Cytokines as key players in the pathophysiology of preeclampsia. *Med Princ Pract.* 2013;22(Suppl 1):8–19.

11. Schwede S, Alfer J, von Rango U. Differences in regulatory T-cell and dendritic cell pattern in decidual tissue of placenta accreta/increta cases. *Placenta.* 2014;35(6):378–385.

12. Konkel JE, Zhang D, Zanvit P, et al. Transforming growth factor-β signaling in regulatory T cells controls T helper-17 cells and tissue-specific immune responses. *Immunity.* 2017;46(4):660–674.

13. Ogasawara MS, Aoki K, Aoyama T, et al. Elevation of transforming growth factor-beta1 is associated with recurrent miscarriage. *J Clin Immunol.* 2000;20(6):453–457.

14. Huber A, Hefler L, Tempfer C, Zeisler H, Lebrecht A, Husslein P. Transforming growth factor-beta 1 serum levels in pregnancy and pre-eclampsia. *Acta Obstet Gynecol Scand.* 2002;81(2):168–171.

15. Kaminska B, Kocyk M, Kijewska M. TGF beta signaling and its role in glioma pathogenesis. *Adv Exp Med Biol.* 2013;986:171–187.

16. Zuo Y, Fu Z, Hu Y, et al. Effects of transforming growth factor-β1 on the proliferation and invasion of the HTR-8/SVneo cell line. *Oncol Lett.* 2014;8(5):2187–2192.

17. Duzyj CM, Buhimschi IA, Laky CA, et al. Extravillous trophoblast invasion in placenta accreta is associated with differential local expression of angiogenic and growth factors: a cross-sectional study. *BJOG.* 2018;125(11):1441–1448.

18. Zheng XF, Hu XY, Ma B, et al. Interleukin-35 Attenuates D-Galactosamine/Lipopolysaccharide-Induced Liver Injury via Enhancing Interleukin-10 Production in Kupffer Cells. *Front Pharmacol.* 2018;9:959.

19. Mao H, Gao W, Ma C, et al. Human placental trophoblasts express the immunosuppressive cytokine IL-35. *Hum Immunol.* 2013;74(7):872–877.

20. Yue CY, Zhang B, Ying CM. Elevated serum level of IL-35 associated with the maintenance of maternal-fetal immune tolerance in normal pregnancy. *PLoS One.* 2015;10(6):e0128219.

21. Ozkan ZS, Simsek M, Ilhan F, Deveci D, Godekmerdan A, Sapmaz E. Plasma IL-17, IL-35, interferon-γ, SOCS3 and TGF-β levels in pregnant women with preeclampsia, and their relation with severity of disease. *J Matern Fetal Neonatal Med.* 2014;27(15):1513–1517.

22. Wan YY, Flavell RA. "Yin-Yang" functions of transforming growth factor-beta and T regulatory cells in immune regulation. *Immunol Rev.* 2007;220(1):199–213.

23. Lala PK, Nandi P. Mechanisms of trophoblast migration, endometrial angiogenesis in preeclampsia: the role of decorin. *Cell Adh Migr.* 2016;10(1–2):111–125.

24. Tse WK, Whitley GS, Cartwright JE. Transforming growth factor-beta1 regulates hepatocyte growth factor-induced trophoblast motility and invasion. *Placenta.* 2002;23(10):699–705.

25. Huang Z, Li S, Fan W, Ma Q. Transforming growth factor β1 promotes invasion of human JEG-3 trophoblast cells via TGF-β/Smad3 signaling pathway. *Oncotarget.* 2017;8(20):33560–33570.

26. Fisher SJ. Why is placentation abnormal in preeclampsia? *Am J Obstet Gynecol.* 2015;213(4 Suppl):S115–S122.

27. Fu YP, Yi Y, Cai XY, et al. Overexpression of interleukin-35 associates with hepatocellular carcinoma aggressiveness and recurrence after curative resection. *Br J Cancer.* 2016;114(7):767–776.

28. Liao KL, Bai XF, Friedman A. Mathematical modeling of interleukin-35 promoting tumor growth and angiogenesis. *PLoS One.* 2014;9(10):e110126.

29. Cao W, Wang X, Chen T, et al. The expression of notch/notch ligand, IL-35, IL-17, and Th17/Treg in preeclampsia. *Dis Markers.* 2015;2015(6):1–9.

The Frequency of Discordant Variant Classification in the Human Gene Mutation Database: A Comparison of the American College of Medical Genetics and Genomics Guidelines and ClinVar

Kyoung-Jin Park, MD, PhD,[1] Woochang Lee, MD, PhD,[2*] Sail Chun, MD, PhD,[2]
Won-Ki Min, MD, PhD[2]

ABSTRACT

Objective: Discordant variant classifications among public databases is one of the well-documented limitations when interpreting the pathogenicity of variants. The aim of this study is to investigate the level of germline variant misannotation from the Human Gene Mutation Database (HGMD) and the annotation concordance between databases.

Methods: We used a total of 188,106 classified variants (disease-causing mutations [n = 179,454] and polymorphisms [n = 8652]) in 6466 genes from the HGMD. All variants were reanalyzed based on the American College of Medical Genetics and Genomics (ACMG) guidelines and compared to ClinVar database variants.

Results: When variants were classified based on the ACMG guidelines, misclassification was observed in 3.47% (2289/65,896) of variants. The overall concordance between HGMD and ClinVar was 97.62% (52,499/53,780) of variants studied.

Conclusion: Variants in databases must be used with caution when variant pathogenicity is interpreted. This study reveals the frequency of misannotation of the HGMD variants and annotation concordance between databases in depth.

Keywords: classification, ClinVar, database, Human Gene Mutation Database, pathogenicity, variant

Abbreviations:

aP/aLP, pathogenic/likely pathogenic based on ACMG-AMP guideline; aB/aLB, benign/likely benign based on ACMG-AMP guideline; cP/cLP, pathogenic/likely pathogenic based on ClinVar annotation; cB/cLB, benign/likely benign based on ClinVar annotation; dbSNP, Single Nucleotide Polymorphism Database; HGMD, Human Gene Mutation Database; ACMG, American College of Medical Genetics and Genomics; ACMG-AMP, American College of Medical Genetics and Genomics and Association for Molecular Pathology; 1000GP, 1000 Genomes Project; gnomAD, Genome Aggregation Database; DM, disease-causing mutations; DP, disease-associated polymorphisms; FP, functional polymorphism; DFP, disease-associated polymorphisms with supporting functional evidence; R, Retired records; P/LP, pathogenic/likely pathogenic; B/LB, benign/likely benign; VUS, variants of unknown significance; UTR, untranslated region.

[1]Department of Laboratory Medicine, Myongji Hospital, Hanyang University College of Medicine, Goyang-Si, Gyeonggi-Do, Korea, [2]Department of Laboratory Medicine, Asan Medical Center, University of Ulsan College of Medicine, Seoul, Korea

*To whom correspondence should be addressed.
wlee1@amc.seoul.kr

Accurate variant classification and identification of a pathogenic variant are essential for medical decisions such as tailored therapy, risk stratification, and diagnosis of diseases.[1] However, researchers' understanding of the classification and interpretation of variants is far from perfect. In a clinical laboratory, germline variant classification is based on professional guidelines such as the American College of Medical Genetics and Genomics and the Association for Molecular Pathology (ACMG-AMP) guidelines for the standardized interpretation of these variants.[2]

To find pathogenic (or benign) evidence and prioritize disease-associated variants, disease databases such as the Human Gene Mutation Database (HGMD; http://www.hgmd.cf.ac.uk/ac/index.php) and ClinVar (http://www.ncbi.nlm.nih.gov/clinvar/) are routinely annotated. In addition, general population databases such as the 1000 Genomes Project of the International Genome Sample Resource (1000GP; http://

www.internationalgenome.org), the National Heart, Lung, and Blood Institute Exome Sequencing Project Exome Variant Server (http://evs.gs.washington.edu/EVS/), and the Genome Aggregation Database (gnomAD; http://gnomad.broadinstitute.org/) are used to filter out common benign variants. However, the information in the databases should be used with caution because of the risk that the variant classification may not be correct.[3-9] It is important to understand the frequency of misclassification or annotation discordance in public databases before the assignment of variant pathogenicity.

There have been several efforts to investigate the misclassification of variants from public databases and re-evaluate the pathogenicity in several genes.[3-9] A study by Shah et al[4] showed that ClinVar includes a significant number of misclassified variants that lead to the overestimation of pathogenicity. Another study revealed that up to 27% of *BRCA1* and *BRCA2* variants have discordant classification between ClinVar and a commercial testing laboratory.[3] On the other hand, other studies have shown that pathogenic variants have been identified in general population databases such as gnomAD.[7-9]

Currently, little study regarding the classification of the HGMD variants, which are widely used as a comprehensive collection of germline pathogenic variants causing human inherited diseases, has been performed.[10,11] There are 6 variant annotations classified by the HGMD curators: disease-causing mutations (DM), likely disease-causing mutations but with questionable pathogenicity (DM?), disease-associated polymorphisms (DP); in vitro or in vivo functional polymorphism (FP), disease-associated polymorphisms with supporting functional evidence (DFP), and retired records (R).[10] Several studies have reported that many disease-associated variants in the HGMD have little or no effect on clinical phenotype.[1,12,13] This finding might be explained by the possibility of variant misclassification and variable penetrance. Here we aimed to investigate the level of annotation discordance of the HGMD through the application of ACMG-AMP guidelines as the current standard criteria. In addition, we evaluated whether variant type and allele frequency were associated with annotation discordance. Finally, we evaluated the annotation concordance between the HGMD and ClinVar.

Materials and Methods

We used a total of 190,157 classified variants, which were annotated as DM, DP, DFP, and FP among a total of

229,161 variants in 6970 genes from the HGMD (professional version 2019.01). We removed the DM? (n = 38,630) and R (n = 347) variants. For simplicity, we grouped the variants into 2 sets: the mutSet (consisting of the DM variants; n = 180,092) and the snpSet (sum of the DP [n = 3677], DFP [n = 2293], and FP [n = 4095] variants; n = 10,065; **Figure 1**). In addition, a total of 2051 variants within noncoding RNAs and intergenic areas were excluded. A total of 188,106 HGMD variants in 6466 genes (mutSet [n = 179,454] and snpSet [n = 8652]) were selected for the analyses (**Figure 1**).

First, the ACMG-AMP criteria were applied using the ANNOVAR and InterVar software (intervar_20180118), which generates an automated interpretation of variants.[14,15] In this study, we considered pathogenic and likely pathogenic classification as equivalent and grouped these variants together as P/LP. Similarly, benign and likely benign variants were considered equivalent and categorized as B/LB. After manual reviews of the evidence of pathogenicity, a total of 122,210 unclassified variants were excluded for more simplified and clear analyses. Finally, a total of 65,896 variants (P/LP [n=62,509] + B/LB [n=3,387]) in 4214 genes were analyzed to investigate the frequency of misannotated variants (**Figure 1**). Misclassified variants were defined as either mutSet variants that would be changed into B/LB variants or snpSet variants that would be interpreted as P/LP variants. Because the sample-level information was not available in variant call format downloaded from the HGMD professional version, we calculated the frequency of misclassified variants among the total studied variants.

Second, to assess annotation concordance between databases, we selected 70,026 variants that were registered in both the HGMD and ClinVar (clinVar_20190305: available from March 2019). ClinVar variants with uncertain significance (n = 8374) and ClinVar annotations including *conflicting interpretations of pathogenicity* (n = 2945), *others* (n = 375), and *not provided* (n=4552) were excluded. ClinVar annotations with *risk factor, affects, association, protective,* or *drug response* (n = 596) were considered as clinically significant polymorphisms. Finally, a total of 53,780 variants were considered to check for concordance between HGMD and ClinVar (**Figure 1**).

All studied variants were assigned a pathogenicity category as follows: "P/LP and B/LB" according to ACMG-AMP guidelines and ClinVar annotations were described
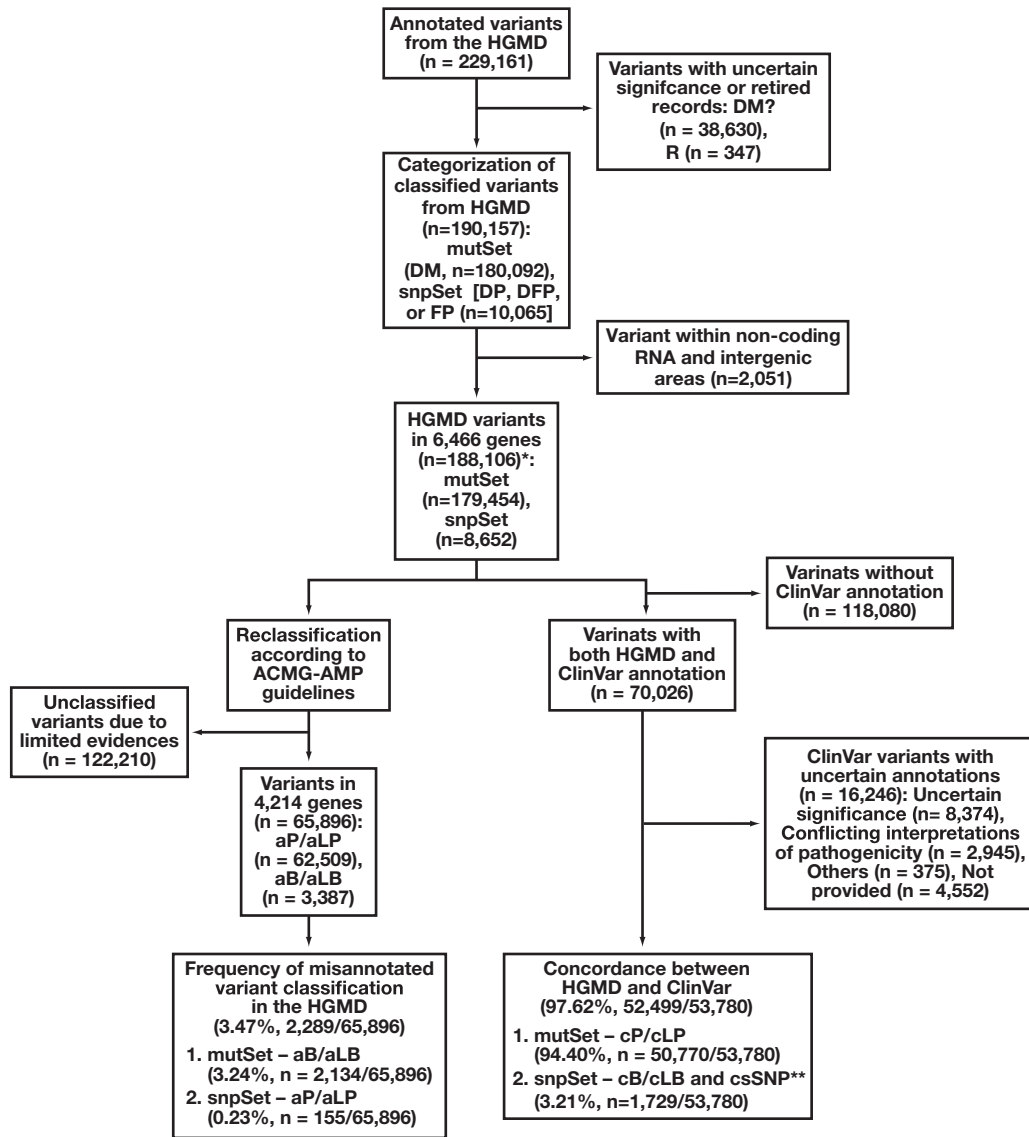
Figure 1

Overall workflow. *Variants with exonic, intronic, promoter, 5 prime, and 3 prime untranslated regions. ** ClinVar annotations with *risk factor, affects, association, protective,* and *drug response* (n = 596) were considered as clinically significant polymorphism (csSNP).

as "aP/aLP and aB/aLB" and "cP/cLP and cB/cLB", respectively. (**Figure 1**). Differences in variant type between discordance and concordance and differences in the ClinVar review status between discordance and concordance were analyzed using the χ^2 test. The statistical significance was analyzed with MedCalc ver11.5.1.0 (Mariakerke, Belgium)

Results

When ACMG-AMP guidelines-based variant classifications were applied to HGMD variants, overall discordance was observed in 3.47% (2289/65,896) of the variants: 3.24% (2134/65,896) of mutSet and 0.24% (155/65,896)

of snpSet (**Table 1**). The discordance was identified in 20.03% (844/4214) of the genes studied. When the misannotated HGMD variants were further compared with the available ClinVar variants (n = 1,128), the 46.81% (1,128; n = 528) of variants was concordant with the ClinVar annotations [mutSet–aB/aLB–cB/cLB (n = 496) or snpSet–aP/aLP–cP/cLP (n=32)]. Among a total of 496 variants misannotated as DM from the HGMD (mutSet–aB/aLB–cB/cLB), a total of 33 variants reviewed by expert panel from ClinGen were shown in **Table 2**. About 21.45% (491/2289) of variants with discordance between the HGDM and ACMG-AMP guidelines were located in 41 known clinically actionable genes; *APC, APOB, BRCA1, BRCA2, COL3A1, DSC2, DSG2, DSP, FBN1, GLA, KCNH2, KCNQ1, LDLR, LMNA, MEN1, MLH1, MSH2, MSH6, MUTYH, MYBPC3, MYH11, MYH7, MYL2, PCSK9, PKP2, PMS2, PTEN, RB1, RET, RYR1, RYR2, SCN5A, SDHD, STK11, TMEM43, TNNI3, TNNT2, TP53, TSC1, TSC2,* and *VHL* (**Table 2**, complete data available upon request).[15]

Discordance differed substantially by variant type (*P* <.0001; **Figure 2**). A total of 65,845 variants in exonic and splicing regions were analyzed. Loss-of-function variants such as frameshift, nonsense, and splicing variants were more observed in concordant variants than discordant variants, and missense and synonymous variants were more common in discordant variants (frameshift: 27.37%, n = 17,393/63,557 vs 0.35%, n = 8/2288; nonsense: 34.96%, n = 22,219/63,557 vs 2.49%, n = 57/2288; splicing: 3.70%, n = 2354/63,557 vs 0.09%, n = 2/2288; missense: 33.49%, n = 21,288/63,6557 vs 81.38%, n = 1862/2288;

and synonymous: 0.48%, n = 303/63,557 vs 15.69%, n = 359/2288; **Figure 2A**). This pattern was replicated in the comparison data between the HGMD and ClinVar (**Figure 2B**).

In addition to variant type, discordance differed by ClinVar review status: the lower the ClinVar review status, the higher the discordance rate (*P* <.0001; **Figure 3**). Discordance was more common in variants for which the ClinVar review status was described as *no assertion criteria provided* (0 gold stars); *criteria provided, single submitter* (1 gold star); and *criteria provided, conflicting interpretations* (1 gold star). On the other hand, concordance was frequently shown in the ClinVar variants, for which the review status was *criteria provided, multiple submitters, no conflicts* (2 gold stars); *reviewed by expert panel* (3 gold stars); and *practice guideline* (4 gold stars) (**Figure 3**).

Overall concordance between the HGMD and ClinVar was 97.62% (52,499/53,780; **Table 1**). Among a total of 1281 discordant variants between the HGMD and ClinVar, a total of 62 variants that were reviewed by expert panel (in ClinVar, 3 gold stars) are shown in **Table 3**. Clinically actionable variants were observed in up to 13.11% (168/1281) of the variants with discordance between the HGMD and ClinVar. These 168 variants were located in 33 known clinically actionable genes; *APC, APOB, BRCA1, BRCA2, CACNA1S, COL3A1, DSP, FBN1, GLA, KCNH2, LDLR, MEN1, MLH1, MSH2, MSH6, MUTYH, MYBPC3, MYH7, PCSK9, PKP2, PTEN, RB1, RET, RYR1, RYR2, SCN5A, SDHD, TMEM43, TNNI3, TP53, TSC1,* and *TSC2* (**Table 3**; complete data available upon request).[15]

Table 1. Concordance of Variant Annotation between HGMD and ACMG-AMP Guidelines-Based Classification and ClinVar

	HGMD vs ACMG-AMP (n = 65,896)		HGMD vs ClinVar (n = 53,780)	
	Concordant, % (n)	**Discordant, % (n)**	**Concordant, % (n)**	**Discordant, % (n)**
mutSet				
DM	91.62% (n = 60,375)	3.24% (n = 2134)	94.40% (n = 50,770)	2.20% (n = 1183)
snpSet				
DFP	1.12% (n = 741)	0.03% (n = 20)	1.04% (n = 558)	0.05% (n = 25)
DP	2.68% (n = 1764)	0.05% (n = 31)	1.53% (n = 821)	0.04% (n = 23)
FP	1.10% (n = 727)	0.16% (n = 104)	0.65% (n = 350)	0.09% (n = 50)
Subtotal	4.90% (n = 3232)	0.24% (n = 155)	3.21% (n = 1729)	0.18% (n = 98)
Total	96.53% (n = 63,607)	3.47% (n = 2289)	97.62% (n = 52,499)	2.38% (n = 1281)

ACMG, American College of Medical Genetics and Genomics; AMP, Association for Molecular Pathology; DM, disease-causing mutation; DP, disease-associated polymorphisms; FP, functional polymorphism; DFP, disease-associated polymorphisms with supporting functional evidence; HGMD, Human Gene Mutation Database.
Concordance includes both mutSet-P/LP pairs and snpSet-B/LB pairs. Discordance includes both mutSet-B/LB pairs and snpSet-P/LP pairs.

Table 2. Examples of Benign or Likely Variants Among Variants Misannotated as DM from the HGMD

Gene Symbol	Transcript	NT	AA	Type	dbSNP	ACMG-AMP	Evidence	Review status[a]	ClinVar	HGMD
MSH2	NM_000251.2	c.4G>A	p.A2T	Missense	rs63750466	aB/aLB	BP1, BP6	3	cB/cLB	DM
MSH2	NM_000251.2	c.304G>A	p.V102I	Missense	rs193922373	aB/aLB	BP1, BP6	3	cB/cLB	DM
MSH2	NM_000251.2	c.593A>G	p.E198G	Missense	rs63750327	aB/aLB	BP1, BP6	3	cB/cLB	DM
MSH2	NM_000251.2	c.1690A>G	p.T564A	Missense	rs55778204	aB/aLB	BP1, BP6	3	cB/cLB	DM
MSH2	NM_000251.2	c.2714C>G	p.T905R	Missense	rs267608022	aB/aLB	BP1, BP6	3	cB/cLB	DM
MSH6	NM_000179.2	c.161G>C	p.G54A	Missense	rs63751098	aB/aLB	BP1, BP6	3	cB/cLB	DM
MSH6	NM_000179.2	c.1019T>C	p.F340S	Missense	rs61753793	aB/aLB	BP1, BP6	3	cB/cLB	DM
MSH6	NM_000179.2	c.1403G>A	p.R468H	Missense	rs41295268	aB/aLB	BP1, BP6	3	cB/cLB	DM
MLH1	NM_000249.3	c.803A>G	p.E268G	Missense	rs63750650	aB/aLB	BP1, BP6	3	cB/cLB	DM
MLH1	NM_000249.3	c.845C>G	p.A282G	Missense	rs63750360	aB/aLB	BP1, BP6	3	cB/cLB	DM
MLH1	NM_000249.3	c.977T>C	p.V326A	Missense	rs63751049	aB/aLB	BS2, BP1, BP6	3	cB/cLB	DM
MLH1	NM_000249.3	c.1733A>G	p.E578G	Missense	rs63751612	aB/aLB	BP1, BP6	3	cB/cLB	DM
MLH1	NM_000249.3	c.1742C>T	p.P581L	Missense	rs63751684	aB/aLB	BS2, BP1, BP6	3	cB/cLB	DM
MLH1	NM_000249.3	c.1853A>C	p.K618T	Missense	rs63750449	aB/aLB	BS1, BS2, BP1, BP6	3	cB/cLB	DM
MLH1	NM_000249.3	c.2074T>C	p.S692P	Missense	rs587779957	aB/aLB	BP1, BP4	3	cB/cLB	DM
MLH1	NM_000249.3	c.2101C>A	p.Q701K	Missense	rs63750114	aB/aLB	BS1, BS2, BP1, BP6	3	cB/cLB	DM
BRCA2	NM_000059.3	c.231T>G	p.T77=	Synonymous	rs114446594	aB/aLB	BS1, BS2, BP4, BP6, BP7	3	cB/cLB	DM
BRCA2	NM_000059.3	c.1395A>T	p.V465=	Synonymous	rs11571641	aB/aLB	BP4, BP6, BP7	3	cB/cLB	DM
BRCA2	NM_000059.3	c.4656T>C	p.G1552=	Synonymous	rs41293491	aB/aLB	BP4, BP6, BP7	3	cB/cLB	DM
BRCA2	NM_000059.3	c.5710C>G	p.L1904V	Missense	rs55875643	aB/aLB	BS2, BP1, BP6	3	cB/cLB	DM
BRCA2	NM_000059.3	c.7992T>A	p.I2664=	Synonymous	rs80359800	aB/aLB	BS2, BP4, BP6, BP7	3	cB/cLB	DM
MYH7	NM_000257.3	c.77C>T	p.A26V	Missense	rs186964570	aB/aLB	BS1, BP6	3	cB/cLB	DM
CDH1	NM_004360.4	c.892G>A	p.A298T	Missense	rs142282590	aB/aLB	BS2, BP6	3	cB/cLB	DM
CDH1	NM_004360.4	c.1018A>G	p.T340A	Missense	rs116093741	aB/aLB	BS2, BP4	3	cB/cLB	DM
CDH1	NM_004360.4	c.2494G>A	p.V832M	Missense	rs35572355	aB/aLB	PS3, PM1, PM2, PP3, PP5	3	cB/cLB	DM
BRCA1	NM_007294.3	c.5095C>A	p.R1699=	Synonymous	rs55770810	aB/aLB	BP4, BP6, BP7	3	cB/cLB	DM
BRCA1	NM_007294.3	c.4955T>C	p.M1652T	Missense	rs80356968	aB/aLB	BP1, BP6	3	cB/cLB	DM
BRCA1	NM_007294.3	c.4910C>T	p.P1637L	Missense	rs80357048	aB/aLB	BP1, BP6	3	cB/cLB	DM
BRCA1	NM_007294.3	c.3022A>G	p.M1008V	Missense	rs56321129	aB/aLB	BS2, BP1, BP4, BP6	3	cB/cLB	DM
BRCA1	NM_007294.3	c.2322T>A	p.G774=	Synonymous	rs397508958	aB/aLB	BP4, BP6, BP7	3	cB/cLB	DM
BRCA1	NM_007294.3	c.1865C>T	p.A622V	Missense	rs56039126	aB/aLB	BP1, BP4, BP6	3	cB/cLB	DM
BRCA1	NM_007294.3	c.1486C>T	p.R496C	Missense	rs28897676	aB/aLB	BP1, BP4, BP6	3	cB/cLB	DM
BRCA1	NM_007294.3	c.736T>G	p.L246V	Missense	rs28897675	aB/aLB	BS2, BP1, BP6	3	cB/cLB	DM

AA, amino acid; ACMG, American College of Medical Genetics and Genomics; AMP, Association for Molecular Pathology; DM, disease-causing mutation; aB/aLB, benign/likely benign based on ACMG-AMP guideline; cB/cLB, benign/likely benign based on ClinVar annotation; HGMD, Human Gene Mutation Database; NA, not applicable; NT, nucleotide; dbSNP, Single Nucleotide Polymorphism Database.

[a]The evidences from ACMG-AMP guideline include BP1 (missense variant in a gene for which truncating variants cause diseases), BP4 (multiple lines of computational evidences suggest no impact), BP6 (Recent source reports variants as benign), BP7 (synonymous variant predict to have no impact by splicing prediction algorithms), BS1 (allele frequency greater than expected for diseases), BS2 (variant observed in a healthy individual with full penetrance) PM1 (variant located in a mutational hotspot or critical functional domain), PM2 (variant with extremely low frequency in control databases), PP3 (multiple lines of computational evidence support a deleterious effect, and PP5 (Recent source reports variants as pathogenic).
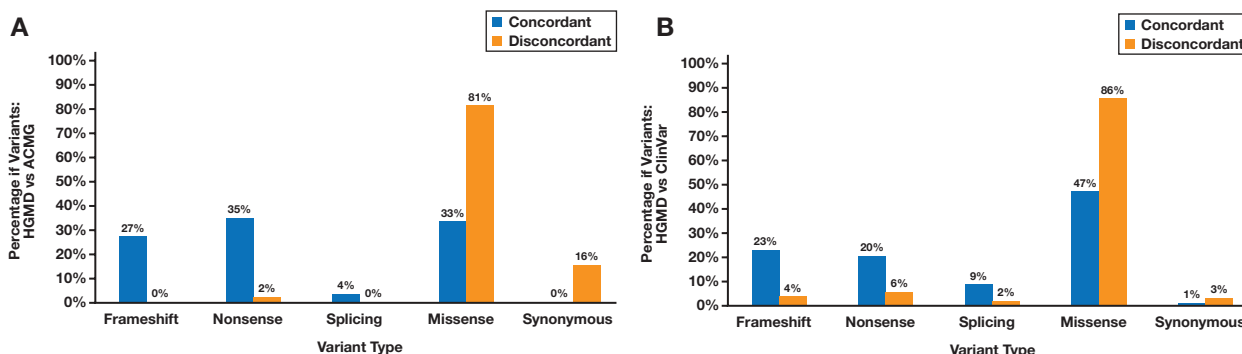
Figure 2

Comparison of HGMD variant type and concordance. **A**, HGMD annotations vs ACMG-AMP guidelines-based variant interpretation. **B**, HGMD annotations vs ClinVar annotations.
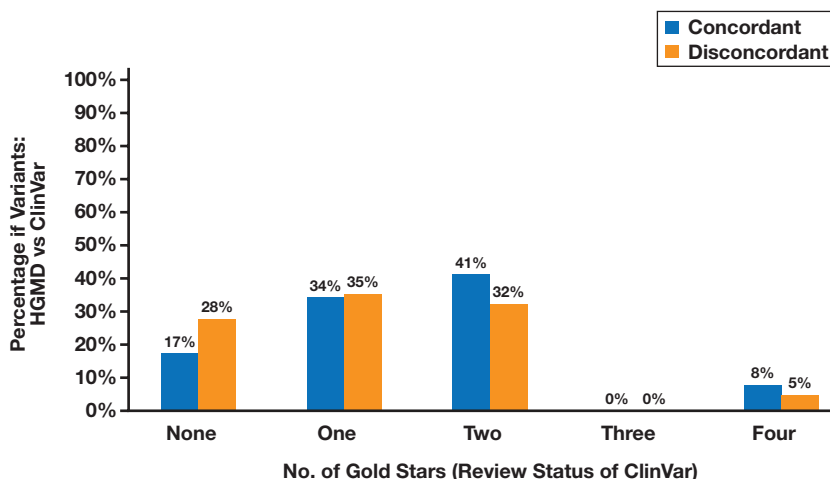
Figure 3

Comparison of review status of ClinVar and database concordance. Number of gold stars: none (no assertion criteria provided), 1 (criteria provided, single submitter or criteria provided, conflicting interpretations), 2 (criteria provided, multiple submitters, no conflicts), 3 (reviewed by expert panel), or 4 (practice guideline).

Discussion

This study highlighted the annotation discordance between databases and the misclassification level in the HGMD. Our findings revealed that the overall discordance was less than 4% of the total studied variants of the HGMD and that the annotation concordance between these public databases was approximately 98%. It is interesting that the frequency of discordance in mutSet (from DM to aB/aLB, 3.24% [2134/65,896]) was higher than those in snpSet (from DP/DFP/FP to aP/aLP, 0.24% [155/65,896]). This reflects the

tendency of the ACMG-AMP guidelines to minimize false positives and a curation policy of the HGMD that aims to minimize false negatives.[10]

Furthermore, classifications of 47% of these discordant variants were supported by ClinVar annotations, indicating that concurrent use of multiple databases including the HGMD and ClinVar would be recommended for the accurate classification of germline variants. In particular, information about the review status of ClinVar could contribute significantly to the concordance between databases and the accuracy of germline variant interpretation (**Figure 3**).

Table 3. Examples of Discordant Variants Between the HGMD and ClinVar

Gene Symbol	Transcript	NT	AA	Type	dbSNP	Review Status	ClinVar	HGMD
DPYD	NM_000110.3	c.2846A>T	p.D949V	Missense	rs67376798	3	Drug response	DM
DPYD	NM_000110.3	c.1905 + 1G>A	NA	Splicing	rs3918290	3	Drug response	DM
DPYD	NM_000110.3	c.1679T>G	p.I560S	Missense	rs55886062	3	Drug response	DM
MSH2	NM_000251.2	c.4G>A	p.A2T	Missense	rs63750466	3	cB/cLB	DM
MSH2	NM_000251.2	c.279_281delTCT	p.(Leu94del)	Nonframeshift deletion	rs267607919	3	cB/cLB	DM
MSH2	NM_000251.2	c.304G>A	p.V102I	Missense	rs193922373	3	cB/cLB	DM
MSH2	NM_000251.2	c.593A>G	p.E198G	Missense	rs63750327	3	cB/cLB	DM
MSH2	NM_000251.2	c.1690A>G	p.T564A	Missense	rs55778204	3	cB/cLB	DM
MSH2	NM_000251.2	c.2714C>G	p.T905R	Missense	rs267608022	3	cB/cLB	DM
MSH6	NM_000179.2	c.161G>C	p.G54A	Missense	rs63751098	3	cB/cLB	DM
MSH6	NM_000179.2	c.1019T>C	p.F340S	Missense	rs61753793	3	cB/cLB	DM
MSH6	NM_000179.2	c.1403G>A	p.R468H	Missense	rs41295268	3	cB/cLB	DM
MSH6	NM_000179.2	c.2398G>C	p.V800L	Missense	rs61748083	3	cB/cLB	DM
MLH1	NM_000249.3	c.-107C>G	NA	5 prime UTR	rs587778886	3	cB/cLB	DM
MLH1	NM_000249.3	c.803A>G	p.E268G	Missense	rs63750650	3	cB/cLB	DM
MLH1	NM_000249.3	c.845C>G	p.A282G	Missense	rs63750360	3	cB/cLB	DM
MLH1	NM_000249.3	c.977T>C	p.V326A	Missense	rs63751049	3	cB/cLB	DM
MLH1	NM_000249.3	c.1733A>G	p.E578G	Missense	rs63751612	3	cB/cLB	DM
MLH1	NM_000249.3	c.1742C>T	p.P581L	Missense	rs63751684	3	cB/cLB	DM
MLH1	NM_000249.3	c.1853A>C	p.K618T	Missense	rs63750449	3	cB/cLB	DM
MLH1	NM_000249.3	c.2074T>C	p.S692P	Missense	rs587779957	3	cB/cLB	DM
MLH1	NM_000249.3	c.2101C>A	p.Q701K	Missense	rs63750114	3	cB/cLB	DM
MYO6	NM_004999.3	c.2836C>T	p.R946C	Missense	rs141845119	3	cB/cLB	DM
EGFR	NM_005228.4	c.2369C>T	p.T790M	Missense	rs121434569	3	Drug response	DM
CFTR	NM_000492.3	c.220C>T	p.R74W	Missense	rs115545701	3	Drug response	DM
CFTR	NM_000492.3	c.330C>A	p.D110E	Missense	rs397508537	3	Drug response	DM
CFTR	NM_000492.3	c.577G>A	p.E193K	Missense	rs397508759	3	Drug response	DM
CFTR	NM_000492.3	c.1736A>C	p.D579A	Missense	rs397508288	3	Drug response	DM
CFTR	NM_000492.3	c.2930C>T	p.S977F	Missense	rs141033578	3	Drug response	DM
CFTR	NM_000492.3	c.3154T>G	p.F1052V	Missense	rs150212784	3	Drug response	DM
CFTR	NM_000492.3	c.3179A>C	p.K1060T	Missense	rs397508513	3	Drug response	DM
CFTR	NM_000492.3	c.3199G>A	p.A1067T	Missense	rs121909020	3	Drug response	DM
CFTR	NM_000492.3	c.3208C>T	p.R1070W	Missense	rs202179988	3	Drug response	DM
CFTR	NM_000492.3	c.3209G>A	p.R1070Q	Missense	rs78769542	3	Drug response	DM
CFTR	NM_000492.3	c.3222T>A	p.F1074L	Missense	rs186045772	3	Drug response	DM
CFTR	NM_000492.3	c.3454G>C	p.D1152H	Missense	rs75541969	3	Drug response	DM
PTEN	NM_000314.6	c.235G>A	p.A79T	Missense	rs202004587	3	cB/cLB	DM
PTEN	NM_000314.6	c.1026 + 32T>G	NA	Intronic	rs555895	3	cB/cLB	DM
TECTA	NM_005422.2	c.701A>G	p.Q234R	Missense	rs144682235	3	cB/cLB	DM
PTPN11	NM_002834.4	c.925A>G	p.I309V	Missense	rs201787206	3	cB/cLB	DM
PTPN11	NM_002834.4	c.1678C>T	p.L560F	Missense	rs397516797	3	cB/cLB	DM
BRCA2	NM_000059.3	c.231T>G	p.T77=	Synonymous	rs114446594	3	cB/cLB	DM
BRCA2	NM_000059.3	c.1395A>T	p.V465=	Synonymous	rs11571641	3	cB/cLB	DM
BRCA2	NM_000059.3	c.4656T>C	p.G1552=	Synonymous	rs41293491	3	cB/cLB	DM
BRCA2	NM_000059.3	c.5710C>G	p.L1904V	Missense	rs55875643	3	cB/cLB	DM
BRCA2	NM_000059.3	c.7992T>A	p.I2664=	Synonymous	rs80359800	3	cB/cLB	DM
BRCA2	NM_000059.3	c.8969G>A	p.W2990*	Nonsense	rs80359148	3	cP/cLP	FP
BRCA2	NM_000059.3	c.9256G>T	p.G3086*	Nonsense	rs80359192	3	cP/cLP	FP
MYH7	NM_000257.3	c.77C>T	p.A26V	Missense	rs186964570	3	cB/cLB	DM
CDH1	NM_004360.4	c.892G>A	p.A298T	Missense	rs142822590	3	cB/cLB	DM
CDH1	NM_004360.4	c.1018A>G	p.T340A	Missense	rs116093741	3	cB/cLB	DM
CDH1	NM_004360.4	c.2413G>A	p.D805N	Missense	rs200894246	3	cB/cLB	DM
CDH1	NM_004360.4	c.2494G>A	p.V832M	Missense	rs35572355	3	cB/cLB	DM
BRCA1	NM_007294.3	c.5095C>A	p.R1699=	Synonymous	rs55770810	3	cB/cLB	DM
BRCA1	NM_007294.3	c.4955T>C	p.M1652T	Missense	rs80356968	3	cB/cLB	DM
BRCA1	NM_007294.3	c.4910C>T	p.P1637L	Missense	rs80357048	3	cB/cLB	DM

Table 3. Continued

Gene Symbol	Transcript	NT	AA	Type	dbSNP	Review Status	ClinVar	HGMD
BRCA1	NM_007294.3	c.3022A>G	p.M1008V	Missense	rs56321129	3	cB/cLB	DM
BRCA1	NM_007294.3	c.2322T>A	p.G774=	Synonymous	rs397508958	3	cB/cLB	DM
BRCA1	NM_007294.3	c.1865C>T	p.A622V	Missense	rs56039126	3	cB/cLB	DM
BRCA1	NM_007294.3	c.1486C>T	p.R496C	Missense	rs28897676	3	cB/cLB	DM
BRCA1	NM_007294.3	c.736T>G	p.L246V	Missense	rs28897675	3	cB/cLB	DM
MAP2K2	NM_030662.3	c.818A>G	p.K273R	Missense	rs539555837	3	cB/cLB	DM

B/LB, benign/likely benign; DM, disease-causing mutation; FP, functional polymorphism; HGMD, Human Gene Mutation Database, NA, not applicable; P/LP, pathogenic/likely pathogenic; UTR, untranslated region.

Even if the number of discordant variants was relatively small, it is important to acknowledge these variants. Considering that some of the discordances were identified in clinically actionable genes such as *BRCA1,* they are not negligible (**Table 2**). Because accurate variant interpretation is critical in medical decision-making regarding procedures such as prophylactic bilateral salpingo-oophorectomy or cancer screening, careful use of annotations from public databases is required.

The current classification of germline variants is based on the allelic data, clinical data (de novo data, segregation data), functional data, computational data, and population data.[2] Different databases and a number of computational methods have been used to annotate germline variants, and annotation resources and databases are continuously updating and improving at different intervals. Furthermore, the databases do not share the same collection of variants and have different curation policies. In addition, the HGMD and ClinVar have different systems for variant classification: the HGMD has 6 classifications—DM, DM?, DFP, DP, FP, and R—and the ClinVar has a set of clinical significance terms such as *uncertain significance, not provided, benign, likely benign, likely pathogenic, pathogenic, drug response, histocompatibility, other, confers sensitivity, risk factor, association, protective,* and affects. Here, ClinVar annotations with *risk factor, affects, association, protective,* or *drug response* were considered as clinically significant polymorphisms.

A recent study using the ClinVar database revealed that variant types, clinical testing methods, and penetrance could affect concordance rates of within-database annotations.[16] We have shown that loss-of-function variants such as nonsense variants were frequently observed in concordant variants compared with discordant variants. This finding is in line with the results from the previous study.[16]

It may reflect that the PVS1 criterion, which was defined as "null variant in a gene where loss-of-function is a known mechanism of disease" is very strong criteria in ACMG-AMP guidelines-based classification and indicates that further application of the PVS1 criterion could improve the reliability of HGMD annotation.

The current study has some limitations. First, both the aP/aLP and aB/aLB variants defined by the 18 criteria from the ACMG-AMP guidelines were included and 122,210 unclassified variants were totally excluded for a more simplified workflow. To minimize the controversial interpretation of variant pathogenicity, the variants of unknown significance (VUSs) were excluded and both P/LP variants and B/LB variants by criteria were included. The discordance rate in this study may be underestimated because of the exclusion of a number of VUS. A previous study showed that the discordance rate of *BRCA1* and *BRCA2* variants between a public database and single laboratory was 14%.[3] In comparison, the discordance rate of this study was low (<4% vs 14%).[3] The lower rate of discordance can be attributed to the differences in the studied genes, the number of genes studied, the databases used, and the inclusion or exclusion of VUSs.

Second, we used computational tools such as ANNOVAR and InterVar, which is based on 18 criteria to diminish interpretation variability. Even if these tools have been widely used for variant annotation, automatic tools may generate annotation errors.[17,18] For example, InterVar considered the variant of NM_004360.4(CDH1):c.2494G>A (p.V832M) to be a P/LP variant. However, we concluded that the variant was B/LB with manual annotation per classification under the BS1 and BS2 criteria and per the review status of ClinVar (considered as *reviewed by expert panel*). Comprehensive annotation depends on the databases used and the

evidence available for variant interpretation. To avoid inaccurate classification, we manually reviewed the evidence of pathogenicity using multiple databases. In the current study, it was not possible to consider complicated genetic factors or clinical information. Further studies are recommended to improve the process of variant annotation.

Third, the current ACMG-AMP guidelines-based classification is not complete.[2] Previous research has reported that the initial concordance of ACMG-AMP guidelines-based variant classification was only 34% across laboratories.[19] Furthermore, all variants with an allele frequency >0.05 in population databases are classified as benign variants in the current ACMG-AMP guideline. However, a recent study revealed that a few pathogenic variants with an allele frequency >0.05 were associated with hemochromatosis or deafness.[20] Rule BA1, which is defined variants with allele frequency >5% in control databases could result in an overestimation of the discordance in certain genes. In this study, discordance because of rule BA1 occurred in 0.01% (8/62,509) of the DM variants.

MMoreover, the cutoff of the PM2 criterion, which is defined as "the variants with extremely low frequency from controls" in population databases, applied in this study was <0.005, as previously described.[15] However, there is no defined cutoff in the guidelines.[2] Previous studies have reported that ethnicity-specific criteria and gene/disease-specific criteria should be applied to the cutoff of allele frequency to interpret pathogenicity.[21,22] Ethnicity-specific allele frequency was not available in this study. Although some criteria are subjective and uncertain, ACMG-AMP guidelines are the de facto method for clinical variant interpretation.

Conclusion

In summary, the present study adds to the discussion on the possible risks of interpreting germline variants using public databases. Variant classification from public databases must be used with caution. We found that a significant number of benign variants were misannotated as pathogenic variants, whereas pathogenic variants were misannotated as polymorphism in the HGMD. This study revealed a misclassification burden of the HGMD variants and an annotation concordance between databases. Although

a number of unclassified variants were excluded, this study contributes to germline variant interpretation by providing a valuable resource for accurate variant classification. Further clinical studies using well-characterized datasets and updating resources are recommended to improve the process of variant annotation and establish uniform standards for variant classification. **LM**

References

1. Manrai AK, Funke BH, Rehm HL, et al. Genetic misdiagnoses and the potential for health disparities. *N Engl J Med.* 2016;375(7):655–665.

2. Richards S, Aziz N, Bale S, et al.; ACMG Laboratory Quality Assurance Committee. Standards and guidelines for the interpretation of sequence variants: a joint consensus recommendation of the American College of Medical Genetics and Genomics and the Association for Molecular Pathology. *Genet Med.* 2015;17(5):405–424.

3. Gradishar W, Johnson K, Brown K, Mundt E, Manley S. Clinical variant classification: a comparison of public databases and a commercial testing laboratory. *Oncologist.* 2017;22(7):797–803.

4. Shah N, Hou YC, Yu HC, et al. Identification of misclassified ClinVar variants via disease population prevalence. *Am J Hum Genet.* 2018;102(4):609–619.

5. Vail PJ, Morris B, van Kan A, et al. Comparison of locus-specific databases for BRCA1 and BRCA2 variants reveals disparity in variant classification within and among databases. *J Community Genet.* 2015;6(4):351–359.

6. Norton N, Robertson PD, Rieder MJ, et al.; National Heart, Lung, and Blood Institute GO Exome Sequencing Project. Evaluating pathogenicity of rare variants from dilated cardiomyopathy in the exome era. *Circ Cardiovasc Genet.* 2012;5(2):167–174.

7. Tarailo-Graovac M, Zhu JYA, Matthews A, van Karnebeek CDM, Wasserman WW. Assessment of the ExAC data set for the presence of individuals with pathogenic genotypes implicated in severe Mendelian pediatric disorders. *Genet Med.* 2017;19(12):1300–1308.

8. Soussi T, Leroy B, Devir M, Rosenberg S. High prevalence of cancer-associated TP53 variants in the gnomAD database: a word of caution concerning the use of variant filtering. *Hum Mutat.* 2019;40(5):516–524.

9. Kobayashi Y, Yang S, Nykamp K, Garcia J, Lincoln SE, Topper SE. Pathogenic variant burden in the ExAC database: an empirical approach to evaluating population data for clinical variant interpretation. *Genome Med.* 2017;9(1):13.

10. Stenson PD, Mort M, Ball EV, et al. The Human Gene Mutation Database: towards a comprehensive repository of inherited mutation data for medical research, genetic diagnosis and next-generation sequencing studies. *Hum Genet.* 2017;136(6):665–677.

11. Abouelhoda M, Faquih T, El-Kalioby M, Alkuraya FS. Revisiting the morbid genome of Mendelian disorders. *Genome Biol.* 2016;17(1):235.

12. Ghouse J, Have CT, Weeke P, et al. Rare genetic variants previously associated with congenital forms of long QT syndrome have little or no effect on the QT interval. *Eur Heart J.* 2015;36(37):2523–2529.

13. Ghouse J, Have CT, Skov MW, et al. Numerous Brugada syndrome-associated genetic variants have no effect on J-point elevation, syncope susceptibility, malignant cardiac arrhythmia, and all-cause mortality. *Genet Med.* 2017;19(5):521–528.

14. Liu X, Wu C, Li C, Boerwinkle E. dbNSFP v3.0: a one-stop database of functional predictions and annotations for human nonsynonymous and splice-site SNVs. *Hum Mutat.* 2016;37(3):235–241.

15. Kalia SS, Adelman K, Bale SJ, et al. Recommendations for reporting of secondary findings in clinical exome and genome sequencing, 2016 update (ACMG SF v2.0): a policy statement of the American College of Medical Genetics and Genomics. *Genet Med.* 2017;19(2):249–255.

16. Yang S, Lincoln SE, Kobayashi Y, Nykamp K, Nussbaum RL, Topper S. Sources of discordance among germ-line variant classifications in ClinVar. *Genet Med.* 2017;19(10):1118–1126.

17. McCarthy DJ, Humburg P, Kanapin A, et al. Choice of transcripts and software has a large effect on variant annotation. *Genome Med.* 2014;6(3):26.

18. Steward CA, Parker APJ, Minassian BA, Sisodiya SM, Frankish A, Harrow J. Genome annotation for clinical genomic diagnostics: strengths and weaknesses. *Genome Med.* 2017;9(1):49.

19. Amendola LM, Jarvik GP, Leo MC, et al. Performance of ACMG-AMP variant-interpretation guidelines among nine laboratories in the clinical sequencing exploratory research consortium. *Am J Hum Genet.* 2016;99(1):247.

20. Ghosh R, Harrison SM, Rehm HL, Plon SE, Biesecker LG; ClinGen Sequence Variant Interpretation Working Group. Updated recommendation for the benign stand-alone ACMG/AMP criterion. *Hum Mutat.* 2018;39(11):1525–1530.

21. Shearer AE, Eppsteiner RW, Booth KT, et al. Utilizing ethnic-specific differences in minor allele frequency to recategorize reported pathogenic deafness variants. *Am J Hum Genet.* 2014;95(4):445–453.

22. Mester JL, Ghosh R, Pesaran T, et al. Gene-specific criteria for PTEN variant curation: recommendations from the ClinGen PTEN Expert Panel. *Hum Mutat.* 2018;39(11):1581–1592.

The Association Between Serum Human Epididymis Protein 4 Level and Cardiovascular Events in Patients with Chronic Obstructive Pulmonary Disease

Hui Lin, MD,[1] Jianhong Xiao, BD,[1] Xianghua Su, BD,[2] Bin Song, MD[1]*

ABSTRACT

Objective: Serum human epididymis protein 4 (HE4) is associated with immune and inflammatory responses. This study aimed to assess the performance of serum HE4 in the early detection of cardiovascular (CV) events in patients with chronic obstructive pulmonary disease (COPD).

Methods: Serum HE4 levels were measured in 199 patients with COPD, all of whom were prospectively followed up for a median period of 36 months (range = 3 months–38 months). Logistic regression analysis was performed to assess the association between cardiovascular disease (CVD) history and HE4 in patients with COPD. Cox proportional hazard analysis was performed to assess the prognostic value of serum HE4 for predicting CV events.

Results: Serum HE4 levels were higher in patients with COPD with CV events than in those without CV events (252.6 pmol/L [186.4–366.8] vs 111.0 pmol/L [84.8–157.1]; P <.001). The multivariate logistic regression model revealed that serum HE4 (odds ratio = 1.639; 95% confidence interval [CI], 1.213–2.317; P_{trend} =.009) was independently associated with CVD history after adjusting for age, sex, body mass index, current smoking status, current alcohol consumption status, admission systolic blood pressure and diastolic blood pressure, hyperlipidemia, left ventricular ejection fraction, primary diseases, and laboratory measurements in patients with COPD at baseline. The multivariate Cox proportional hazard analysis revealed that serum HE4 (hazard ratio = 2.012; 95% CI, 1.773–4.469; P <.001) was an independent prognostic factor for CV events in these patients. The Kaplan-Meier analysis showed that the rate of CV events was higher in patients with COPD with HE4 levels above the median (187.5 pmol/L) than in those with HE4 levels below the median.

Conclusion: Our results showed that serum HE4 was significantly and independently associated with CVD history and had independent predictive value for CV events in patients with COPD. Serum HE4 may enable early recognition of CV complication development among patients with COPD.

Keywords: human epididymis protein 4, chronic obstructive pulmonary disease, cardiovascular events, cardiovascular events, Cox regression, prognosis

Chronic obstructive pulmonary disease (COPD) is one of the main causes of morbidity and mortality worldwide. Patients with COPD are at increased risk of cardiovascular disease (CVD).[1,2] The early detection of CVD in patients with COPD may provide an opportunity to develop strategies to reduce medical burden and improve prognosis.

Human epididymis protein 4 (HE4), encoded by the *WFDC2* gene located on chromosome 20q12-13.1, is a secretory protein highly expressed in the human epididymis.[3] The HE4 sequence shows a similarity to proteinase inhibitors, which suggests that HE4 may be involved in sperm maturation.[4] The mature HE4 protein is a 20 to 25 kDa glycoprotein found in the cytoplasm and on membranes of cells and in circulation. Studies have reported that HE4 is highly expressed in malignant tumors such as ovarian cancer and endometrial cancer tumors.[5,6] In addition, some studies have shown that HE4 is moderately expressed in multiple normal and abnormal tissues in the human body, such as

Abbreviations

HE4, human epididymis protein 4; CV, cardiovascular; COPD, chronic obstructive pulmonary disease; CVD, cardiovascular disease; CI, confidence interval; HF, heart failure; BMI, body mass index; BP, blood pressure; LVEF, left ventricular ejection fraction; Hb, hemoglobin; FBG, blood glucose; ALB, albumin; NT-proBNP, N-terminal prohormone of B-type natriuretic peptide; eGFR, estimated glomerular filtration rate; HOMA-IR, homeostasis model assessment of insulin resistance; HR, hazard ratio.

[1]Department of Respiratory Medicine and [2]Neurosurgery Department, Mindong Hospital of Fujian Medical University, Fuan, Fujian, China

*To whom correspondence should be addressed.
2990931499@qq.com

the respiratory tract, convoluted tubules of the kidney, and other tissues,[7,8] and it plays a very important role in processes related to immune defense.

Other WFDC proteins with antiproteinase activity have also been correlated with inflammatory processes.[9-11] It has been widely recognized that inflammation is involved in the occurrence and development of CVDs. As a chronic inflammatory disease, COPD can hasten the progression of atherosclerosis and contribute to a higher rate of CVD death.[12,13] Several previous studies have suggested that serum HE4 is associated with worsening cardiac function in patients with heart failure (HF) and has a predictive value for progressive HF.[14-16] Given the close association between HE4 and inflammation,[7,8] we hypothesized that HE4 may be associated with cardiovascular (CV) outcomes in patients with COPD. However, to date, no relevant study has explored the relationship between serum HE4 and CV events in patients with COPD. The aim of this study was to investigate whether increased HE4 levels contribute to the increased risk for CV events, independent of confounding factors. This was also the first study to explore the prognostic value of HE4 for predicting CV events in patients with COPD.

Materials and Methods

Study Population

We studied 199 patients from the National Population Health Science Data Center database in China who were hospitalized because of COPD in an acute stage between January 2015 and December 2016. This database contains the original data of various medical industries in China, so this study has sufficient data to be analyzed. All patients with COPD had been stable for 3 months without other serious acute illnesses before admission. After standardized hospital treatment, all patients were clinically stable during hospitalization and were prospectively followed up after discharge. The diagnosis of COPD was performed by 2 respiratory specialists who used the same diagnostic criteria for these patients according to the Global Initiative for Chronic Obstructive Lung Disease.[17] Of these patients, 40 had a history of CVDs. For the purposes of the study, CVD history was defined as myocardial infarction (n = 16), stroke (n = 14), and HF (n = 10). Patients with a history of acute

or chronic kidney disease, neoplastic diseases, or other serious diseases were excluded, including 14 patients with chronic kidney disease, severe liver or lung diseases, or ovarian cancer or other malignant diseases.

The diagnosis of primary diseases, including coronary heart disease, hypertension, and diabetes mellitus, was based on patients' current or previous medical records. Other data on clinical characteristics, including age, sex, body mass index (BMI), current smoking status, current alcohol consumption status, blood pressure (BP), hyperlipidemia, and left ventricular ejection fraction (LVEF), were collected from patient interviews or medical records. According to the Declaration of Helsinki guidelines, the Ethics Committee of Mindong Hospital of Fujian Medical University approved this study, and all patients gave written informed consent.

Follow-Up

All patients were prospectively followed up for a median of 36 months (range = 3 months–38 months) by telephone or review of the medical record 3 times a year until the occurrence of endpoints (ie, CV events). The endpoints in this study were myocardial infarction, stroke, HF, and CV death, which was defined as death because of myocardial infarction, stroke, or progressive HF confirmed by 2 attending doctors.

Measurement of HE4

Fasting venous blood specimens from patients with COPD were obtained in the early morning within the first 24 hours after admission. The specimens were prepared immediately by centrifugation and processed for determination of HE4 levels. Serum HE4 levels were tested by electrochemiluminescence immunoassay (Cobas e 601, F. Hoffmann-La Roche Ltd). Specimens with HE4 levels >1500 pmol/L were tested again (coefficient of variation of precision = <5%; measurement range = 15 pmol/L –1500 pmol/L; detection limit = 5 pmol/L). To further ensure the reliability of HE4 measurement, serum HE4 was measured twice in each patient's serum specimen, and the final HE4 value was the average of the 2 results, which was analyzed in our study.

Laboratory Measurements and Definition

The venous blood specimens were also tested for hemoglobin (Hb), blood glucose (FBG), and albumin (ALB) with

the use of the Siemens ADVIA 2400 automatic biochemistry analyzer (Siemens AG). The N-terminal prohormone of the B-type natriuretic peptide (NT-proBNP) levels were measured by immunoassay on an ELECSYS2010 instrument (ELECSYS proBNP, Roche Diagnostics, Germany). The estimated glomerular filtration rate (eGFR) was calculated using the Modification of Diet in Renal Disease formula.[18] The homeostasis model assessment of insulin resistance (HOMA-IR) was used to calculate insulin resistance.

Statistical Analyses

The normality of the data was analyzed by the Kolmogorov-Smirnov test combined with Q-Q plots. The data that were not normally distributed were expressed as the median (interquartile range) and analyzed by the Mann-Whitney U test. Data are presented as the mean ± SD for normally distributed data and were analyzed by independent t-test. Categorical variables were analyzed by the χ^2 test. Multivariate logistic regression analysis was performed to identify the independent association between serum HE4 levels and CVD history in patients with COPD at baseline. The Cox proportional hazard model was used to identify the independent prognostic factors for CV events in patients with COPD. The factors (P <.05) by univariate analysis were entered into the Cox proportional hazard analyses. In addition, we also adjusted for clinical data relevant to CVDs even if the factors were not significantly associated with CV events in the univariate analysis because they are key clinical variables and may be associated with CV events in the multivariate but not univariate analyses. We constructed CV event-free curves according to the Kaplan-Meier method and compared them using the log-rank test. All of the analyses were performed using SPSS 24.0. A P ≤.05 was considered to be statistically significant.

Results

Clinical Characteristics of Patients at Baseline (N = 199)

To evaluate the serum levels of HE4 in patients with COPD, 212 age and sex-matched patients who underwent physical examination without COPD or any other severe illnesses were selected as the control group. Our results showed

that serum HE4 levels in patients with COPD were significantly higher compared with those in the control patients (Table 1). The clinical characteristics of patients with COPD are presented in Table 2. We identified CV events in 115 (57.8%) patients with COPD. All the patients with COPD were divided into 2 groups: those with and those without CV events. Patients with CV events tended to be current alcohol consumers, be older (76.2 [68.7–84.3]), and have a higher BMI than patients without CV events (P <.05). Patients with CV events had lower LVEF, eGFR, Hb, and ALB levels and higher HE4, NT-proBNP, FBG, and HOMA-IR levels than those without CV events (all P <.001). There were no significant differences in other variables, including sex, current smoking status, hyperlipidemia, and primary diseases including hypertension, diabetes mellitus, and coronary heart disease, between patients with COPD with and without CV events (all P >.05).

Independent Association of HE4 with History of CVDs

Multivariate logistic regression analyses were performed to determine the association of serum HE4 levels in patients with COPD with a history of CVDs (Table 3). Model 1 indicated that higher serum HE4 levels were significantly associated with CVD history after adjusting for age and sex. After adjusting for age, sex, BMI, current smoking status, current alcohol consumption status, admission systolic BP and diastolic BP, hyperlipidemia, LVEF, and primary diseases (eg, hypertension, diabetes mellitus, coronary heart disease), the results of Model 2 were similar to those of Model 1. This association remained statistically significant and changed minimally after adding laboratory measurements to Model 2 (to create Model 3). The fully adjusted odds ratio of CVD history in Model 3 was 1.639 (1.213–2.317) in quartile 4 (the highest) vs 1.104 (1.001–1.382) quartile 1 (the lowest) of the serum HE4 levels.

Table 1. Baseline Characteristics of Patients with COPD and Control Patients

Variables	Control Patients (n = 212)	Patients with COPD (n = 199)	P Value
Age, y	73.7 (64.9–78.5)	74.2 (66.3–80.4)	.764
Sex (male/female)	108/104	110/89	.844
HE4 (pmol/L)	74.3 (44.5–99.6)	187.5 (146.9–282.4)	<.001

COPD, chronic obstructive pulmonary disease; HE4, human epididymis protein 4. Data are presented as mean ± SD for normally distributed data and as median (interquartile range) for nonnormally distributed data.

Table 2. Comparison of Clinical Characteristics Between 199 Patients with COPD at Baseline

Variables	All Patients (n = 199)	COPD without CV Events (n = 84)	COPD with CV Events (n = 115)	P Value
Age, y	74.2 (66.3–80.4)	72.3 (63.8–75.3)	76.2 (68.7–84.3)	.021
Sex (male/female)	110/89	45/39	65/50	.679
BMI	25.3 (22.3–26.2)	24.2 (21.5–25.3)	26.9 (23.7–27.8)	.016
Current smoker, n (%)	30 (15)	12 (14)	18 (16)	.790
Current drinker, n (%)	85 (43)	32 (38)	53 (46)	.010
LVEF	60.4 ± 7.51	61.4 ± 6.33	59.3 ± 8.71	.049
CVD history	40 (20.1)	14 (16.7)	26 (22.6)	.009
Hyperlipidemia, n (%)	60 (30)	27 (32)	33 (29)	.601
Admission systolic BP (mm Hg)	126.3 (109.3–144.1)	125.6 (107.3–143.4)	127.3 (110.2–146.9)	.707
Admission diastolic BP (mm Hg)	77.6 (70.1–85.4)	76.4 (67.2–79.1)	78.5 (75.4–87.2)	.400
Primary diseases				
Hypertension, n (%)	46 (23)	20 (24)	26 (23)	.788
Diabetes mellitus, n (%)	61 (31)	25 (30)	36 (31)	.674
Coronary heart disease, n (%)	38 (19)	15 (18)	23 (20)	.076
Others, n (%)	21 (10)	8 (9)	13 (11)	.601
Laboratory measurements				
eGFR (mL/min/1.73 m^2)	57.93 (46.09–64.85)	64.01 (58.25–69.07)	61.34 (54.48–68.73)	<.001
NT-proBNP (pg/mL)	733 (539–892)	548 (388–781)	799 (632–1022)	<.001
Hb (g/L)	116 (102–130)	124 (109–137)	112 (96–123)	<.001
ALB (g/L)	39.0 (36.5–42.1)	40.1 (38.3–44.9)	38.2 (35.1–40.2)	<.001
FBG (mmol/L)	5.41 (4.19–7.37)	5.24 (4.02–6.20)	6.40 (4.82–8.33)	.010
HOMA-IR	2.25 ± 0.94	2.04 ± 0.74	2.45 ± 1.15	<.001
HE4 (pmol/L)	187.5 (146.9–282.4)	111.0 (84.8–157.1)	252.6 (186.4–366.8)	<.001

ALB, albumin; BMI, body mass index; BP, blood pressure; COPD, chronic obstructive pulmonary disease; CV, cardiovascular; CVD, cardiovascular disease; eGFR, estimated glomerular filtration rate; FBG, fasting blood glucose; Hb, hemoglobin; HE4, human epididymis protein 4; HOMA-IR, homeostasis model assessment of insulin resistance; LVEF, left ventricular ejection fraction; NT-proBNP, N-terminal prohormone of B-type natriuretic peptide.
Data are presented as mean ± SD for normally distributed data, as median (interquartile range) for nonnormally distributed data, and as n (%) for categoric variables.

Cox Proportional Hazard Analyses of CV Event Prediction

All included patients (n = 199) were prospectively followed up for a median period of 36 months (range = 3 months–38 months). We found that CV events occurred in 115 of the patients with COPD. Twenty-two patients died, and 20 of those deaths were caused by CVDs, which included progressive HF (n = 3), myocardial infarction (n = 9), and stroke (n = 8). In addition, 95 events requiring rehospitalization (myocardial infarction, stroke, and progressive HF) took place during the follow-up period.

To determine the risk factors for CV events, univariate and multivariate Cox proportional hazard regression analyses were performed (**Table 4**). Univariate analysis showed that higher HE4 levels were significantly associated with a higher risk of CV events (hazard ratio [HR] = 2.316; 95% confidence interval [CI], 1.125–5.247). Moreover, age, BMI, current alcohol consumption status, LVEF, CVD history, eGFR, NT-proBNP, Hb, FBG, HOMA-IR, and ALB were

associated with the endpoints (ie, myocardial infarction, stroke, HF, and CV death). The multivariate Cox proportional hazard analysis revealed that HE4 (HR = 2.012; 95% CI, 1.773–4.469; P <.001) was an independent prognostic factor for CV events after adjustments for age, BMI, current smoking status, current alcohol consumption status, hyperlipidemia, history of CVDs, LVEF, admission systolic BP, NT-proBNP, FBG, HOMA-IR, Hb, ALB, and eGFR. Kaplan-Meier analysis showed that patients with COPD with serum HE4 levels above the median had a significantly higher rate of CV events than patients with serum HE4 levels below the median value (log-rank test, P <.001; **Figure 1**).

We performed an additional sensitivity analysis to evaluate the association of serum HE4 with CV events in patients with COPD who did not have a previous CVD history (n = 159). In these patients, the number of total CV events was 78. The multivariate Cox analysis showed that higher HE4 levels were still independently associated with a higher risk of CV events (data not shown). Similarly, compared with patients who had HE4 levels below the median value,

Table 3. Logistic Regression Analysis of Relationship Between CVD History and HE4 in Patients with COPD

Variables	Model 1	Model 2	Model 3
Serum HE4 level			
Quartile 1 (low)	1.000 (referent)	1.000 (referent)	1.000 (referent)
Quartile 2	1.193 (1.009–1.589)	1.136 (1.005–1.497)	1.104 (1.001–1.382)
Quartile 3	1.365 (1.124–1.813)	1.304 (1.109–1.744)	1.244 (1.072–1.640)
Quartile 4 (high)	1.853 (1.352–3.348)	1.730 (1.285–2.884)	1.639 (1.213–2.317)
P trend	<.001	<.001	.009

BMI, body mass index; BP, blood pressure; COPD, chronic obstructive pulmonary disease; CVD, cardiovascular disease; HE4, human epididymis protein 4; LVEF, left ventricular ejection fraction.
Model 1: Adjusted for age and sex. Model 2: Adjusted for age, sex, BMI, current smoker, current drinker, admission systolic BP and diastolic BP, hyperlipidemia, LVEF, and primary diseases (hypertension, diabetes mellitus, coronary heart disease and other diseases). Model 3: Adjusted for age, sex, BMI, current smoker, current drinker, admission systolic BP and diastolic BP, hyperlipidemia, LVEF, primary diseases (eg, hypertension, diabetes mellitus, coronary heart disease), and laboratory measurements.

Kaplan-Meier survival curves showed that the rate of CV events was still higher in patients with HE4 levels above the median (log-rank test, *P* <.001; data not shown).

Discussion

Our results suggested that patients with COPD with CV events had higher serum HE4 levels than those without CV events. Serum HE4 was independently related to CVD history in patients with COPD in the multivariate logistic regression analysis. The multivariate Cox proportional hazard analysis suggested that HE4 was an independent prognostic factor for CV events (myocardial infarction, stroke, and HF). Kaplan-Meier analysis showed that patients with COPD with higher HE4 levels had a significantly higher rate of CV events.

Research has shown that CVDs such as ischemic heart disease and stroke are increasing in prevalence and are responsible for one-quarter of deaths globally.[19] Despite advances in the understanding of risk factors, CV events related to atherosclerosis remain unacceptably common. Risk is particularly high among patients with proinflammatory comorbidities, including COPD,[20] and COPD is a leading cause of CV complications because of sympathetic activation, oxidative stress, and systemic inflammation.[21,22]

Table 4. Univariate and Multivariate Cox Proportional Hazard Analyses of Predicting CV Events in 199 Patients with COPD

Variables	HR	95% CI	P Value
Univariate analysis			
Age (per 1-year increase)	1.227	1.081–1.634	.037
Sex	1.180	0.791–1.176	.418
BMI (per 1-year increase)	1.402	1.113–1.984	.013
Current smoker	1.186	0.762–2.168	.346
Current drinker	1.313	1.102–2.054	.023
CVD history	1.809	1.071–3.490	.017
Hyperlipidemia	0.731	0.604–1.436	.147
LVEF (per 1-SD increase)	0.404	0.282–0.827	.002
Admission systolic BP (per 1-SD increase)	1.752	1.103–2.342	.069
Admission diastolic BP (per 1-SD increase)	1.304	0.709–1.367	.205
Primary diseases			
Hypertension	1.209	0.907–1.847	.490
Diabetes mellitus	1.181	0.922–2.334	.366
Coronary heart disease	1.125	0.604–1.434	.355
Others	1.303	0.712–1.471	.216
Laboratory measurements			
eGFR (per 1-SD increase)	0.966	0.958–0.974	<.001
NT-proBNP (per 1-SD increase)	1.002	1.002–1.003	<.001
Hb (per 1-SD increase)	0.974	0.965–0.983	<.001
ALB (per 1-SD increase)	0.955	0.918–0.992	.018
HE4 (per 1-SD increase)	2.316	1.125–5.247	<.001
FBG (per 1-SD increase)	1.452	1.110–3.048	.030
HOMA-IR (per 1-SD increase)	1.847	1.202–3.153	.018
Multivariate analysis			
Age (per 1-year increase)	0.995	0.972–1.019	.205
BMI (per 1-year increase)	1.402	1.113–1.984	.013
Current smoker	1.142	0.701–1.981	.409
Current drinker	1.151	0.803–1.903	.078
Hyperlipidemia	0.822	0.712–1.525	.309
LVEF (per 1-SD increase)	0.485	0.251–0.68	.003
Admission systolic BP (per 1-SD increase)	1.524	1.042–1.957	.090
History of CVDs	1.793	1.019–3.291	.019
FBG (per 1-SD increase)	1.350	1.100–2.942	.098
HOMA-IR (per 1-SD increase)	1.307	1.092–2.244	.064
NT-proBNP (per 1-SD increase)	2.310	1.833–3.092	.008
Hb (per 1-SD increase)	0.994	0.982–1.007	.360
ALB (per 1-SD increase)	1.020	0.971–1.071	.432
HE4 (per 1-SD increase)	2.012	1.773–4.469	<.001
eGFR (per 1-SD increase)	0.723	0.552–0.912	<.001

ALB, albumin; BMI, body mass index; BP, blood pressure; COPD, chronic obstructive pulmonary disease; CV, cardiovascular; CVD, cardiovascular disease; eGFR, estimated glomerular filtration rate; FBG, fasting blood glucose; Hb, hemoglobin; HE4, human epididymis protein 4; HOMA-IR, homeostasis model assessment of insulin resistance; LVEF, left ventricular ejection fraction; NT-proBNP, N-terminal prohormone of B-type natriuretic peptide; SD, standard deviation.

Chronic vascular inflammation is the main pathophysiological basis of CV events. Disproportionate increases in inflammation play an important role in the occurrence and
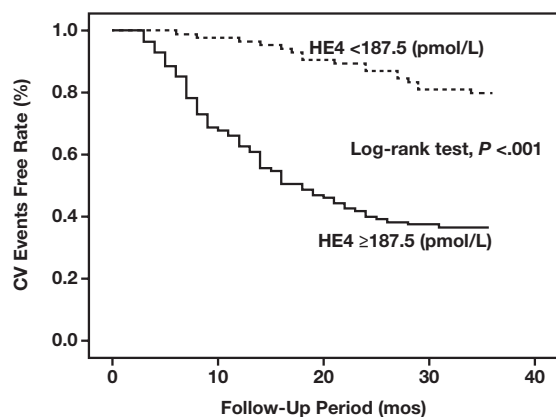
Figure 1

Kaplan-Meier analysis of CV events experienced by patients, stratified into 2 groups by median levels of serum HE4. CV, cardiovascular; H%4, human epididymis protein 4.

development of CV events in patients with COPD.[12,13] As a small-molecule and secretory protein, HE4 can be easily secreted from tissues and enter the circulating blood in multiple normal or abnormal tissues in the human body, such as the respiratory tract, convoluted tubules of the kidney, and other tissues, which play a very important role in the process of immune defense.[7,8] For instance, serum HE4 levels were found to be increased in patients with pelvic inflammatory disease and upper respiratory tract infection.[23,24] Other WFDC proteins have also been correlated with inflammatory processes.[9]

In our study, we first showed that serum HE4 had a close association with CVD history at baseline and CV events by multivariate analyses, which may be partly or mostly explained by the mechanistic research performed in previous studies.[21,22] These studies have shown that chronic vascular inflammation caused by COPD promotes atherosclerosis-related CVD events. Increased HE4 levels may be the result of the aggravation of inflammation in patients with COPD, which promotes the occurrence of CV events.[7,8,12,13] Some studies have also suggested that higher serum HE4 levels are associated with worsening cardiac function in patients with HF patients. Higher serum HE4 levels have been considered an independent factor for predicting the prognosis in patients with HF.[14-16] Previous studies have proven that HE4 is not overexpressed in normal or abnormal cardiovascular tissues.[5-8] Increased HE4 levels are not mainly attributable to pathological changes in CV tissue itself. The mechanism of chronic inflammation may be a better

explanation of increased HE4, which is consistent with our hypothesis and results.

In addition, some studies have suggested that increased HE4 levels are closely related to renal dysfunction.[16,25,26] The eGFR of our COPD patients was normal, so the negative influence of renal function abnormalities on our results was excluded. Studies have also reported that HE4 is associated with cancer (eg, ovarian, cervical, lung, and breast cancers) and other serious diseases.[5,6,8,10,24] To eliminate the impact of the diseases on this study, patients with COPD with these diseases were excluded from the baseline assessment. It is of great clinical significance to determine the independent risk factors or predictors of CV events in patients with COPD. The early detection of CVDs in these patients may provide an opportunity to develop strategies to reduce the medical burden and improve prognosis. Our results seemed to imply that serum HE4 is a highly sensitive biomarker for the early recognition of CV events in patients with COPD.

This study has some notable strengths. We first found that serum HE4 can be used as an effective prognostic factor for CV events in patients with COPD, and the serum test is simple and convenient for patients. In addition, the study population exhibited a broad spectrum of risks, including primary and secondary prevention populations. We ensured comprehensive follow-up and rigorous adjudication of CV events. Finally, the HE4 assay chosen for this analysis is both widely available and analytically stable (with a coefficient of variation of precision <5%).

Limitations

The limitation of the study is the small sample size. More studies must be performed to identify the value of serum HE4 for predicting CV events. Given the close relationships between serum HE4 and many malignant tumors or renal function, the results of this study are not applicable to the general population.

Conclusions

Serum HE4 is an independent prognostic factor for predicting CV events in patients with COPD. Serum HE4

may enable the early recognition of patients with COPD at risk of developing CV complications. **LM**

Acknowledgments

References

1. Leitao FF, Sin DD. COPD and cardiovascular diseases: now is the time for action! *Thorax.* 2018;73(9):799–800.

2. Schneider C, Bothner U, Jick SS, Meier CR. Chronic obstructive pulmonary disease and the risk of cardiovascular diseases. *Eur J Epidemiol.* 2010;25(4):253–260.

3. Kirchhoff C, Habben I, Ivell R, Krull N. A major human epididymis-specific cDNA encodes a protein with sequence homology to extracellular proteinase inhibitors. *Biol Reprod.* 1991;45(2): 350–357.

4. Kirchhoff C. Molecular characterization of epididymal proteins. *Rev Reprod.* 1998;3(2):86–95.

5. Hellström I, Raycraft J, Hayden-Ledbetter M, et al. The HE4 (WFDC2) protein is a biomarker for ovarian carcinoma. *Cancer Res.* 2003;63(13):3695–3700.

6. Plebani M; HE4 Study Group. HE4 in gynecological cancers: report of a European investigators and experts meeting. *Clin Chem Lab Med.* 2012;50(12):2127–2136.

7. Hertlein L, Stieber P, Kirschenhofer A, et al. Human epididymis protein 4 (HE4) in benign and malignant diseases. *Clin Chem Lab Med.* 2012;50(12):2181–2188.

8. Galgano MT, Hampton GM, Frierson HF Jr. Comprehensive analysis of HE4 expression in normal and malignant human tissues. *Mod Pathol.* 2006;19(6):847–853.

9. Bingle CD, Vyakarnam A. Novel innate immune functions of the whey acidic protein family. *Trends Immunol.* 2008;29(9): 444–453.

10. Escudero JM, Auge JM, Filella X, Torne A, Pahisa J, Molina R. Comparison of serum human epididymis protein 4 with cancer antigen 125 as a tumor marker in patients with malignant and nonmalignant diseases. *Clin Chem.* 2011;57(11):1534–1544.

11. Drapkin R, von Horsten HH, Lin Y, et al. Human epididymis protein 4 (HE4) is a secreted glycoprotein that is overexpressed by serous and endometrioid ovarian carcinomas. *Cancer Res.* 2005;65(6):2162–2169.

12. King PT. Inflammation in chronic obstructive pulmonary disease and its role in cardiovascular disease and lung cancer. *Clin Transl Med.* 2015;4(1):68.

13. Parris BA, O'Farrell HE, Fong KM, Yang IA. Chronic obstructive pulmonary disease (COPD) and lung cancer: common pathways for pathogenesis. *J Thorac Dis.* 2019;11(Suppl 17):S2155–S2172.

14. Piek A, Meijers WC, Schroten NF, Gansevoort RT, de Boer RA, Silljé HH. HE4 serum levels are associated with heart failure severity in patients with chronic heart failure. *J Card Fail.* 2017;23(1):12–19.

15. de Boer RA, Cao Q, Postmus D, et al. The WAP four-disulfide core domain protein HE4: a novel biomarker for heart failure. *JACC Heart Fail.* 2013;1(2):164–169.

16. Huang Y, Jiang H, Zhu L. Human epididymis protein 4 as an indicator of acute heart failure in patients with chronic kidney disease. *Lab Med.* 2020;51(2):169–175.

17. Antuni JD, Barnes PJ. Evaluation of individuals at risk for COPD: beyond the scope of the Global Initiative for Chronic Obstructive Lung Disease. *Chronic Obstr Pulm Dis.* 2016;3(3):653–667.

18. Levey AS, Stevens LA, Schmid CH, et al.; CKD-EPI (Chronic Kidney Disease Epidemiology Collaboration). A new equation to estimate glomerular filtration rate. *Ann Intern Med.* 2009;150(9):604–612.

19. Lozano R, Naghavi M, Foreman K, et al. Global and regional mortality from 235 causes of death for 20 age groups in 1990 and 2010: a systematic analysis for the Global Burden of Disease Study 2010. *Lancet.* 2012;380(9859):2095–2128.

20. Müllerova H, Agusti A, Erqou S, Mapel DW. Cardiovascular comorbidity in COPD: systematic literature review. *Chest.* 2013;144(4):1163–1178.

21. Lévy P, Kohler M, McNicholas WT, et al. Obstructive sleep apnoea syndrome. *Nat Rev Dis Primers.* 2015;1(3):15015.

22. Onishi K. Total management of chronic obstructive pulmonary disease (COPD) as an independent risk factor for cardiovascular disease. *J Cardiol.* 2017;70(2):128–134.

23. Orfanelli T, Jayaram A, Doulaveris G, Forney LJ, Ledger WJ, Witkin SS. Human epididymis protein 4 and secretory leukocyte protease inhibitor in vaginal fluid: relation to vaginal components and bacterial composition. *Reprod Sci.* 2014;21(4):538–542.

24. Bingle L, Cross SS, High AS, et al. WFDC2 (HE4): a potential role in the innate immunity of the oral cavity and respiratory tract and the development of adenocarcinomas of the lung. *Respir Res.* 2006;7(3):61–64.

25. LeBleu VS, Teng Y, O'Connell JT, et al. Identification of human epididymis protein-4 as a fibroblast-derived mediator of fibrosis. *Nat Med.* 2013;19(2):227–231.

26. Allison SJ. Fibrosis: HE4–a biomarker and target in renal fibrosis. *Nat Rev Nephrol.* 2013;9(3):124–126.

Trimester-Specific Reference Intervals of Serum Urea, Creatinine, and Uric Acid Among Healthy Pregnant Women in Zhengzhou, China

Yuhua Gao, MD,[1] Jia Jia, PhD,[2] Xianan Liu, PhD,[1] Shuren Guo, PhD,[1] Liang Ming, PhD[1]*

ABSTRACT

Objective: To verify the differences in serum levels of urea, creatinine, and uric acid (UA) between pregnant and nonpregnant women and establish specific reference intervals of serum urea, creatinine, and UA for pregnant women, and thus help for the detection of kidney disease in pregnancy.

Methods: Based on the selection criteria, 1312 apparently healthy pregnant women and 1301 nonpregnant women were enrolled in this study. The levels of serum urea, creatinine, and UA were compared between the pregnant and nonpregnant women. The differences in the 3 indicators among different age groups and trimesters in pregnant women were studied. Finally, reference intervals were established by nonparametric methods according to the recommendation of Clinical and Laboratory Standards Institute guideline C28-A3.

Results: Compared with nonpregnant women, pregnant women had a significantly lower level of serum urea, creatinine, and UA (all *P* <.01),

and no significant age-related differences in the 3 indicators were observed among the pregnant women (*P* >.05). However, the levels of these indicators were significantly different among the 3 trimesters (all *P* <.01 or *P* =.01). Accordingly, trimester-specific reference intervals of serum urea (1.6–4.4 mmol/L; 1.6–4.2 mmol/L; 1.6–4.4 mmol/L), creatinine (36–68 µmol/L; 34–66 µmol/L; 36–68 µmol/L), and UA (122–297 µmol/L; 129–327 µmol/L; 147–376 µmol/L) for trimesters 1, 2, and 3, respectively, were established.

Conclusion: These newly established reference intervals will be valuable for the detection and monitoring of kidney disease in pregnancy.

Keywords: pregnant women, reference intervals, urea, creatinine, uric acid, kidney disease

Abbreviations:

UA, uric acid; GFR, glomerular filtration rate; CLSI, Clinical and Laboratory Standards Institute.

Chronic kidney disease is a public health problem with high morbidity and mortality worldwide. It affects up to 6% of women of childbearing age in high-income countries and is estimated to affect 3% of pregnant women.[1] Biomarkers are often used to detect renal function and prevent severe damage to the kidneys because no obvious clinical symptoms can be observed in the early stages of the disease.[2] Clinically, serum urea, creatinine, and uric acid (UA) are 3 of the most widely used biomarkers to evaluate renal function.

Among these, serum urea and creatinine are classical biomarkers for their relatively higher accuracy, and UA, which is renally excreted and related to renal dysfunction, can also be used to indicate kidney damage.[3,4] In addition, serum creatinine is recommended by the kidney disease: improving global outcomes (KDIGO) 2012 clinical practice guidelines to estimate the glomerular filtration rate (GFR) for disease assessment.[2] Therefore, the evaluations of these 3 biomarkers can provide essential information for clinical decisions regarding kidney disease.

Reference intervals are critical for the interpretation of clinical biomarkers for kidney disease. Whereas most reference values of biomarkers are usually defined based on blood specimens from healthy men or nonpregnant women, reference intervals for pregnant women are scarce but are prerequisites for their specificity in assessing physiological characteristics during pregnancy.[5] Compared with levels in nonpregnant women, renal blood

[1]Department of Clinical Laboratory, The First Affiliated Hospital of Zhengzhou University, Zhengzhou, China, [2]School of Environment, Beijing Normal University, Beijing, China

*To whom correspondence should be addressed.
mingliang3072@163.com

flow and GFR levels can increase significantly during normal pregnancy.[6] Furthermore, blood volume and composition vary even in different trimesters during pregnancy.[7] As a result, the levels of biomarkers for kidney disease such as serum urea, creatinine, and UA may be significantly different between pregnant and nonpregnant women.[8,9] However, reference intervals of serum urea, creatinine, and UA in pregnant women are rarely established or are measured in few participants.[5,10,11] Moreover, the International Federation for Clinical Chemistry and the Clinical and Laboratory Standards Institute (CLSI) also recommend that each laboratory should establish its own reference intervals.[12,13]

To help clinicians detect and monitor kidney disease in pregnant women, we recruited 1312 apparently healthy pregnant and 1301 nonpregnant women to (i) verify the differences in serum levels of urea, creatinine, and UA between pregnant and nonpregnant women and (ii) establish specific reference intervals for these biomarkers for pregnant women.

Materials and Methods

Patients

We recruited apparently healthy pregnant women who were examined in our hospital from May 2018 to February 2019. The inclusion criteria were as follows: (i) aged 20 to 45 years, and (2) normal pregnancy test results (ie, routine blood and urine tests; routine biochemical tests, eg, total protein, albumin, total cholesterol, alanine aminotransferase, aspartate aminotransferase triglycerides, fasting blood glucose). The exclusion criteria were as follows: (i) major organ diseases such as liver, kidney, heart, and lung disease; (ii) positive urine protein ; (iii) recent medication, surgery, or other treatments; (iv) acute trauma or acute or chronic inflammation; (v) history of hypertension and diabetes before pregnancy; (vi) other complications, eg, ectopic pregnancy, gestational diabetes, or gestational hypertension (including preeclampsia, eclampsia, chronic hypertension with pregnancy, chronic hypertension with preeclampsia, or hemolysis, elevated liver enzymes, low platelet count syndrome); and (vii) infectious diseases such as hepatitis B virus, hepatitis C virus, and human immunodeficiency virus. Patients

were divided into 3 groups according to trimester: first trimester (1–12 weeks), second trimester (13–27 weeks), and third (28–40 weeks).

To prove the necessity of establishing specific reference intervals for pregnant women, we also recruited healthy women aged 20 to 45 years who were not pregnant during the same period. The levels of serum urea, creatinine, and UA of these nonpregnant women were all within normal reference intervals.

Physical examination and certain clinical laboratory tests were performed for all participants. Through the selection criteria, 1312 apparently healthy pregnant women (first trimester, n = 431; second trimester, n = 429; third trimester, n = 452) and 1301 nonpregnant women were included in our study. We also divided the ages of the pregnant women into 4 groups (ages 20–25 years, n = 155; ages 26–30 years, n = 699; ages 31–35 years, n = 331; ages 36–45 years, n = 127) to analyze whether serum urea, creatinine, and UA levels were age-related during pregnancy. The study was approved by the ethics committee of The First Affiliated Hospital of Zhengzhou University and conducted in accordance with the ethical standards of the Helsinki Declaration.

Laboratory Analysis

Venous blood specimens were taken from all patients after fasting for 8 to 12 hours. Blood specimens were collected using 5 mL tubes with separating gel (BD Bioscience, Franklin Lakes, NJ). All the specimens were centrifuged at 3500 rpm for 5 minutes and tested within 8 hours. All the tests were measured by using the Roche Cobas c701 system and reagents (Roche Diagnostics GmbH, Mannheim, Germany). The calibrators and controls were also provided by Roche. The laboratory conducted internal quality control every day and participated in the national external quality assessment every year, and all analytes were qualified. The lower limits of detection of urea, creatinine, and UA were 0.5 mmol/L, 5 μmol/L, and 11.9 μmol/L, respectively. The details of the 3 analytes are shown in Supplementary Table 1.

Outlier Test

According to the recommendations of CLSI guideline C28-A3,[13] outliers were detected by the Dixon method. Outliers were removed when D/R ≥ 1/3, where D was the absolute

difference between an extreme value (smallest or largest) and the next value (small or large) and R was the range of all observations. This process was repeated on the remaining data until all outliers were deleted.

Statistical Analysis

The Kolmorov-Smirnov test was used to determine the normality of the data, and all the data were shown to be nonnormally distributed. Continuous variables were expressed as means ± standard deviation and were compared using the Mann-Whitney U test or the Kruskal-Wallis H test. Reference intervals were established by nonparametric methods according to the recommendation of CLSI C28-A3.[13] All statistical analyses were conducted using SPSS 19.0 (SPSS, Chicago, IL). All tests were 2-tailed, and P <.05 was considered statistically significant.

When we compared these indicators in the different age groups among the pregnant women, we observed no significant age-related differences (P >.05; Table 1). However, the levels were significantly different among the different trimesters (all P <.01 or P =.01, respectively; Table 2, Figure 1). Therefore, different reference intervals of urea, creatinine, and UA should be established according to trimester. For urea and creatinine, further comparisons revealed that there were no significant differences in levels between the first and third trimester (all P > .05). However, when urea and creatinine levels during those trimesters were each compared with levels during the second trimester, there were significant differences for both the first and the third trimester (all P <.05). Thus, the first and third trimester should use the same reference intervals for urea and creatinine, respectively (Table 3). For UA, there were significant differences between any 2 trimesters (All P <.01). Thus, it is essential to establish 3 different reference intervals for UA according to trimester. The results are shown in Table 3.

Results

A total of 2613 participants (1312 pregnant women and 1301 nonpregnant women) were included in this study. The characteristics of the participants are shown in Table 1. The distributions of urea, creatinine, and UA for nonpregnant women and pregnant women each are shown in Figure 1. Compared with the nonpregnant women, the pregnant women had a significantly lower level of urea (2.75 ± 0.70 mmol/L vs 4.07 ± 0.95 mmol/L; P <.01), creatinine (48.97 ± 8.10 μmol/L vs 60.75 ± 8.97 μmol/L; P <.01), and UA (213.35 ± 53.99 μmol/L vs 246.26 ± 48.67 μmol/L; P <.01), respectively. Therefore, it is essential to establish specific reference intervals of these 3 indicators for pregnant women.

Discussion

With the dramatic hormonal and hemodynamic changes of pregnancy, renal function is altered, and these changes must be considered when assessing renal function in pregnancy.[14] Because blood volume begins to increase after conception, renal blood flow and GFR also increase significantly: During normal pregnancy, renal blood flow and GFR can be increased by 50% to 85% and 40% to 65%, respectively.[6] As a result, serum urea, creatinine, and UA are vastly decreased during pregnancy.[8] In this study, significantly lower levels of serum urea, creatinine, and UA were observed (P <.01) during pregnancy, which confirmed the necessity of establishing specific reference intervals of

Table 1. Characteristics of Pregnant and Nonpregnant Participants

Parameters	Pregnant Women	Nonpregnant Women	P Value	Pregnant Women Divided by Age (y)				P Value
				20–25	26–30	31–35	36–45	
Participants	1312	1301	…	155	699	331	127	…
Age, y	29.66 ± 4.12	30.15 ± 4.86	.07	23.48 ± 1.65	28.13 ± 1.31	32.53 ± 1.52	38.16 ± 1.86	<.01
Urea, mmol/L	2.75 ± 0.70	4.07 ± 0.95	<.01	2.72 ± 0.69	2.73 ± 0.68	2.79 ± 0.73	2.79 ± 0.72	.33
Creatinine, μmol/L	48.97 ± 8.10	60.75 ± 8.97	<.01	47.65 ± 7.33	48.38 ± 8.93	49.29 ± 7.62	49.91 ± 8.54	.06
UA, μmol/L	213.35 ± 53.99	246.26 ± 48.67	<.01	209.00 ± 52.50	215.62 ± 54.04	210.69 ± 54.8	213.11 ± 53.43	.36

UA, uric acid.
Continuous variables were compared by Mann-Whitney U test (comparison between 2 groups) or Kruskal-Wallis H test (comparison among 3 groups).
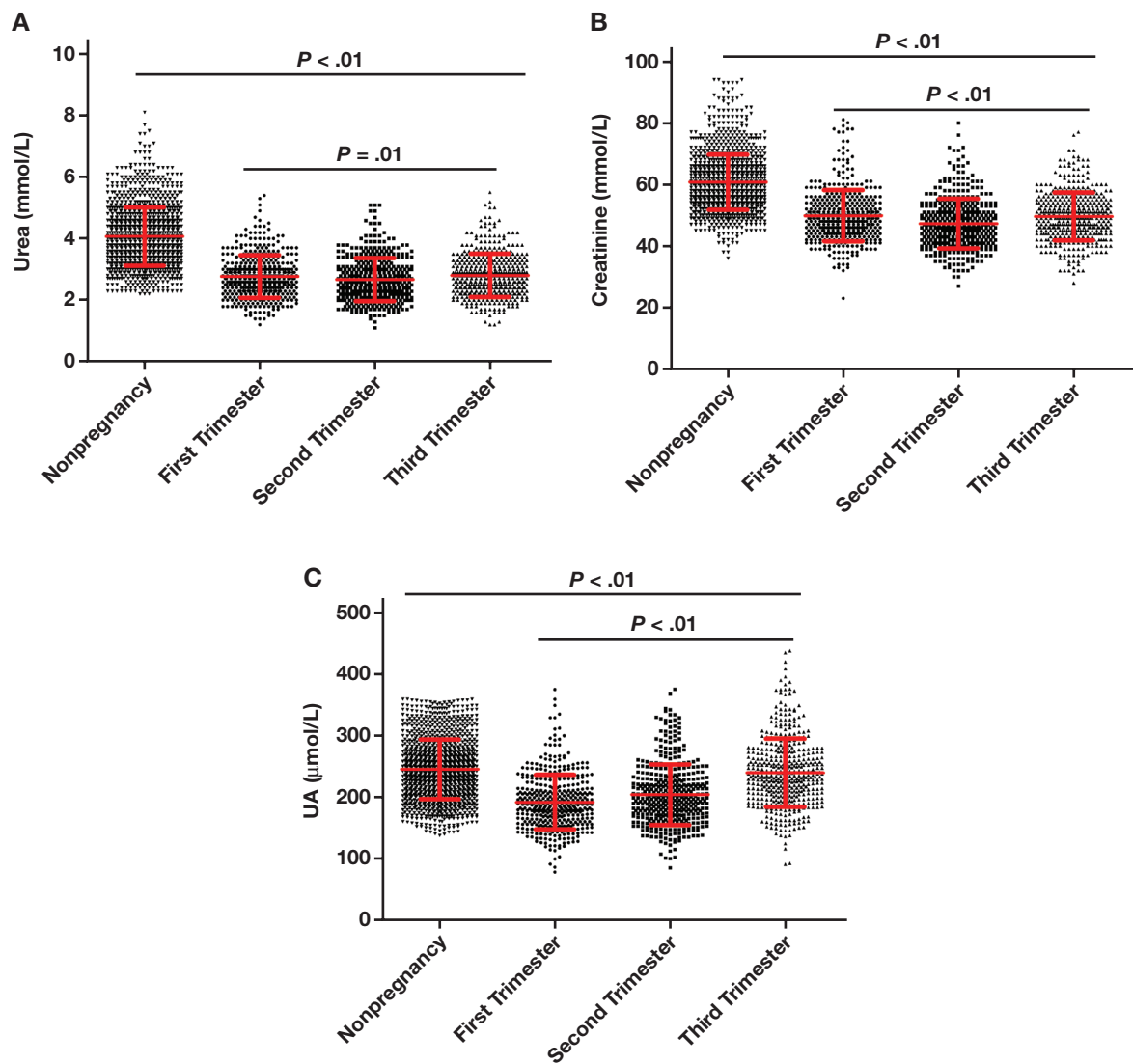
Figure 1

Data distributions of serum urea (A), creatinine (B), and UA (C) for nonpregnancy and pregnancy.

these indicators for pregnant women. However, the variations in these 3 indicators during different periods of pregnancy are not completely consistent.

Urea is the major product of protein nitrogen metabolism and is freely filtered by the glomeruli, and approximately 50% of urea is reabsorbed by renal tubules under normal conditions.[15] Apart from being affected by kidney disease, serum urea levels can also be influenced by a high-protein diet or by oral corticosteroids.[16] Nevertheless, as a classical indicator that has been used for decades, serum

urea level can still reflect renal function to some extent, and it is increased during acute and chronic renal disease. Compared with the nonpregnant women in our study, pregnant women had a significantly lower level of serum urea (2.75 ± 0.70 mmol/L vs 4.07 ± 0.95 mmol/L; P <.01), indicating that serum urea in pregnant women may be reduced by approximately 32%. Moreover, patients in their second trimester showed the lowest levels of serum urea; their serum urea concentrations were considered to exceed the upper limit of normal if they were >4.2 mmol/L. However, the upper limit of normal for serum urea in the

Table 2. Levels of Serum Urea, Creatinine, and UA Among Different Trimesters

Parameters	First Trimester, Group A	Second Trimester, Group B	Third Trimester, Group C	P Value
Participants	431	429	452	…
Age, y	29.49 ± 4.01	29.71 ± 4.03	30.05 ± 4.27	$P = .08^a$
Urea, mmol/L	2.77 ± 0.69	2.67 ± 0.70	2.81 ± 0.70	$P = .01$
				$P_{AB} = .02$
				$P_{AC} = .45$
				$P_{BC} < .01$
Creatinine, µmol/L	49.91 ± 8.32	47.32 ± 8.04	49.63 ± 7.72	$P < .01$
				$P_{AB} < .01$
				$P_{AC} = .84$
				$P_{BC} < .01$
UA, µmol/L	192.79 ± 44.33	205.11 ± 49.28	240.78 ± 55.45	$P < .01$
				$P_{AB} < .01$
				$P_{AC} < .01$
				$P_{BC} < .01$

UA, uric acid.

Continuous variables were compared by Mann-Whitney U test (comparison between 2 groups) or Kruskal-Wallis H test (comparison among 3 groups).

[a]P, P value of comparison among the 3 groups; P*AB*, P value of comparison between Group A and Group B; P*AC*, P value of comparison between Group A and Group C; P*BC*, P value of comparison between Group B and Group C.

Table 3. Reference Intervals of Serum Urea, Creatinine, and UA for Pregnant Women

Analytes	First Trimester	Second Trimester	Third Trimester
Urea, mmol/L	1.6 (1.6–1.7)–4.4 (4.2–4.5)	1.6 (1.5–1.7)–4.2 (4.0–4.4)	1.6 (1.6–1.7)–4.4 (4.2–4.5)
Creatinine, µmol/L	36 (34–37)–68 (67–71)	34 (32–35)–66 (63–69)	36 (34–37)–68 (67–71)
UA, µmol/L	122 (114–127)–297 (286–316)	129 (114–136)–327 (317–335)	147 (138–154)–376 (353–389)

UA, uric acid.

Numbers in brackets represent 90% confidence intervals.

general population of our hospital is 8.2 mmol/L. This finding means that large numbers of pregnant patients with potential renal damage may miss a diagnosis without there being specific reference intervals for pregnant women. Similar to our results, Dai et al[11] also found that pregnant women had a significantly lower level of serum urea nitrogen, especially in the middle of the trimester (13–35 week). Both these results confirm that it is essential to establish specific reference intervals of serum urea for pregnancy.

Creatinine is one of the most widely available and commonly used biomarkers of renal function.[17] It is a decomposition product of creatine phosphate in muscle and is usually produced at a relatively constant rate by the body (depending on muscle mass). Under normal conditions,

creatine is freely filtered by the glomeruli and is not reabsorbed by the tubules. Moreover, outside of pregnancy, serum creatinine concentration is used to estimate GFR, which can be further used for the diagnosis of chronic kidney disease and the grading of kidney disease severity.[2] However, creatinine-based equations to estimate GFR may misclassify renal function during pregnancy because they depend on a steady state of creatinine balance (dietary protein intake, muscle mass, plasma volume and glomerular filtration).[18] In addition, a 24-hour collection of urine (collect the total urine of the patient within 24 hours) to measure creatinine clearance is impractical.[19]. Accordingly, physicians typically rely on serum creatinine levels measured at routine visits during pregnancy.[7,20]

In this study, serum creatinine levels during pregnancy were significantly lower than those in the nonpregnant patients (48.97 ± 8.10 µmol/L vs 60.75 ± 8.97 µmol/L; $P < .01$), which is consistent with other studies.[11,20,21] Furthermore, pregnancy in the second trimester showed the lowest level of serum creatinine. Wiles et al[7] also found the lowest level of serum creatinine to be in the second trimester, and the upper limits of normal of serum creatinine in their study were 76 µmol/L, 72 µmol/L, and 77 µmol/L in sequential trimesters. In contrast, in the current study, the upper limits of normal for serum creatinine were 68 µmol/L, 66 µmol/L, and 68 µmol/L in sequential trimesters. The inconsistency may come from different patient populations (eg, different regions, countries, races),

reagents, and methods, which also further indicates the necessity for each laboratory to establish its own reference intervals.

Research has shown that UA is the final product of urine metabolism and is renally excreted.[3] Therefore, elevated serum UA levels are seen in patients with kidney disease. The well-known effects of elevated UA levels on the kidneys include nephrolithiasis and acute kidney injury in the setting of tumor lysis.[22] Moreover, recent data suggest that UA may be an important factor in the pathogenesis of acute kidney injury in general and of chronic kidney disease and hypertension.[3,22] Therefore, the establishment of a correct reference interval of serum UA is helpful for detecting renal damage early. In this study, compared with the nonpregnant patients, pregnant women had a significantly lower level of serum UA (213.35 ± 53.99 µmol/L vs 246.26 ± 48.67 µmol/L; P <.01). However, serum UA began to increase significantly in sequential trimesters (Table 3). These results were similar to those of other studies, and the increased serum UA concentration in late pregnancy may be related to an altered renal handling concentration of urate.[10,11]

Aside from the changes in UA levels, we noticed that the differences in urea and creatinine levels were not very large across all 3 trimesters. This slight renal impairment is easy to neglect based on serum creatinine and urea because of their insensitivities in the early stages of kidney disease (serum urea and creatinine levels may not increase with mild renal impairment).[4] The small increases above the normal (ie, for nonpregnancy) reference interval levels of these 2 indicators may have indicated renal impairment,[5,11] although the values were minimal. Thus, trimester-specific reference intervals of serum creatinine and urea may improve the detection rate of kidney disease during pregnancy.

Conclusion

We have verified the necessity of establishing specific reference intervals of serum urea, creatinine, and UA for pregnant women and trimester-specific reference intervals of these 3 indicators. These findings will be helpful for clinicians to detect and monitor kidney disease in pregnancy. **LM**

References

1. Webster P, Lightstone L, McKay DB, Josephson MA. Pregnancy in chronic kidney disease and kidney transplantation. *Kidney Int.* 2017;91(5):1047–1056.

2. KDIGO CKD Work Group. KDIGO 2012 clinical practice guideline for the evaluation and management of chronic kidney disease. *Kidney Int Suppl.* 2013;3:1–150.

3. Giordano C, Karasik O, King-Morris K, Asmar A. Uric acid as a marker of kidney disease: review of the current literature. *Dis Markers.* 2015;2015:382918.

4. Gounden V, Jialal I. *Renal Function Tests*. Treasure Island, FL: StatPearls Publishing; 2020.

5. Larsson A, Palm M, Hansson LO, Axelsson O. Reference values for clinical chemistry tests during normal pregnancy. *BJOG.* 2008;115(7):874–881.

6. Jeyabalan A, Conrad KP. Renal function during normal pregnancy and preeclampsia. *Front Biosci.* 2007;12:2425–2437.

7. Wiles K, Bramham K, Seed PT, Nelson-Piercy C, Lightstone L, Chappell LC. Serum creatinine in pregnancy: a systematic review. *Kidney Int Rep.* 2019;4(3):408–419.

8. Carlin A, Alfirevic Z. Physiological changes of pregnancy and monitoring. *Best Pract Res Clin Obstet Gynaecol.* 2008;22(5):801–823.

9. Torgersen KL, Curran CA. A systematic approach to the physiologic adaptations of pregnancy. *Crit Care Nurs Q.* 2006;29(1):2–19.

10. Klajnbard A, Szecsi PB, Colov NP, et al. Laboratory reference intervals during pregnancy, delivery and the early postpartum period. *Clin Chem Lab Med.* 2010;48(2):237–248.

11. Dai Y, Liu J, Yuan E, et al. Gestational age-specific reference intervals for 15 biochemical measurands during normal pregnancy in China. *Ann Clin Biochem.* 2018;55(4):446–452.

12. Solberg HE; International Federation of Clinical Chemistry (IFCC), Scientific Committee, Clinical Section, Expert Panel on Theory of Reference Values, and International Committee for Standardization in Haematology (ICSH), Standing Committee on Reference Values. Approved recommendation (1986) on the theory of reference values. Part 1. The concept of reference values. *J Clin Chem Clin Biochem.* 1987;25(5):337–342.

13. Clinical and Laboratory Standards Institute. *Defining, Establishing, and Verifying Reference Intervals in the Clinical Laboratory; Approved Guideline*. 3rd ed. Wayne, PA: Clinical and Laboratory Standards Institute; 2010.

14. Maynard SE, Thadhani R. Pregnancy and the kidney. *J Am Soc Nephrol.* 2009;20(1):14–22.

15. Wang H, Ran J, Jiang T. Urea. *Subcell Biochem.* 2014;73:7–29.

16. Becker J, Friedman E. Renal function status. *Am J Roentgenol.* 2013;200(4):827–829.

17. Treacy O, Brown NN, Dimeski G. Biochemical evaluation of kidney disease. *Transl Androl Urol.* 2019;8(Suppl 2):S214–S223.

18. Smith MC, Moran P, Ward MK, Davison JM. Assessment of glomerular filtration rate during pregnancy using the MDRD formula. *BJOG.* 2008;115(1):109–112.

19. Ahmed SB, Bentley-Lewis R, Hollenberg NK, Graves SW, Seely EW. A comparison of prediction equations for estimating glomerular filtration rate in pregnancy. *Hypertens Pregnancy.* 2009;28(3):243–255.

20. Harel Z, McArthur E, Hladunewich M, et al. Serum creatinine levels before, during, and after pregnancy. *JAMA.* 2019;321(2):205–207.

21. Jia L, Yongmei J, Leiwen P, Yi Y. The reference intervals for renal function indexes in Chinese pregnant women. *Pak J Pharm Sci.* 2017;30(3(Special)):1133–1138.

22. Fathallah-Shaykh SA, Cramer MT. Uric acid and the kidney. *Pediatr Nephrol.* 2014;29(6):999–1008.

Plasma Cell Proliferation Is Reduced in Myeloma-Induced Hypercalcemia and in Co-Culture with Normal Healthy BM-MSCs

Nader Vazifeh Shiran, PhD,[*1] Saeid Abroun, PhD,[1]

ABSTRACT

Objective: In multiple myeloma (MM), stimulation of osteoclasts and bone marrow (BM) lesions lead to hypercalcemia, renal failure, and anemia. Co-culture of the myeloma cells in both hypocalcemia and hypercalcemia concentrations with bone marrow-mesenchymal stem cells were evaluated.

Materials and Methods: Viability and survival of myeloma cells were assessed by microculture tetrazolium test and flow cytometric assays. Mesenchymal stem cells (MSCs) were extracted from normal and myeloma patients and were co-cultured with myeloma cells.

Results: Myeloma cells showed less survival in both hypocalcaemia and hypercalcemia conditions (P <.01). The

paracrine and juxtacrine conditions of demineralized bone matrix-induced hypercalcemia increased the proliferation and survival of the cells (P <.05). Unlike myeloma MSCs, normal MSCs reduced the survival of and induced apoptosis in myeloma cells (P <.1).

Conclusion: Normal healthy-MSCs do not protect myeloma cells, but inhibit them. However, increasing the ratio of myeloma cells to MSCs reduces their inhibitory effects of MSCs and leads to their myelomatous transformation.

Keywords: myeloma line, hypercalcemia, co-culture, mesenchymal stem cells, demineralized bone matrix

Multiple myeloma (MM) accounts for nearly 20% of plasma cell dyscrasias that are distinguished by International Myeloma Working Group criteria.[1] The new definition of active multiple myeloma is clonal bone marrow (BM) plasma cells >10% or biopsy-proven bony or extramedullary plasmacytoma, and any one or more of the following features and myeloma-defining events (MDE): evidence of end organ damage that can be attributed to the underlying plasma cell proliferative disorder, specifically CRAB [**C**) Hypercalcemia: serum calcium >0.25 mmol/L (>1 mg/dL) higher than the upper limit of normal or > 2.75 mmol/L (>11 mg/dL), **R**) Renal insufficiency: creatinine clearance < 40 mL/min or serum creatinine >177mol/L (>2 mg/dL), **A**) Anemia: hemoglobin value of >2 g/dL below the lowest limit of normal, or a hemoglobin value <10 g/dL, and **B**) Bone lesions: one or more osteolytic lesion on skeletal radiography, computed tomography (CT), or positron emission tomography (PET)/CT. If bone marrow has <10% clonal plasma cells, more than one bone lesion is required to be distinguished from solitary plasmacytoma with minimal marrow involvement. Any one or more of the following biomarkers of malignancy (MDEs): i) ≥60% clonal plasma cells on BM examination, ii) Serum involved/uninvolved free light chain (FLC) ratio of ≥100, provided the absolute level of the involved light chain is at least 100 mg/L (a patient's involved FLC, either κ or λ, is above the normal reference range; the uninvolved FLC is typically in, or below the normal range), and iii) More than one focal

Abbreviations:

MM, multiple myeloma; BM, bone marrow; MTT, microculture tetrazolium test; MSC, mesenchymal stem cells; MDE, myeloma-defining events; CRAB, hypercalcemia, renal insufficiency, anemia, bone lesions; DKK, Dickkopf homologue-1; IGF-1, insulin-like growth factor; IL-6, interleukin-6; VEGF, vascular endothelial growth factor; FLC, free light chain; PTHrP, parathyroid hormone-related protein; RANKL, receptor activator of nuclear factor kappa B ligand; DBM, demineralized bone matrix; HMCL, human myeloma cell lines; DMEM, Dulbecco's modified Eagle medium; PFS, progression-free survival.

[1]Department of Hematology and Blood Banking, Faculty of Medical Sciences, Tarbiat Modares University, Tehran, Iran

*To whom correspondence should be addressed.
nadershirani@yahoo.com

lesion on magnetic resonance imaging (MRI) that is ≥5 mm in size.[2]

Myeloma cells originate from BM plasma cells that continuously receive growth and survival factors, such as B cell activating factor, A proliferation-inducing ligand , Insulin-like growth factor-1 (IGF-1), Interleukin-6 (IL-6), Vascular endothelial growth factor (VEGF), and IL-21 from BM myeloma niche cells, which leads to the activation of nuclear factor kappa-light-chain-enhancer of activated B cells (NF-κB), Janus kinase/signal transducers, and activators of transcription and phosphoinositide-3-kinase/RAC-alpha serine/threonine-protein kinase signaling pathways.[3] At times this pathway is sustainably activated due to quantitative and qualitative chromosomal abnormalities and mutations in regulatory proteins, which in turn activate the parallel signaling pathways, and cause myeloma neoplasms. Malignant plasma cells can stimulate osteoporosis severely, and lead to the development of BM lesions by producing Dickkopf homologue-1 (DKK), Receptor activator of nuclear factor kappa B ligand (RANKL), IL-3, Growth/differentiation factor 15 (GDF-15), Transforming growth factor beta (TGF-β), and parathyroid hormone related protein (PTHrP), direct and indirect stimulation of osteoclasts, and the inhibition of osteoblasts. All these are manifested by increased blood calcium level, kidney damage, anemia, and other symptoms of hypercalcemia. CRAB tetrad, especially hypercalcemia, is a symptom that is exclusively observed in MM and not in any other plasma cell dyscrasia.[4]

Considering the exacerbation of hypercalcemia in MM patients along with progression of the disease, the question is whether hypercalcemia or hypocalcaemia can affect the proliferation and survival rates of myeloma cells, and if hypercalcemia in MM acts as a growth factor and positive feedback? To answer these questions, mild and severe hypocalcemia conditions were induced by calcium chelators such as sodium citrate and ethylene diamine tetra acetic acid (EDTA), respectively. Also, calcium chloride and calcium lactate were used to create various concentrations of hypercalcemia. Meanwhile, culture media treated by 3-dimensional-demineralized bone matrix (DBM) scaffolds were employed to imitate BM environment and to create hypercalcemic conditions. The proliferation and survival of myeloma cells (vitality and viability) in each mode were analyzed by a methylthiazole tetrazolium test or microculture tetrazolium test (MTT) and flow cytometric assays, respectively. Myeloma cells acquire their immortality and

survival properties partially from BM niche cells. Therefore, co-culture of mesenchymal stem cells (MSCs) derived from normal and myeloma BMs with human myeloma cell lines (HMCL) in different ratios was the target of another investigation. For this purpose, combined Roswell Park Memorial Institute-1640 (RPMI-1640) and Dulbecco's modified Eagle medium (DMEM) culture media were used. Another difference in calcium concentration is the condition of cell culture in the two RPMI-1640 and DMEM media. Calcium concentration in DMEM is nearly 4.5 times that of RPMI-1640. Cell survival and proliferation in both media were compared by MTT assay, and then co-culture effects of normal and myeloma MSCs on HMCL was assessed.

Materials and Methods

Culture and Treatment of Myeloma Cells in Different Calcium Concentrations

The human myeloma cell lines (HMCLs) used in this study include RPMI-8226, JJN-3,U266, LP-1, L-363, KMM-1, and KMS-12BM. The myeloma cell is a post-germinal B lymphocyte, so a pre-germinal center B lymphocyte (Nalm-6), a non-B lymphocyte (Molt-4), and a nonlymphocytic myeloid cell (K562) were used as controls to determine the possible effects of calcium concentration for each lineage in similar conditions. Incubated with 5% CO_2 in 37°C and 85% humidity, cells were cultured in RPMI-1640 media supplemented by fetal bovine serum (FBS) 10%, penicillin 100 U/mL, and streptomycin 100 μg/mL. Calcium concentrations in all media were measured by Ion Selective Electrode (ISE) method (**Table 1**), despite the fact that the concentration of total calcium in RPMI, DMEM, and blood is known to be 0.4 mM (1.6 mg/dL), 1.8 mM (7 mg/dL), and 2–3 mM (8–10 mg/dL), respectively. In order to create hypocalcemic condition (Ca <2.5 mg/dL), sodium citrate (molecular weight: 294.1) and EDTA (MW: 372.24) (Sigma Aldrich-Germany) were used. Hypercalcemia condition (Ca >10 mg/dL) was created by using cell culture-specific calcium lactate (MW: 218.2) and calcium chloride (MW: 147.02) (Sigma Life-Science). Working solutions were prepared from a 10 mM initial stock using $C1V1 = C_2V_2$ formula. The basic medium of all wells was RPMI-1640 supplemented with 10% FBS. According to the designed experiment (**Table 1**), certain amounts of EDTA, sodium citrate, calcium chloride,

Table 1. Calcium Concentrations in Each of the Conditions Under Study

Ca Concentration (mg/dl)	Culture Media	Ca Concentration (mg/dl)	Culture Media
5.1±0.2	DMEM=RPMI+10%FBS	14.1 ± 0.2	FBS
5 ± 0.2	RPMI+10%FBS+3µl Ca Cloride 10mM	1.6 ± 0.2	RPMI-1640
10 ± 0.5	RPMI+10%FBS+6µl Ca Cloride 10mM	2.7 ± 0.2	RPMI+10%FBS
15 ± 1.1	RPMI+10%FBS+9.2µl Ca Cloride 10mM	0.8 ± 0.2	RPMI+ 3µl K3EDTA+10%FBS
20 ± 2.2	RPMI+10%FBS+12.5µl Ca Cloride 10mM	0.3 ± 0.1	RPMI+6µl K3EDTA+10%FBS
5 ± 0.2	RPMI+10%FBS+2.3µl Ca Lactate 10mM	1.9 ± 0.2	RPMI+20µl Citrate3.2%+10%FBS
10 ± 0.6	RPMI+10%FBS+4.6µl Ca Lactate 10mM	1.4 ± 0.2	RPMI+40µl Citrate3.2%+10%FBS
15 ± 1.2	RPMI+10%FBS+7µl Ca Lactate 10mM	7.0 ± 0.2	DMEM-High Glucose
20 ± 2.3	RPMI+10%FBS+9.6µl Ca Lactate 10mM	7.8 ± 0.2	DMEM+10%FBS

and calcium lactate were added to each well, and the concentration of calcium in each well was measured. 20×10^3 cells per microliter (95% viability) were transferred to 96W plate wells, and the above treatments were made. After 24 and 48 h, MTT and trypan blue tests were performed for each well. Cell apoptosis was examined by flow cytometry after 48 h for KMS-12BM cell line (as selective sample).

Co-Culture of Myeloma Cells in DBM-Containing Medium

DBMs are allograft bones converting to a 3D matrix with 40%–60% porosity, lacking blood, cells and minerals, but containing collagen I and noncollagen proteins such as adhesion proteins osteonectin, matrix metalloproteinase-2 (BMP2), and BMP-7 (belonging to TGF-β family) during decalcification with acid extraction, which are osteogenic and can be used to repair bone defects as well as in tissue engineering and regenerative medicine.

Simultaneously, with the study of the effects of hypercalcemia conditions on proliferation, metabolism, and survival of myeloma cells, DBM scaffold (Hans Biomed, DFDBA) was used to investigate a similar effect. For this purpose, 20×10^3 KMS-12BM myeloma cells were added to each well of 48W plates containing RPMI-1640 media supplemented with 10% FBS. Then 20 DBM beads were added to the wells in direct contact and discrete conditions through 0.3 µ meshed Transwell to provide new physicochemical conditions (juxtacrine and paracrine) for the proliferation and survival of myeloma cells in addition to DBM-conditioned media (DBM-cm). In this media, which is a combination of DBM, RPMI-1640, and FBS, calcium and other factors leak into and enrich the media. In fact, meshed transwells inhibit the juxtaposition of cells and DBM (paracrine condition). Treated

and control cells (lacking DBM) were cultured for 48 h in 37°C incubator with 5% CO_2. After 48 h, DBM beads and transwell were removed from the main wells by a sterile forceps and MTT assay was performed on all cells. Given the impossibility of taking 2D images, 3D images of DBMs in terms of their interaction and attachment to myeloma cells were taken and evaluated by scanning electron microscope (SEM).

Isolation and Identification of MSCs from BM

To isolate MSC cells, a standard protocol was followed. 1.5 mL of BM aspirate of an MM patient and an asymptomatic *Normal Healthy* individual were cultured in a T75 flask containing 15 mL of DMEM (Gibco, UK) containing 20% FBS (Gibco, Germany), NaHCO3 (3.7 mg/mL), and L-glutamin and penicillin/ streptomycin (100 U/mL and 100 mg/mL, respectively) (Sigma) in 5% CO_2 and 37°C. The adherent elongated cells, MSCs, exhibited homogeneous fibroblast-like morphology with a spindle or triangular-shaped cell bodies, large and ellipse nuclei, and growing outward in a "swirling fibroblast-like" pattern. The nonadherent cells were removed after 48 h with medium change. After 3–4 days, the cultures at 80%–90% confluence were tripsinized using 0.05% trypsin/1 mM EDTA, and then passaged at 1:2 ratios into fresh 25 cm^2 culture flasks. Subculture was repeated till passage 3 when sufficient cells were provided for the next stage of experiment. Finally, having been passaged 3 times, cells authenticated by multi lineage differentiation and flowcytometric analysis of CD105, CD29, CD73, CD44, CD45, and CD34 were used for the next stages of the study (**Figures 1** and **2**).

To promote multi lineage differentiation, MSCs at passage 3 were plated in a concentration of 3×10^4/mL in 6-well culture
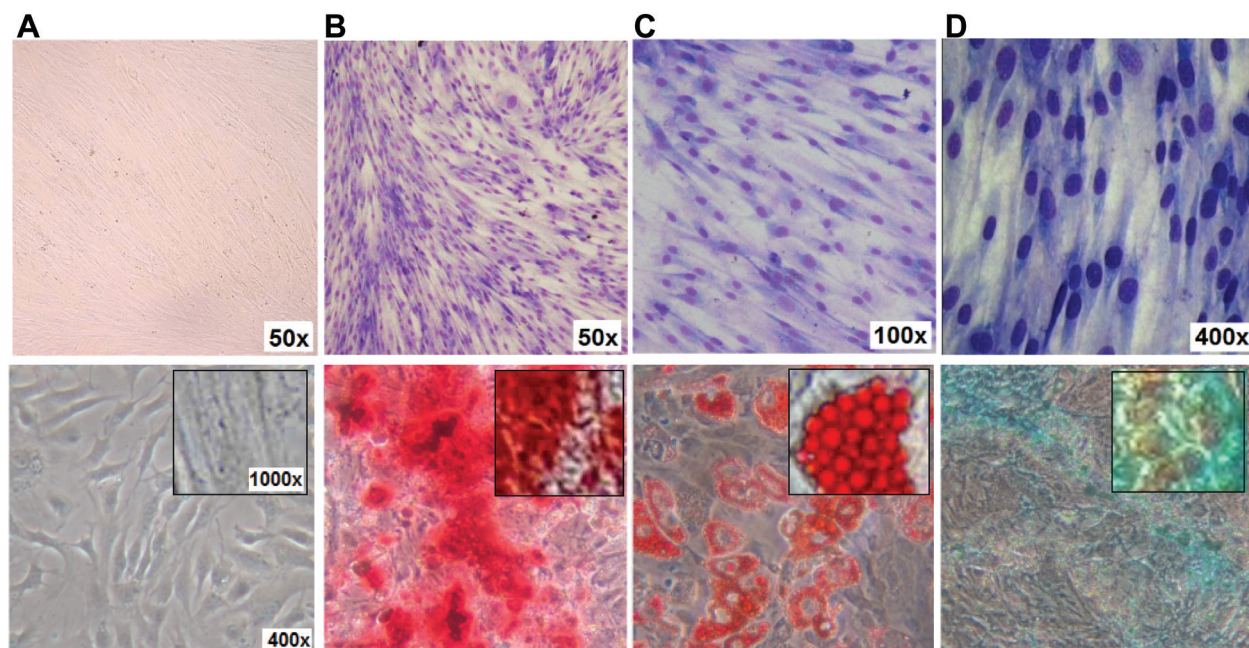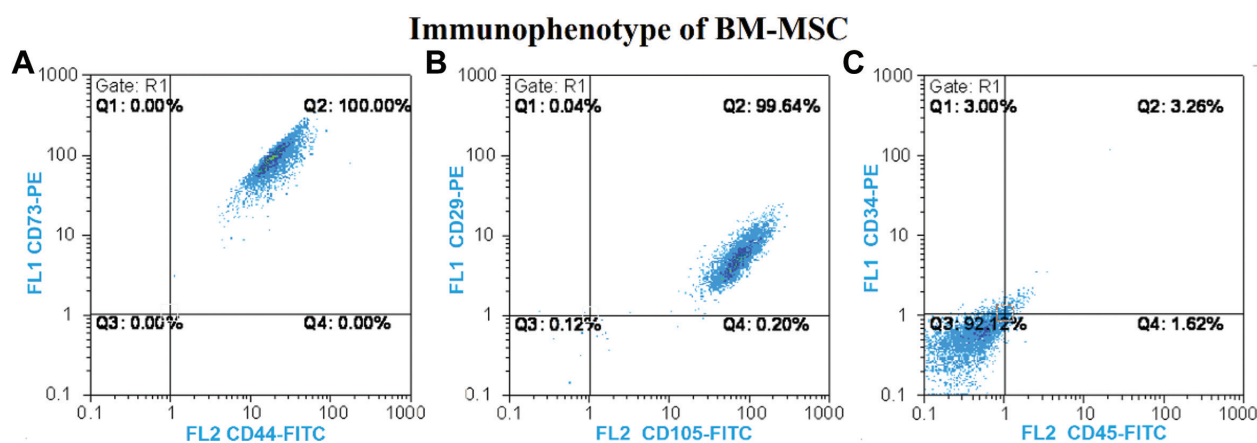
Figure 1

Top: Phase contrast image and right-Giemsa staining of primary culture of NH-MSC cells at the surface of the well with 70% confluency by 50, 100, and 400x magnification, showing spindle or triangular-shaped cell bodies, large and ellipse nuclei and growing outward in a "swirling fibroblast-like" pattern with transparent cytoplasm lacking granules. MSCs showed a varying cellular morphology from spindle-shaped towards more cuboidal fibroblast-like cells. Elongated fusiform cells were mostly observed after day 5 of the culture. Bottom: Compared with undifferentiated control MSCs (**A**), Osteogenic differentiation showed marked morphological changes and extensive extracellular calcium deposition in BM derived MSCs as demonstrated by positive Alizarin Red S staining (**B**). In adipogenic cultures, formation of lipid droplets within the cytoplasm of the cells was quite slow and were gradually occupied the whole cells. Accumulation of intracellular lipid droplets was determined as red loci following oil red O staining (**C**), in chondrogenic culture, the metachromatic nature of the matrix was determined by the toluidine blue staining of glycos-aminoglycans as purple stained loci in bone marrow (**D**).

plates until 70%–80% confluence. The proliferation medium was replaced by adipogenic differentiation (consisting of DMEM supplemented with 10% FBS, 50 μg/mL ascorbic 3-phosphate, 0.5 mM isobutyl-methylxanthine, 100 nM dexamethasone, and 50 μg/mL indomethacin), Osteogenic differentiation (DMEM medium supplemented with 10% FBS, 50 μg/mL ascorbic 3-phosphate, 10 nM dexamethasone, 0.5 mM isobutyl-methylxanthine, and 10 mM β glycerol phosphate), and chondrogenic differentiation (DMEM supplemented with 10% FBS, 10 ng/mL TGF-β1, 0.1 μM dexamethasone, 50 μg/mL ascorbic acid, and 50 mg/mL *I*nsulin, *T*ransferrin, *S*elenous acid (ITS+) premix (Becton Dickinson), 6.25 μg/mL of insulin, transferrin, and selenius acid, each) media (all from Sigma-Aldrich). The cultures were kept for 3 weeks during which differentiation medium

was changed twice weekly, and then specific staining was performed and identified under an inverted microscope (Olympus, Meridian).

The first sign of the adipogenic differentiation became evident 2–3 weeks after culture when lipid droplets appeared in the differentiating cells. Eventually, the lipid-rich vacuoles within cells combined together and filled the cells. Accumulation of lipid in these vacuoles was assayed histologically by oil red O (ORO) staining (Merck). Briefly, the intracellular accumulation of lipid-rich vacuoles was stained with 0.3% Oil Red O solution. To this end, the cells were washed by PBS and fixed in 40% paraformaldehyde for 20 min, washed and dehydrated with 70% isopopanol for 5 min, and stained with 2% oil red O solution in 99%

Figure 2

Immunophenotype of MSC that were positive for CD73, CD44, CD29, CD105, CD34, and CD45 that authenticated based on literature.

isopropanol for 10–15 min at room temperature. After 3 times washing with PBS, the intracellular lipid-rich vacuoles were stained as red foci.

At the end of the osteogenic period, the number and size of mineralizing nodules were maximized. To evaluate mineralized matrix, cells were stained with 2% Alizarin-Red S (ARS) solution (Behnogen). Briefly, the differentiated cells were washed twice with PBS and fixed with 40% paraformaldehyde for 15 min at room temperature. The cells were then washed thoroughly with PBS and stained with 2% ARS (pH = 4–4.2) within 0.5% NH_4OH for 2–5 min. After 2 min or 3 times washing by water, the mineralized matrix was identified by the presence of red foci in stained specimen.

At the end of chondrogenic period and for the presence of glycosaminoglycans within the extracellular matrix, the cells were stained with Toluidine blue. Briefly, the differentiated cells were fixed with 10% formalin for 10 min at room temperature. After washing, the cells were exposed to Toluidine blue for 30 sec at room temperature. Acid mucopolysaccharides and sulfated mucopolysaccharides within the extracellular matrix were stained as violet foci.

Co-Culture Effect of MSCs on Proliferation, Survival and Metabolism of Myeloma Cell Lines

Since in normal conditions, myeloma cells proliferate in BM in presence of BM stromal cells, co-culture of KMS-12BM

myeloma cells with mesenchymal stem cells from a Multiple Myeloma patient (MM-MSC) and a Normal Healthy subject (NH-MSC) were used to study the effects of MSCs. To provide simultaneous paracrine and juxtacrine conditions, we used direct culture of KMS-12BM cells on NH-MSC and MM-MSC adherent layers. For pure paracrine conditions, KMS-12BM cells were cultured in meshed 0.3 μm pores insert transwells (SPL Polyester/ PETE membrane). Myeloma cells also create autocrine conditions, but this effect was not investigated because of its uniformity in all 3 conditions. In fact, this test was conducted in duplicate for 3 modes: 1) single myeloma type, 2) myeloma cell line on MSC, and 3) myeloma cell line in transwell within an MSC-containing well, followed by MTT assay and the evaluation of the results.

First, in 2 series of 96W wells, 5×10^3 adherent MSCs were cultured from 2 MM patients and an apparently healthy person (DMEM media supplemented with 10% FBS). After 24 h and reaching 80% confluence, by changing the old culture medium, 10×10^3, 20×10^3, and 40×10^3 KM-12BM myeloma cells simultaneously suspended in 100 μL of 1:1 combined culture medium (DMEM + RPMI1640 supplemented with 10% FBS) were added to i) an empty well, (ii) on MSCs, and (iii) meshed insert transwells on MSC surface. After 48 h, myeloma cells were detached from transwell and MSC surface, and transferred to empty wells of 96W, and MTT assay was then performed on all 3 modes. Because DMEM and RPMI-1640 are specific culture media for MSCs and

myeloma cells, and given the lack of significant inter-actions of partly high calcium levels in DMEM on myeloma cells, a 50% combination of the two culture media was used in co-culture stage.

Methylthiazole Tetrazolium Test (MTT Assay)

To perform the MTT, the old culture medium of cells is discharged to remove the metabolites, drugs, and poten-tially reducing agents, leaving live cells as the only reducing agents of tetrazolium in the environment. For this purpose, the plate content is precipitated in a special centrifuge at 200 G for 10 min, so that the cells are not discarded while removing the culture medium. Subsequently, 100 µL of fresh culture medium and one-tenth of the culture medium volume (equivalent of 10 µL) MTT solution (Sigma) at 50 mg/mL con-centration, with final dilution of 5 mg/mL are added to each well. The plate coated with aluminum foil is incubated for 4 h in cell culture incubator for the formation of formazan crystals *on* the surface and interface of the cells. After centrifuging, the whole supernatant of wells is discarded, and 100 µL of solvent and lethal dimethyl sulfoxide (DMSO) is added to the cells. The plate is covered with foil and placed on a rotator for 15 mins so that all cells are killed and cannot form new crystals. Previously formed crystals by live cells are dissolved in DMSO. The plate is placed in enzyme-linked immuno-sorbent assay (ELISA)-Reader (Biotek-ELx800) and read at 570 and 630 nm wavelengths. OD630 (reference) related to the absorbance of plastic plate and the color of medium are subtracted from OD 570 to obtain final OD. The data are ana-lyzed in Excel and Gen5™ Data Analysis softwares (Biotek), and the following formula is used to calculate the inhibition percentages:

$$\% \, Inhibition = \left\{ 1 - \frac{\begin{array}{c} Absorbance \, of \\ (Test \, dose - initial \, plating) \end{array}}{\begin{array}{c} Absorbance \, of \\ (Control - initial \, plating) \end{array}} \right\} \times 100\%$$

Study the Number and Viability of KMS12BM Cells by 0.4% Trypan Blue Staining in Hypercalcemia and Hypocalcemia Treatments

The final OD obtained in the MTT assay depends on the metabolism of the cells, as well as their numbers, there-fore less absorbance may not be only due to cells' death, but to their decreased metabolism. As a result, a total cell count and the percentage of live cells (vitality) should be separately measured along with the MTT assay. For this purpose, we cultured 20×10^3 KMM-1 cells (as a cell with moderate to high sensitivity to hypercalcemia and hypo-calcemia) in each well of a 96w plate. In order to induce hypercalcemia and hypocalcaemia, 7 and 40 µL of 10 mM calcium chloride and 3.2% sodium citrate were respect-ively added to each well, and the cells were cultured in standard conditions for 24 and 48 h. At the end of each treatment, 50 µL of cell suspension of each well was re-moved and mixed with 50 µL of 0.4% trypan blue vital dye (Invitrogen). After 2 min, 50 µL of the mixture was removed and loaded between stone lamella and hemocytometer (modified Neubauer). After 2 min, total cell count and the number of blue (dead) cells were counted to calculate the vitality of cells (100 minus percentage of dead cells), using the following formula. In this test, dead cells are not able to pump trypan blue dye due to the lack of ATP, and they turn blue because of dye penetration:

Percentage of dead cells = (number of blue cells ÷ total number of cells) × 100

Flow Cytometric Analysis of Apoptosis by Annexin-V/PI Staining

The KMM-1 cell line was used to assess the apoptotic stage induced by hypercalcemia and hypocalcemia be-cause of moderate sensitivity of these cells to both con-ditions. After 24-h treatment, the cells were collected and centrifuged at 200 g for 10 min. 100 µL of binding buffer containing 1 µL Annexin-V (5 mg/mL) and 1 µL propidium iodide (1 mg/mL) dye was added to cells precipitate fol-lowing the removal of supernatant and rinsing with PBS buffer. After incubation in dark and RT for 15 min, the percentage of live, preapoptotic, and apoptotic cells was evaluated by BD-FACS Calibur (USA) and analyzed using FlowMax software.

Preparation of SEM Images of 3D DBM Structures After Culture with KMM-1 Myeloma Cells

To prepare 3D images of DBM treated with myeloma cells, the medium was first gently removed from the surface of the cells and initial fixation was performed in 2.5% glutaraldehyde solution (for 1.5 h at 4°C). After rinsing, sec-ondary fixation was done in 1% osmium tetroxide solution (2 h at 4°C). The samples were each placed in acetone with ascending purity (30, 50, 70, 80, 90, and 100%), for half
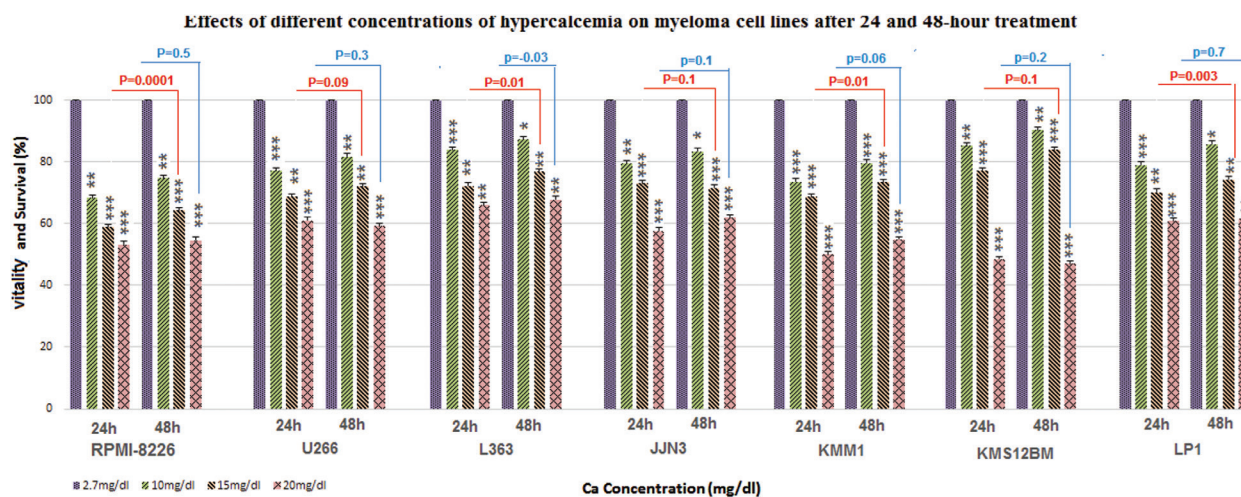
Figure 3

Evaluation of the effects of different concentrations of hypercalcemia on myeloma cells after 24 and 48-hour treatment in RPMI-1640 culture medium supplemented with 10% FBS. The vitality of myeloma cells in 10, 15, and 20 mg/dl concentrations of calcium chloride was 78%, 69%, 56%, respectively, and it was 83%, 73%, and 58% after 48 hours (*P* <.01). These numbers in similar concentrations of calcium lactate were 69%, 61%, 55% after 24 hours and 75%, 64%, and 58% after 48 hours (not shown). The survival of cells after 48 hours was 5% more than that after 24 hours. Cells showed higher survival rate (6%) after calcium chloride treatment compared to calcium lactate treatment, which was not meaningful (*P* >.5). however it was an indactor for compensatory and regulatory mechanisms for adaptation to hypercalcemia.

an hour to eliminate water from DBM. After dehydration, the samples were transferred to and kept for 72 h in 80°C freezer. Cells were then quickly transferred to a lyophilizing device to desiccate the samples in vacuum for 6 h. The opposite side of the sample was embedded in silver glue and attached on metal stabs. The samples were placed in a desiccator for 12–24 h to be dried. Biological samples were enclosed in a thin layer of carbon or heavy metals such as gold to acquire electron dispersion capacity. To this end, the samples were transferred to Spoter Coatering (Bal-Tec Company) to coat them with an approximate 12 nm thickness of gold. The coated samples were transferred to an SEM (Model XL30 of Philips, Netherlands) to take pictures of DBM surface.

Statistical Analysis

All experiments were performed as two or three independent tests and expressed as mean ± SD. For statistical analysis, Mann-Whitney and Kruskal Wallis tests were done using Statistical Package for the Social Sciences (SPSS-21) and Excel. *P* <.05 indicates that the mean difference between the experimental group and the control, and smaller *P* value, lower probability of random findings, and their higher significance are significant.

Results

Hypercalcemia and Hypocalcemia Decrease the Metabolism and Survival of Myeloma Cells in vitro

Both hypocalcemia and hypercalcemia conditions caused a decrease in metabolism and survival of myeloma cells (**Figures 3** and **4**); so that after 24 hours, the mean vitality of myeloma cells in 10, 15, and 20 mg/dl of calcium chloride, compared to controls, reduced to 78%, 69%, and 56%, respectively (*P* <.01). The vitality of the cells in similar concentrations of calcium lactate reduced to 69%, 61%, and 55%, respectively (not shown in the figure). Similarly, after 48 h, the mean vitality of myeloma cells (in same concentration of calcium chloride as above), decreased to 83%, 73%, and 58%, respectively (*P* <.01). The vitality of cells in similar concentrations of calcium lactate decreased respectively to 75%, 64%, and 58% after 48 h. As for nonmyeloma cells, this reduction in vitality was 81%, 69%, and 62% in calcium chloride (**Figure 5**) and 71%, 65%, and 61% in calcium lactate (not shown in the figure). Inhibitory and detrimental effects of hypocalcemia conditions were much more
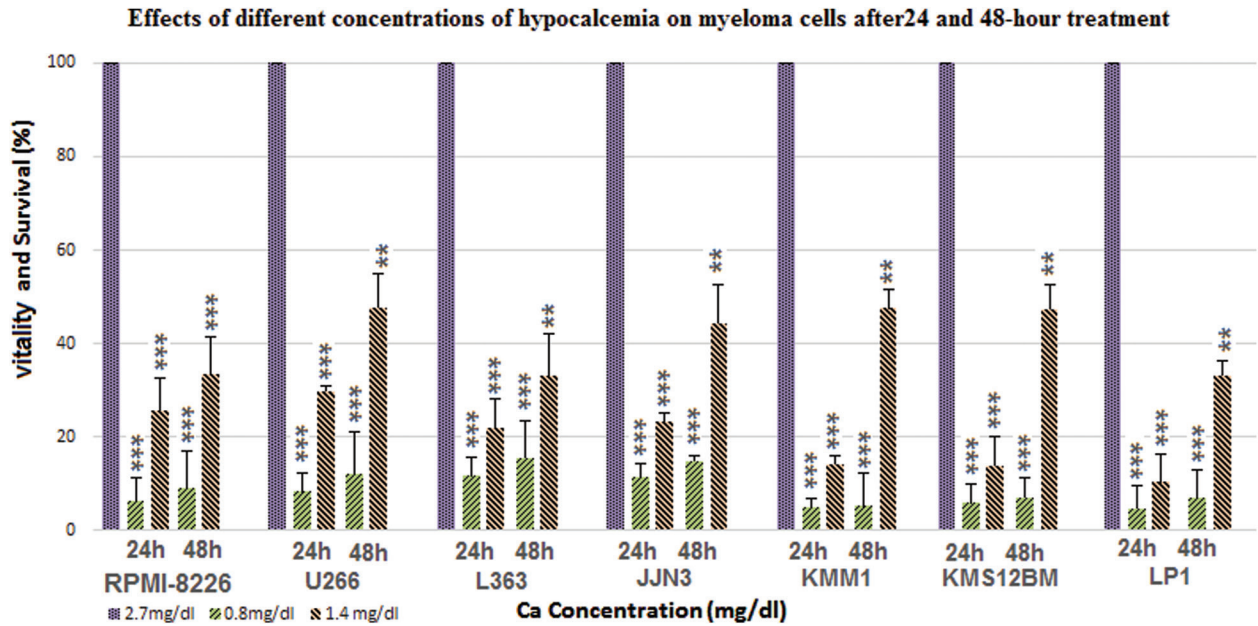
Figure 4

Evaluation of the effects of different concentrations of hypocalcemia on myeloma cells after24 and 48-hour treatment in RPMI-1640 culture medium supplemented with 10% FBS. The vitality of myeloma cells was 19.8% in citrated condition and 7.5% in EDTA containing culture (P <.01). this shows a moderate reduction to 40.9 and 10.1% within 48 hours. In both myeloma and non-myeloma cells inhibitory effects of hypocalcemia and hypercalcemia were more significant after 24 hours compare to 48 hours.
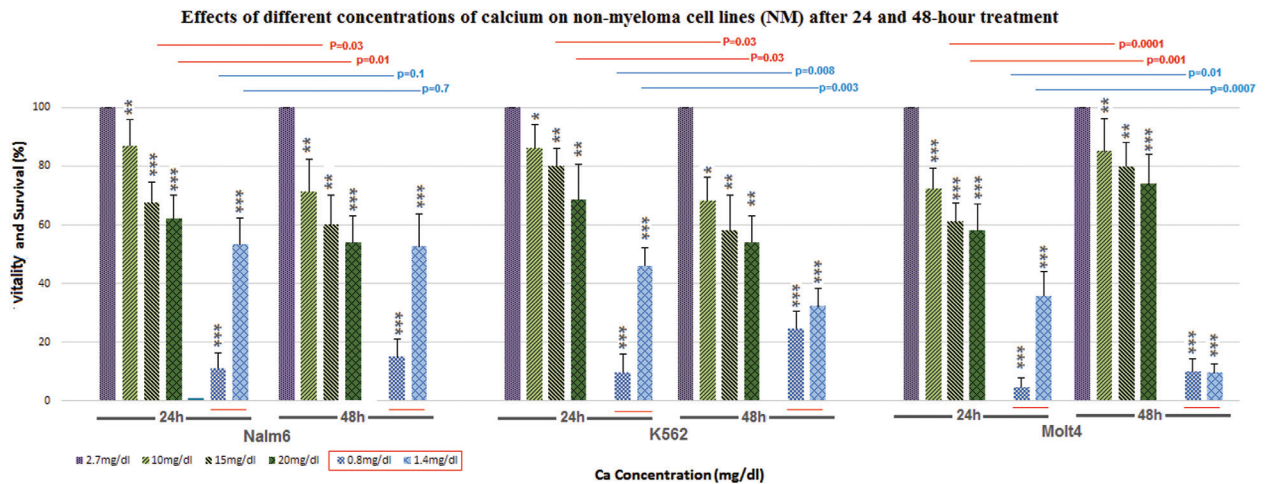
Figure 5

Evaluation of the effects of different concentrations of calcium on non-myeloma cell lines (NM) after 24 and 48-hour treatment in RPMI-1640 culture medium supplemented with 10% FBS. The vitality of non-myeloma cells in 10, 15, and 20 mg/dl concentrations of calcium chloride (81%, 69%, 62%, after 24 hours and 74%, 66%, and 60% after 48 hours, respectively) and calcium lactate (71%, 65% and 61% after 24 hours and 68%, 61% and 56% after 48 hours, respectively) showed a meaningful reduction (results of calcium lactate treatment are not shown). The inhibitory effect of hypocalcemia was so evident in Molt-4 cells (P <.001). the mean survival of NM cells in hypocalcemia conditions (1.9 and 0.8 mg/dl) was 31.5% and 8.5% after 24 hours and 45.1% and 16.6% after 48 hours, respectively. This shows a significant increase after 48 hours in citrate treated conditions.

significant than hypercalcemia conditions, so that 1.9 mg/dL and 0.8 mg/dL concentration of calcium treated with sodium citrate and EDTA reduced cell survival to 19.8% and 7.5% within 24 h and 40.9% and 10.1% within 48 h (P <.001), respectively. Surprisingly, lower inhibitory effects are seen over longer time intervals. Vitality of nonmyeloma control cells, in similar conditions, decreased to 31.5% and 8.5% within 24 h and 45% and 16.6% within 48 h. Among the nonmyeloma cells Molt-4 cell line showed a high sensitivity to hypocalcaemia (**Figure 5**). RPMI-8226 and LP-1 respectively showed the highest sensitivity to hypercalcemia and hypocalcemia conditions among myeloma cells. In both NM and MM cell lines, inhibitory and perhaps cytotoxic effects of calcium lactate which induced hypercalcemia were on average 6 ± 3% higher than calcium chloride, which was not significant (P >.5).

Another important point in this study was a brief reduction in inhibitory effects of hypercalcemia and hypocalcemia with an increase in treatment time from 24 to 48 h, which in all cases (except for citrate) increased metabolic rate and cell viability by 5 ± 3%. An explanation to this could be the regulatory effects of cells in reducing the influx and increasing the efflux of excess calcium, and calcium chelation by cell metabolites and acidic proteins, as well as adaptation of cells to new conditions. In case of citrate hypocalcemia, relative to 24-h treatment, the increase in metabolism and survival within 48 h was nearly 17 ± 5%, which could be attributed to the use of citrate as a nutrient metabolite in Krebs cycle.

The Number and Vitality of KMM-1 Cells are Decreased During Hypercalcemia and Hypocalcemia Treatments in vitro

The result of the MTT test not only depends on the number of live cells, but their metabolism and the level of formazan-producing NADH and NADPH; therefore, a decline in MTT may not exclusively be due to the death of the cells but to reduced metabolism of cells as well. As a result, in addition to MTT assay, the cell count/survival (Vitality) and apoptose kinetic (Viability) should be determined by trypan blue and flow cytometric tests, respectively. In this experiment, KMM-1 cells after 24 and 48 h of incubation in hypercalcemia (12 mg/dL) conditions showed a 27 ± 3.8% and 23.4 ± 3% reduction in the number and survival of cells relative to control, respectively. In terms of hypocalcemia (1.4 mg/dL), these values respectively showed 74 ± 6.6% and 65 ± 4/8% reduction, which was about three times higher than hypercalcemia
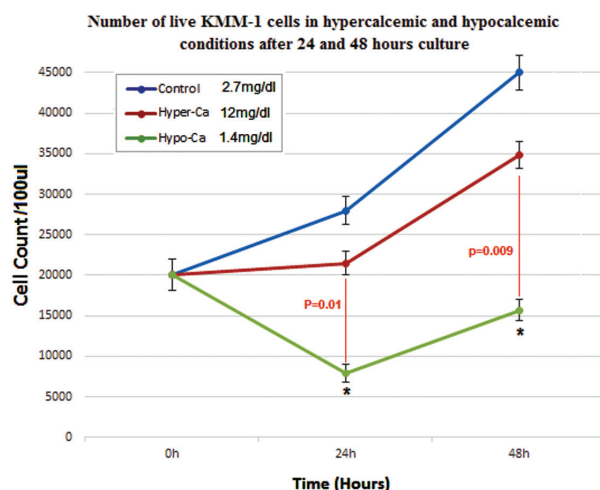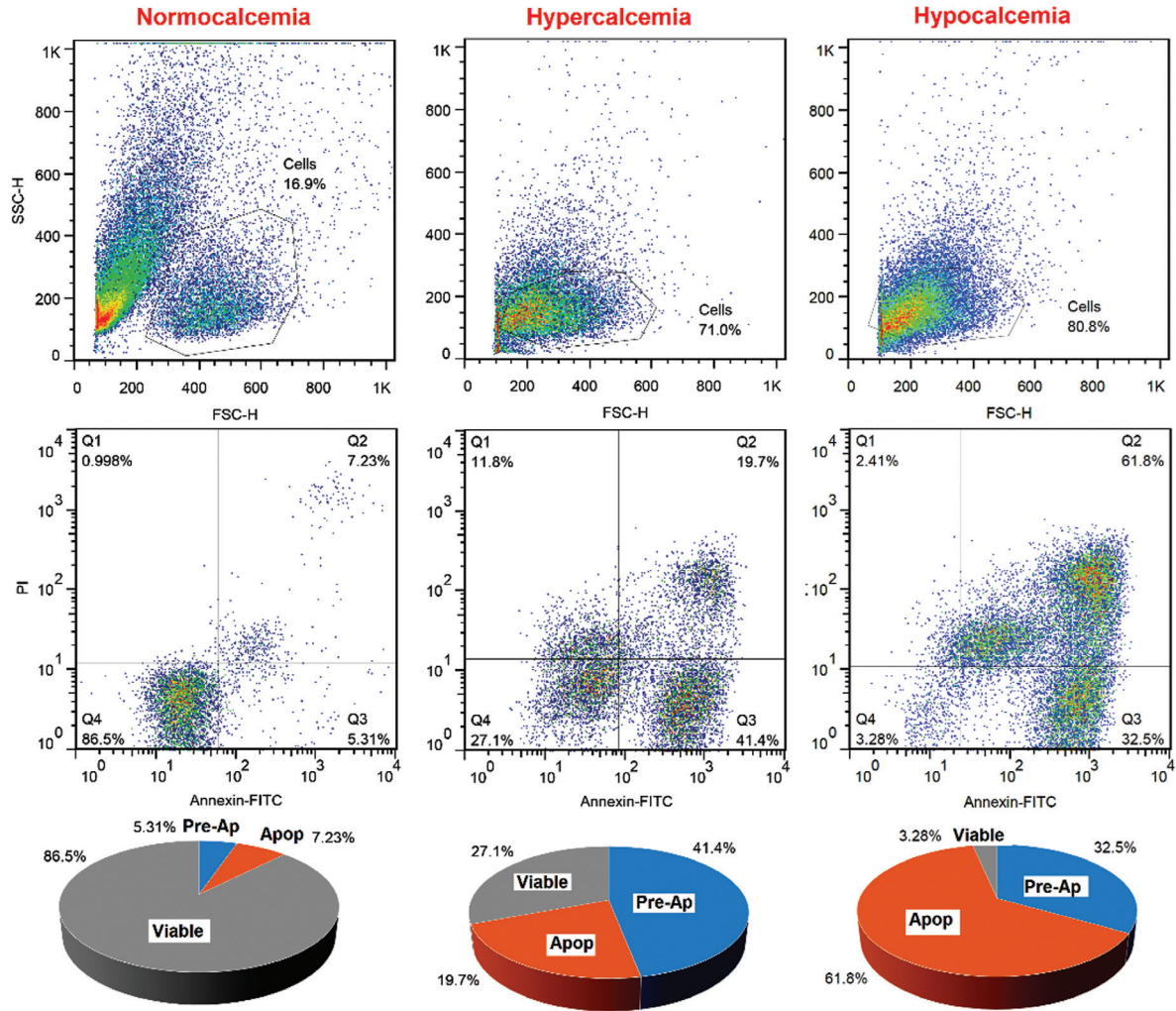

Figure 6

Assessment of the number of live KMM-1 cells in hypercalcemic and hypocalcemic conditions after 24 and 48 hours culture in RPMI-1640 medium supplemented with 10% FBS. The number of control cells increased by 1.4 times from 20000 to 28,000 cells after 24 hours. Under hypercalcemic condition, and over the same span; however, number of treated cells decreased by 27% to 21,500 cells (P <.05). Under hypocalcemic conditions, after 24 hours, the number of cells reduced 74% to 7900 cells (P <.01). In case of 48-hour treatment, the number of control cells increased 2.2 times (from 20,000 to 45,000 cells). However the number of cells under hypercalcemic and hypocalcemic conditions, reduced 23% (to 34,800) (P <.05) and 65% (to 15,700 cells) (P <.01), respectively. In both cases vitality was higher compared to 24-hour treatment. The average and standard deviation of the results from triplicate runs calculated and the P value indicate the meaningfulness of the results statistically compared to the control sample (* equivalent to P <.01 and ** equivalent to P <.001).

in reduction of cell count and vitality (**Figure 6**). it was found that hypercalcemia reduced simultaneous cellular count (27%) and survival (18%) in 24 h, therefor MTT's decline (50%) is not just due to cell death or hypometabolism alone (**Figures 6 and 7**). Also hypocalcemia reduced simultaneous cellular count (74%) and survival (61%) in 24 h, therefore the reduction of MTT (88%) is likely due to decreased proliferation and number of cells (increased apoptosis) as well as reduced cellular metabolism.

The Ratio of Late-Apoptotic to Preapoptotic Cells in Hypocalcemia is Reversed Relative to Hypercalcemia

Assessment of apoptosis by flow cytometry analysis of KMM-1 cell line in hypocalcemia (1.4 mg/dL) and

Viability and Apoptosis Status of KMM-1 Cell Line in Hyper and Hypocalcemic Conditions vs Normocalcemic Condition
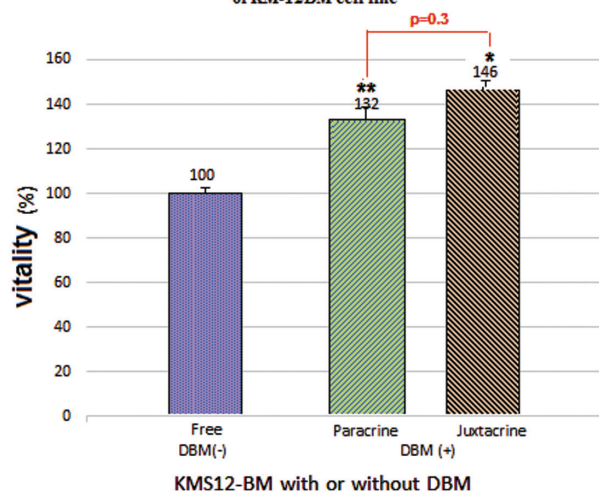

Figure 7

Study of viability and apoptosis status of KMM-1 cell line in 2 different conditions of calcium. Hypercalcemia induced pre-apoptosis more than late-apoptotic conditions (41 to 19%) but hypocalcemia induced late-apoptotic relative to pre-apoptotic conditions (61 to 32 %) over a culture period of 24 hours. The *P* value for the difference between apoptotic and preopoptotic conditions in hypercalcemia and hypocalcemia conditions was 0.003 and 0.05, respectively (meaningfulness).

hypercalcemia (12 mg/dL) revealed that hypercalcemia significantly induced preapoptosis more than late-apoptotic conditions (41% to 19%) and compared to hypocalcemia, it probably has a delayed phase of apoptosis (*P* <.01).

However, hypocalcemia-induced late-apoptosis compared to preapoptosis (61% to 32%) during 24 h (fast effect), but the total number of dead cells (late-apoptotic plus pre-apoptotic) is 1.5 times higher in hypocalcemia (**Figure 7**).

Figure 8

Paracrine and juxtacrine effects of 3D-DBM scaffold on metabolism and survival of KM-12BM cell line, showing a meaningful increase in cell survival up to 132% (P <.01) and 146 % (P <.05). Unlike simple hypercalcemia condition, increase in cell survival is evident. According to Mann-Whitney test P value was .3 and meaningless.

DBM Containing Medium Increases Metabolism and Survival of Myeloma Cells Creates a Mild Hypercalcemia Conditions

Interaction between KMS-12BM cell line and DBM in direct contact and discrete conditions through 0.3 μ meshed transwell, provide new juxtacrine, paracrine, and physicochemical conditions for the proliferation and survival of myeloma cells in addition to DBM-cm. The MTT assay showed 146% (P <.05) and 132% (P <.01) increase of metabolism and survival of cells in juxtacrine and paracrine conditions, respectively (**Figure 8**). This finding suggests that, in addition to DBM-derived growth factors, higher localized concentrations of factors and physicochemical structure of DBM play a role in juxtacrine proliferation of myeloma cells. In the last day, calcium concentration was measured in the culture medium containing DBM, which in both cases was 7.3 mg/dL and nearly 4.6 mg/dL higher than control medium.

DBM images show spongy and high porosity surfaces, which do not indicate any connection of myeloma cells to the surface (**Figure 9**). Imitation of three-dimensional conditions, calcium leakage and some inorganic factors on average increased the proliferation and survival of myeloma

cells in direct contact of cells with DBM by 146%; however, under conditions without direct contact, the mean increase in vitality was 132%.

Unlike MM-MSCs, Co-Culture of NH-MSCs with Myeloma Cell Line Decreases Metabolism and Survival of Myeloma Cells in vitro

Contrary to MM-MSCs, survival of KMS-12BM cells after 48-h co-culture in 4:1 ratio to NH-MSC was not increased. Survival and vitality rate of these cells in juxtacrine and paracrine conditions reduced by 46% and 12%, which was significant in direct contact conditions (P <.01), but the survival of cells in the presence of MM-MSC increased by 133% and 121%, respectively (**Figure 10**). Increased ratio of myeloma cells (8:1) reduced the inhibitory effects of NH-MSC and increased metabolism and survival of cells by 103% and 117% relative to baseline, respectively, while MM-MSC increased this value by 125% and 115%. The inductive effects of juxtacrine conditions were higher than paracrine (contrary to normal MSCs). In 2:1 ratio, the inhibitory effects of NH-MSC and the inductive effects of MM-MSC were significantly high in both juxtacrine and paracrine conditions; nevertheless, due to the difficulty in removing all myeloma cells from the surface of mesenchymal cells in juxtacrine conditions, precision and reproducibility of the test were low and of negligible significance because of coefficient of variation (CV) higher than 45%.

Discussion

Calcium is the most abundant mineral in the human body that plays a role in coagulation, contraction, conduction of electrical current, sleep regulation, bone formation, signaling, intracellular activation, and apoptosis.[5] Approximately 90–140 g of total calcium is found in bones. Calcium level in the body is regulated through 3 hormonal systems in kidney, intestine, and bone. Calcium regulating factors include calcitonin, parathyroid hormone (PTH), and parathyroid hormone-related protein (PTHrP). PTHrP is produced by malignant cells such as myeloma, breast, and lung carcinoma, causing hypercalcemia and increasing cellular adhesion in these patients. PTH and PTHrP stimulate adenylate cyclase and PLC enzymes to produce RANKL and inhibit the production of osteoprotegerin (RANKL antagonist) in osteoblasts.[6,7] RANKL binds to RANK on
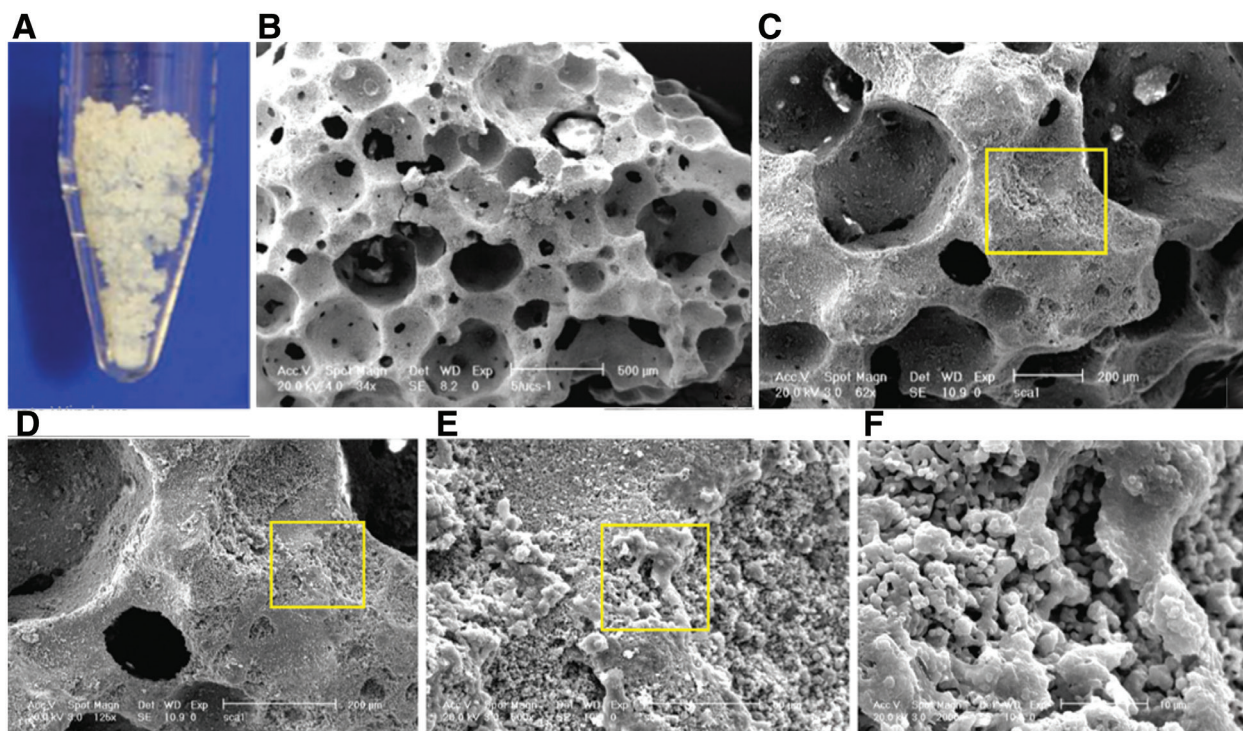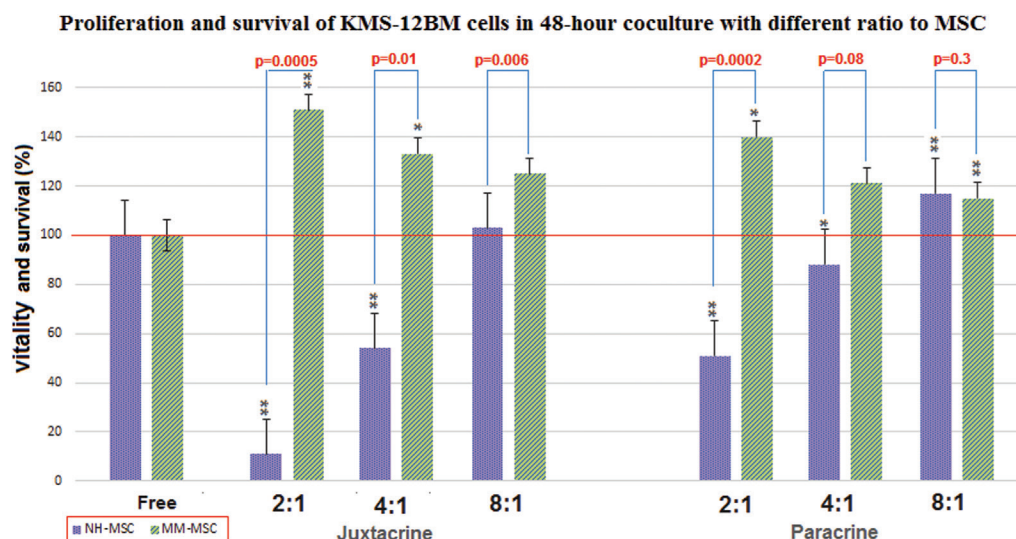
Figure 9

A) SEM image of DBM scaffold (post juxtacrine treatment with KMS-12BM) on **B**) 500µm, **C**) 200µm, **D**) 100µm, **E**) 50µm and **F**) 10µm scales magnifications with 30–40% porosity and surface area of 35–40 g/cm2. As it can be seen, no connection and interaction is observed between DBM and KMS12BM myeloma cells and DBM increased the proliferation of myeloma cells by 132 ± 6% through paracrine effect and secretion of humoral factors; however, the growth conditions in juxtacrine phase was 12% higher than paracrine (146 ± 4.3%).

osteoclasts and stimulates the production of carbonic acid by carbonic anhydrase enzyme, leading to bone destruction and calcium release. In contrast to PTH and PTHrP, sodium pamidronate inhibits calcium reabsorption, which increases bone density and repairs bone lesions in patients with myeloma.[8] Hypercalcemia in MM can also be a function of local osteolysis or humoral changes, thereby increasing IL-6 and PTHrP and decreasing PTH and consequently 1,25(OH) 2-Vit-D3, as well as the percentage of renal tubular reabsorption of phosphate (%TRP) and calcium/creatinine (C_{ca}/C_{cr}) clearance. Although PTH level is normal or decreased in 94% of patients (<68 pg/mL), it increases in 6% of cases, which is often associated with a poor prognosis. These patients also have a higher ratio of BM plasma cells, β2 microglobulin (β_2-MG), creatinine, lactate dehydrogenase (LDH), Igλ and IgA involvement, and paraprotein concentration, but their survival rate is decreased by 50%, and they are often in ISS-III stage (β_2-MG >5.5mg/L). PTH hormone stimulates RANKL, IL-6, and fms like tyrosine

kinase 3 (FLT-3) production, which increase the proliferation of plasma cells and decrease the apoptosis of plasma cells and hematopoietic stem cells. As a result, in patients with hyperparathyroidism, the risk of gammopathy is increased and the plasma cell ratio is higher in MM patients having high PTH levels.[4]

Myeloma cells produce DKK1, RANKL, IL-3, macrophage inflammatory protein 1-alpha (MIP-1α), MIP-3α, activin-A, GDF-15, TGF-β, hepatocyte growth factor (HGF), secreted frizzled-related protein 2 (sFRP2), sclerostin, VEGF, IL-6, IL-7, tumour necrosis factor-alpha (TNF-α), and can inhibit osteoblasts, stimulate osteoclasts, and induce osteolysis; therefore, serum calcium levels are highly increased which can affect the proliferation, survival, and activity of cells, as well as clinical symptoms of hypercalcemia.[9,10] A calcium level higher than 12 mg/dL (equivalent to 3 mmol/L) is called hypercalcemia, which is associated with dry mouth, polydipsia, polyuria, nausea, and anorexia. Calcium

Figure 10

Unlike MM-MSCs, proliferation and survival of KMS-12BM cells in 48-hour coculture with 4:1 ratio to NH-MSC, was not increased. vitality of these cells in both juxtacrine and paracrine modes was decreased by 46% and 12%, respectively. This shows that the reduction in survival of myeloma cells in direct contact (juxtacrine) conditions was significant (P <.01). However, survival of these cells in both juxtacrine and paracrine modes increased by 133% and 121%, respectively in the presence of MM-MSC cells. As the ratio of myeloma cells (8:1) increased, the inhibitory effects of NH-MSC decreased and the survival of cells increased by 3% and 17%. MM-MSC increased these values to 125% and 115%, although the induction effects of juxtacrine mode were greater than paracrine (contrary to NH-MSCs). Indeed, a high ratio of myeloma cells to MSC changed the nature of NH-MSC to a form similar to MM-MSC through the production of certain cytokines causing myeloma progress, in which the number of KMS-12BM cells increased to a level higher than baseline. In 2:1 ratio, the inhibitory effects of NH-MSC and the inductive effects of MM-MSC were high in both juxtacrine and paracrine conditions; however, due to the difficulty of removing all myeloma cells from the surface of mesenchymal cells in juxtacrine conditions, precision and reproducibility of the test were low and of lower significance because of CV higher than 45%. By calculating Kruskal-Wallis H and conducting Mann-Whitney test, P values between paracrine and juxtacrine groups of MMSs were calculated. The P value indicate the meaningfulness of the results statistically compared to the control sample (* equivalent to P <.01 and ** equivalent to P <.001).

levels >15 mg/dL (equivalent to 4 mmol/L) indicate acute hypercalcemia which is a medical emergency, and is accompanied by heart disease, crisis, and coma.[11]

The 48 h survival rate of myeloma and nonmyeloma cells lines in citrated and EDTA-containing hypocalcemic medium show significant reduction. on the other hand, inhibitory effects of hypocalcaemia and hypercalcemia were lower within 48 h than 24 h, which may be related to the compensatory effects, cellular compatibility, and the re-release of chelated calcium in 48 h. In this regard, a study was conducted indicating that somatic cells have a number of calcium influx channels, for example, Orai, Transient Receptor Potential-Canonical (TRPC), N-methyl-D-aspartate receptor (NMDA), voltage-operated channels (VOC), and mitochondrial calcium uniporter (MCU), as well as calcium efflux

channels [e.g., Na^+/Ca^{2+} exchanger (NCX) and plasma membrane Ca^{2+} ATPase (PMCA)] that during hypercalcemia, increasing expression of efflux channels and decreasing expression of influx channels cause adaptation to conditions.[12–15] To verify this phenomenon in myeloma cells, a similar study was conducted in line with calcium metabolism in myeloma cells, the results of which will be released in the future, but no clinical and in vivo studies have been conducted in this area.

In this study, the myeloma cells better tolerated hypercalcemia than hypocalcemia; nevertheless, these conditions did not increase their proliferation and survival *in vitro* and myeloma-induced hypercalcemia, resulting neither a positive feedback nor a vicious cycle. Obviously, moderate hypercalcemia caused by DBM slightly increases

the metabolism, survival, and vitality of myeloma cells, which is due to the release of growth factors and the expression of certain adhesion molecules in loose connection of DBM with myeloma cells. Therefore, this effect was greater in juxtacrine than paracrine conditions (146 ± 8% vs. 132 ± 7.3%), but this difference is not significant (*P* >.05).

DBMs are allograft bones converting to a 3D matrix with 40%–60% porosity lacking blood, cells, and minerals, but containing collagen I and noncollagen proteins such as adhesion proteins osteonectin, BMP2, and BMP-7 (belonging to TGF-β family) during decalcification with acid extraction, which are osteogenic and can be used to repair bone defects, as well as in tissue engineering and regenerative medicine. In addition, among the 4 cell lines of B lymphocyte, T lymphocyte, myeloid and myeloma, the Molt-4 T-cell line had a higher sensitivity to hypocalcaemia. Apoptosis rate is concentration-dependent, and EDTA treatment showed more severe effects in comparison with citrate, which may be associated with chelation of other ions such as Mg and Mn, along with the degradation of calcium-containing proteins.

Despite general similarities, RPMI-1640 and DMEM media have significant differences in their ingredients; for example, DMEM lacks biotin, para-aminobenzoic acid (PABA), cobalamin, calcium pentothenate, asparagine, aspartate, glutamine, glutamate and proline, and in turn has 2-fold glucose, leucine, serine, isoleucine, methionine, magnesium sulfate, and riboflavin, 3-fold glycine, histidine, lysine, tryptophan, and tyrosine, and 4-fold phenylalanine, calcium, nicotinamide, thiamine, pyridoxine, threonine, and folate. Unlike DMEM medium, RPMI-1640 lack iron.[16] The final calcium level measured by the ISE method in pure and FBS-supplemented RPMI-1640 was 1.6 mg/dL and 2.7 mg/dL, respectively, and these values for DMEM were 7 mg/dL and 7.8 mg/dL, respectively. Combination of the two culture media reached calcium concentration to 5.1 mg/dL, and according to the optimum culture of myeloma cells in RPMI-1640, cell survival was favorable in these conditions; nevertheless, calcium reduction to a threshold lower than pure RPMI-1640 significantly reduced cell survival.[17] At Ca >10 mg/dL concentration, a slight reduction in metabolism and survival of cells was also observed, which rejected the hypothesis of induced effects of myeloma hypercalcemic conditions.[18–21]

Hence, to kill myeloma cells, first their connection to mesenchymal cells and myeloma niches should be disengaged, followed by their sensitization to chemotherapy or bortezomib by anoikis support.[22] The development of

myeloma can be secondary to myeloma niche and vice versa. In other words, the mutation and transformation of plasmacyte niche to myeloma niche both amplify and activate plasmacyte signaling, causing its malignancy, or myeloma cells produce and secrete cytokines and growth factors providing for transformation of the natural niche to myeloma niche, forming a vicious circle developing myeloma.[23] At the onset of these myeloma changes, epigenetic and genetic changes such as aneuploidy, translocation, and mutations are of paramount importance. The expression of a large number of genes is different between MM-MSC and NH-MSC cells, including an increase in the expression of IL-6, DKK1, GDF-15, IL-10, IL-1β, Homeobox B (HOX-B), MMP-2/4–6, and TNF-α and the decrease of FGF expression in the former.[24] Application of NH-MSC in cell therapy not only kills MM cells but leads to differentiation into osteoblast, which improves the disease.[25,26] Alternatively, low FasL NH-MSC can be differentiated into supportive MM-MSCs, and increases the proliferation and survival of myeloma cells. The higher the expression of Fas-L/CD178 on the surface of normal MSCs, the greater their inhibitory effects on myeloma cells, which even increases the expression of Fas/CD95 on the surface of myeloma cells, while MM-MSCs show lower Fas-L expression and increase the survival of myeloma cells.[27–30]

In this research, based on the article by Anderson and Jakubikova, articlit was found that mesenchymal cells derived from myeloma patients act as a niche or a promoting factor for myeloma, but mesenchymal cells of healthy individuals are inhibitors of myeloma, which may lead to the development of a new strategy for the treatment of these patients via injection of normal MSCs into MM patients.[31] Obviously, a higher number of myeloma than mesenchymal cells over longer treatment periods changes the nature of NH-MSCs to MM-MSC such as forms with the production of certain myeloma inducing cytokines in which the number of KMS-12BM cells compared to baseline increases. Indeed, multiple myeloma in the long run causes the niche to change in its own right and contribute to the progression of myeloma. The proliferation and survival of KMS-12BM cells in 48-h co-culture with 4:1 ratio to NH-MSC did not increase in contrast to MM-MSC, and the metabolism and survival of these cells in juxtacrine and paracrine modes decreased significantly in direct contact condition (juxtacrine), But the proliferation and survival of cells in presence of MM-MSC cells increased.

Alternatively, with the increase in the ratio of myeloma cells (8:1), the inhibitory effect of NH-MSC was decreased, and the metabolism and survival of cells increased relative to

baseline. MM-MSC increased this value. Moreover, the induction effects of juxtacrine conditions were higher than paracrine (contrary to normal MSC). In 2:1 ratio, the inhibitory effects of NH-MSC and inductive effects of MM-MSC were greater than 4:1 ratio in juxtacrine conditions and inhibitory effects of normal mesenchymal cells is attributed to high expression of FasL by them, which was not investigated in this study.

In the MM mouse model, treatment of MSCs with highly expressed Fas ligand (FasLhigh MSCs) showed remarkable inhibitory effects on MM indenization in terms of extending the mouse survival rate and inhibiting tumor growth, bone resorption in the lumbus and collum femoris, and MM cell metastasis in the lungs and kidneys. In addition, reduced proliferation and increased apoptosis of MM cells were observed when co-cultured with FasL high MSCs in vitro. Furthermore, mechanistically, the binding between Fas and Fas Ligand (Fas-L) significantly induced apoptosis in MM cells, as evidenced through an increase in the expression of apoptosis marker and Fas in MM cells. In contrast, FasLnull MSCs promote MM growth. Fas-L/Fas-induced MM apoptosis plays a crucial role in the MSC-based inhibition of MM growth. it is possible that the higher stromal culture is just "sucking" up the hypercalcium either by cell influx or chealation by acidic proteins on the much larger cell surface of MSCs.[32]

Although MTT or a specific statistical study was not conducted for the survival of mesenchymal cells, there was evidence of an increase in apoptotic and degenerated NH-MSCs (narrow and dark cells) despite the increase in their number. But in the case of MM-MSC cells, the number of apoptotic cells was much lower (not shown). It was found that hypercalcemia in MM does not increase the proliferation or survival of myeloma cells, but the increase in the number of myeloma cells in BM or in vitro leads to the production of growth and differentiation factors, converting normal and anti-malignant stroma to myeloma promoting stroma exacerbating hypercalcemia and associated complications in MM by stimulating myeloma cells and osteoclasts.[33]

The main function of MSCs in BM is formation of endosteal and perivascular niches. Both of these niches are disrupted in MM, as evidenced by neoangiogenesis, osteolytic lesions, impaired hematopoiesis and immunosuppression, and the changes allow a subset of MM cells to escape dormancy and proliferate. BM MSCs can differentiate into adipocytes, which increase with age, and are considered negative regulators of hematopoiesis. MM induces

proliferation and expansion of MSCs, but other studies showed that MM cells elicit a premature senescence phenotype in MSCs. Osteoblasts and osteocytes are suppressed, particularly in areas of MM involvement. Yaccoby et al. showed that MSCs from patients with MM had changes in expression of genes associated with cellular proliferation, and a higher proportion of senescent cells and lower proliferative potential than those from age-matched healthy donors. Co-culturing normal MSCs with myeloma cells suppressed MSC differentiation to adipocytes and osteoblasts, and reduced expression of insulin-like growth factor-binding protein 2 (IGFBP2) and adiponectin.[34]

Drucker and Attar showed that BM resident mesenchymal stem cells (BM-MSCs) are altered in MM, and in vitro studies indicate their transformation by MM proximity is within hours. The response time frame suggested that protein translation may be implicated. BM-MSCs (ND and MM) co-cultured with MM cell lines displayed elevated proliferation and death, as well as increased expression/activity of major translation initiation factors (eIF4E, eIF4GI). MM cell lines co-cultured with MM-MSCs also displayed higher proliferation and death rates coupled with augmented translation initiation factors; in contrast, MM cell lines co-cultured with ND-MSCs did not display elevated proliferation only death and had no changes in eIF4GI levels/activity. EIF4E expression was increased in cell lines. there is direct dialogue between the MM and BM-MSCs populations that includes translation initiation manipulation and critically affects cell fate.[35]

Multiple myeloma MSC gene expression signatures can differentiate multiple myeloma from monoclonal gammopathy and smoldering multiple myeloma (SMM), as well as from healthy controls and treated multiple myeloma patients who have achieved a complete remission. Schinke and Yaccoby identified a prognostic gene score based on 3 MSC specific genes, type IV collagen alpha, natriuretic peptide receptor 3 (NPR3), and integrin beta like 1 (ITGBL1), that was able to predict progression-free survival (PFS) in multiple myeloma patients, and progression into multiple myeloma from SMM. A MSC gene score derived from overexpression of COL4A1, and underexpression of NPR3 and ITGBL1 in multiple myeloma microenvironment, had a significant impact on PFS and was also able to reliably predict the PFS of treated multiple myeloma patients who had achieved a complete remission (CR). Furthermore, a high-risk MSC gene score was associated with progression of MGUS/SMM patients to multiple myeloma. These results emphasize that progression of MM towards a more

aggressive phenotype and of SMM to MM does not solely rely on intrinsic plasma cells factors, but are independently impacted by the biology of the surrounding microenvironment. *COL4A1* interacts with other extracellular matrix components, controls the formation of new capillaries, and also regulates HIF-1α and VEGF expression (anti-angiogenic effect) and modulates progression of MGUS to MM. *NPR3* and *ITGBL1* play important roles within the extracellular matrix, though few reports suggest they contribute to tumor growth and carcinogenesis.[36]

Cell–cell communication is mediated by exosomes (Exs). Rocarro and Anderson showed that MM BM-MSCs release exosomes that are transferred to MM cells, thereby result in modulation of tumor growth in vivo. Exosomal microRNA (miR) content differed between MM and normal BM-MSCs, with a lower content of the tumor suppressor miRNAs.[37] MM patients exhibit distinguishable elevations in some of their contents such as miR-21, miR-146a, let-7b and miR-18a, while some molecules such as miR-15a are markedly downregulated in EXs of MM patients compared to healthy individuals. These findings make EXs desirable biomarkers for early prediction of disease progression and drug resistance in the context of MM.[38] In addition, MM BM-MSC-derived exosomes had higher levels of oncogenic proteins, cytokines (chemokines including CXCL1, IL6, IL-8, IP-10, MCP-1, and CCL-5), and adhesion molecules compared with exosomes from the cells of origin. Importantly, whereas MM BM-MSC-derived exosomes promoted MM tumor growth, normal BM-MSC exosomes inhibited the growth of MM cells. In summary, exosome transferred from BM-MSCs to clonal plasma cells represents a previously undescribed and unique mechanism that highlights the contribution of BM-MSCs to MM disease progression. a positive feedback loop between MM cells and MSC. MM cells promote the increase of miR146a in MSC which leads to more cytokine secretion, which in turn favors MM cell growth and migration.[39]

In the 3D model of Jakubikova and Anderson, MSC with conserved phenotype (CD73 + CD90 + CD105+) formed compact clusters with active fibrous connections, and retained lineage differentiation capacity. Extracellular matrix molecules, integrins, and niche-related molecules including N-cadherin and CXCL12 are expressed in the 3D MSC model. Furthermore, activation of osteogenesis (*MMP13*, *SPP1*, *ADAMTS4*, and *MGP* genes) and osteoblastogenic differentiation were confirmed in 3D MSC model. Co-culture of patient-derived BM mononuclear cells with either autologous or allogeneic MSC in 3D model increased proliferation of MM cells, CXCR4 expression, and SP cells. Importantly, resistance to novel agents (IMiDs, bortezomib, carfilzomib) and conventional agents (doxorubicin, dexamethasone, melphalan) was observed in 3D MSC system, reflective of clinical resistance.[31]

Conclusions

In this study, both hypercalcemia and hypocalcemia conditions decreased the survival of myeloma cells in vitro, although hypercalcemic conditions showed better results in these cells. The proliferation and survival of myeloma cells depend on stromal cells which are transformed into malignant forms, so NH-MSCs cannot protect, but inhibit myeloma cells. However, increasing the ratio of myeloma cells to MSCs reduces the inhibitory effects on MSCs and leads to myelomatous transformation. More studies are required to answer the questions in this field. **LM**

Authors' contributions

N.V.S conceived the manuscript and revised it and performed the technical tests; S. A wrote and revised the manuscript, provided data and information.

Compliance with ethical guidelines

Ethical approval

"All procedures performed in studies involving human participants were in accordance with the 1964 Helsinki declaration and its later amendments or comparable ethical standards."

References

1. Willan J, Eyre TA, Sharpley F, Watson C, King AJ, Ramasamy K. Multiple myeloma in the very elderly patient: challenges and solutions. *Clin Interv Aging.* 2016;11:423–435.

2. Kyle RA, Rajkumar SV. Criteria for diagnosis, staging, risk stratification and response assessment of multiple myeloma. *Leukemia.* 2009;23(1):3–9.

3. Terpos E, Ntanasis-Stathopoulos I, Gavriatopoulou M, Dimopoulos MA. Pathogenesis of bone disease in multiple myeloma: from bench to bedside. *Blood Cancer J.* 2018;8(1):7.

4. Rajkumar SV, Dimopoulos MA, Palumbo A, et al. International Myeloma Working Group updated criteria for the diagnosis of multiple myeloma. *Lancet Oncol.* 2014;15(12):e538–e548.

5. Haupt S, Raghu D, Haupt Y. p53 Calls upon CIA (Calcium Induced Apoptosis) to Counter Stress. *Front Oncol.* 2015;5:57.

6. Mascia F, Denning M, Kopan R, Yuspa SH. The black box illuminated: signals and signaling. *J Invest Dermatol.* 2012;132(3 Pt 2):811–819.

7. Pedriali G, Rimessi A, Sbano L, et al. Regulation of endoplasmic reticulum-mitochondria Ca2+ transfer and its importance for anti-cancer therapies. *Front Oncol.* 2017;7:180.

8. Krebs J, Agellon LB, Michalak M. Ca(2+) homeostasis and endoplasmic reticulum (ER) stress: An integrated view of calcium signaling. *Biochem Biophys Res Commun.* 2015;460(1):114–121.

9. Wu X, Lin M, Li Y, Zhao X, Yan F. Effects of DMEM and RPMI 1640 on the biological behavior of dog periosteum-derived cells. *Cytotechnology.* 2009;59(2):103–111.

10. Arora M. Cell culture media: a review. *Mater Methods* 2013(3):175.

11. Sigel A, Sigel H, Sigel RK, editors. Interrelations Between Essential Metal Ions and Human Diseases. Netherlands: Springer Netherlands; 2013;13:81–137.

12. Ritter CS, Haughey BH, Miller B, Brown AJ. Differential gene expression by oxyphil and chief cells of human parathyroid glands. *J Clin Endocrinol Metab.* 2012;97(8):E1499–E1505.

13. Lappas D, Noussios G, Anagnostis P, Adamidou F, Chatzigeorgiou A, Skandalakis P. Location, number and morphology of parathyroid glands: results from a large anatomical series. *Anat Sci Int.* 2012;87(3):160–164.

14. Davey RA, Turner AG, McManus JF, et al. Calcitonin receptor plays a physiological role to protect against hypercalcemia in mice. *J Bone Miner Res.* 2008;23(8):1182–1193.

15. Poole KE, Reeve J. Parathyroid hormone - a bone anabolic and catabolic agent. *Curr Opin Pharmacol.* 2005;5(6):612–617.

16. Silbermann R, Roodman GD. Myeloma bone disease: Pathophysiology and management. *J Bone Oncol.* 2013;2(2):59–69.

17. Hens JR, Wysolmerski JJ. Key stages of mammary gland development: molecular mechanisms involved in the formation of the embryonic mammary gland. *Breast Cancer Res.* 2005;7(5):220–224.

18. Broadus AE, Mangin M, Ikeda K, et al. Humoral Hypercalcemia of Cancer. *N Engl J Med*. 1988;319:556–563.

19. Ring ES, Lawson MA, Snowden JA, Jolley I, Chantry AD. New agents in the treatment of myeloma bone disease. *Calcif Tissue Int.* 2018;102(2):196–209.

20. Fairfield H, Falank C, Avery L, Reagan MR. Multiple myeloma in the marrow: pathogenesis and treatments. *Ann N Y Acad Sci.* 2016;1364:32–51.

21. Heusschen R, Muller J, Duray E, et al. Molecular mechanisms, current management and next generation therapy in myeloma bone disease. *Leuk Lymphoma.* 2018;59(1):14–28.

22. Heusschen R, Muller J, Withofs N, Baron F, Beguin Y, Caers J. Multiple myeloma bone disease: from mechanisms to next generation therapy. *Belgian J Hematol*. 2017;8(2):66–74.

23. Gunn WG, Conley A, Deininger L, Olson SD, Prockop DJ, Gregory CA. A crosstalk between myeloma cells and marrow stromal cells stimulates production of DKK1 and interleukin-6: a potential role in the development of lytic bone disease and tumor progression in multiple myeloma. *Stem Cells.* 2006;24(4):986–991.

24. Xu S, De Veirman K, De Becker A, Vanderkerken K, Van Riet I. Mesenchymal stem cells in multiple myeloma: a therapeutical tool or target? *Leukemia*. 2018;32.14–1500(7).

25. Garcia-Gomez A, Sanchez-Guijo F, Del Cañizo MC, San Miguel JF, Garayoa M. Multiple myeloma mesenchymal stromal cells: Contribution to myeloma bone disease and therapeutics. *World J Stem Cells.* 2014;6(3):322–343.

26. Xu S, Menu E, De Becker A, Van Camp B, Vanderkerken K, Van Riet I. Bone marrow-derived mesenchymal stromal cells are attracted by multiple myeloma cell-produced chemokine CCL25 and favor myeloma cell growth in vitro and in vivo. *Stem Cells.* 2012;30(2):266–279.

27. Filho GS, Caballé-Serrano J, Sawada K, et al. Conditioned medium of demineralized freeze-dried bone activates gene expression in periodontal fibroblasts in vitro. *J Periodontol.* 2015;86(6):827–834.

28. Becerra J, Andrades JA, Ertl DC, Sorgente N, Nimni ME. Demineralized bone matrix mediates differentiation of bone marrow stromal cells in vitro: effect of age of cell donor. *J Bone Miner Res.* 1996;11(11):1703–1714.

29. Honsawek S. *"The Quantitative Assessment of Osteoinductivity of Human Demineralized Bone Matrix and cDNA Array Analysis of Osteogenic Differentiation in Human Periosteal Cells" (2003)*. Doctor of Philosophy (PhD), Dissertation, Old Dominion University, DOI:10.25777/a527-vm76.

30. Reagan MR, Ghobrial IM. Multiple myeloma mesenchymal stem cells: characterization, origin, and tumor-promoting effects. *Clin Cancer Res.* 2012;18(2):342–349.

31. Jakubikova J, Cholujova D, Hideshima T, et al. A novel 3D mesenchymal stem cell model of the multiple myeloma bone marrow niche: biologic and clinical applications. *Oncotarget.* 2016;7(47):77326–77341.

32. Atsuta I, Liu S, Miura Y, et al. Mesenchymal stem cells inhibit multiple myeloma cells via the Fas/Fas ligand pathway. *Stem Cell Res Ther.* 2013;4(5):111.

33. Mehdi SJ, Johnson SK, Epstein J, et al. Mesenchymal stem cells gene signature in high-risk myeloma bone marrow linked to suppression of distinct IGFBP2-expressing small adipocytes. *Br J Haematol.* 2019;184(4):578–593.

34. André T, Meuleman N, Stamatopoulos B, et al. Evidences of early senescence in multiple myeloma bone marrow mesenchymal stromal cells. *PLoS One.* 2013;8(3):e59756.

35. Attar-Schneider O, Zismanov V, Dabbah M, Tartakover-Matalon S, Drucker L, Lishner M. Multiple myeloma and bone marrow mesenchymal stem cells' crosstalk: Effect on translation initiation. *Mol Carcinog.* 2016;55(9):1343–1354.

36. Schinke C, Qu P, Mehdi SJ, et al. The Pattern of Mesenchymal Stem Cell Expression Is an Independent Marker of Outcome in Multiple Myeloma. *Clin Cancer Res.* 2018;24(12):2913–2919.

37. Roccaro AM, Sacco A, Maiso P, et al. BM mesenchymal stromal cell-derived exosomes facilitate multiple myeloma progression. *J Clin Invest.* 2013;123(4):1542–1555.

38. Moloudizargari M, Abdollahi M, Asghari MH, Zimta AA, Neagoe IB, Nabavi SM. The emerging role of exosomes in multiple myeloma. *Blood Rev.* 2019;38:100595.

39. De Veirman K, Wang J, Xu S, et al. Induction of miR-146a by multiple myeloma cells in mesenchymal stromal cells stimulates their pro-tumoral activity. *Cancer Lett.* 2016;377(1):17–24.

Case Study

Monocytic Acute Myeloid Leukemias with KM2TA Translocations to Chromosome 17q that May Clinically Mimic Acute Promyelocytic Leukemia

Raisa I. Balbuena-Merle, MD, MHS,[1,2] Christopher A. Tormey, MD,[1] Autumn DiAdamo, BS,[3] Henry M. Rinder, MD,[1,4] Alexa J. Siddon, MD[1]

ABSTRACT

Objective: Acute promyelocytic leukemia (APL) with variant *RARA* translocation, eg, t(11;17), is not sensitive to all-trans retinoic acid and requires distinct chemotherapy. However, there are some leukemic entities that may mimic aspects of the clinical and/or laboratory picture of APL and cause confusion because of karyotype nomenclature. Therefore, recognition of such entities may be of therapeutic and prognostic significance.

Methods: We present 2 cases of acute myeloid leukemia (AML) with t(11;17) that were clinically concerning for APL based primarily on clinical presentation but were ultimately diagnosed as AML with monocytic differentiation.

Results: Both leukemias harbored *KMT2A* translocations, one located near but not involving *RARA* and the other with *SEPT9*.

Conclusion: In leukemias that clinically and/or immunophenotypically mimic APL, identification of specific gene translocations can lead to the correct diagnosis and may carry therapeutic/prognostic implications.

Keywords: acute myeloid leukemia, *RARA* variants, acute promyelocytic leukemia, genetic sequencing, karyotype, fluorescence in situ hybridization, molecular diagnostics

De novo acute myeloid leukemia (AML) with t(11;17) mimics other leukemic entities, creating a difficult diagnostic approach.[1-3] Specifically, morphologic findings may be nonspecific, creating confusion regarding the leukemic cell lineage (myeloid, monocytic, or promyelocytic), and could potentially lead to inappropriate therapies early in the disease course. Translocations involving the *KMT2A* gene (previously known as *MLL*), if not specifically identified, can be misconstrued as variant acute promyelocytic leukemia (APL), especially when there is a similar clinical presentation.[2] We report 2 cases of de novo AML with *KMT2A* translocations that illustrate these points by their clinical features, which were suggestive of APL. We reviewed the literature from 1961 to the present for acute leukemias with *KMT2A* translocations (11q23) involving either 17q12 or 17q21 (near or involving *RARA*) and 17q25 (*SEPT9*), research for which also reported the results of immunophenotyping and morphology.

Abbreviations:

APL, acute promyelocytic leukemia; AML, acute myeloid leukemia; rr, reference range; NSE, nonspecific esterase; MPO, myeloperoxidase; AMoL, acute monocytic/monoblastic leukemia; FISH, fluorescence in situ hybridization; NGS, next-generation sequencing; DIC, disseminated intravascular coagulation; PCR, polymerase chain reaction; ATRA, all-trans retinoic acid.

[1]Department of Laboratory Medicine, Yale University School of Medicine, New Haven, Connecticut, [2]Pathology and Laboratory Medicine Service, VA Connecticut Healthcare System, West Haven, Connecticut, [3]Department of Genetics and [4]Internal Medicine (Hematology), Yale University School of Medicine, New Haven, Connecticut

*To whom correspondence should be addressed.
Alexa.siddon@yale.edu

Case Series

Case 1

A male patient aged 26 years presented with new-onset weakness, decreased appetite, weight loss, rigors, and diaphoresis, but no bleeding was noted. His white blood cell count was $5.5\times10^3/\mu L$ (reference range [rr] = $4–10\times10^3/\mu L$) with 44% blasts, hemoglobin 3.6 g/dL (rr = 12 g/dL–18 g/dL), and platelets $103\times10^3/\mu L$ ($140–440\times10^3/\mu L$).

Coagulation studies were normal. The hematologist reviewed the blood smear (**Figure 1A**, Image A) and was concerned for APL; however, blasts were strongly positive for nonspecific esterase (NSE) staining (**Figure 1B**, Image B) and negative for myeloperoxidase (MPO) by cytochemical staining. The patient refused a bone marrow examination. Immunophenotyping of blood showed CD34- HLADR++ blasts (**Table 1**) with additional markers that favored the diagnosis of acute monocytic/monoblastic leukemia (AMoL). Blastic plasmacytoid dendritic cell neoplasm in leukemic phase was also considered based on dim CD56 expression.

Fluorescence in situ hybridization (FISH) was negative for t(15;17) and t(9;22). Specifically, FISH for t(15;17) was performed using dual color probes for the *PML* gene at 15q24.1 and for the *RARA* gene at 17q21 (Cytocell Inc). Of the 200 interphase cells examined, 100% had the normal pattern of 2 independent signals for each probe consistent with absence of fusions; this result also ruled out *RARA* gene rearrangement. Final cytogenetics (**Table 1**) showed a t(11;17)(q23;q12) translocation in all 15 metaphase cells examined with *KMT2A* (11q23; Cytocell Inc) rearrangement in 89% of blood leukocytes (200 interphase cells examined; **Figure 2**). The karyotype was 46,XY, t(11;17)(q23;q12)[15]. Next-generation sequencing (NGS) using our in-house custom 49-gene panel (See Supplemental Table 1), including commonly mutated genes in AML, did not detect pathologic variants. The final diagnosis was AMoL with t(11;17) translocation. After red cell transfusion but before specific therapy, the patient left against medical advice and was lost to follow-up.

Case 2

A female patient aged 70 years presented with acute-onset left-sided abdominal pain. Her white blood cell count was $71 \times 10^3/\mu L$ with 30% blasts, hemoglobin 10.5 g/dL, and platelets $61 \times 10^3/\mu L$. Computed tomography revealed hemoperitoneum. Coagulation studies were abnormal (prothrombin time 20.2 seconds [rr = 9.6–12.4 seconds], d-dimer 23.78 mg/L fibrinogen equivalent units (FEU) [rr = <0.75 mg/L FEU], and fibrinogen 94 mg/dL [209 mg/dL–444 mg/dL]), interpreted as being consistent with disseminated intravascular coagulation (DIC) by the primary team and raising clinical suspicion for APL (among other leukemic entities). Blood cytochemical stains showed MPO-positive, NSE-negative blasts. Immunophenotyping showed blasts to be CD34- and HLADR+ with additional markers favoring AMoL (**Table 2**).

In the marrow, polymerase chain reaction (PCR) detected an *FLT3* D835 mutation, and FISH/cytogenetics showed a t(11;17)(q23;q25) rearrangement within a hyperdiploid karyotype (**Table 2**). The patient's final karyotype was 48,XX,+6,t(11;17)(q23;q25),+13[15]/50,idem,+4,+8[3]/46,XX[2]. Through NGS, we detected a pathogenic *EZH2* variant and confirmed the *FLT3* D835 variant. The final diagnosis was AMoL with an *FLT3* tyrosine kinase mutation, a presumptive *KMT2A-SEPT9* translocation, and an *EZH2* variant. The patient achieved complete remission after induction but relapsed 2 months later with 60% blasts of the identical immunophenotype and acute intracranial hemorrhage; she died within 24 hours of admission.

Discussion

Certain clinical scenarios prompt pathologists to err on the side of caution by favoring a more actionable diagnosis, such as APL, in the scenario of a new leukemia with distinctive morphological and immunophenotypic characteristics. Certainly, when coagulation studies in a patient with de novo leukemia suggest DIC, as in case 2, there is strong suspicion for APL, which can also show monocytic-like morphology. Even when the blast immunophenotype is compatible with AMoL, the presence of a possible APL variant translocation creates a diagnostic challenge.[4] Although rapid PCR testing may be an aid in this setting, it is generally specific for the product of t(15;17); therefore, FISH is a better and more broad-based tool for variant APL. Specifically, if a patient has a translocation involving 17q, then FISH studies are necessary for confirming whether or not the *RARA* gene is actually involved. A significant number of genes have been associated with AML translocations of 11q23 within the 17q12–25 region, including *MLL-LASP1, MLL-MLLT6/AF17,* and *MLL-ACACA*.[5,6] Previous research in patients with AML has shown that the breakpoints in these regions do not directly involve the *RARA* gene.[7,8] These variant translocations generally do not result in all-trans retinoic acid (ATRA) sensitivity of the leukemia; hence, it is necessary to identify these specific AML translocations to institute appropriate therapy.[9]
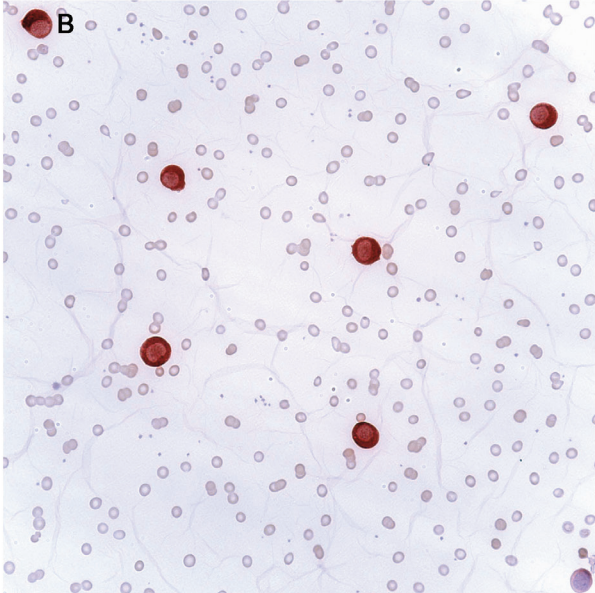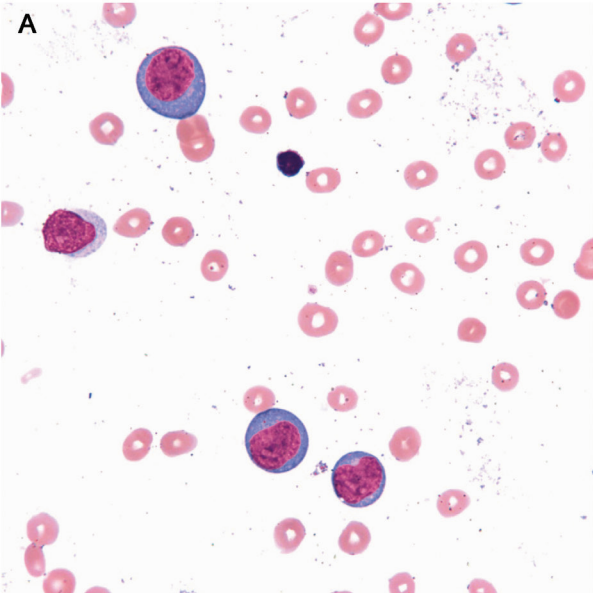
AML with t(11;17)(q23;q12 or q21)

Per our literature review, we identified 6 individual case reports where a *KMT2A* (*MLL*) gene rearrangement was
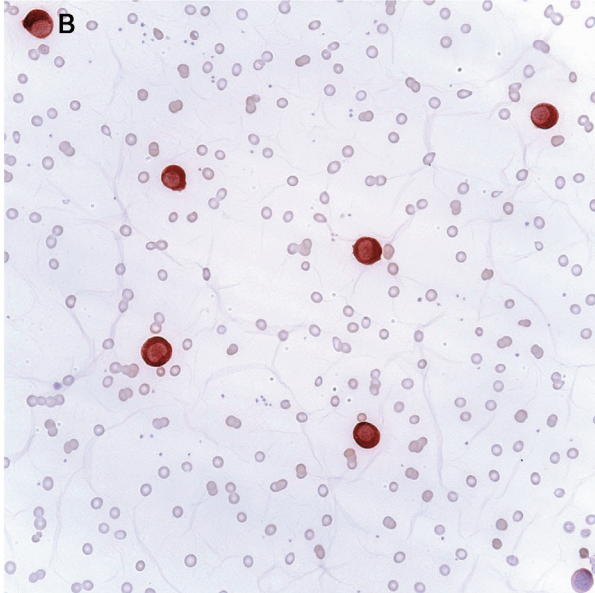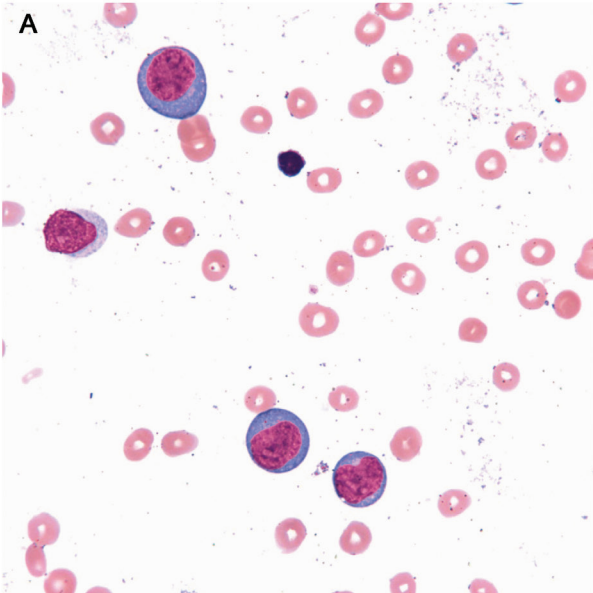
Figure 1A

Image A. Hematoxylin and eosin 1000×. Peripheral smear from case 1 showing blasts with open chromatin, prominent nucleoli, basophilic cytoplasm, and occasional vacuolization.
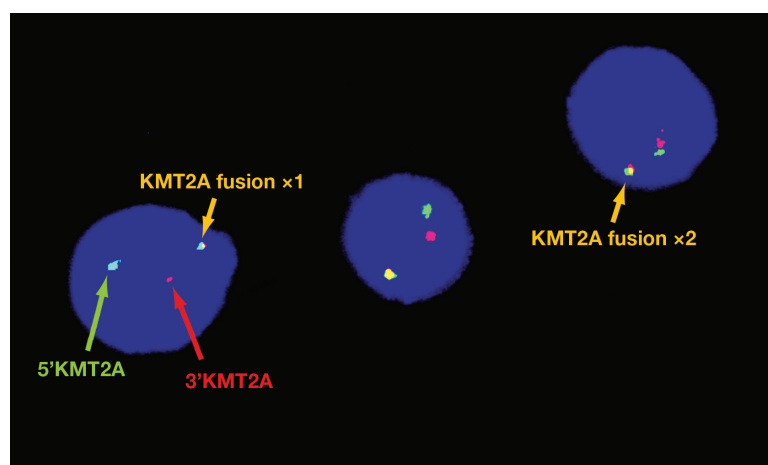

Figure 1B

Image B. Hematoxylin and eosin 400×. Blasts showing strong positivity for nonspecific esterase staining.

Table 1. Summary of Reported Patients with t(11;17)(q23;q12 or q21)

Case Reference	Age	Sex	Cytogenetics	Diagnosis (WHO 2016)	NSE/ANAE	Immunophenotype by Flow Cytometric Analysis										Reported Outcome
						CD34	CD13	CD33	CD117	HLA-DR	CD56	MPO	CD4	CD14	CD64	
Reeves et al[10]	4mo	M	46,XY, t(11;17)(q23;q11-21)	AMoL	NR	-	+	+	NR	+	+	-	NR	NR	NR	NR
Shekhter-Levin et al[11]	39	M	47,XY,+5,t(11;17)(q23;q12) in 22 cells; 47,XY, +5,t(11;17)(q23;q12),del(9)(q34)	AMoL	+	dim+	+	NR	+	+	NR	+	+	NR	NR	<1 week to death
Dal Cin et al[12]	36	M	46 XY, t(11;17)(q23;q21)	AMoL	+	NR	-	+	NR	+	NR	NR	NR	NR	NR	Remission after transplant
Dubé et al[8]	13	F	46,XX,t(4;20)(q2?1;p11.2),t(8;16)(q11.2;p11.2),t(11;17)(q23;q21),t(11;18)(q13;p11.2)	AMoL	NR	NR	NR	+	+	+	NR	NR	NR	NR	NR	Remission after transplant
Classen et al[13]	11	F	46, XX,t(11;17)(q23;q21)	AMoL	NR	+	-	+	var	+	var	-[a]	NR	+	+	Remission after chemotherapy
Kang et al[2]	61	F	46XX,t(11;17)(q23;q21)	AMoL	+	+	-	+	var+	+	var+	NR	+	+	+	Relapsed disease 8 months after chemotherapy
[b]	26	M	46,XY,t(11;17)(q23;q12)	AMoL	+	-	dim+	+	+	+	-	var+	dim+	dim	dim+	NR

M, male; F, female; AMoL, acute monoblastic/monocytic leukemia; -, negative; +, positive; ++, bright positive; var, variable; dim+, dim positive; NR, not reported; NSE/ANAE, nonspecific esterase/alpha naphthyl acetate esterase; MPO, myeloperoxidase.
[a]By cytochemical stain.
[b]Case 1 of the current report.

Figure 2

Fluorescence in situ hybridization image from case 1 showing a normal cell with 2 *KMT2A* fusions and abnormal cells showing *KMT2A* break-apart.

shown and partnered with a region of the *RARA* gene or in close approximation to the *RARA* gene, showing a t(11;17) rearrangement (**Table 1**). We emphasize that our case (Case 1) did not involve the *RARA* gene, as was confirmed by negative *RARA* FISH, yet the translocation was in close proximity to the *RARA* gene. Like

Table 2. Summary of Reported Patients with t(11;17)(q21;q25)

Case Reference	Age	Sex	Cytogenetics	Diagnosis (WHO 2016)	NSE/ANAE	Immunophenotype by Flow Cytometric Analysis										Reported Outcome
						CD34	CD13	CD33	CD117	HLA-DR	CD56	MPO	CD4	CD14	CD64	
Baer et al[4]	19	M	46, XY, t(11;17)(q23;q25)	AMoL	NR	-	+	-	NR	+	-		dim+	+	+	Alive 4 months from diagnosis
Yamamoto et al[25]	64	M	46, XY, t(11;17)(q23;q25)	AMML	+	NR	+	+	NR	NR	NR	+[a]	+	+	NR	Alive 18 months from diagnosis
Kang et al[2]	57	M	46, XY,t(11;17)(q23;q25)	AML	weak+	-	+	+	+	dim+	-	+[a]	-	-	-	Complete remission after 2nd chemotherapy induction
Kurosu et al[6]	32	M	46, XY,t(11;17)(q23;q25)	AMoL	NR	NR	+	+	NR	+	NR	NR	NR	+	NR	Alive 10 months from diagnosis
Saito et al[25]	71	M	46,XY,t(11;17)(q23;q25)/46,XY,t(1;6)(p36.3;q23)	AML	NR	+	+	NR	NR	NR	NR	NR	NR	NR	NR	Alive 33 months from diagnosis
Lee et al[26]	72	M	45,XY,-7,t(11;17)(q23;q25)[5]/46,XY,-7,+8,t(11;17)(q23;q25)[15]	AMML	+	-	+	+	-	NR	NR	-[a]	NR	+	NR	Conservative care because of patient condition
Forlenza et al[27]	2	F	46, XX, t(11;17)(q23;q25)	Acute megakaryoblastic leukemia	NR	NR	NR	NR	+	NR	NR	NR	NR	NR	NR	Remission after transplant
Altahan et al[1]	21	F	46,XX,t(11;17)(q23;q25)	AMoL	NR	-	NR	+	+	+	-	+	+	NR	+	Remission after transplant
[b]	70	F	46,XY,t(11;17)(q23;q12)[15]	AMoL	dim+	dim+	+	+	+	+	var+	dim+	dim+	dim+	dim+	Relapsed 2 months after induction and died

M, male; F, female; AML, acute myeloid leukemia; AMoL, acute monoblastic/monocytic leukemia; AMML, acute myelomonocytic leukemia; -, negative; +, positive; ++, bright positive; var, variable; dim+, dim positive; NR, not reported; NSE/ANAE, nonspecific esterase/alpha naphthyl acetate esterase; MPO, myeloperoxidase.
[a]By cytochemical stain.
[b]Case 2 of the current report.

our patient in case 1, these 6 unique patients all had normal coagulation parameters and no evidence of DIC. Further, all 6 leukemias showed morphologic and immunophenotypic features consistent with a diagnosis of AMoL.[2,7,8,10-13] The NSE/ANE (non-specific esterase/alpha naphthyl acetate esterase) cytochemistry stains were positive in all reported case reports, also consistent with monocytic differentiation.[2,12,14] Flow cytometry showed consistent expression of *HLA-DR,* which further aids in establishing the diagnosis of AMoL and essentially eliminates the possibility of acute promyelocytic leukemia. Notably, all but 1 of the patients survived at least 1 year after diagnosis, consistent with the prognosis of AMoL.

The majority of patients with APL have a canonical t(15;17)(q22;q21), formerly known as t(15;17)(q22;q12),[15] but several variant translocations have been described. The most common variants are *RARA* with the alternate fusion partners *ZBTB16* (11q23.2), *NUMA1* (11q13.4), *NPM1* (5q35.1), and *STAT5B* (17q21.2).[16] These variant t(11;17) are reported mostly in patients with ATRA-resistant APL and most frequently involve the (q23;q21) region resulting in fusion of *ZBTB16-RARA*.[17,18] The majority of these ATRA-resistant

t(11;17)(q23;q21) leukemias show a morphology distinct from classic APL, but some can be indistinguishable from the classic t(15;17).[18,19] Patients with *ZBTB16-RARA* often exhibit normal nuclei, Pelger-like neutrophils, and granularity but absence of Auer rods.[19,20]

AML with t(11;17) (q23;q25) *KMT2A-SEPT9*

We identified 8 unique case reports of AML with the *KMT2A-SEPT9* rearrangement found in our second case (**Table 2**), all of which included immunophenotyping. The presentation of bleeding with DIC in our second case clearly shifted the initial diagnostic concern toward APL. Research on 2 other patients with AMoL with t(11;17)(q23;q25) and DIC on presentation similarly noted APL at the top of their differential diagnosis,[1,21] although 1 case report did not note immunophenotyping. Morphologically, the blasts in case 2 had a monocytic appearance, yet NSE was negative, further suggesting the possibility of a variant APL.

Two of the 8 literature case reports identified atypical promyelocytes,[1,2] unlike our patients, including 1 of the patients with DIC.[1] Immunophenotypic expression of *HLA-DR*

was present in all of the patients tested, but only half of the 8 case reports noted this result, unlike all the case reports noting *HLA-DR* positivity in the patients with t(11;17)(q23;q12 or q21).

The t(11;17)(q23;q25) resulting in a *KMT2A-SEPT9* fusion transcript is consistent with the cytogenetic abnormality seen in our second case. *SEPT9* belongs to the septin family of genes and has been previously described in cases of secondary AML, de novo AML with or without monocytic differentiation, and myelodysplastic syndrome.[1,2,22,23] Unlike in the patients with *RARA* translocation, acute leukemias with *KMT2A-SEPT9* gene rearrangement include variants of AML in addition to AMoL.[2,24-27] Specifically, 1 instance of *KMT2A-SEPT9*-rearranged acute megakaryoblastic leukemia (identified by targeted RNA sequencing) in a child without trisomy 21 was reported by Forlenza et al.[27]

Our review suggests that acute leukemias with *KMT2A-SEPT9* gene rearrangement have a shorter survival compared to those showing *KMT2A-RARA* rearrangement. The overall survival for 11q23 *KMT2A* gene rearrangements in AML has been reported to be approximately 8.5 months.[28] Patients with *KMT2A-SEPT9* gene rearrangement have a reported survival of 44% at 1 year postdiagnosis compared to a survival of 83% in those with the *KMT2A-RARA* rearrangement. The latter resembles the survival of patients with AML with t(9;11)(p21;q23) (the *KMT2A-MLLT3* rearrangement), which has the best overall survival among *KMT2A* gene rearrangements.[29]

Conclusion

Research has shown that AML with *KMT2A* translocated to chromosome 17q is a rare entity that presents with a highly variable immunophenotype. Reported cases of patients with these leukemias involve a region near the *RARA* gene in the translocation. It is not surprising that the former can emulate APL characteristics; indeed, the 17q25 rearrangements involving the *SEPT9* gene can present with a clinical and morphologic scenario resembling APL. An AML with monocyte-like morphology and/or DIC is concerning for APL, but the presence of t(11;17) by simple karyotyping is insufficient for diagnosis. The combination of morphologic, immunophenotypic, and molecular

findings should be considered in reaching the correct diagnosis. **LM**

Supplementary Data

The supplemental table can be found in the online version of this article at www.labmedicine.com.

References

1. Altahan R, Altahan S, Khalil S. Non-acute promyelocytic leukemia variant, acute myeloid leukemia with translocation (11;17). *Clin Case Rep.* 2019;7(3):558–563.

2. Kang LC, Smith SV, Kaiser-Rogers K, Rao K, Dunphy CH. Two cases of acute myeloid leukemia with t(11;17) associated with varying morphology and immunophenotype: rearrangement of the MLL gene and a region proximal to the RARalpha gene. *Cancer Genet Cytogenet.* 2005;159(2):168–173.

3. Rubnitz JE, Behm FG, Downing JR. 11q23 rearrangements in acute leukemia. *Leukemia.* 1996;10(1):74–82.

4. Baer MR, Stewart CC, Lawrence D, et al. Acute myeloid leukemia with 11q23 translocations: myelomonocytic immunophenotype by multiparameter flow cytometry. *Leukemia.* 1998;12(3):317–325.

5. Meyer C, Burmeister T, Gröger D, et al. The MLL recombinome of acute leukemias in 2017. *Leukemia.* 2018;32(2):273–284.

6. Kurosu T, Tsuji K, Ohki M, et al. A variant-type MLL/SEPT9 fusion transcript in adult de novo acute monocytic leukemia (M5b) with t(11;17)(q23;q25). *Int J Hematol.* 2008;88(2):192–196.

7. Asleson AD, Morgan V, Smith S, Velagaleti GV. Amplification of the RARA gene in acute myeloid leukemia: significant finding or coincidental observation? *Cancer Genet Cytogenet.* 2010;202(1):33–37.

8. Dubé S, Fetni R, Hazourli S, Champagne M, Lemieux N. Rearrangement of the MLL gene and a region proximal to the RARalpha gene in a case of acute myelocytic leukemia M5 with a t(11;17)(q23;q21). *Cancer Genet Cytogenet.* 2003;145(1):54–59.

9. Fenaux P, Castaigne S, Dombret H, et al. All-transretinoic acid followed by intensive chemotherapy gives a high complete remission rate and may prolong remissions in newly diagnosed acute promyelocytic leukemia: a pilot study on 26 cases. *Blood.* 1992;80(9):2176–2181.

10. Reeves BR, Kempski H, Jani K, et al. A case of acute monocytic leukemia with t(11;17) involving a rearrangement of MLL-1 and a region proximal to the RARA gene. *Cancer Genet Cytogenet.* 1994;74(1):50–53.

11. Shekhter-Levin S, Gollin SM, Kaplan SS, Redner RL. Involvement of the MLL and RARalpha genes in a patient with acute monocytic leukemia with t(11;17)(q23;q12). *Leukemia.* 2000;14(3):520–522.

12. Dal Cin P, Sherman L, Marzelli M, McLaughlin C, Zukerberg L, Amrein PC. A new case of t(11;17)(q23;q21) with MLL rearrangement. *Cancer Genet Cytogenet.* 2004;148(2):178–179.

13. Classen CF, Teigler-Schlegel A, Röttgers S, Reinhardt D, Döhner K, Debatin KM. AML bearing the translocation t(11;17)(q23;q21): involvement of MLL and a region close to RARA, with no differentiation response to retinoic acid. *Ann Hematol.* 2005;84(12):774–780.

14. Arber DA, Orazi A, Hasserjian R, et al. The 2016 revision to the World Health Organization classification of myeloid neoplasms and acute leukemia. *Blood.* 2016;127(20):2391–2405.

15. De Braekeleer E, Douet-Guilbert N, De Braekeleer M. RARA fusion genes in acute promyelocytic leukemia: a review. *Expert Rev Hematol.* 2014;7(3):347–357.

16. Zelent A, Guidez F, Melnick A, Waxman S, Licht JD. Translocations of the RARalpha gene in acute promyelocytic leukemia. *Oncogene.* 2001;20(49):7186–7203.

17. Dowse RT, Ireland RM. Variant ZBTB16-RARA translocation: morphological changes predict cytogenetic variants of APL. *Blood.* 2017;129(14):2038.

18. Park DJ, Vuong PT, de Vos S, Douer D, Koeffler HP. Comparative analysis of genes regulated by PML/RAR alpha and PLZF/RAR alpha in response to retinoic acid using oligonucleotide arrays. *Blood.* 2003;102(10):3727–3736.

19. Han SB, Lim J, Kim Y, Kim HJ, Han K. A variant acute promyelocytic leukemia with t(11;17) (q23;q12); ZBTB16-RARA showing typical morphology of classical acute promyelocytic leukemia. *Korean J Hematol.* 2010;45(2):133–135.

20. Adams J, Nassiri M. Acute promyelocytic leukemia: a review and discussion of variant translocations. *Arch Pathol Lab Med.* 2015;139(10):1308–1313.

21. Santos J, Cerveira N, Correia C, et al. Coexistence of alternative MLL-SEPT9 fusion transcripts in an acute myeloid leukemia with t(11;17)(q23;q25). *Cancer Genet Cytogenet.* 2010;197(1):60–64.

22. Taki T, Ohnishi H, Shinohara K, et al. AF17q25, a putative septin family gene, fuses the MLL gene in acute myeloid leukemia with t(11;17) (q23;q25). *Cancer Res.* 1999;59(17):4261–4265.

23. Kreuziger LM, Porcher JC, Ketterling RP, Steensma DP. An MLL-SEPT9 fusion and t(11;17)(q23;q25) associated with de novo myelodysplastic syndrome. *Leuk Res.* 2007;31(8):1145–1148.

24. Yamamoto K, Shibata F, Yamaguchi M, Miura O. Fusion of MLL and MSF in adult de novo acute myelomonocytic leukemia (M4) with t(11;17) (q23;q25). *Int J Hematol.* 2002;75(5):503–507.

25. Saito H, Otsubo K, Kakimoto A, Komatsu N, Ohsaka A. Emergence of two unrelated clones in acute myeloid leukemia with MLL-SEPT9 fusion transcript. *Cancer Genet Cytogenet.* 2010;201(2):111–115.

26. Lee SG, Park TS, Oh SH, et al. De novo acute myeloid leukemia associated with t(11;17)(q23;q25) and MLL-SEPT9 rearrangement in an elderly patient: a case study and review of the literature. *Acta Haematol.* 2011;126(4):195–198.

27. Forlenza CJ, Zhang Y, Yao J, et al. A case of KMT2A-SEPT9 fusion-associated acute megakaryoblastic leukemia. *Cold Spring Harb. Mol. Case Stud.* 2018;4(6):1–6.

28. Chen Y, Kantarjian H, Pierce S, et al. Prognostic significance of 11q23 aberrations in adult acute myeloid leukemia and the role of allogeneic stem cell transplantation. *Leukemia.* 2013;27(4):836–842.

29. Mrózek K, Heinonen K, Lawrence D, et al. Adult patients with de novo acute myeloid leukemia and t(9; 11)(p22; q23) have a superior outcome to patients with other translocations involving band 11q23: a cancer and leukemia group B study. *Blood.* 1997;90(11):4532–4538.

Detection of a Cryptic *EP300/ZNF384* Gene Fusion by Chromosomal Microarray and Next-Generation Sequencing Studies in a Pediatric Patient with B-Lymphoblastic Leukemia

Holly E. Berg, DO,[1] Patrick R. Blackburn, PhD,[2] James B. Smadbeck, PhD,[3] Kirsten E. Swanson, BS,[2] Christopher S. Rice, MS,[2] Matthew R. Webley, BS,[2] Sarah H. Johnson, MS,[3] George Vasmatzis, PhD,[3] Xinjie Xu, PhD,[2] Patricia T. Greipp, DO,[2] Nicole L. Hoppman, PhD,[2] Rhett P. Ketterling, MD,[2] Linda B. Baughn, PhD,[2] Catherine H. Boston, MD,[4] Lisa M. Sutton, MD,[5] Jess F. Peterson, MD[2*]

ABSTRACT

Zinc-finger protein 384 (*ZNF384*) gene fusions with *EP300* have recently been described as a recurrent fusion in B-cell acute lymphoblastic leukemia (B-ALL) with a good response to conventional chemotherapy, suggesting a favorable prognosis. Herein, we report on a female patient aged 12 years with uninformative conventional chromosome and B-ALL panel fluorescence in situ hybridization studies with chromosomal microarray showing multiple copy number gains, including relative gains in the *ZNF384* (12p13.31) and *EP300* (22q13.2)

gene regions, suggesting a cryptic *EP300/ZNF384* fusion. Ultimately, a next-generation sequencing assay, mate pair sequencing, was utilized to confirm *EP300/ZNF384* fusion in this B-ALL clone, which may confer a favorable overall prognosis and potential targeted therapy.

Keywords: B-cell acute lymphoblastic leukemia (B-ALL), *EP300*, *ZNF384*, chromosomal microarray, next-generation sequencing, mate pair sequencing

Clinical History

A female patient aged 12 years with a history of bilateral knee pain for approximately 1 year, diagnosed with

Abbreviations:

B-ALL, B-cell acute lymphoblastic leukemia; FISH, fluorescence in situ hybridization; NSAIDS, nonsteroidal anti-inflammatory drugs; Ph-like, Philadephia-like; MPseq, mate pair sequencing; NGS, next generation sequencing.

[1]Department of Laboratory Medicine and Pathology, [2]Division of Laboratory Genetics and Genomics, Department of Laboratory Medicine and Pathology, and [3]Center for Individualized Medicine-Biomarker Discovery, Mayo Clinic, Rochester, Minnesota, [4]Cancer and Blood Disorders Center and [5]Department of Pathology and Laboratory Medicine, Driscoll Children's Hospital, Corpus Christi, Texas

*To whom correspondence should be addressed.
peterson.jess@mayo.edu

Osgood-Schlatter disease and initially treated with steroids and nonsteroidal anti-inflammatory drugs (NSAIDs), presented to the emergency department with 1 week of worsening pain that had moved to the left ankle and right hip that was unrelieved by NSAIDs. The patient reported increased fatigue, drenching night sweats, and a 15-lb weight loss. She was febrile, and her physical exam revealed bilateral posterior cervical lymphadenopathy, subtle hepatomegaly of 1 cm, and decreased range of motion of the right hip. Imaging of both knees did not show any fractures. A complete blood count revealed mild anemia (hemoglobin, 9.1 g/dL; reference 11.8 g/dL–14.8 g/dL) with normal white blood cell (6.0×10^3/μL; reference, 3.5×10^3/μL –10.5×10^3/μL) and platelet (232×10^3/μL; reference, 150×10^3/μL –450×10^3/μL) counts. However, her peripheral smear contained 16% blasts with large nuclei, open chromatin, and scant cytoplasm. Based on these findings, a hematology workup was initiated.

Hematopathology Evaluation

Flow cytometric analysis of the patient's peripheral blood showed an immature population of B-cells expressing surface CD10 (partial), CD19, CD22 (dim), CD33 (partial), CD34, CD38 (partial, dim), CD45 (dim), and HLA-DR, with intracellular expression of TdT and CD79a (**Figure 1, Image A** and **Figure 1, Image B**). This population lacked expression of all T-cell markers tested, including CD3 (surface and cytoplasmic), CD4, CD5, CD7, and CD8, and was also negative for CD13, CD14, CD15, CD16, CD20, CD22 (cytoplasmic), CD56, CD61, and CD117. Bone marrow aspirate smears showed hypercellularity and were essentially replaced (>90%) by medium to large cells consistent with blasts (**Figure 1, Image C**). Flow cytometric analysis of the bone marrow confirmed involvement by B-cell acute lymphoblastic leukemia (B-ALL). Marrow blasts expressed surface CD10 (partial), CD19, CD22, CD33, CD34, CD38 (dim), CD45, and HLA-DR. Morphologic review of the patient's cerebrospinal fluid was negative for malignant cells.

Cytogenomic Analyses

A bone marrow aspirate was received for conventional chromosome and B-ALL panel fluorescence in situ hybridization (FISH) studies. The B-ALL FISH panel included locus-specific (*CDKN2A*/D9Z1, *TP53*/D17Z1, D4Z1/D10Z1/D17Z1), break-apart (*KMT2A* [*MLL*], *IGH*, *MYC, ETV6, CRLF2, P2RY8*), and dual-color dual-fusion (*BCR/ABL1, PBX1/TCF3, ETV6/RUNX1*) probe sets. Cells from the diagnostic bone marrow aspirate specimen were processed using standard cytogenetic and FISH techniques according to specimen-specific protocols.

Conventional chromosome analysis revealed the following complex karyotype: 45,XX,t(1;13;11)(q25;q14;p11.2),der(6)(6pter→6p25::6q13→6p25::6q13→6q15:: 21q11.2→21qter,-12,der(18)t(12;18)(q13;q23),der(21)t(6;21)(q15;q11.2)[2]/44,idem,+1, der(1;22)(q10;q10)[3]/46,XX[9]. The B-ALL FISH panel studies identified a loss of the *ETV6* gene region (12p13.2) and a gain of the *PBX1* gene region (1q23) in 55.4% and 3.4% of the interphase nuclei, respectively. Because no primary genetic abnormality was identified,

a Philadelphia-like (Ph-like) FISH panel was performed to evaluate the *IKZF1, PDGFRB, JAK2,* and *ABL2* gene regions. A heterozygous *IKZF1* deletion was observed in 11.5% of the interphase nuclei, suggesting a possible subclone; the remaining Ph-like probes were normal.

Chromosomal microarray studies were subsequently pursued because no primary genetic abnormality had been identified. The patient's DNA was processed using the Applied Biosystems CytoScan reagent kit, the CytoScan Amplification kit, and was hybridized to a CytoScan HD Array (Life Technologies, Carlsbad, CA). Data were generated (hg19 genome build) and analyzed using the Applied Biosystems Chromosome Analysis Suite (Applied Biosystems, Foster City, CA). Multiple copy number abnormalities were observed involving chromosomal regions 12p, 12q, 13q, 18q, 21q, and 22q. Notably, a relative gain (82 kb) that encompassed the *ZNF384* gene region (12p13.31) (**Figure 2, Image A**) and a relative gain (44 kb) that encompassed the *EP300* gene region (22q13.2) (**Figure 2, Image B**) were observed.

To further interrogate the suspected cryptic *EP300/ZNF384* gene fusion, mate pair sequencing (MPseq) was pursued. The patient's DNA was processed using the Illumina Nextera Mate Pair library kit (Illumina, San Diego, CA), multiplexed at 2 specimens per lane and sequenced on the Illumina HiSeq 2500 on rapid run mode. Data were aligned to the reference genome (GRCh38) using BIMA V3, and abnormalities were identified and visualized using SVAtools and Ingenium, both in-house developed bioinformatics tools.[1,2] The MPseq detected a 12;22 translocation with breakpoints located within the *EP300* gene (intron 6, NM_001429) at 22q13.2 and within the *ZNF384* gene (intron 2, NM_133476) at 12p13.31 (**Figure 3, Image A**), predicting an *EP300* (exons 1–6)/*ZNF384* (exons 3–10) gene fusion (detailed mechanism in Supplemental Figure 1). A schematic diagram of the EP300/ZNF384 chimeric protein fusion has also been provided (**Figure 3, Image B**).

Discussion

The evolution of cytogenetic analysis from conventional chromosome analysis to molecular methodologies, including next-generation sequencing (NGS), has provided superior genomic resolution and the ability to identify
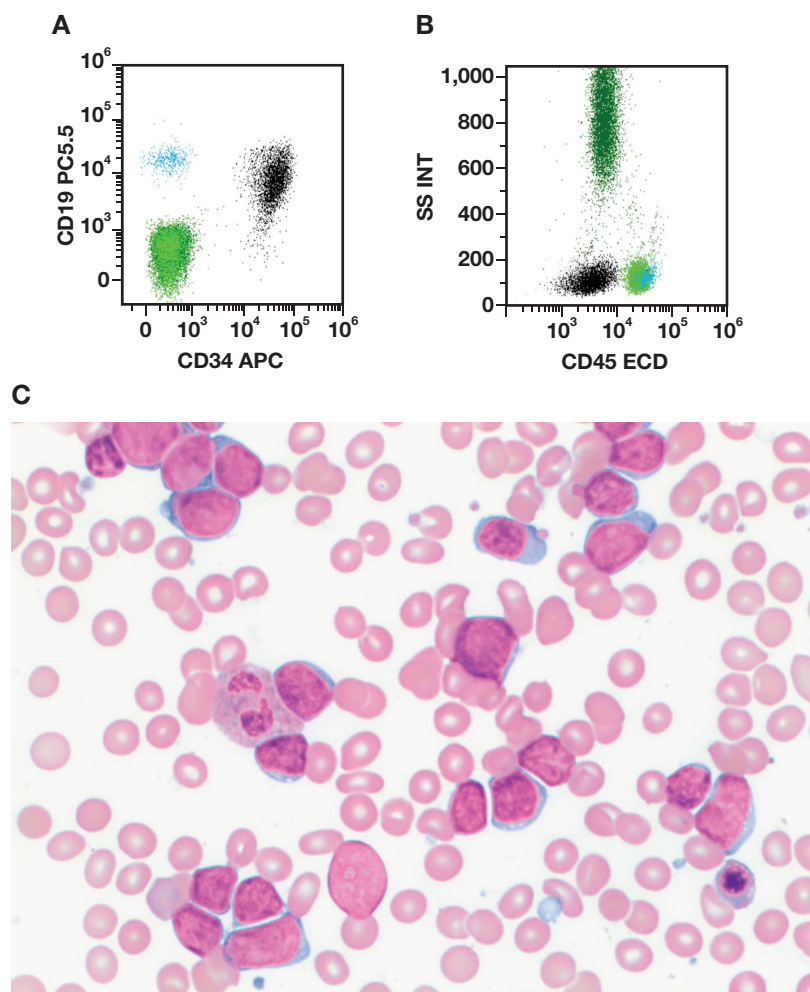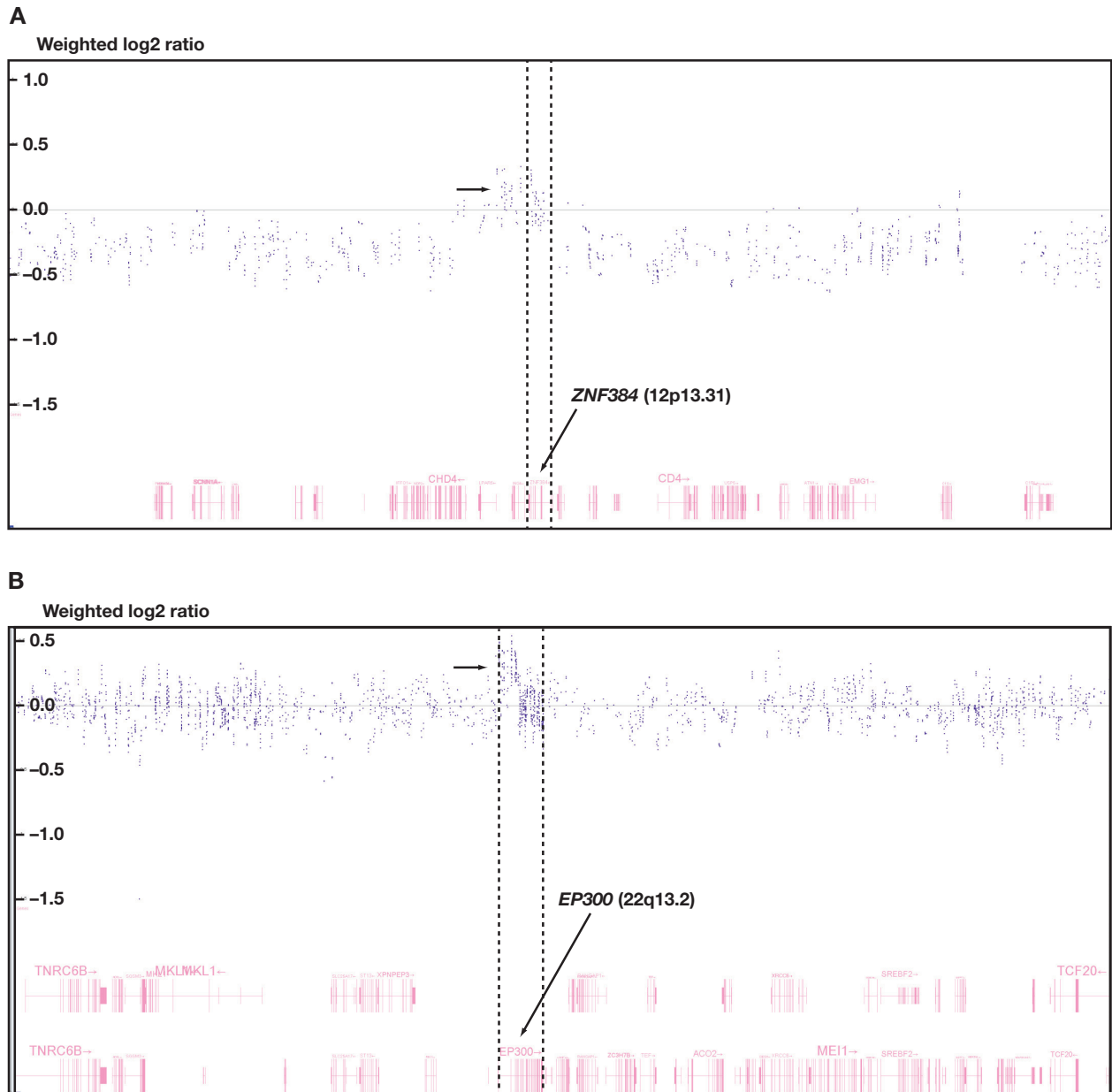
Figure 1

Morphologic and immunophenotypic evaluation. **A,** Bone marrow aspirate smear stained with Wright-Giemsa, showing frequent medium- to large-sized blasts with large nuclei and scant cytoplasm (magnification, × 40). Peripheral blood flow scatter plots show blasts (black) with uniform positive CD19 and CD34 expression (**B**) and blasts with dim CD45 expression (**C**). Other cell populations include normal B-cells (blue), T-cells (light green), and granulocytes (dark green).

innumerable underlying genetic aberrancies. Many of these recurrent cytogenetic abnormalities also have unique morphologic and immunophenotypic features, so several subtypes of B-ALL are now defined by the presence of such abnormalities.[3] More important, because these recurrent abnormalities are increasingly identified as part of routine diagnosis and staging of B-ALL, predictions for response to conventional treatment and recurrence risk stratification are possible. More appropriate stratification allows clinicians to mitigate the potentially lifelong consequences of chemotherapy-associated toxicity, decreasing exposure for patients with lower risks of recurrence while

increasing treatment intensity in patients with a high risk of recurrence.

The leukemogenic properties of many cytogenetic abnormalities have been elucidated and are commonly associated with alterations in cell signaling pathways, regulation of transcription, cytokine receptors, and differentiation capability.[4,5] Although prognostic significance is well documented for several characteristic cytogenetic abnormalities such as *ETV6/RUNX1* and *BCR/ABL1* and multiple Ph-like B-ALL-associated abnormalities, many emerging recurrent abnormalities warrant further investigation to confirm

A

Figure 2

Chromosomal microarray evaluation of the *EP300* and *ZNF384* gene regions. **A,** Relative gain (82 kb; arrow) that disrupts the *ZNF384* gene region (12p13.31). **B,** A gain (44 kb; arrow) that disrupts the *EP300* gene region (22q13.2). These combined results suggest a cryptic *EP300/ZNF384* gene fusion.

prognostic significance and predict potential therapeutic intervention.[6] Recent studies have noted that a minor percentage of precursor B-ALL harbors a *ZNF384* gene fusion, with several fusion partners identified, including genes in the *TET* family genes such as Ewing sarcoma breakpoint

region 1 (*EWSR1,* t[12,22]), TATA box binding protein-associated factor (*TAF15*, t[12;17]), and transcription factor 3 (*TCF3* or *E2A*, t[12;19])).[4,7-9] These studies indicate that approximately 6% of *BCR/ABL1*-negative/Ph-like-negative B-ALL harbors an *EP300/ZNF384* fusion, associated with a

A

B
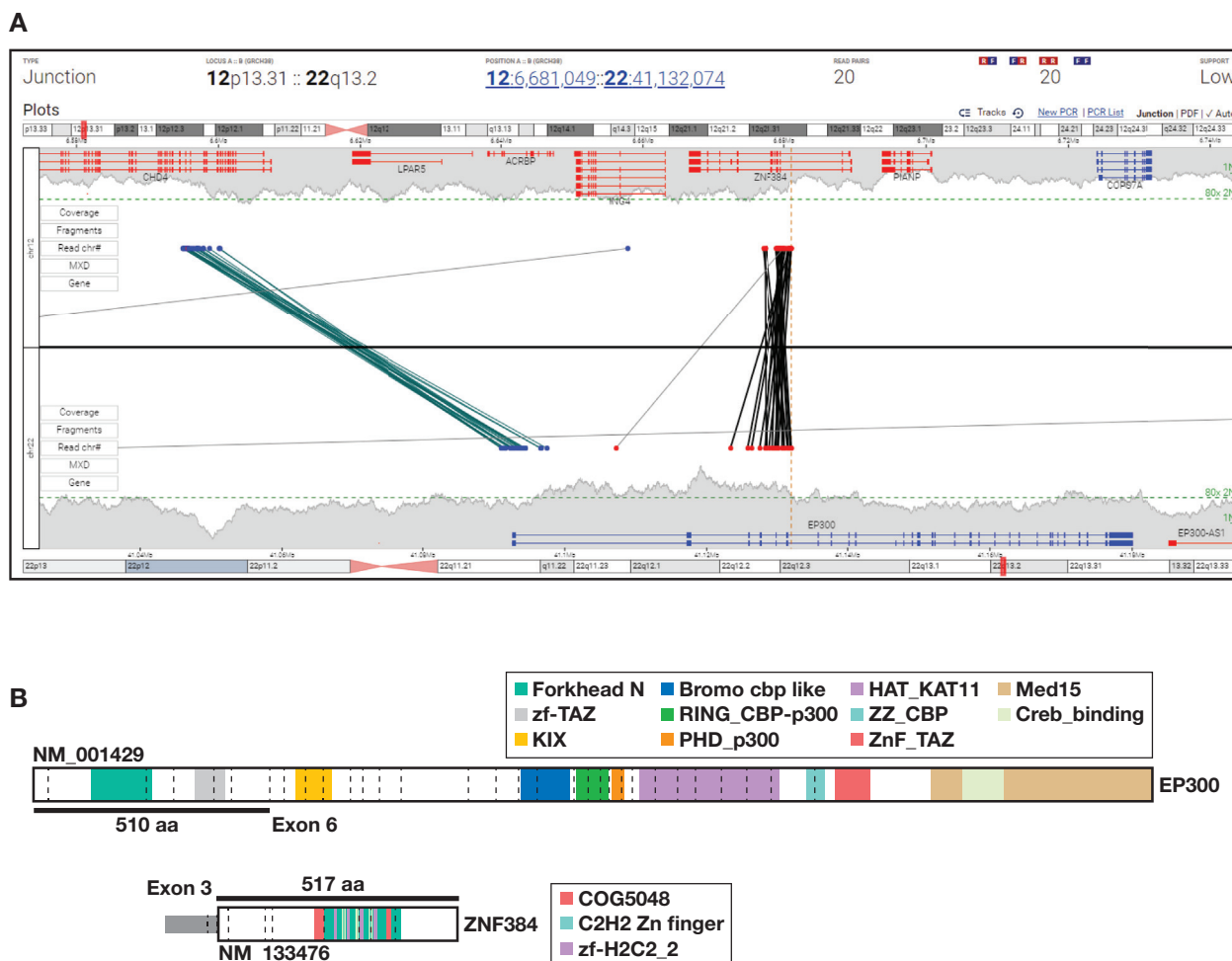
Figure 3

An MPseq evaluation and schematic diagram of EP300/ZNF384 chimeric protein fusion. **A,** Junction plot showing breakpoints located within the *EP300* gene (intron 6, NM_001429) at 22q13.2 and within the *ZNF384* gene (intron 2, NM_133476) at 12p13.31. This translocation resulted in a predicted *EP300* (exons 1–6)/*ZNF384* (exons 3–10) gene fusion. **B,** Schematic diagram of the EP300/ZNF384 chimeric protein fusion, generated with ProteinPaint.[12] MPseq, mate pair sequencing.

characteristic immunophenotype of weak CD10 expression with aberrant CD13 or CD33 expression.[6,7,9,10]

In addition, Hirabayashi et al[9] observed this characteristic immunophenotype in all B-ALL patients with *ZNF384*-related fusion genes. Patients with the *EP300/ZNF384* gene fusion typically present as adolescents (67%; > age 10 years) and with lower initial white blood cell counts (78%; $< 20 \times 10^3/\mu L$). In contrast to other *ZNF384* fusion partners, patients with *EP300/ZNF384* fusions have significantly higher 5-year event-free survival and overall survival (83.3% and 100%, respectively), strongly suggesting a more favorable prognosis.[7,9]

Thus, the identification of this fusion is of clinical importance because it conveys a more favorable prognosis, despite the adverse features of advanced age of presentation. In our patient, an *IKZF1* deletion was also observed in a subset (11.5%) of the interphase nuclei. Although *IKZF1* deletions are associated with an unfavorable prognosis, the clinical significance of *IKZF1* deletions in a subset of the interphase nuclei is uncertain.[11]

Most *EP300/ZNF384* fusions are not identified by classic cytogenetic analysis such as conventional G-banding or by FISH testing because of the lack of commercially available probes to these gene regions.[9] As illustrated in

our patient, despite harboring a complex karyotype, the 12;22 rearrangement was not of value and comprehensive FISH panels for both B-ALL and Ph-like targets were noncontributory other than providing the identification of an *IKZF1* deletion. Chromosomal microarray characterized multiple copy number abnormalities and was ultimately helpful in the prediction of potential cryptic *EP300/ZNF384* gene fusion because of subtle relative gains involving portions of the *ZNF384* and the *EP300* gene regions. However, MPseq was required to characterize the presence of the *EP300/ZNF384* gene fusion.

This case study illustrates that chromosomal microarray and NGS-based technologies, such as MPseq, can be critical to identify cytogenetic abnormalities undetected by traditional methodologies, and that the detection of these cryptic rearrangements can have important prognostic and therapeutic implications.

Patient Outcome

The patient was classified as National Cancer Institute high risk and was treated on the Children's Oncology Group high-risk ALL chemotherapy protocol; she went into complete remission after her second phase. Her treatment was complicated by pancreatitis. **LM**

Supplementary Data

The supplemental figure can be found in the online version of this article at www.labmedicine.com.

Supplemental Figure 1. Reconstruction of *EP300/ZNF384* fusion. The left panel shows the reconstruction of the *EP300/ZNF384* fusion. Green lines indicate the path of the reconstruction. Green dashed lines (J1 and J2) indicate junctions called by the MPseq pipeline connecting the *EP300* gene region of chr22 to the *ZNF384/CHD4* gene regions of chr12. The breakpoints for each junction are indicated by horizontal red lines, and the exact called locations are given in the bottom left of the figure (hg38). Dashed blue lines indicate areas of chr12 and chr22 that are gained as part of rearrangement. Genes are depicted as light blue or light red boxes if they are on the forward or reverse strands of the chromosome, respectively. The right panel shows the final reconstruction of the der(22) chromosome and

the *EP300/ZNF384* fusion with the red solid line indicating regions derived from chr22 and the blue solid line indicating the region of insertion derived from chr12. MPseq, mate pair sequencing.

References

1. Drucker TM, Johnson SH, Murphy SJ, Cradic KW, Therneau TM, Vasmatzis G. BIMA V3: an aligner customized for mate pair library sequencing. *Bioinformatics.* 2014;30(11):1627–1629.

2. Johnson SH, Smadbeck JB, Smoley SA, et al. SVAtools for junction detection of genome-wide chromosomal rearrangements by mate-pair sequencing (MPseq). *Cancer Genet.* 2018;221:1–18.

3. Borowitz MJ, Chan JKC, Downing JR, et al. B-lymphoblastic leukaemia/lymphoma with recurrent genetic abnormalities. In: Swerdlow SH, Campo E, Harris NL et al, eds. *WHO Classification of Tumours of Haematopoietic and Lymphoid Tissues.* 4th ed. Lyon, France: IARC; 2017:203–209.

4. Qian M, Zhang H, Kham SK, et al. Whole-transcriptome sequencing identifies a distinct subtype of acute lymphoblastic leukemia with predominant genomic abnormalities of EP300 and CREBBP. *Genome Res.* 2017;27(2):185–195.

5. Yamamoto H, Hayakawa F, Yasuda T, et al. ZNF384-fusion proteins have high affinity for the transcriptional coactivator EP300 and aberrant transcriptional activities. *FEBS Lett.* 2019;593(16):2151–2161.

6. Liu YF, Wang BY, Zhang WN, et al. Genomic profiling of adult and pediatric B-cell acute lymphoblastic leukemia. *EBioMedicine.* 2016;8:173–183.

7. McClure BJ, Heatley SL, Kok CH, et al. Pre-B acute lymphoblastic leukaemia recurrent fusion, EP300-ZNF384, is associated with a distinct gene expression. *Br J Cancer.* 2018;118(7):1000–1004.

8. Gocho Y, Kiyokawa N, Ichikawa H, et al.; Tokyo Children's Cancer Study Group. A novel recurrent EP300-ZNF384 gene fusion in B-cell precursor acute lymphoblastic leukemia. *Leukemia.* 2015;29(12):2445–2448.

9. Hirabayashi S, Ohki K, Nakabayashi K, et al.; Tokyo Children's Cancer Study Group (TCCSG). ZNF384-related fusion genes define a subgroup of childhood B-cell precursor acute lymphoblastic leukemia with a characteristic immunotype. *Haematologica.* 2017;102(1):118–129.

10. Yaguchi A, Ishibashi T, Terada K, et al. EP300-ZNF384 fusion gene product up-regulates GATA3 gene expression and induces hematopoietic stem cell gene expression signature in B-cell precursor acute lymphoblastic leukemia cells. *Int J Hematol.* 2017;106(2):269–281.

11. Stanulla M, Cavé H, Moorman AV. IKZF1 deletions in pediatric acute lymphoblastic leukemia: still a poor prognostic marker? *Blood.* 2020;135(4):252–260.

12. Zhou X, Edmonson MN, Wilkinson MR, et al. Exploring genomic alteration in pediatric cancer using ProteinPaint. *Nat Genet.* 2016;48(1):4–6.

A Hemolytic Transfusion Reaction Caused by an Unexpected Le^b Antibody

Alexander A. Delk, MT(ASCP)SBBCM, BS,[1] Richard R. Gammon, MD,[2,*] Harold Alvarez, MD,[3] Nancy Benitez, MHS(ASCP)SBB,[1] Frieda Bright, MT(ASCP)SBB, MHA[1]

ABSTRACT

A Black male patient aged 21 years with a history of sickle cell disease and HIV was admitted to the hospital with vaso-occlusive crisis. A transfusion reaction was called after the patient developed a fever (39.5°C), tachycardia, chills, and hematuria after receiving 300 mL of red blood cells. A posttransfusion specimen was submitted to the Immunohematology Reference Laboratory for investigation. Antibody identification revealed an anti-Le^b as the probable cause of the immediate acute hemolytic transfusion reaction. Lewis antibodies are considered clinically insignificant. This case shows the importance of considering cold antibodies, including Lewis antibodies, as a possible cause of an acute hemolytic transfusion reaction.

Keywords: Lewis b, hemolysis, transfusion reaction, antibodies, immunohematology, sickle cell disease

Patient History

A Black male patient aged 21 years with a history of sickle cell disease and HIV was admitted to the hospital with a diagnosis of vaso-occlusive crisis. Specimens from the patient with a history of cold and warm autoantibodies and an anti-M (IgM) were submitted to the Immunohematology Reference Laboratory (IRL) at OneBlood Inc (Orlando, FL) for antibody investigation. Approximately one year prior the IRL provided 3 compatible red blood cell (RBC) units previously, and no antibodies were identified at this time. The antibody identification was resolved, and no new alloantibodies or apparent unexpected results were noted at the low ionic strength saline (LISS)- anti-human globulin phase of testing.

Abbreviations:

IRL, Immunohematology Reference Laboratory; RBC, red blood cell; LISS, low ionic strength saline; IAT, indirect antiglobulin testing; DAT, direct antiglobulin testing; DTT, dithiothreitol.

[1]Immunohematology Reference Laboratory and [2]Scientific Medical and Technical Direction, OneBlood, Inc, Orlando, Florida, USA, [3]Pathology Department, Baptist Health, Miami, Florida, USA

*To whom correspondence should be addressed.
richard.gammon@oneblood.org.

Two units that were phenotypically matched for the clinically significant common blood group antigens (E-, K-, Fy (a-), Jk(b-), and S-) and crossmatch-compatible at tube LISS-indirect antiglobulin testing (IAT) for RBC units were issued.

Shortly after physicians started to transfuse the first unit, a transfusion reaction was called. The patient developed a fever (39.5°C), tachycardia, chills, and hematuria after he received 300 mL of RBC. A transfusion reaction investigation was initiated by the hospital. The clerical checks on the blood container and compatibility labels were in agreement. The pretransfusion specimen was icteric, and the posttransfusion specimen was hemolyzed. The pre- and posttransfusion direct antiglobulin testing results (DAT) were both positive and characterized as weakly reactive. Laboratory results showed an elevated lactic acid dehydrogenase (LDH) level of 2476 U/L (normal level, 34 U/L–246 U/L) and a decreased haptoglobin level of less than 31 mg/dL (normal level, 30 mg/dL–200 mg/dL). Urinalysis showed large blood and bilirubin (normal negative). Because of the findings in the posttransfusion specimen and the blood and urine analysis, this overall condition was reported as an acute hemolytic transfusion reaction and was treated with methylprednisolone. We report here a case of an acute hemolytic transfusion reaction because of a hemolytic

anti-Le[b] that was not identified in the pretransfusion antibody evaluation but was strongly reactive in posttransfusion testing.

Methods

After the patient experienced the transfusion reaction, a posttransfusion specimen was collected by the hospital and submitted to the IRL for antibody identification. When the initial assessment of the transfusion reaction results and the patient's medical and transfusion history were evaluated, the IRL determined that additional testing was warranted. This panel of testing included, from both pre- and posttransfusion patient specimens and donor units, ABO Rh, antigen typing, and DAT on the patient's cells using monospecific anti-IgG (Immucor, Norcross, GA) and anti-C3b,-C3d (Immucor, Norcross, GA); repeat crossmatch; 0.01 M dithiothreitol (DTT) (Sigma Aldrich, St. Louis, MO) treatment of plasma; comparative testing with serum vs plasma at LISS 37C; neutralization; and acid elution.

Antibody detection and identification were performed according to standard IRL techniques and protocols. The patient's plasma was tested against reagent RBCs performed at immediate spin (IS; screen cells only) in tube saline and tube polyethylene glycol-IAT (Immucor, Norcross, GA), enhancement (screen and panel cells), and tube LISS-IAT using monospecific anti-IgG to determine or exclude any additional antibody specificities. We used 0.01 M DTT to treat the patient's serum to determine if the Lewis antibodies were solely IgM or a combination of IgG and IgM. In addition, neutralization using the Lewis Blood Group System (Immucor, Norcross, GA) was used per manufacturer instructions to aid in the exclusion of additional alloantibodies.

Results

The patient was A Rh (D)-positive, and the historical red cell antigen profile had been previously performed (Table 1). As previously determined, the patient had a history of cold and warm autoantibodies and a directly agglutinating anti-M that was most likely an IgM antibody as previously determined by testing with 0.01 M DTT–treated plasma. Two phenotypically matched units that were crossmatch-compatible at LISS-IAT were issued to the referring hospital. By chance, 1 unit previously tested was M–, and the other was untested.

Early the next morning, the IRL was notified that the patient had a transfusion reaction and that specimens would be submitted for additional antibody identification. After receipt of the posttransfusion specimen in the IRL, a clerical check showed no evidence of discrepancy when compared with the pretransfusion specimen. The pretransfusion specimen seemed icteric, and the posttransfusion specimen was hemolyzed (Image 1). Both pre- and post-DAT were positive; however, they were recorded as invalid because the saline control was reactive. After treatment with 0.01 M DTT, the pretransfusion specimen was negative and the posttransfusion specimen remained invalid (spontaneously agglutinated). Although the IgG DAT was negative or invalid, an eluate was prepared from the pre- and posttransfusion specimens. The resulting eluates were nonreactive with all cells tested. The blood types of the patient and donors were retested and found to be A-positive and to match the patient's type. The crossmatch was performed at LISS-IAT with a tube test and found to be compatible.

However, because the posttransfusion specimen was hemolyzed and the patient seemed to have an acute transfusion reaction, additional investigation was performed. The pretransfusion workup was evaluated, and it was noted that the auto control and an Le (a–b–) cell were the only negative reactions. The phenotype of the patient was Le (a–b–), and Lewis antibodies were the suspected cause of the transfusion reaction. Subsequent tube testing using the patient's pretransfusion serum specimen was performed with an array of M– panel cells of varying Le types (Table 2). Anti-Le[a] and Le[b] were identified. The serum was treated with 0.01 M DTT, and it was determined that the anti-Le[a] was both IgM and IgG whereas the anti-Le[b] was only IgM in nature. Lewis neutralization was performed using a commercially available Lewis substance to exclude additional common alloantibodies. The 2 units previously

Table 1. Patient's Historical Antigen Profile															
D	C	c	E	e	K	Le[a]	Le[b]	Fy[a]	Fy[b]	Jk[a]	Jk[b]	M	N	S	s
+	+	+	0	+	0	0	0	0	+	+	0	0	+	0	+

The patient also had a history of cold and warm autoantibodies and an anti-M (IgM).

Image 1

The pretransfusion sample (right) appeared icteric and the post-transfusion sample was hemolyzed (left).

sent for transfusion were typed for Lewis antigens and found to be Le (a+b–), and Le (a-b+). The unit implicated in the transfusion reaction was Le (a–b+); M–. The patient's veno-occlusive crisis resolved, he was discharged from the hospital 6 days later, and additional transfusion was not needed.

The clinical significance of the anti-M was not definitively determined. Because the anti-M was directly agglutinating at IS it was most likely IgM in nature; moreover, M+ cells

that were previously tested with 0.01 M DTT–treated serum were nonreactive. Based on these results, the anti-M was not considered clinically significant by the IRL. In addition, the unit implicated in the transfusion reaction was M–. A specimen was not submitted for monocyte monolayer assay (MMA) studies of the anti-M because the MMA assay performed by the testing laboratory only assessed the clinical significance of IgG antibodies and did not assess the clinical significance of IgM antibodies.

Discussion

Similar to a case previously described,[1] the following evidence strongly suggested that this patient's hemolytic transfusion reaction was caused by anti-Le[b]: (i) the antibody was hemolytic in vitro, seen with almost all clinically significant Lewis antibodies; (ii) the units the patient received at the time of the first transfusion were positive for Le[b] and negative for M, as was the unit involved with the hemolytic transfusion reaction; (iii) the patient's phenotype was Le(a–b–), the most common type that produces Lewis antibodies; and (iv) the patient was not taking any medications that could be implicated in drug-induced hemolysis.[1]

In general, Lewis antibodies are not considered clinically significant.[2] Red cells that are compatible in tests at 37°C, regardless of Lewis phenotype, are expected to have normal in vivo survival.[2] It is not necessary to transfuse antigen-negative red cells in most patients.[2] Unlike ABO antigens, Lewis antigens are extrinsic glycolipid antigens that are readily eluted and shed from transfused red cells within a few days of transfusion.[3] Lewis antigens in transfused plasma can neutralize Lewis antibodies in the recipient.[2] For these reasons, hemolysis in vivo is very rare after transfusion.[2] We have found only 5 other reported patients with anti-Le[b] causing hemolysis.[1,4-7] All, including the one presented here, were hemolytic transfusion reactions,

Table 2. Tube Testing Using Pretransfusion Serum Specimen				
Reaction Phase	IS	37°C LISS	LISS-IAT	PeG-IAT
Le (a+b–), M–	3+	Hemolysis	3+	3+
Le (a–b+), M–	3+	Slight hemolysis	1+	3+
Le (a–b–), M–	0	0	0	0

PeG, polyethylene glycol.
Testing used an array of M– panel cells of varying Lewis types.

either acute or delayed. Note that in reviewing the literature, we found only 6 published hemolytic reactions to anti-Le[a].[3,8-13] Anti-Le[a] is more frequently associated with acute hemolytic transfusion reactions than is anti-Le[b].[4,8-13]

This case study shows the importance of investigating Lewis antibodies as a possible cause of a hemolytic transfusion reaction. Both anti-Le[a] and anti-Le[b] have been associated with mild hemolytic disease of the fetus and newborn.[14,15] In addition, when cold autoantibodies are present, it is critical to continue to include direct agglutination testing at 37°C. The auto control will serve as a guide to the acceptable reactivity. This study also highlights the fact that current platforms for automated testing use plasma. This means that at least in this particular case, the clinically significant Le[b] would have escaped detection by automated methods. Two general takeaways for directly agglutinating antibodies are that first, what matters most is that if there is true reactivity at 37°C, then the antibody is possibly clinically significant, regardless of antibody class (eg, IgM and/or IgG). Second, it is important to consider evaluating serum, when available, instead of plasma specimens at 37°C to observe for hemolysis. The patient should be advised to carry an antibody identification card for any hospital admissions where there may be a need for blood transfusion. **LM**

Acknowledgments

References

1. Irani MS, Figueroa D, Savage G. Acute hemolytic transfusion reaction due to anti-Le(b). *Transfusion.* 2015;55(10):2486–2488.

2. Westman JS, Olsson ML. ABO and other carbohydrate blood group systems. In: Fung MK, Eder AF, Spitalnik SL, Westhoff CM, eds. *AABB technical manual.* 19th ed. Bethesda, MD: AABB Press, 2017:458–463.

3. Combs MR. Lewis blood group system review. *Immunohematology.* 2009;25(3):112–118.

4. Quiroga H, Leite A, Baia F, et al. Clinically significant anti-Leb [abstract]. *Vox Sang.* 2000;78 Suppl 1:P125.

5. Jesse JK, Sheek KJ. Anti-Leb implicated in acute hemolytic transfusion reaction: a rare occurrence. *Transfusion.* 2000;40:115S.

6. Weir AB 3rd, Woods LL, Chesney C, Neitzer G. Delayed hemolytic transfusion reaction caused by anti-LebH antibody. *Vox Sang.* 1987;53(2):105–107.

7. Contreras M, Mollison PL. Delayed haemolytic transfusion reaction caused by anti-LebH antibody. *Vox Sang.* 1989;56(4):290.

8. Höglund P, Rosengren-Lindquist R, Wikman AT. A severe haemolytic transfusion reaction caused by anti-Le(a) active at 37 °C. *Blood Transfus.* 2013;11(3):456–459.

9. De Vries SI, Smitskamp HS. Haemolytic transfusion reaction due to an anti-Lewis agglutinin. *Br Med J.* 1951;1(4701):280–281.

10. Brendemoen OJ, Aas K. Hemolytic transfusion reaction probably caused by anti-Lea. *Acta Med Scand.* 1952;141(6):458–460.

11. Roy RB, Wesley RH, Fitzgerald JD. Haemolytic transfusion reaction caused by anti-Le. *Vox Sang.* 1960;5(6):545–550.

12. Marchese M. Postpartum acute hemolytic transfusion reactions associated with anti-Lea in two pregnancies complicated by preeclampsia. *Immunohematology.* 2017;33(3):114–118.

13. Duncan V, Pham HP, Williams LA 3rd. A possible case of a haemolytic transfusion reaction caused by anti-Le(a) antibody. *Blood Transfus.* 2015;13(3):535–536.

14. Carreras Vescio LA, Torres OW, Virgilio OS, Pizzolato M. Mild hemolytic disease of the newborn due to anti-Lewis(a). *Vox Sang.* 1993;64(3):194–195.

15. Bharucha ZS, Joshi SR, Bhatia HM. Hemolytic disease of the newborn due to anti-Le. *Vox Sang.* 1981;41(1):36–39.

Case Study

Cording in Disseminated *Mycobacterium chelonae* Infection in an Immunocompromised Patient

Gregory Olson, MD,[1][*][o] Moira C. McNulty, MD,[1] Kathleen Mullane, DO,[1]
Kathleen G. Beavis, MD,[2] Vera Tesic, MD[2]

ABSTRACT

Cording is a phenomenon in which acid fast bacilli grow in parallel and was previously used as a means of presumptive microscopic identification of *Mycobacterium tuberculosis* (TB). However, this process has been shown in multiple other nontuberculous mycobacterial (NTM) species. Here we present the case of an immunocompromised adult who presented with wrist pain, weight loss, and cough. A positron emission tomography scan showed uptake in the right ulna, multiple soft tissue sites, and the left lung. Biopsies and cultures were obtained from multiple sites,

and the patient was ultimately diagnosed with disseminated *Mycobacterium chelonae* infection. The organism showed cording in culture. As seen in this patient, cording may occur in multiple NTM species and is not reliable as the sole indicator of the presence of TB.

Keywords: *Mycobacterium*, *Mycobacterium chelonae*, cording, transplant, nontuberculous mycobacteria, stem cell transplant

Clinical History

A male patient aged 64 years with a history of chronic lymphocytic leukemia with transformation to diffuse large B-cell lymphoma presented to the outpatient clinic 6 months after stem cell transplant (SCT) with right wrist pain of 6 weeks duration. He reported a weight loss of 30 pounds since his SCT and a mild cough. He had no fevers, chills, night sweats, or diarrhea. His wife noted that she had tested positive for latent tuberculosis (TB) many years ago and was not treated; she had no cough.

Abbreviations:

TB, tuberculosis; NTM, nontuberculous mycobacterial; SCT, stem cell transplant; PET, positron emission tomography; AFB, acid fast bacilli.

[1]Infectious Diseases and Global Health and [2]Department of Pathology, University of Chicago Medical Center, Chicago, Illinois

*To whom correspondence should be addressed.
Gregory.olson@uchospitals.edu

His wrist pain was initially thought to result from gout, but when he did not improve with treatment, magnetic resonance imaging was performed showing a possible tumor in the right ulnar bone. A positron emission tomography (PET) scan showed highly metabolic uptake of the right distal ulna, soft tissue uptake in both thighs and the anterior abdominal wall, and nodular opacities in the left lower lobe of the lung. He was thus admitted to the hospital for further workup. Upon hospitalization he had normal vital signs with the exception of a reduced oxygen saturation of 92% on room air. Physical examination found the patient to be weak and deconditioned, with two nodular skin lesions on his bilateral thighs and painful swelling of the right wrist. Laboratory results showed white blood cells of 1.5×10^3/μL (reference range, 3.5–11.0) with a left shift (78% neutrophils, 8% lymphocytes, and 13% monocytes), hemoglobin of 6.0 g/dL (13.5 g/dL–17.5 g/dL), and platelets of 60×10^3/μL (150–450). Kidney and liver function were normal.

Biopsies of the right ulnar and left thigh lesions were obtained for pathology, bacterial culture, and acid fast bacilli (AFB) cultures. Direct AFB smears were positive with 4+ AFB from

the thigh and 2+ from the arm. A sputum smear was positive for 1+ AFB, and AFB grew in blood cultures as well. Bone marrow biopsy revealed hypocellular marrow and rare AFB. A 16S rRNA sequencing at the reference laboratory confirmed that the patient had disseminated *Mycobacterium chelonae* infection. Cultures of the bone, skin, sputum, and blood were ultimately positive and showed cording (**Images 1**, **2**).

This patient was initially started on rifabutin, isoniazid, pyrazinamide, ethambutol, and azithromycin. When cultures revealed *M. chelonae,* antibiotics were changed to imipenem, amikacin, and clarithromycin. Susceptibility results showed sensitivity to amikacin, tobramycin,
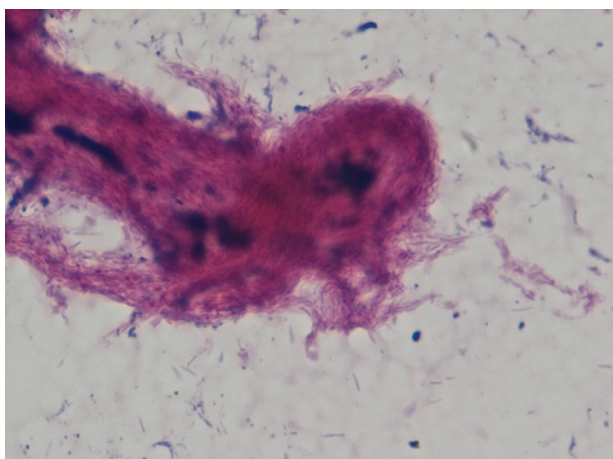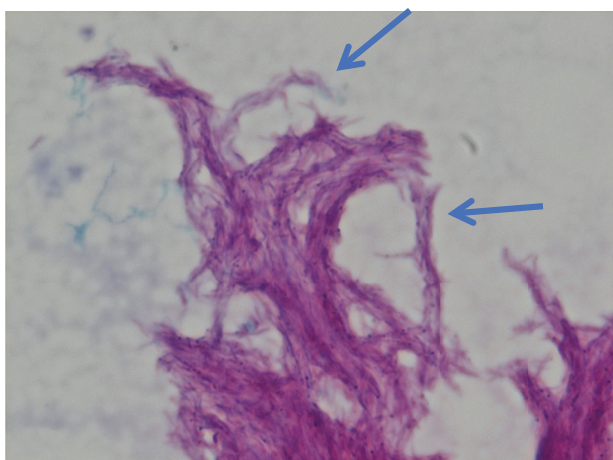
doxycycline, linezolid, and clarithromycin, intermediate resistance to imipenem, and resistance to cefoxitin, fluoroquinolones, and trimethoprim-sulfamethoxazole. His regimen was changed to azithromycin, doxycycline, and linezolid, but linezolid was later stopped because of bone marrow suppression. The patient has continued on this therapy with improvement in symptoms, and treatment was ultimately stopped when a repeat PET scan showed resolution of the prior areas of uptake.

Discussion

Most often described with *Mycobacterium tuberculosis,* cording is a phenomenon in which AFB grow in parallel, end-to-end and side-to-side, forming ropelike structures in liquid culture media.[1-3] Although this process was thought to primarily occur in TB and was used as a means of presumptive microscopic identification of TB,[1,2] it has been shown in multiple other nontuberculous mycobacterial (NTM) species.[2-5] Cording is linked to increased virulence with enhanced intracellular survival in macrophages, more extracellular replication, and the ability to evade the immune system via the formation of abscesses and granulomas.[3,4]

M. chelonae is a rapidly growing mycobacterium found in the environment.[6] It most commonly causes infection of the skin, bone, and soft tissue. Disseminated disease can also occur in patients who are immunosuppressed, often accompanied by a characteristic skin lesion. Pulmonary disease can occur, but less commonly than with other NTM species. There have also been patients with keratitis associated with contact lenses and eye surgery. Treatment is generally multidrug therapy based on susceptibility testing, and surgical debridement may be necessary.[6]

As shown in this case of disseminated *M. chelonae* infection, cording may occur in multiple NTM species and is not reliable as the sole indicator of the presence of TB. **LM**

Image 1

Wide view of AFB smear. AFB, acid fast bacilli.

Image 2

Magnified view of AFB smear. The arrows indicate the presence of cording. AFB, acid fast bacilli.

References

1. Tu HZ, Chang SH, Huaug TS, Huaug WK, Liu YC, Lee SS. Microscopic morphology in smears prepared from MGIT broth medium for rapid presumptive identification of *Mycobacterium tuberculosis* complex,

Mycobacterium avium complex and *Mycobacterium kansasii*. *Ann Clin Lab Sci.* 2003;33(2):179–183.

2. Sánchez-Chardi A, Olivares F, Byrd TF, Julián E, Brambilla C, Luquin M. Demonstration of cord formation by rough *Mycobacterium abscessus* variants: implications for the clinical microbiology laboratory. *J Clin Microbiol.* 2011;49(6):2293–2295.

3. Julián E, Roldán M, Sánchez-Chardi A, Astola O, Agustí G, Luquin M. Microscopic cords, a virulence-related characteristic of *Mycobacterium tuberculosis*, are also present in nonpathogenic mycobacteria. *J Bacteriol.* 2010;192(7):1751–1760.

4. Bernut A, Herrmann JL, Kissa K, et al. *Mycobacterium abscessus* cording prevents phagocytosis and promotes abscess formation. *Proc Natl Acad Sci U S A.* 2014;111(10):E943–E952.

5. Staropoli JF, Branda JA. Cord formation in a clinical isolate of *Mycobacterium marinum*. *J Clin Microbiol.* 2008;46(8):2814–2816.

6. Griffith DE, Aksamit T, Brown-Elliott BA, et al.; ATS Mycobacterial Diseases Subcommittee; American Thoracic Society; Infectious Disease Society of America. An official ATS/IDSA statement: diagnosis, treatment, and prevention of nontuberculous mycobacterial diseases. *Am J Respir Crit Care Med.* 2007;175(4):367–416.

Case Study

Acute Myeloid Leukemia Case Harboring Unusual *FLT3* Variant: Somatic vs Germline?

Nirupama Singh, MD, PhD,[1] Diana Morlote, MD,[1] Cindy Vnencak-Jones, PhD,[2]
Nikolaos Papadantonakis, MD, PhD,[3] Shuko Harada, MD[1,*]

ABSTRACT

FLT3 mutations are considered a prognostic and predictive marker. Here we report on a patient with a rare *FLT3* germline variant in the context of relapsed acute myeloid leukemia (AML). A female patient aged 57 years presented with AML with mutations in the *IDH2, ASXL1,* and *DNMT3A* genes. She underwent allogenic hematopoietic stem cell transplant but relapsed 2 years posttransplant. Targeted next generation sequencing identified a new missense variant in the *FLT3* tyrosine kinase domain c.2440G > T (p.A814S). The treating team considered the possibility of patient eligibility for an *FLT3* inhibitor. Because both somatic and germline mutations

can be identified in tumor tissue with high-throughput sequencing, it becomes important to distinguish the origin of these alterations when possible—especially, in this challenging case, to define the treatment modality. Simultaneous tumor/germline sequencing allows for the identification of rare germline mutations and may help in determining their significance in the pathogenesis of disease.

Keywords: Hematopathology, Molecular pathology, Highthroughput sequencing, Somatic vs Germline alterations/mutations, *FLT3*, Cytogenetically normal (CN)-AML

Acute myeloid leukemia (AML) is the most common leukemia in adults, involving clonal myeloid precursor proliferation with a decreased capacity to differentiate. It is a heterogenous group of diseases with variable prognoses; for example, acute promyelocytic leukemia has a good prognosis, with complete remission rates of 100% and cure rates exceeding 80%,[1] whereas AML with mutations in *TP53* or *RUNX1* has a worse prognosis.[2] Historically, AML was classified based on morphology and cytogenetics analysis,[3] which together provided diagnostic and prognostic markers.[4] However, the majority (50%) of AML is cytogenetically normal (CN-AML), lacking structural abnormalities.[4]

Abbreviations:

AML, acute myeloid leukemia; CN-AML, cytogenetically normal acute myeloid leukemia; ITD, internal tandem duplications; TKD, tyrosine kinase domain; VAF, variant allele frequency; RTK, receptor tyrosine kinase.

[1]Department of Pathology, Department of Medicine, University of Alabama at Birmingham, Birmingham, Alabama, [2]Department of Pathology, Vanderbilt University, Nashville, Tennessee, [3]Division of Hematology and Medical Oncology, Emory Winship Cancer Institute, Emory University, Atlanta, Georgia

*To whom correspondence should be addressed.
sharada@uabmc.edu

For these patients, it is difficult to predict the prognosis and define the treatment modality.

With the recent advent of high-throughput sequencing, new mutations in AML are identified, and many of these mutations help in defining the prognosis and treatment regimen. Many of these recurrent mutations are present in *FLT3, DNMT3A, IDH1, IDH2,* and others. Some mutations are considered in the most recent World Health Organization (2016) AML subtype classification, such as AML with mutated *NPM1* and biallelic mutations of *CEBPA*.[5] The previously recognized cytogenetics risk (t(15;17), t(11;19), monosomy karyotype) and recent identification of molecular subtypes (NPM1 mutation, biallelic CEBPA mutation) are used in the 2016 World Health Organization guidelines[5] for AML risk stratification (favorable, intermediate, and adverse).

The clinical presentation overlaps in different subtypes of AML, but patient management is complicated and based on these recent molecular subsets and available drug targets. We report a challenging case of a patient with an unusual *FLT3* alteration. In this study, we discuss the relevance of an *FLT3* germline alteration in relapsed AML and the significance of this finding on patient therapy.

Case Report

A female patient aged 57 years presented to our hospital with a recent diagnosis of AML. Cytogenetics and fluorescence in situ hybridization revealed CN-AML. Molecular profiling, performed at a reference laboratory, revealed mutations in the *IDH2, ASXL1,* and *DNMT3A* genes but no internal tandem duplications (ITD) or codon 835 tyrosine kinase domain (TKD) recurrent hotspot mutations in *FLT3* (**Table 1**). The patient received Fludarabine, Arabinofuranosyl cytidine (cytarabine), granulocyte colony-stimulating factor (FLAG) treatment as a second induction therapy that consisted of fludarabine and cytarabine daily on days 1 to 5 and then an allogenic hematopoietic stem cell transplant. The donor was a related donor with a 12/12 allele match.

Eighteen months after her discharge from the hospital with a successful engraftment, the patient developed leukopenia that fluctuated; almost 2 years after the first engraftment, a bone marrow biopsy was performed that revealed relapsed disease with a blast population of approximately 10%. In-house targeted next-generation sequencing identified the previously reported *IDH2, ASXL1,* and *DNMT3A* mutations with a variant allele frequency (VAF) corresponding to 5 to 10%, consistent with the reported blast percentage (**Table 1**). In addition, a missense variant, c.2440G > T, in the *FLT3* TKD resulting in p.A814S was detected at a VAF of approximately 50% (**Figure 1**). The treating team considered the variant as a newly evolved variant and raised the possibility of eligibility for a clinical trial with an *FLT3* inhibitor.

Previous research has reported *FLT3* p.A814S in 1 patient with myelodysplastic syndrome in the COSMIC database and has not been reported in the general population (ExAc database).[6] In-silico algorithms modeling predictions such as SIFT and Polyphen2 predict deleterious/probably damaging effect of *FLT3* p.A814S. However, these predictions are not confirmed by functional studies, and their biologic effect has not been characterized.

In our patient, the variant was present at a VAF of 40 to 50%, higher than the expected VAF from the blast percentage of 10%, raising a possibility that this variant was present in the germline. A sequencing analysis of *FLT3* exon 20 on DNA extracted from a buccal swab revealed that the patient was heterozygous for variant c.2440G > T, with similar amounts of each nucleotide. Based on these results, an *FLT3* inhibitor was not favored. The patient received several lines of treatment and eventually was able to proceed to a second allogenic hematopoietic stem cell transplant with a matched unrelated donor. Seven months posttransplant, the patient is doing well.

Discussion

Research has shown that *FLT3* is a member of the class III receptor tyrosine kinase (RTK) family. It contains 5 functional domains: immunoglobin-like loops, the transmembrane domain, the extracellular domain, the juxtamembrane domain, and the tyrosine kinase 1 and 2 domains, similar to other members of the RTK family such as *KIT* and *PDGFR*. The *FLT3* gene is expressed in early myeloid progenitor cells and the hematopoietic stem cell compartment.[7] The FLT3 ligand is a growth factor for immature myeloid cells and stem cells. The *FLT3* receptor binds to the FLT3 ligand and induces the downstream signaling pathways, activating proteins like STAT5 and ERK, that are responsible for growth and proliferation, of early hematopoietic progenitor cells.[7]

Targeted high-throughput sequencing has identified many recurrent mutations in AML, including *FLT3, NPM1, CEBPA, DNMT3A, IDH1/2,* and *TET2*.[8] One study identified *FLT3* mutations in 30% of patients with AML,[8] most of whom had a normal karyotype. In another study, mutations in *FLT3* included ITD in the juxtamembrane domain, identified in 25% of patients with AML, and point mutations in the TKD at codon 835, in approximately 7% of patients with AML.[9] Both ITD and TKD mutations lead to constitutive activation of tyrosine kinase[9] and therefore present a potential for therapeutic

Table 1. Summary of Molecular Findings at Initial Diagnosis and Relapsed Disease

Gene	Initial Diagnosis	Relapsed
IDH2	p.R172W (25%)	p.R172W (5-10%)
DNMT3A	p.S770L (30%)	p.S770L (5-10%)
FLT3-ITD[a]	negative	negative
FLT3-TKD[a]	negative	p.A814S (40-50%)[b]

ITD, internal tandem duplication; PCR, polymerase chain reaction; TKD, tyrosine kinase domain.
[a]ITD was detected by using PCR followed by detection and fragment size analysis using capillary electrophoresis. TKD mutation (codon D835) was identified by amplification of exon 20 followed by EcoRV digestion (This restriction enzyme recognizes GAT^ATC sites to cut) with detection and fragment size analysis using capillary electrophoresis.
[b]FLT3 TKD (p.A814S) was identified by using a next-generation sequencing platform.
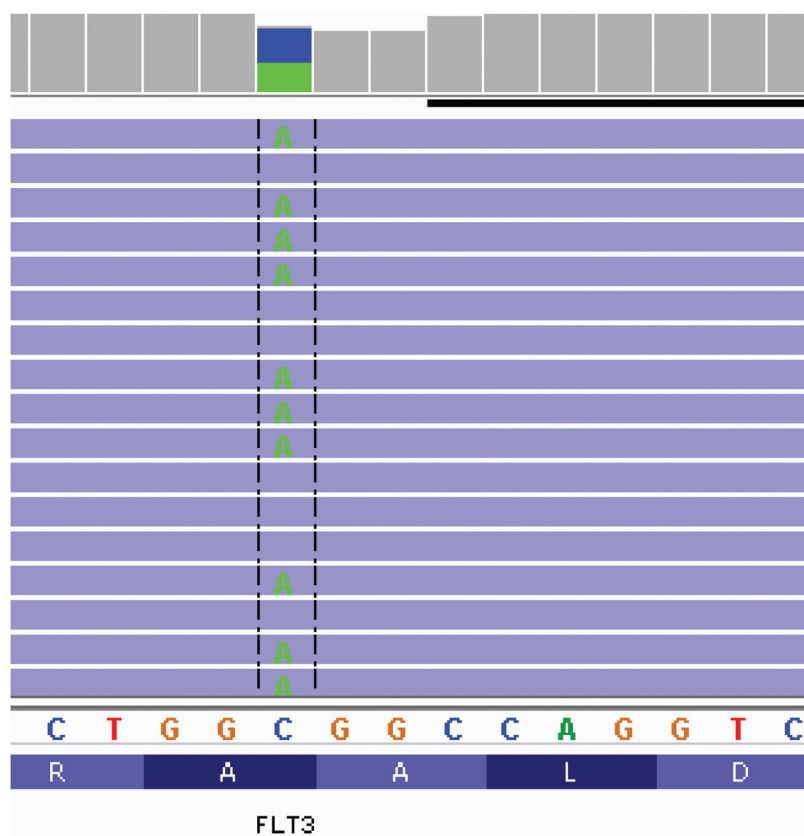
Figure 1

Integrative genomic viewer of *FLT3* exon 20. In-house myeloid comprehensive panel, consisting of 50 genes, uses target enrichment with Agilent HaloPlex HS, and next-generation sequencing was performed on the Illumina MiSeq instrument.[11]

targets. Patients with AML with *FLT3* mutations historically have had significantly worse outcomes compared to those with *FLT3* wild type; however, with the advent of *FLT3* inhibitors, the prognosis has improved.[10] These mutations may be redefining the management and prognosis of AML with intermediate prognosis (mostly in CN-AML).[10]

US Food & Drug Administration–approved *FLT3* inhibitors are available for *FLT3*-mutated AML as a first-line therapy in relapsed and refractory AML and recently as a first-line treatment with chemotherapy in primary AML.[11] There are 2 generations of *FLT3* inhibitors available based on their specificity. Type II inhibitors such as sorafenib work against only *FLT3* ITD, whereas Type I second-generation inhibitors such as crenolanib and gilteritinib work in the presence of either ITD or TKD with higher potency.[12] Thus, identifying *FLT3* mutations to identify potential targeted therapy is important for patient management.

Our patient had an unusual *FLT3* alteration in the TKD. Her condition initially caused some confusion among the treatment team because the initial molecular profile failed to report this unique *FLT3* germline variant because the assay was designed to detect only hotspot mutations. The detection of this variant at relapse was initially thought to be a newly acquired disease-associated mutation. Germline testing using DNA extracted from a buccal swab revealed that the variant was constitutional. Research has shown that *FLT3* somatic mutations are a common occurrence in AML, but the role of an *FLT3* germline mutation is poorly understood. This case study illustrates the importance of distinguishing germline and somatic mutations and highlights the significance of reporting potential germline variants in next generation sequencing conducted on tumor tissue only or of reporting confirmed germline variants when side-by-side testing is performed. In addition to alerting the healthcare provider and patient about a germline variant over time, these data provide

evidence to help distinguish which rare germline gene/variants may predispose a patient to cancer.

Conclusion

With the advent of high-throughput sequencing, the ability to distinguish between somatic and germline variants is crucial for patient management and will aid in the understanding of predisposition to cancer and tumorigenesis. **LM**

References

1. Lo-Coco F, Avvisati G, Vignetti M, et al.; Gruppo Italiano Malattie Ematologiche dell'Adulto; German-Austrian Acute Myeloid Leukemia Study Group; Study Alliance Leukemia. Retinoic acid and arsenic trioxide for acute promyelocytic leukemia. *N Engl J Med.* 2013;369(2):111–121.

2. Papaemmanuil E, Gerstung M, Bullinger L, et al. Genomic classification and prognosis in acute myeloid leukemia. *N Engl J Med.* 2016;374(23):2209–2221.

3. Kalousek DK, Wiersma SR, et al. Morphologic, immunologic, and cytogenetic classification of acute myeloid leukemia and myelodysplastic syndrome in childhood: a report from the Children's Cancer Group. *Leukemia* 1996;10(1):5–12.

4. Byrd JC, Mrózek K, Dodge RK, et al.; Cancer and Leukemia Group B (CALGB 8461). Pretreatment cytogenetic abnormalities are predictive of induction success, cumulative incidence of relapse, and overall survival in adult patients with de novo acute myeloid leukemia: results from Cancer and Leukemia Group B (CALGB 8461). *Blood.* 2002;100(13):4325–4336.

5. Arber DA, Orazi A, Hasserjian R, et al. The 2016 revision to the World Health Organization classification of myeloid neoplasms and acute leukemia. *Blood.* 2016;127(20):2391–2405.

6. Papaemmanuil E, Gerstung M, Malcovati L, et al. Clinical and biological implications of driver mutations in myelodysplastic syndromes. *Blood.* 2013;122(22):3616–3627.

7. Rappold I, Ziegler BL, Köhler I, et al. Functional and phenotypic characterization of cord blood and bone marrow subsets expressing FLT3 (CD135) receptor tyrosine kinase. *Blood.* 1997;90(1):111–125.

8. Ley TJ, Miller C, Ding L, et al. Genomic and epigenomic landscapes of adult de novo acute myeloid leukemia. *N Engl J Med*. 2013;368(22):2059–2074.

9. Jiang J, Paez JG, Lee JC, et al. Identifying and characterizing a novel activating mutation of the FLT3 tyrosine kinase in AML. *Blood.* 2004;104(6):1855–1858.

10. Bacher U, Haferlach C, Kern W, Haferlach T, Schnittger S. Prognostic relevance of FLT3-TKD mutations in AML: the combination matters–an analysis of 3082 patients. *Blood.* 2008;111(5):2527–2537.

11. Larrosa-Garcia M, Baer MR. FLT3 inhibitors in acute myeloid leukemia: current status and future directions. *Mol Cancer Ther.* 2017;16(6):991–1001.

12. Morlote D, Janowski K, Siniard RC, et al. Effects of DNA integrity on next generation sequencing quality metrics: comparison of two harvesting methods from paraffin embedded tissue. *Am J Clin Pathol*. 2019;152(1):27–35.

Erratum

In the article "Case Report and Literature Review of Nodular Hiradenoma, a Rare Adnexal Tumor That Mimics Breast Carcinoma, in a 20-Year-Old Woman", the word "Hidradenoma" was misspelled as "Hiradenoma" in the initial publication of this article. This has been corrected.